



University  
of Glasgow

McCaig, Alison M. (2010) *Investigation of dual Src/c-Abl tyrosine kinase inhibition as a novel therapeutic approach for chronic lymphocytic leukaemia*. PhD thesis.

<http://theses.gla.ac.uk/2008/>

Copyright and moral rights for this thesis are retained by the author

A copy can be downloaded for personal non-commercial research or study, without prior permission or charge

This thesis cannot be reproduced or quoted extensively from without first obtaining permission in writing from the Author

The content must not be changed in any way or sold commercially in any format or medium without the formal permission of the Author

When referring to this work, full bibliographic details including the author, title, awarding institution and date of the thesis must be given

**Investigation of Dual Src/c-Abl Tyrosine Kinase Inhibition as a  
Novel Therapeutic Approach for Chronic Lymphocytic Leukaemia**

**Alison M<sup>c</sup>Caig**

A thesis submitted for the Doctor of Philosophy  
at the University of Glasgow

Faculty of Medicine

Submitted: April 2010

© Alison M<sup>c</sup>Caig

## Summary

Chronic lymphocytic leukaemia (CLL) is the most common leukaemia in the western world, and remains incurable with current chemotherapy. Although CLL was long-regarded as an autonomous accumulation of functionally incompetent lymphocytes that escape apoptosis, significant rates of clonal proliferation and death have now been elegantly demonstrated in CLL patients *in vivo*. This, coupled with the high rates of spontaneous apoptosis observed on *ex-vivo* culture, confirms that CLL is a dynamic disorder, in which the tumour microenvironment is central to leukemic cell survival. Recent advances in CLL cell biology implicate signalling through the B cell antigen receptor (BCR) in the pathogenesis and progression of the disease. The absence of significant somatic hypermutation of the immunoglobulin heavy chain variable region (IgV<sub>H</sub>), which largely correlates with the expression of ZAP-70, in CLL cells is a significant adverse prognostic marker. CLL cases expressing an unmutated IgV<sub>H</sub> gene generally retain the ability to signal through the BCR. Components of the BCR signalling pathway are therefore attractive novel therapeutic targets, with potential selectivity for adverse prognostic groups. The non-receptor tyrosine kinases Lyn (a Src kinase) and c-Abl are both required for effective BCR signalling. Both are over-expressed, and constitutively active in CLL, and inhibition of either induces a degree of apoptosis. Dasatinib is a Src/c-Abl tyrosine kinase inhibitor in clinical use in chronic myeloid leukaemia. The main objective of this project was to conduct translational studies to determine the anti-leukaemic effects of dasatinib on CLL cells *in vitro*.

While the Src kinase inhibitor PP2, and the c-Abl inhibitor imatinib induced apoptosis of CLL cells at micromolar concentrations, dasatinib induced apoptosis of CLL cells at clinically achievable nanomolar concentrations, with an EC<sub>50</sub> in the region of 10-30 nM, and plateau in effect above 100 nM. CLL cell treatment with 100 nM dasatinib for 48 hr led to a mean reduction in viability of 33.7%, but with significant inter-sample variability. No correlation was observed between dasatinib sensitivity and the established prognostic factors clinical stage, ZAP-70 status, or cytogenetic subgroup. Notably, CLL cells known to contain the 17p deletion, resulting in p53 dysfunction, responded similarly to other samples. Apoptosis induced by dasatinib involved loss of mitochondrial membrane potential and was caspase-dependent. Although dasatinib treatment alone rarely induced apoptosis of over 50% of CLL cells, synergy was observed between dasatinib and the

current first-line chemotherapeutic agents fludarabine and chlorambucil. Moreover, dasatinib exhibited synergy with a novel Bcl-2 inhibitor, and the HSP90 inhibitor 17-DMAG.

Recently, antigen-independent 'tonic' BCR signalling has been linked to the pathogenesis of B cell lymphomas. Tonic signalling is proposed to be mediated by basal activity of Lyn and Syk kinases recruited to the BCR. As Syk is also over-expressed in CLL, we hypothesised that dasatinib sensitivity may correlate with inhibition of components of tonic BCR signal transduction. Indeed, CLL cells contained constitutively phosphorylated Syk<sup>Y348</sup>. Furthermore, a significant inverse correlation was observed between basal Syk<sup>Y348</sup> phosphorylation and dasatinib sensitivity in individual samples, suggesting its' utility as a biomarker of response. Dasatinib consistently inhibited an increase in Syk<sup>Y348</sup> phosphorylation on BCR crosslinking. In addition, dasatinib inhibited calcium flux, and prevented Akt and MAPK phosphorylation on BCR stimulation. Moreover, dasatinib prevented up-regulation of Mcl-1 and blocked the increase in CLL cell survival observed on prolonged BCR stimulation, confirming inhibition of BCR signalling as a functionally relevant treatment strategy in CLL. Although dasatinib prevented CXCR4 down-regulation following BCR stimulation of CLL cells, dasatinib also specifically inhibited PI-3K/Akt activation upon CXCR4 stimulation by SDF-1, resulting in reduced actin polymerization and migration following SDF-1 stimulation. While the full translational implications of these observations remain to be determined, these data demonstrate that the anti-leukaemic effects of dasatinib extend beyond direct inhibition of BCR signal transduction.

It is well recognised that bone marrow (BM) stromal cells and blood-derived 'nurse-like' cells protect CLL cells from spontaneous apoptosis *in vitro*. More recently, proliferating CLL cells have been identified within specialised 'proliferation centres', admixed with appreciable numbers of T lymphocytes, predominantly activated CD4<sup>+</sup> T cells expressing CD40 ligand (CD154), and interleukin 4 (IL-4). CD40/IL-4 stimulation of CLL cells *in vitro* leads to up-regulation of the anti-apoptotic Bcl-2 family proteins Bcl-x<sub>L</sub> and Mcl-1, and the proliferative protein survivin, mimicking the expression profile of CLL cells isolated from patient lymph nodes (LNs). We were interested to determine whether the effects of dasatinib on CLL cells were modulated by these microenvironmental factors. To achieve this, CLL cells were co-cultured with either the murine BM

stromal cell line NT-L, or NT-L cells stably transfected to express CD154, the latter with IL-4 added to the culture medium (154L/IL-4 system). The pro-apoptotic effect of dasatinib in CLL cells was abrogated by stromal cell co-culture, with or without CD154 and IL-4. Stromal cell-mediated resistance to dasatinib involved Akt and MAPK signalling, as evidenced by the ability of both the PI-3K inhibitor LY294002, and the MEK inhibitor PD98059 to restore dasatinib sensitivity of cells in NT-L co-culture. 154L/IL-4 co-culture activated multiple MAPK, associated with up-regulation of Bcl-x<sub>L</sub>, Mcl-1, and survivin, which was not inhibited by dasatinib. Dasatinib also failed to inhibit CLL cell proliferation in the 154L/IL-4 system. While dasatinib retained the ability to sensitise CLL cells to both fludarabine and chlorambucil in NT-L co-culture, the addition of CD154 and IL-4 rendered cells resistant to all drug combinations. Dasatinib did however retain the ability to sensitise CLL cells to the HSP90 inhibitor 17-DMAG in both NT-L and 154L/IL-4 co-culture.

In conclusion, these studies demonstrate that dasatinib offers much as a novel therapeutic strategy for CLL, overcoming pro-survival signalling through the BCR. However, our data suggest that dasatinib may be best utilised in combination treatment strategies with agents that can target antigen-independent signalling networks within the microenvironment. Collectively, this work provides valuable information that will inform future clinical trials of Src/c-Abl inhibitors in CLL.

## **Declaration**

This work represents original work carried out by the author and has not been submitted in any form to any other University.

Alison M<sup>c</sup>Caig

April 2010

## **Acknowledgements**

I am extremely grateful to my supervisor, Dr. Alison Michie, for continued guidance and inspiration throughout this project. I am very privileged to have been able to complete my PhD research programme within Dr. Michie's laboratory, and am truly indebted to her for the scientific training I have received over the last three years, which will prove invaluable to me in my future career progression. Her unwavering patience, optimism, and support have enabled me to achieve far more than I initially thought possible. I would also very much like to thank Professor Tessa Holyoake for her longstanding support and advice, which has been instrumental in enabling me to pursue my academic interests. In addition, I am very appreciative of the help I have received from all members of Professor Holyoake's, Professor Margaret Harnett's, and Dr. Helen Wheadon's laboratories, for opportunities to present my work, and many helpful discussions. In particular, I would like to thank Dr. Rinako Nakagawa for her help with flow cytometry and western blotting, Dr. Hwee Kee Tay for training me to perform calcium assays, Peixun Zhou for assistance with confocal microscopy, and Milica Vukovic for help with TaqMan<sup>®</sup> PCR. I am grateful to my advisor, Dr. Mike Leach for help with obtaining CLL patient samples, and for many useful discussions throughout this project. Furthermore, I am grateful to all patients who have donated blood samples that have enabled this work to be carried out. I would also like to acknowledge the University of Glasgow, the Medical Research Council, and Tenovus Scotland for funding this work, to all of whom I am very grateful for support. Finally, I would like to thank my family, friends, and my fiancé Indran Raju for much patience and moral support throughout the course of my PhD studies.

<b>Contents</b>	<b>Page</b>
Summary	ii
Declaration	v
Acknowledgements	vi
List of Contents	vii
List of Tables	xiii
List of Figures	xiv
List of Equations	xviii
Abbreviations	xix
<b>Chapter 1: Introduction</b> .....	<b>1</b>
1.1 B lymphocyte development and function.....	2
1.1.1 Overview of B lymphocyte development.....	2
1.1.2 The humoral immune response .....	4
1.1.2.1 The germinal centre reaction .....	4
1.2 Chronic lymphocytic leukaemia .....	6
1.2.1 Epidemiology and diagnosis of CLL .....	6
1.2.2 Clinical features of CLL.....	7
1.2.3 Prognostic factors in CLL.....	8
1.2.3.1 Clinical prognostic factors .....	8
1.2.3.2 IgV <sub>H</sub> mutation status.....	9
1.2.3.3 ZAP-70 .....	9
1.2.3.4 CD38 .....	10
1.2.3.5 Cytogenetic abnormalities .....	10
1.2.3.6 Other biological prognostic indicators .....	11
1.2.4 Treatment of CLL.....	12
1.2.4.1 A history of developments in CLL therapy .....	12
1.2.4.2 Limitations of current therapy .....	15
1.3 Overview of CLL biology .....	16
1.3.1 Historical understanding of CLL biology .....	16
1.3.2 Current understanding of CLL biology .....	17
1.4 The role of antigen in the pathogenesis of CLL.....	18
1.5 B cell receptor signal transduction .....	24

1.5.1	Early events following BCR engagement by antigen .....	24
1.5.2	Signal transduction .....	25
1.5.2.1	MAPK signalling pathway.....	26
1.5.2.2	PI-3K/Akt signalling pathway.....	27
1.5.2.3	NF- $\kappa$ B signalling .....	28
1.5.3	Tonic BCR signalling .....	29
1.6	BCR signalling in CLL cells .....	30
1.6.1	BCR signal transduction in CLL cells.....	30
1.6.2	Evidence for dysregulated tonic BCR signalling in CLL.....	34
1.6.2.1	Lyn kinase .....	34
1.6.2.2	c-Abl kinase.....	36
1.7	The role of the microenvironment in CLL .....	36
1.7.1	The role of stromal cells in CLL .....	37
1.7.1.1	SDF-1/CXCR4 axis .....	39
1.7.1.2	Integrins .....	40
1.7.1.3	Angiogenic cytokines .....	41
1.7.2	Nurse-like cells .....	42
1.7.2.1	BAFF and APRIL.....	42
1.7.2.2	CD31/CD38 axis .....	43
1.7.3	T lymphocytes in CLL .....	43
1.7.3.1	CD40 signalling in CLL.....	45
1.7.3.2	IL-4 signalling in CLL.....	47
1.8	Potential novel therapeutic strategies based on knowledge of CLL biology .....	48
1.8.1	Rationale for investigation of the Src/c-Abl TKI dasatinib .....	48
1.8.2	The rationale for inhibition of Bcl-2 family proteins in CLL.....	50
1.8.3	Rationale for inhibition of heat shock protein 90 .....	53
1.9	Aims and objectives .....	55
<b>Chapter 2: Materials and Methods .....</b>		<b>56</b>
2.1	Cells and reagents .....	57
2.1.1	CLL patient samples .....	57
2.1.2	Normal blood samples .....	57
2.1.3	Drugs and inhibitors .....	57
2.1.4	Chemokines and cytokines.....	58
2.1.5	Antibodies .....	58

2.2	Tissue culture .....	58
2.2.1	Purification of CLL cells from patient samples .....	59
2.2.2	Cell counting using a haemocytometer .....	59
2.2.3	Cryopreservation of cells .....	59
2.2.4	Recovery of cryopreseved samples .....	60
2.2.5	Culture of CLL cells .....	60
2.2.6	Isolation of B lymphocytes from buffy coats .....	60
2.2.6.1	Mononuclear cell preparation .....	60
2.2.6.2	CD19 selection using magnetic cell sorting .....	60
2.2.7	Cell Lines .....	61
2.2.7.1	NT-L and CD154L cells .....	61
2.2.7.2	M2-10B4 cells .....	61
2.2.7.3	Ramos cells .....	61
2.2.7.4	HT29 cells .....	62
2.2.8	CLL cell stimulation .....	62
2.2.8.1	Short term BCR stimulation using biotinylated anti-IgM .....	62
2.2.8.2	Long term BCR stimulation with anti-IgM F(ab') <sub>2</sub> fragments .....	62
2.2.8.3	Long term BCR stimulation with immobilised anti-IgM .....	62
2.2.8.4	Short-term stimulation with SDF-1 .....	63
2.2.8.5	Long term SDF-1 stimulation .....	63
2.2.8.6	Co-culture with stromal cells .....	63
2.2.8.7	Co-culture with soluble CD154 and IL-4 .....	64
2.2.9	CLL cell proliferation assay .....	64
2.2.9.1	CFSE staining of CLL cells .....	64
2.2.9.2	12 day 154L/IL-4 co-culture .....	65
2.3	Flow cytometry .....	65
2.3.1	Assessment of surface antigen expression .....	65
2.3.2	Analysis of intracellular proteins .....	66
2.3.3	Measurement of Syk <sup>Y348</sup> phosphorylation by intracellular phosphospecific flow cytometry .....	66
2.3.4	Annexin V / Viaprobe staining .....	67
2.3.5	Assessment of mitochondrial membrane potential .....	67
2.3.6	Chemotaxis assay .....	68
2.3.7	Actin polymerisation assay .....	68
2.3.8	Pseudoemperipolesis assay .....	69
2.3.9	FACS for CFSE proliferation experiments .....	70

2.3.9.1	Cell counting by flow cytometry.....	70
2.3.9.2	Analysis of cell division using CFSE .....	71
2.3.9.3	Calculation of percentage recovery of input cells.....	71
2.4	Assessment of calcium flux following BCR stimulation by fluorescence spectrophotometry .....	72
2.5	Assessment of actin polymerisation using confocal fluorescence microscopy.....	73
2.6	Western blotting .....	74
2.6.1	Cell lysate preparation .....	74
2.6.2	Protein quantification .....	74
2.6.3	Sodium dodecyl sulphate-polyacrylamide gel electrophoresis (SDS-PAGE) and transfer.....	75
2.6.4	Immunolabelling and detection .....	75
2.6.5	Membrane stripping and re-probing.....	76
2.7	Quantitative PCR.....	76
2.7.1	RNA extraction.....	76
2.7.2	Reverse transcription PCR .....	76
2.7.3	TaqMan® real-time PCR .....	77
2.8	Statistical analysis .....	77
2.8.1	Software used for statistical analysis.....	77
2.8.2	Statistical analysis of data generated in drug combination experiments .....	78

**Chapter 3: Dasatinib induces apoptosis of CLL cells *in vitro*, and shows synergy with established and novel chemotherapeutic agents. . 99**

3.1	Introduction.....	100
3.2	Aims and Objectives.....	100
3.3	Results .....	101
3.3.1	The Src/c-Abl TKI dasatinib induces apoptosis of CLL cells <i>in vitro</i> . 101	101
3.3.2	Dasatinib-induced apoptosis is independent of established prognostic factors. ....	102
3.3.3	Dasatinib-induced apoptosis in CLL cells is caspase-dependent.....	103
3.3.4	Duration of dasatinib exposure required to induce apoptosis of CLL cells <i>in vitro</i> . ....	104
3.3.5	Dasatinib also induces a degree of apoptosis in normal B lymphocytes. ....	105

3.3.6	Bcl-2 inhibitors and HSP90 inhibitors induce apoptosis of CLL cells <i>in vitro</i> .....	105
3.3.7	Dasatinib exhibits synergy with fludarabine, chlorambucil, and novel therapeutic agents <i>in vitro</i> .....	107
3.4	Discussion .....	109
<b>Chapter 4: Dasatinib inhibits BCR signalling in CLL cells, and reduces CLL cell migration towards SDF-1.</b> .....		<b>135</b>
4.1	Introduction.....	136
4.1.1	Evidence for the therapeutic potential of inhibiting tonic signalling in B cell malignancies .....	136
4.1.2	The link between BCR signal transduction and migration of B lymphocytes.....	137
4.2	Aims and Objectives.....	138
4.3	Results .....	139
4.3.1	Dasatinib inhibits tonic BCR signalling in CLL cells.....	139
4.3.2	CLL sensitivity to dasatinib correlates with basal Syk phosphorylation. ....	140
4.3.3	Dasatinib inhibits signalling induced by BCR ligation in CLL cells....	141
4.3.4	Dasatinib inhibits BCR-mediated up-regulation of Mcl-1 and survival of CLL cells. ....	143
4.3.5	Dasatinib prevents CXCR4 down-regulation on BCR stimulation ...	144
4.3.6	Dasatinib inhibits Akt phosphorylation on CXCR4 stimulation in CLL cells. ....	145
4.3.7	Dasatinib inhibits SDF-1-induced actin polymerisation, chemotaxis, and pseudoemperipolesis.....	146
4.3.8	Dasatinib inhibits pro-survival SDF-1 signalling in CLL cells <i>in vitro</i> .	147
4.4	Discussion .....	149
<b>Chapter 5: CLL cell co-culture with stromal cells, in the presence or absence of CD154 and IL-4, modulates the anti-leukaemic effects of dasatinib.</b> .....		<b>176</b>
5.1	Introduction.....	177
5.1.1	Modelling the CLL microenvironment <i>in vitro</i> .....	177
5.2	Aims and Objectives:.....	179
5.3	Results .....	180

5.3.1	Stromal cell or CD154/IL-4 co-culture greatly reduces apoptosis induced by dasatinib .....	180
5.3.2	PI-3K/Akt and MAPK activation in NT-L and 154L/IL-4 co-cultured CLL cells abrogates the pro-apoptotic effect of dasatinib .....	180
5.3.3	Dasatinib fails to inhibit the up-regulation of anti-apoptotic Bcl-2 family proteins and survivin on 154L/IL-4 co-culture .....	182
5.3.4	CLL cell proliferation in 154L/IL-4 co-culture is not inhibited by dasatinib .....	183
5.3.5	Dasatinib retains the ability to sensitise CLL cells to fludarabine and chlorambucil in NT-L, but not 154L/IL-4 co-culture .....	184
5.3.6	Synergy between dasatinib and Bcl-2 inhibitor I is lost on NT-L or 154L/IL-4 co-culture .....	185
5.3.7	Dasatinib sensitises CLL cells to the HSP90 inhibitor 17-DMAG sensitises in both NT-L and 154L/IL-4 co-culture .....	185
5.4	Discussion .....	188
<b>Chapter 6: General Discussion .....</b>		<b>218</b>
6.1	Summary of results .....	219
6.2	What could dasatinib add to current treatment algorithms in CLL? .....	219
6.3	Is there a potential role for dasatinib as maintenance therapy for CLL? .....	221
6.4	Novel therapeutic agents with the potential to target the leukaemic microenvironment in CLL .....	222
6.5	The potential for assessment of novel dasatinib combination therapies in mouse models of CLL .....	225
6.6	The future of targeted therapy in CLL .....	226
6.7	Concluding remarks .....	227
<b>Bibliography .....</b>		<b>229</b>

## List of Tables

<b>Table 1.1</b>	Immunophenotypic scoring system for CLL .....	7
<b>Table 1.2</b>	Binet clinical staging system for CLL .....	8
<b>Table 1.3</b>	Cytogenetic abnormalities identified in CLL .....	10
<b>Table 1.4</b>	2008 IWCLL guideline indications for treatment of CLL.....	12
<b>Table 2.1</b>	Suppliers addresses.....	80
<b>Table 2.2</b>	Details of CLL samples stored .....	82
<b>Table 2.3</b>	Details of inhibitor preparation and storage .....	84
<b>Table 2.4</b>	Antibodies used for FCM.....	85
<b>Table 2.5</b>	Antibodies used for western blotting .....	86
<b>Table 2.6</b>	Definitions of drug synergism and antagonism .....	87
<b>Table 3.1</b>	Degree of synergy observed in CLL cells treated with dasatinib in combination with established and novel therapeutic agents. ...	116
<b>Table 6.1</b>	Current phase I/II clinical trials of dasatinib in relapsed/refractory CLL.....	228

## List of Figures

<b>Figure 1.1</b>	Overview of B lymphocyte development .....	2
<b>Figure 1.2</b>	Structure of the B cell antigen receptor .....	3
<b>Figure 1.3</b>	The germinal centre reaction .....	5
<b>Figure 1.4</b>	Proposed model of antigen stimulation in the pathogenesis of CLL, adapted from the review by Chiorazzi (17) .....	23
<b>Figure 1.5</b>	B cell cytoplasmic spreading and contraction response on antigen stimulation .....	24
<b>Figure 1.6</b>	An overview of the B cell antigen receptor signalling pathway .....	26
<b>Figure 1.7</b>	Regulation of MAPK activation.....	27
<b>Figure 1.8</b>	An outline of the PI-3K/Akt signalling pathway.....	28
<b>Figure 1.9</b>	Diagram of the regulation of Lyn kinase activity.....	35
<b>Figure 1.10</b>	Key interactions between CLL cells and the microenvironment.....	38
<b>Figure 1.11</b>	CXCR4 signalling pathway.....	40
<b>Figure 1.12</b>	Overview of CD40 signalling .....	46
<b>Figure 1.13</b>	Overview of IL-4 signalling .....	47
<b>Figure 1.14</b>	The chemical structure of dasatinib .....	49
<b>Figure 1.15</b>	Outline of intrinsic and extrinsic apoptotic pathways.....	51
<b>Figure 2.1</b>	FCM plot of a representative CLL patient sample following Rosettesep™ purification .....	88
<b>Figure 2.2</b>	Enrichment of B lymphocytes from buffy coat using MACS sorting. ....	89
<b>Figure 2.3</b>	Confirmation of CD154 expression on CD154L cells by FCM .....	90
<b>Figure 2.4</b>	Gating strategy used to determine percentage of CLL cells containing activated caspase 3. ....	91
<b>Figure 2.5</b>	Example of gating strategy used to assess apoptosis in CLL cells stained with Annexin V and Viaprobe. ....	92
<b>Figure 2.6</b>	Pseudoemperipolexis of CLL cells beneath M2-10B4 stromal cells .....	93
<b>Figure 2.7</b>	Gating strategy used to perform CLL cell counts using CountBright™ beads .....	94
<b>Figure 2.8</b>	Gating strategy used to assess CLL proliferation using CFSE. ....	95
<b>Figure 2.9</b>	Example of the determination of calcium flux following BCR crosslinking in Ramos B cells by fluorescence spectrophotometry. ....	96

<b>Figure 2.10</b>	Illustration of the constant ratio combination design of drug synergy experiments .....	97
<b>Figure 2.11</b>	Classical isobologram and illustration of synergistic or antagonistic effects. ....	98
<b>Figure 3.1</b>	Lyn and c-Abl are over-expressed in CLL cells compared to normal B lymphocytes.....	117
<b>Figure 3.2</b>	The Src kinase inhibitor PP2 induces apoptosis of CLL cells .....	118
<b>Figure 3.3</b>	Comparison of imatinib, PP2, and dasatinib on CLL cell viability.	119
<b>Figure 3.4</b>	Time course of apoptosis induced by dasatinib in CLL cells.....	120
<b>Figure 3.5</b>	Effect of increasing concentrations of dasatinib on CLL cell viability following 48 hr continuous treatment.....	121
<b>Figure 3.6</b>	Effect of 48 hr treatment with 100 nM dasatinib on individual CLL sample viability. ....	122
<b>Figure 3.7</b>	Correlation of dasatinib response to prognostic factors. ....	123
<b>Figure 3.8A</b>	Dasatinib induces loss of MMP and leads to caspase 3 activation. ....	124
<b>Figure 3.8B</b>	Annexin V positivity correlates with loss of MMP and caspase activation following dasatinib treatment.....	125
<b>Figure 3.9</b>	Dasatinib-induced apoptosis is caspase-dependent. ....	126
<b>Figure 3.10</b>	Pro-caspase 8 and pro-caspase 9 are cleaved during dasatinib-induced apoptosis.....	127
<b>Figure 3.11</b>	Caspase cleavage occurs within hours of dasatinib treatment. ...	128
<b>Figure 3.12</b>	Comparison of fixed-time versus continuous dasatinib exposure on CLL cell viability.....	129
<b>Figure 3.13</b>	Dasatinib induces a degree of apoptosis in normal B lymphocytes. ....	130
<b>Figure 3.14</b>	Bcl-2 inhibitors induce apoptosis of CLL cells <i>in vitro</i> . ....	131
<b>Figure 3.15</b>	17-DMAG induces apoptosis of CLL cells <i>in vitro</i> . ....	132
<b>Figure 3.16</b>	An example of graphs generated by CalcuSyn software during analysis of dasatinib combination experiments. ....	133
<b>Figure 3.17</b>	EC <sub>50</sub> combination indices for dasatinib in combination with established and novel agents.....	134
<b>Figure 4.1</b>	Dasatinib inhibits Syk <sup>Y348</sup> phosphorylation in unstimulated and BCR-stimulated CLL cells. ....	158
<b>Figure 4.2</b>	Relationship between Syk <sup>Y348</sup> phosphorylation and apoptosis induced by dasatinib. ....	159

<b>Figure 4.3</b>	Inhibition of Lyn <sup>Y396</sup> and Syk <sup>Y352</sup> phosphorylation on 30 min treatment with dasatinib. ....	160
<b>Figure 4.4</b>	Correlation of levels of total and phosphorylated Syk and Lyn with dasatinib sensitivity. ....	161
<b>Figure 4.5</b>	Dasatinib inhibits calcium flux following BCR stimulation in CLL cells. ....	162
<b>Figure 4.6</b>	Effect of dasatinib on Akt and MAPK activation following BCR crosslinking. ....	163
<b>Figure 4.7</b>	Dasatinib inhibits actin reorganisation following BCR crosslinking. ....	164
<b>Figure 4.8</b>	Morphology of CLL cells stimulated with soluble and immobilised anti-IgM in the presence or absence of dasatinib. ...	165
<b>Figure 4.9</b>	Effect of dasatinib on viability of CLL cells on prolonged BCR stimulation <i>in vitro</i> . ....	166
<b>Figure 4.10</b>	Dasatinib inhibits upregulation of Mcl-1 on prolonged BCR stimulation. ....	167
<b>Figure 4.11</b>	Dasatinib inhibits down-regulation of CXCR4 expression following BCR stimulation. ....	168
<b>Figure 4.12</b>	Dasatinib inhibits Akt phosphorylation following SDF-1 stimulation of CLL cells <i>in vitro</i> . ....	169
<b>Figure 4.13</b>	Effect of dasatinib on actin polymerisation following SDF-1 stimulation of CLL cells. ....	170
<b>Figure 4.14</b>	Dasatinib inhibits chemotaxis of CLL cells towards SDF-1. ....	171
<b>Figure 4.15</b>	Analysis of SDF-1 RNA expression in the murine BM stromal cell lines M2-10B4 and NT-L. ....	172
<b>Figure 4.16</b>	Appearance of M2-10B4 stromal cell layers following 5 hr co-culture with CLL cells in the presence or absence of dasatinib. ...	173
<b>Figure 4.17</b>	Dasatinib inhibits pseudoemperipolesis of CLL cells under M2-10B4 cells. ....	174
<b>Figure 4.18</b>	The anti-apoptotic effect of SDF-1 is overcome by dasatinib. ....	175
<b>Figure 5.1</b>	CLL cells co-cultured with stromal cells are significantly less sensitive to dasatinib. ....	199
<b>Figure 5.2</b>	Dasatinib retains the ability to inhibit tyrosine phosphorylation in CLL cells in NT-L or 154L/IL-4 co-culture. ....	200
<b>Figure 5.3</b>	NT-L and 154L/IL-4 co-culture induces activation of MAPK and Akt, which is not inhibited by dasatinib. ....	201

<b>Figure 5.4</b>	PD98059 and LY294002 specifically inhibit ERK and Akt phosphorylation respectively in co-cultured CLL cells. ....	202
<b>Figure 5.5</b>	PD98059 and LY294002 resensitise CLL cells to dasatinib in NT-L, but not 154L/IL-4 co-culture. ....	203
<b>Figure 5.6A</b>	Effects of dasatinib on Bcl-2 family protein and survivin expression in CLL cells cultured in media alone, or NT-L or 154L/IL-4 co-culture. ....	204
<b>Figure 5.6B</b>	Densitometric analysis of Bcl-2 family protein expression in CLL cells cultured in media alone, NT-L, and 154L/IL-4 co-culture in the presence or absence of dasatinib.....	205
<b>Figure 5.7</b>	Effect of dasatinib on Bcl-2 family protein expression induced by sCD154 and IL-4, alone and in combination. ....	206
<b>Figure 5.8</b>	Effect of dasatinib on CLL cell proliferation in the 154L/IL-4 system. ....	207
<b>Figure 5.9</b>	Assessment of cell counts and percentage recovery of input cells in the 12 day 154L/IL-4 co-culture proliferation experiment. ....	208
<b>Figure 5.10</b>	Photographs of CLL cells following 12 days of co-culture in the 154L/IL-4 system with or without 100 nM dasatinib. ....	209
<b>Figure 5.11</b>	Comparison of the effect of dasatinib in combination with fludarabine or chlorambucil on CLL cells cultured in media or stromal co-culture systems. ....	210
<b>Figure 5.12</b>	Dasatinib retains the ability to sensitise CLL cells co-cultured with NT-L stromal cells to chlorambucil and fludarabine.....	211
<b>Figure 5.13</b>	Comparison of apoptosis induced by dasatinib in combination with Bcl-2 inhibitor I in CLL cells cultured in media alone or stromal co-culture.....	212
<b>Figure 5.14</b>	HSP90 expression is increased in co-cultured CLL cells.....	213
<b>Figure 5.15</b>	Comparison of apoptosis induced by dasatinib and 17-DMAG in CLL cells cultured in media or stromal co-culture. ....	214
<b>Figure 5.16</b>	Effects of dasatinib and 17-DMAG on viability of NT-L and 154L cells. ....	215
<b>Figure 5.17</b>	Effect of dasatinib and 17-DMAG, alone and in combination, on CLL cells stimulated with sCD154 and IL-4. ....	216
<b>Figure 5.18</b>	17-DMAG selectively inhibits p70 s6 kinase phosphorylation in CLL cells following sCD154 and IL-4 stimulation. ....	217

## List of Equations

<b>Equation 2.1</b>	Equation to determine cell number by FCM.....	71
<b>Equation 2.2</b>	Equation to calculate cell recovery.....	71
<b>Equation 2.3</b>	Equation to calculate calcium concentration .....	72
<b>Equation 2.4</b>	Equation to calculate the fraction affected for synergy experiments.....	78
<b>Equation 2.5</b>	Median effect equation.....	78
<b>Equation 2.6</b>	Logarithmic expression of the median effect equation used to construct median effect plots .....	79
<b>Equation 2.7</b>	Combination index equation.....	79

## Abbreviations

AID	activation-induced cytidine deaminase
ALL	acute lymphoblastic leukaemia
AML	acute myeloid leukaemia
Apaf-1	apoptosis protease activating factor-1
APC	allophycocyanin
APRIL	a proliferation-inducing ligand
ATM	ataxia telangiectasia mutated
ATP	adenosine triphosphate
BAFF	B cell activation factor
Bam32	B lymphocyte adaptor molecule of 32 kDa
BCA	bicinchoninic acid
BCMA	B-cell maturation antigen
BCR	B cell antigen receptor
Bcr/Abl	Breakpoint cluster region/Abl fusion tyrosine kinase
bFGF	basic fibroblast growth factor
BLNK	B cell linker protein
BM	bone marrow
BSA	bovine serum albumin
Btk	Bruton's tyrosine kinase
[Ca <sup>2+</sup> ]	calcium concentration
CARD	caspase recruitment domain
CD	cluster of differentiation
cdk	cyclin-dependent kinase
CDR3	complementarity determining region 3
CFSE	carboxyfluorescein diacetate succinimidyl ester
CI	combination index
CLL	chronic lymphocytic leukaemia
C <sub>max</sub>	maximum tolerated plasma concentration
CML	chronic myeloid leukaemia
CpG ODN	CpG oligodeoxynucleotides
CR	complete response
CREB	Ca <sup>2+</sup> /cAMP response element binding protein
CSR	class switch recombination
CT	cycle threshold

D	diversity
DAG	diacylglycerol
DLBCL	diffuse large B cell lymphoma
17-DMAG	17-desmethoxy-17-N,N-dimethylaminoethylamino-geldanamycin
DMEM	Dulbecco's Modified Eagle Medium
DMSO	dimethylsulphoxide
DNA	deoxyribonucleic acid
ELISA	enzyme-linked immunosorbent assay
EBMT	European group for bone marrow transplantation
EC <sub>50</sub>	half-maximal effect concentration
EDTA	ethylenediaminetetraacetic acid
ERK	extracellular signal-regulated kinase
FADD	Fas-associated death domain
FAK	focal adhesion kinase
FBS	fetal bovine serum
FC	fludarabine and cyclophosphamide
FCM	flow cytometry
FCR	fludarabine, cyclophosphamide, and rituximab
FDA	Food and Drug Administration
FDC	follicular dendritic cell
FISH	fluorescence in-situ hybridisation
FITC	fluorescein isothiocyanate
FSC	forward-scatter
GA	geldanamycin
GC	germinal centre
H	heavy
<sup>2</sup> H <sub>2</sub> O	deuterated water
HRP	horseradish peroxidase
HS1	haematopoietic lineage cell-specific protein-1
HSP90	heat shock protein 90 kDa
IC <sub>50</sub>	inhibitory concentration required to achieve a 50% reduction in cell viability
ICAM	intercellular adhesion molecule
IFN	interferon

Ig	immunoglobulin
IL	interleukin
I(1,4,5)P <sub>3</sub>	inositol triphosphate
IRS-1	insulin-receptor substrate 1
ITAM	immunoreceptor tyrosine-based activation motif
J	joining
JAK	Janus kinase
JNK	c-Jun N-terminal kinase
kb	kilobase
LDT	lymphocyte doubling time
LFA-1	Leukocyte Function-associated Antigen-1
L	light
LN	lymph node
LSCs	leukaemia stem cells
MAPK	mitogen activated protein kinase
MAPKK	MAPK kinase
MBL	monoclonal B cell lymphocytosis
MFI	mean fluorescence intensity
MHC	major histocompatibility complex
MMP-9	matrix metallo-protease 9
MNC	mononuclear cell
MRD	minimal residual disease
mTOR	mammalian target of rapamycin
MYHIIA	non-muscle myosin heavy chain IIA
MZ	marginal zone
NAL	N-acetyllactosamine
NCI-WG	National Cancer Institute-Working Group
NFAT	nuclear factor of activated T cells
NF-κB	nuclear factor kappa-light-chain enhancer of activated B cells
NLC	nurse-like cell
ORR	overall response rate
OS	overall survival
Par-4	prostate-apoptosis regulatory protein
PARP	poly ADP ribose polymerase

PBMC	peripheral blood mononuclear cells
PBS	phosphate buffered saline
PCR	polymerase chain reaction
PDGFR $\beta$	platelet-derived growth factor receptor $\beta$
PE	phycoerythrin
PFS	progression-free survival
PH	pleckstrin-homology
PHA	phytohaemagglutinin
PI	propidium iodide
PI-3K	phosphatidylinositol-3-kinase
PIP <sub>2</sub>	phosphatidylinositol-4,5-bisphosphate
PIP <sub>3</sub>	phosphatidylinositol-3,4,5-triphosphate
PKC	protein kinase C
PLC $\gamma$ 2	phospholipase C $\gamma$ 2
PP2A	protein phosphatase 2A
PR	partial remission
PTPROt	protein tyrosine phosphatase receptor-type O truncated
PVDF	polyvinylidene fluoride
RT	room temperature
qRT-PCR	quantitative reverse transcription PCR
RAG	recombination activating gene
RIC	reduced intensity conditioning
RCN	relative cell number
RGS1	regulator of G protein signalling 1
RNA	ribonucleic acid
sCD154	recombinant soluble CD154
SDF-1	stromal cell derived factor-1
SDS-PAGE	Sodium dodecyl sulphate-polyacrylamide gel electrophoresis
SEM	standard error of the means
SH	Src homology
SHM	somatic hypermutation
SHP-1	SH2-domain-containing tyrosine phosphatase
siRNA	short interfering RNA

SOCS3	suppressor of cytokine signalling 3
SOS	son of sevenless
SpA	staphylococcus aureus protein A
SSC	side-scatter
STAT	Signal Transducer and Activator of Transcription
Syk	spleen tyrosine kinase
TACI	transmembrane activator and calcium modulator and cyclophilin ligand-interactor
tBid	truncated Bid
TBS	Tris buffered saline
Tcl-1	T-cell leukaemia 1
TCR	T cell receptor
Th	T helper
Thr	threonine
TKI	tyrosine kinase inhibitor
TLR9	Toll-like receptor 9
TLS	tumour lysis syndrome
TMRM	tetramethylrhodaminemethylester
TNF	tumour necrosis factor
TRAF	TNF receptor-associated factor protein
TRAIL	TNF-related apoptosis-inducing ligand
TSP-1	thrombospondin 1
Tyr	tyrosine
V	variable
VCAM-1	vascular cell adhesion molecule-1
VEGF	vascular endothelial growth factor
VLA-4	Very Late Antigen-4
XIAP	X-linked inhibitor of apoptosis protein
ZAP-70	zeta-chain-associated protein kinase 70 kDa
Z-VAD-fmk	Z-Val-Ala-DL-Asp(OMe)-fluoromethylketone

**Chapter 1:**  
**Introduction**

## 1.1 B lymphocyte development and function

### 1.1.1 Overview of B lymphocyte development

B lymphocytes are key cells of the adaptive immune system, with the main role of mature B lymphocytes to recognise pathogens via the B cell antigen receptor (BCR). Following recognition, B lymphocytes are also key effector cells in the immune response, both by producing specific antibodies, and in activating cognate CD4<sup>+</sup> T lymphocytes. A subset of B cells also retains immunological memory, in order to react to re-infection. At all stages of life, B cells require strict control in order to prevent the development of autoimmunity and malignancy.

B lymphocytes develop from pluripotent haematopoietic stem cells, and development is governed by the successful formation of a unique cell surface antigen receptor through the recombination of variable (V), diversity (D), and joining (J) genes in the immunoglobulin (Ig) loci (1). The key stages of B lymphocyte development, which occur within the bone marrow (BM) and peripheral lymphoid organs, are illustrated in Figure 1.1, and described below.

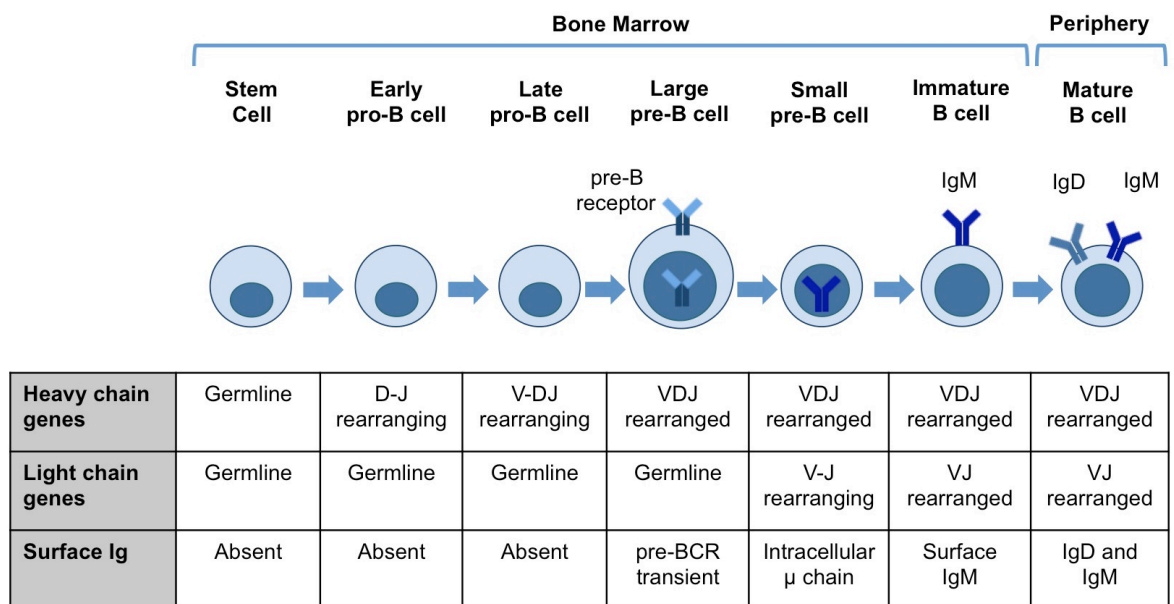


**Figure 1.1 Overview of B lymphocyte development**

Adapted from Janeway *et al.* (1)

During the early pro-B cell stage, transcription factors such as E2A and EBF regulate the expression of the recombination-activating gene-1 (RAG-1) and RAG-2, which form part of the enzymatic complex responsible for V(D)J recombination. The Ig heavy chain gene recombines first, and D to J<sub>H</sub> recombination marks the

transition to the late pro-B stage. Progression to the pre-B cell stage is dependent upon successful  $V_H$  to  $DJ_H$  recombination. At this stage, terminal deoxynucleotidyl transferase inserts additional nucleotides between the rearranged gene segments, to enhance the diversity of the resulting Ig  $\mu$  heavy chain. The heavy chain associates with invariant surrogate light chain proteins to form the pre-BCR. Signalling through the pre-BCR is essential for survival and development past this stage; pre-B cells with non-functional pre-BCRs are deleted by apoptosis. On successful pre-BCR signalling, a process termed allelic exclusion prevents further Ig heavy chain recombination, pre-B cells then proliferate and rearrange Ig light chain genes. On successful  $V_L$  to  $J_L$  recombination, surface IgM is expressed, and the B cell termed an immature B lymphocyte (1).

The BCR comprises membrane-associated Ig heavy and light chains non-covalently associated with a heterodimer of Ig $\alpha$  and Ig $\beta$  proteins (2), and is shown diagrammatically in Figure 1.2. The Ig $\alpha$  and Ig $\beta$  chains contain immunoreceptor tyrosine activation motifs (ITAMs), which are essential for signal transduction during B cell development and in response to antigenic stimulation of mature B cells (3). The BCR signal transduction pathway is described in detail in Section 1.5.

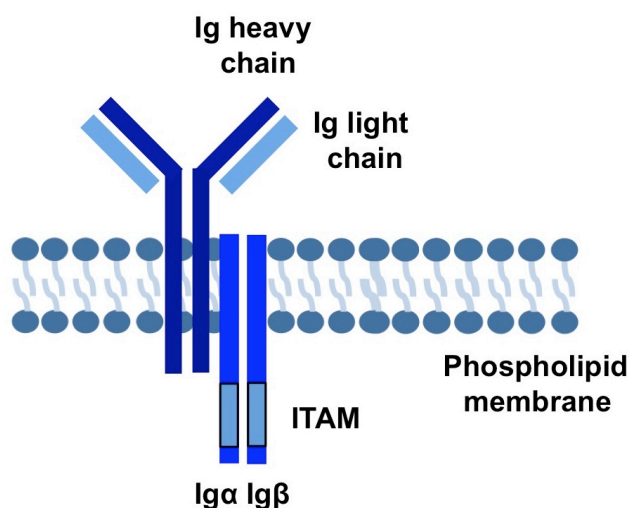


**Figure 1.2 Structure of the B cell antigen receptor**

Prior to egress of immature B lymphocytes from the BM, assessment of self-reactivity occurs. There are three main fates for B cells which are able to generate a BCR signal on interaction with self antigen; elimination by apoptosis, alteration of the BCR to change reactivity (receptor editing), or survival with inactivation of BCR reactivity (anergy) (4). Should developing B cells survive these hurdles they are

released into the circulation as mature B lymphocytes, which can express both surface IgM and IgD.

### **1.1.2 The humoral immune response**

The humoral immune response refers to the eradication of extracellular pathogens by the production of antibodies by activated B lymphocytes which have differentiated to plasma cells. In the majority of instances, plasma cell differentiation requires a process of interaction of activated B and T lymphocytes that recognise the same antigen. On antigen recognition by the BCR, antigen is internalised, processed, and presented on the surface of the B cell associated with major histocompatibility complex (MHC) class II (1). In response to interaction with antigen-MHC II complexes, antigen-specific CD4<sup>+</sup> 'helper' T lymphocytes secrete cytokines that promote the proliferation and differentiation of B cells towards antibody-secreting plasma cells. A limited range of antigens, including bacterial polysaccharides, may activate B cells without T cell co-stimulation, termed T-independent antigens (1). However, in most cases, B and T lymphocyte interaction occurs within specialised secondary lymphoid tissue, and leads to a germinal centre (GC) reaction (5).

#### **1.1.2.1 The germinal centre reaction**

Initial antigen-specific B-T lymphocyte interaction occurs at the margin between the T cell zone and B cell follicle within lymph nodes (LN) (6). Although a few activated B cells differentiate into plasma cells in the primary immune follicle, the majority of antigen-specific B cells form a GC, in which the processes of class switch recombination (CSR), somatic hypermutation (SHM), and affinity maturation occur in order to generate plasma cells which produce antibody with increased ability to eradicate the invading pathogen, and produce long-lived memory B cells (5).

Activated B lymphocytes migrate along chemokine gradients towards areas of the LN rich in T lymphocytes and follicular dendritic cells (FDCs) (7). FDCs can immobilise immune complexes, and are efficient antigen presenting cells (7).

Activated B lymphocytes up-regulate MHC class II and compete for interaction with cognate CD4<sup>+</sup> T cells which provide co-stimulatory signals. Signalling through CD40 expressed on the activated B cell membrane induced by interaction with the CD40-ligand (CD154) expressed on activated CD4<sup>+</sup> T cells is essential for GC function and memory B cell genesis (8). Within a few days, a classical GC

becomes evident by histology, comprising a light zone, rich in FDCs, and a dark zone, filled with densely packed proliferating B cells, termed centroblasts (5). A schematic representation of the GC is shown in Figure 1.3.

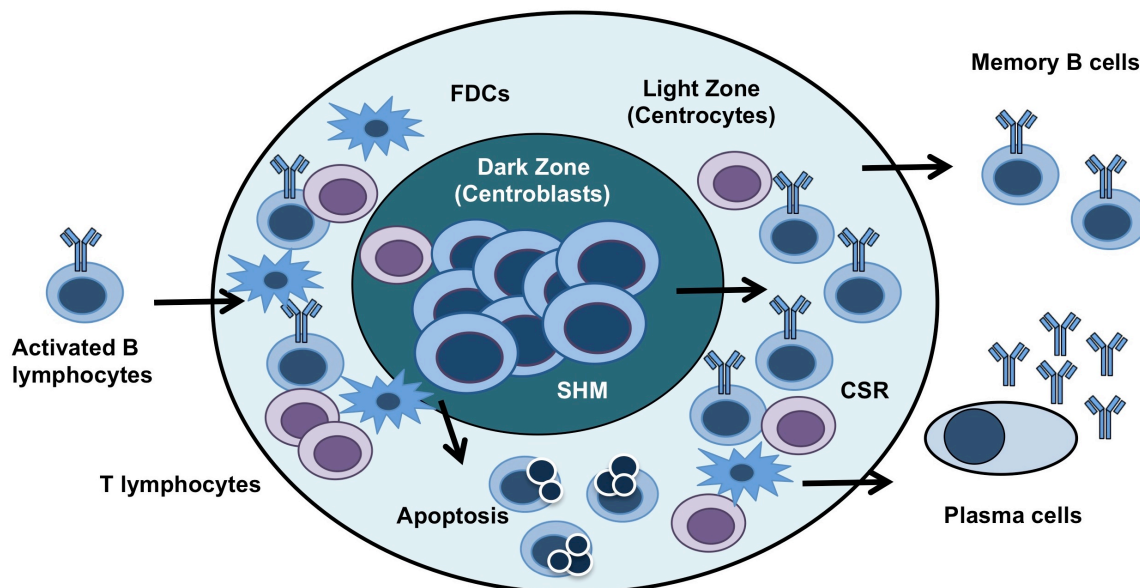


**Figure 1.3 The germinal centre reaction**

Fully activated B cells in the light zone migrate towards the chemokine stromal-cell derived factor-1 (SDF-1; CXCL12) expressed by stromal cells within the dark zone, which signals through the receptor CXCR4 expressed by B lymphocytes (9). Within the dark zone, in addition to intense proliferation, SHM occurs, as a result of the enzymatic action of activation-induced cytidine deaminase (AID) (10). Although debated, current evidence suggests AID acts directly on DNA, specifically deaminating deoxycytidine residues within IgV<sub>H</sub> genes, which trigger DNA repair mechanisms that introduce single nucleotide substitutions (11) at a rate of around  $10^{-3}$  per base pair per generation (12). Centroblasts tolerate this significant amount of DNA mutation in part due to Bcl-6-mediated suppression of p53-mediated DNA damage response pathways (13). Following proliferation and SHM, the B cells are termed centrocytes. Centrocytes are believed to down-regulate CXCR4, and in turn become more sensitive to the attraction of the chemokine CXCL13 in the light zone due to continued expression of the CXCL13 receptor CXCR5 on the B cell surface (9). Within the light zone, CSR occurs, again under the control of AID. During CSR DNA double-strand breaks are introduced, which enable the unique VDJ region to associate with a different class

of Ig constant gene, changing the Ig isotype from IgM to IgG, IgA, or IgE (10). The function of the centrocyte BCR is stringently tested during the process of affinity maturation. GC B cells are primed to die by apoptosis unless they are successful in again securing T cell co-stimulation delivered by CD154, the ligand for CD40 expressed on the B cell surface. The intense ongoing B cell competition for T cell support ensures that only centrocytes bearing a BCR with high specificity for antigen differentiate into antibody-secreting plasma cells, while the majority of centrocytes are lost by apoptosis (8). Given the significant level of DNA editing and proliferation that occurs during the GC reaction, it is easy to appreciate that a failure of selection and regulation may lead to both autoimmunity and malignancy. Indeed, many B cell lymphoproliferative disorders are believed to arise as the B cell transits the GC (14). In follicular lymphoma, the vast majority of cases are characterised by translocation of the anti-apoptotic protein Bcl-2 to the IgH gene locus t(14;18)(q32;q21) (15). Although the malignant lymphocytes in chronic lymphocytic leukaemia (CLL) also over-express Bcl-2, such translocations involving Ig genes are exceptionally rare (16). Evidence to suggest the normal counterpart of the CLL cell is presented in Section 1.4.

## **1.2 Chronic Lymphocytic Leukaemia**

### **1.2.1 Epidemiology and diagnosis of CLL**

CLL is a malignant B cell lymphoproliferative disorder characterised by variable accumulation of mature CD5<sup>+</sup> lymphocytes within the blood, BM, and LN (17). CLL is the most common adult leukaemia in the western world, with an incidence of 2-6 per 100,000 individuals per year. There is a male preponderance for CLL, with a male:female ratio of 1.5-2:2, and a mean age of diagnosis of 65 years (18). Although predominantly a disease of the elderly, a third of patients are diagnosed before the age of 55 (19). Unlike other B cell lymphoproliferative disorders, there is strong evidence of genetic predisposition to CLL. Whilst common in western countries, CLL is much less frequent in Asian countries, and exceptionally rare in Japan (20). In addition, familial CLL occurs in around 5% of cases, with evidence of anticipation and aggressive disease in successive generations (21).

The diagnosis of CLL requires the identification of at least  $5 \times 10^9/L$  clonal B-lymphocytes in the peripheral blood, present for at least 3 months, and demonstration of a characteristic immunophenotype by flow cytometry (FCM) (22). CLL cells co-express surface CD5, CD19, and CD23, while expression of CD20,

CD79b, and surface Ig is weak. A scoring system has been developed (Table 1.1), which has a specificity of 96.8% for the diagnosis of CLL in patients scoring 3-5 points (23). Morphologically, the malignant lymphocytes in CLL resemble mature small lymphocytes, however frequently demonstrate membrane fragility which results in the generation of 'smudge cells' during blood film preparation (20).

Marker	Expression	Score	Expression	Score
Surface Ig	weak	1	mod/strong	0
CD5	positive	1	negative	0
CD23	positive	1	negative	0
FMC7	negative	1	positive	0
CD79b	weak	1	strong	0

**Table 1.1 Immunophenotypic scoring system for CLL (23)**

With the availability of FCM, it has been increasingly recognised that clonal B cell populations with a CLL phenotype are present at levels below  $5 \times 10^9/L$  in around 3% of unselected populations (24). This led to the development of a new diagnostic entity, termed monoclonal B cell lymphocytosis (MBL) (25), and the suggestion that, akin to multiple myeloma, there may be a precursor disorder to CLL. MBL is sub-classified as to whether a typical CLL phenotype is present or not. In longitudinal studies, individuals with CLL-type MBL have been shown to have a low rate of progression to CLL, with a likelihood of requiring CLL therapy of 1-2% per year, however additional oncogenic events are believed to be required for progression (26).

### **1.2.2 Clinical features of CLL**

With the routine availability of diagnostic FCM, CLL is now frequently diagnosed incidentally on blood samples analysed for unrelated reasons. Although CLL may lead to significant peripheral blood lymphocytosis, this rarely directly causes significant organ dysfunction. Symptoms are caused by the accumulation of malignant lymphocytes in LN and BM, leading to painful lymphadenopathy and BM failure. Patients with LN and BM involvement and minimal circulating CLL cells are considered to have the related disorder of small lymphocytic lymphoma (22). CLL is also particularly characterised by pathologies that occur as a result of the secondary immune dysregulation induced by the malignant clone. Over 65% of

patients develop hypogammaglobulinaemia during the course of the disease (27), leading to recurrent infections which are the most common cause of death in CLL (20). In addition, autoimmune disorders, almost exclusively directed towards the haematopoietic system, are common. The incidence of autoimmune haemolytic anaemia has been reported as 10-20%, immune thrombocytopenia occurs in around 2% of patients, and pure red cell aplasia has been reported (28). Importantly, autoantibodies in CLL have been demonstrated to be polyclonal, and of different isotype to the CLL clone, demonstrating that autoimmunity occurs due to a breach in self-tolerance in the residual normal immune system, rather than being directly produced by CLL cells (29). Immune incompetence is also believed to underlie the significantly increased risk of other malignancies in patients with CLL (30).

### 1.2.3 Prognostic factors in CLL

#### 1.2.3.1 Clinical prognostic factors

Over thirty years ago, two clinical staging systems (Rai and Binet) based on measures of the extent of LN and BM involvement with CLL were described (31, 32). The Binet staging system is detailed in Table 1.2. These simply assessable clinical staging systems remain central to guiding treatment decisions in CLL.

Stage	Clinical Features	Median Survival
A	No anaemia, no thrombocytopenia Less than 3 lymphoid regions enlarged	14 years
B	No anaemia, no thrombocytopenia 3 or more lymphoid areas enlarged	5 years
C	Anaemia (Hb < 10 g/dl) Thrombocytopenia (platelet count < 100 x 10 <sup>9</sup> /L)	2 years

**Table 1.2 Binet clinical staging system for CLL**

The lymphocyte doubling time (LDT; projected or actual length of time for peripheral blood lymphocyte count to double) is another established clinical prognostic factor (33), still used to guide treatment decisions. Although the pattern of BM infiltration has been reported to have prognostic significance (34), this invasive measure has been rendered obsolete with the identification of powerful biological prognostic factors.

### **1.2.3.2 IgV<sub>H</sub> mutation status**

Just over a decade ago, it was identified that CLL cells in around half of all patients show evidence of SHM in their IgV<sub>H</sub> genes (mutated CLL) whilst the rest use IgV<sub>H</sub> genes with a near-germline sequence (unmutated CLL) (35). Several groups subsequently reported that patients with unmutated IgV<sub>H</sub> genes had a significantly poorer prognosis than those with evidence of mutated IgV<sub>H</sub> genes (36-38). Most groups used a cut-off of 2% variance from germline sequence as a threshold for considering IgV<sub>H</sub> genes to be mutated. In one study that followed the course of stage A patients, the median survival for those with unmutated CLL was 95 months, compared with 293 months for those with mutated CLL (38).

### **1.2.3.3 ZAP-70**

Assessment of IgV<sub>H</sub> mutation analysis requires access to DNA sequencing technology, not available in most clinical centres. Much attention was thus focussed on identifying surrogate markers for IgV<sub>H</sub> status that may be assessed in routine diagnostic laboratories. The most successful candidate that has emerged is zeta-chain-associated protein kinase 70 (ZAP-70), which has been reported to correlate with U-CLL in around 93% of cases (39, 40). ZAP-70 is a non-receptor tyrosine kinase that has a key role in propagating signals downstream of the T cell antigen receptor (TCR). Briefly, following TCR engagement ZAP-70 associates with phosphorylated ITAM sequences in the  $\zeta$ -chains of the TCR, and in turn recruits and activates key downstream signalling kinases (41). Although not normally expressed in naïve mature B lymphocytes, ZAP-70 is transiently expressed during B cell development at the pro-B to pre-B cell transition stage (42), and has been shown to be expressed by activated mature tonsillar B lymphocytes (43). ZAP-70 can be measured by numerous methods including immunohistochemistry and FCM (39, 40), and optimised FCM protocols have been developed in order to standardise assessment (44, 45). ZAP-70 expression largely remains stable over time (39), strengthening its utility as a prognostic marker. In addition, ZAP-70 expression has recently been established as an independent negative prognostic indicator, regardless of Ig mutational status (46), and is now a standard part of the clinical prognostic assessment of CLL patients.

#### 1.2.3.4 CD38

Another recently identified biological prognostic marker in CLL is surface expression of CD38, which was again initially investigated as a surrogate marker for IgV<sub>H</sub> mutational status. An initial report found that CD38 expression by over 30% of the CLL clone to be strongly predictive of unmutated IgV<sub>H</sub> CLL (37). Subsequent studies failed to reproduce the correlation between CD38 expression and IgV<sub>H</sub> mutational status (47, 48); rather, CD38 has also been confirmed as an independent poor prognostic marker, unrelated to IgV<sub>H</sub> mutational status (47, 49, 50). Recent studies have confirmed that combined analysis of IgV<sub>H</sub> mutations, CD38, and ZAP-70 expression together have greater prognostic power than each alone, and provided evidence that discordant results in analysis of these prognostic markers explain at least part of the clinical heterogeneity of CLL (51, 52).

#### 1.2.3.5 Cytogenetic abnormalities

The low mitotic rate of peripheral blood CLL cells is a hindrance for traditional cytogenetic techniques. Despite this, cytogenetic abnormalities were detected by conventional methods in 55% of patients in a large study, with the most common abnormalities detected being trisomy of chromosome 12 and deletion of chromosome 13q (53). With the advent of techniques not reliant on cell cycle entry, in particular, interphase fluorescence in-situ hybridisation (FISH), abnormalities have been detected in over 80% of all cases (54, 55), as shown in Table 1.3.

Abnormality	Gene(s) affected (if known)	% of Patients	Median Survival (months)
13q deletion	<i>miR15a, miR16-1</i>	55	133
11q deletion	<i>ATM</i>	18	79
12q trisomy		16	114
17p deletion	<i>p53</i>	7	32
6q deletion		6	n/a
Others		12	n/a
Normal karyotype		18	111

**Table 1.3 Cytogenetic abnormalities identified in CLL (55)**

The most frequently identified recurrent abnormality is a deletion of chromosome 13q14, detected in over 50% of all cases (55), and isolated 13q14 deletion is associated with slowly progressive disease (53). Detailed analysis of the deleted region on chromosome 13q identified a 30 kb commonly deleted segment of DNA, present in 68% of patients (56). The conserved region contains DNA encoding two micro-RNAs, miR15 and miR16, suggesting that dysregulation of miRNA function may be involved in the pathogenesis of CLL in these patients (56). Supporting this hypothesis, miR15a and miR16-1 have been demonstrated to negatively regulate Bcl-2 expression, and an inverse correlation between miR15a and miR16-1 expression and Bcl-2 expression has been demonstrated in primary CLL cells (57). Very recently, deletion of this region, including the genes encoding *DLEU2*, *miR-15a*, and *miR16-1*, in mice has been shown to result in a clonal B-lymphoproliferative disorder (58), strengthening the evidence that these genes are involved in the pathogenesis of CLL.

The most adverse cytogenetic abnormality is mono-allelic deletion of chromosome 17p13, which includes the *p53* gene locus (55). In the vast majority of cases with 17p13 deletion, p53 function is lost through inactivating mutations of the remaining allele (59-61). These studies also identified single p53 gene mutations, in the absence of 17p deletion in up to an additional 5% of patients, which also predicted for an adverse prognosis (60). The commonly deleted region on chromosome 11q23 spans the *ataxia telangiectasia mutated (ATM)* gene locus (62). ATM functions in the DNA damage response pathway, activating p53 (63), therefore deletion can lead indirectly to p53 dysfunction. Mutation of *ATM* has also been reported in CLL at a similar frequency to deletions (64). 11q23 deletion is associated with bulky lymphadenopathy and rapid progression (65). Deletion of chromosome 6q21 and trisomy of chromosome 12q13 have both been reported to be associated with atypical lymphocyte morphology, high white cell counts, progressive disease, and an intermediate prognosis (66-68).

#### **1.2.3.6 Other biological prognostic indicators**

A number of additional adverse prognostic indicators have been reported in the literature, including finding over 10% of prolymphocytes in the peripheral blood, raised levels of  $\beta$ 2-microglobulin, serum thymidine kinase, or soluble CD23 in serum (20), however these have also largely been superseded by the assessment of the new biological indicators.

## 1.2.4 Treatment of CLL

### 1.2.4.1 A history of developments in CLL therapy

As CLL is predominantly a disease of the elderly, with an extremely heterogeneous clinical course, many patients may never develop symptoms of, or require treatment for their CLL. However, the majority of patients diagnosed below sixty years of age will require treatment, and many will die of CLL-related causes (69). With progressive improvements in chemotherapy, the aim of treatment has changed for most from palliating symptoms of painful lymphadenopathy towards aiming to produce durable complete remissions.

Historical studies have addressed the question of treating stage A patients at diagnosis. Several groups demonstrated that treatment with chlorambucil at diagnosis did not improve overall survival (OS) compared to treatment on progression to stage B or C disease (70-72). These studies form the basis for the current recommendation in the 2008 IWCLL guidelines that stage A patients may be managed by observation until clinical progression (22). A current area of intense debate and research centres upon how to incorporate biological prognostic factors into treatment decisions in this patient group, in particular patients with adverse cytogenetic features such as 17p deletion or mutation. Current IWCLL indications for treatment are listed in Table 1.3.

Indication	
1	Evidence of progressive BM failure, worsening anaemia or thrombocytopenia.
2	Massive (>6 cm below costal margin) progressive splenomegaly.
3	Massive lymphadenopathy (>10 cm) or progressive symptomatic lymphadenopathy.
4	Progressive lymphocytosis with an increase of > 50% in 2 months, or doubling time < 6 months.
5	Autoimmune anaemia and or thrombocytopenia poorly responsive to immunosuppressive therapy.
6	One or more constitutional symptoms: Unintentional weight loss > 10% in 6 months Significant fatigue Unexplained fevers of over 38°C for over 3 weeks Night sweats for over 1 month without evidence of infection

**Table 1.4 2008 IWCLL guideline indications for treatment of CLL**

Historically, the sensitivity of CLL cells to steroid therapy has been recognised (73), however durable responses are not achieved, and frequent infectious complications limit the benefit of this approach. For several decades, treatment with alkylating agents such as chlorambucil was the gold standard approach to treatment. Although overall response rates (ORR) of over 70% were typically seen, complete response (CR), defined by the National Cancer Institute-Working Group (NCI-WG) as eradication of clonal lymphocytes from blood, with normalisation of physical examination and blood counts, three months from the end of therapy (22), was very rarely achieved. During the 1970's and 1980's several combination chemotherapy regimes including COP (cyclophosphamide, vincristine, and prednisolone), chlorambucil and epirubicin, CHOP (cyclophosphamide, doxorubicin, vincristine, and prednisolone), were compared to chlorambucil alone, however none were found superior (72). The 1990's heralded a turning point in the treatment of CLL, with the recognition that purine analogues such as fludarabine were highly effective against CLL (74). A large randomised controlled trial of single-agent fludarabine or chlorambucil in previously untreated CLL patients demonstrated the superiority of fludarabine in first-line treatment, with CR rates of 20% compared to 4% for fludarabine and chlorambucil respectively (75). However, as chlorambucil causes less net myelo- and immuno-suppression than fludarabine, it remains a recommended first-line agent in elderly patients with comorbidities, who may benefit greatly from symptomatic control, and would be at great risk of infection with purine analogues (76).

With the recognition that purine analogues may achieve durable remissions, research focussed on assessing purine analogue combination regimens to improve CR rates. Phase II trials of fludarabine in combination with the alkylating agent cyclophosphamide (FC) suggested a higher CR rate than historical controls treated with fludarabine alone (77, 78). The superiority of FC was confirmed in the pivotal UK CLL4 trial, a phase III randomised controlled trial that compared FC to either single agent chlorambucil or fludarabine, with CR rates of 38%, 15%, and 7% respectively (79). This trial also reported a significantly increased progression-free survival (PFS) with FC compared to single agent therapy, leading to the recommendation of FC as first-line therapy for fit patients.

Combination regimens combining FC with additional cytotoxic agents have been performed in patients with relapsed CLL. FC in combination with mitoxantrone produced CR in 50% of patients, however with appreciable toxicity (80).

Undoubtedly the most significant advance in combination therapy in this setting has been the development of chemo-immunotherapy. Rituximab is a chimaeric monoclonal antibody with specificity to the CD20 antigen expressed on the surface of mature B cells (81). Initial trials of single-agent rituximab in relapsed CLL were disappointing, with ORR in the region of 40%, suggested to be due to the relatively low CD20 expression on the surface of CLL cells, and raised soluble CD20 in the plasma of CLL patients (82-84). However, studies of rituximab in combination with fludarabine were more promising (22), and a non-randomised trial of rituximab in combination with FC (FCR) reported an ORR of 73% and CR rate of 25% in previously treated patients (85). Given these data in the relapse setting, FCR was assessed in untreated CLL patients requiring therapy, and reported to achieve CR in 70% of patients (86). The German CLL Study Group CLL8 trial compared FC with FCR in a randomised study, and reported a significantly higher CR rate with FCR (44.5%) than with FC (22.9%), leading to FCR replacing FC as the recommended initial treatment in biologically fit patients (76).

The monoclonal antibody alemtuzumab (Campath-1H) is a fully humanised monoclonal antibody with specificity for CD52, an antigen expressed on the surface of both B and T lymphocytes (76). Alemtuzumab has been demonstrated to induce responses in pre-treated patients, including those with p53 dysfunction, in 30-50% of patients, and has also been approved by the US Food and Drug Administration (FDA) for front-line therapy of CLL (76).

With advances in molecular haematology, techniques to assess low levels of minimal residual disease (MRD) have been assessed in acute leukaemias and chronic myeloid leukaemia (CML), and found to predict for relapse and OS (87-89). With increasingly intensive chemo-immunotherapy regimes achieving higher CR rates in CLL, research focussed on the value of monitoring MRD in CLL. Sensitive methods to monitor MRD in CLL using PCR or multi-parameter FCM have been developed, the latter has a sensitivity of 1 in  $10^4$ - $10^5$  cells (90). Studies in relapsed CLL patients treated with FCM or alemtuzumab identified an improvement in OS in those reaching an MRD negative remission (80, 91). Alemtuzumab has been investigated as an agent to eradicate MRD following conventional chemotherapy, however has been complicated by significant infective toxicity in some studies (76). The role of MRD monitoring in guiding treatment decisions in CLL remains a subject of current clinical trials.

Allogeneic stem cell transplantation remains the only curative option for CLL, however due to the epidemiology of the disease, the associated transplant-related mortality outweighs benefit in the large majority. Current European Group for Bone Marrow Transplantation (EBMT) guidelines currently recommend allogeneic transplantation in a limited number of settings, specifically in young patients either with 17p deletion, or those refractory to purine analogue containing therapy (92). As early trials of reduced-intensity conditioning (RIC) allogeneic transplantation provided evidence to support a graft-versus-leukaemia effect in CLL (93), RIC transplantation has received more attention, and can extend a transplantation option to an older patient population. Allogeneic transplantation carries significant long-term risks of complications such as graft-versus host disease, and the overall benefit of allotransplantation is still under active investigation in randomised trials (93). Autologous transplantation in CLL has been extensively studied over the last two decades, however significant relapse rates, and also frequent late complications including secondary myelodysplasia, have led to the wide acceptance that autologous transplantation has no place in routine clinical practice (94).

#### **1.2.4.2 Limitations of current therapy**

A major clinical problem in the management of CLL is the treatment of patients who are refractory to purine analogues, largely due to p53 dysfunction (95). This group of patients has a median survival in the region of 12 months (96, 97). As fludarabine induces a p53-dependent gene-expression response in CLL cells (98), there is concern that purine analogues may select for p53 dysfunctional clones. Recent studies confirming acquired p53 dysfunction following treatment suggest this is a substantiated concern (60).

The only conventional agent with noted activity in p53 dysfunctional patients is high-dose methylprednisolone, which produces responses in around 50% of patients, but is complicated by a significant rate of infection (99). As a single agent in purine analogue refractory patients, alemtuzumab induces responses in 30-40% of patients, however the median time to progression in these studies was only 4-8 months (100, 101). Alemtuzumab is markedly less efficacious in patients with significant lymphadenopathy (over 5 cm) (91), therefore often requires initial steroid therapy to reduce initial LN bulk. There is some evidence that fludarabine used in chemoimmunotherapy combinations with rituximab such as FCR with or

without mitoxantrone may induce responses in patients refractory to fludarabine alone (102), again accepting significant risks of toxicity. As more patients are receiving chemo-immunotherapy with FCR as initial treatment, an emerging problem will be the lack of additional second-line agents for those who relapse early following treatment.

Other patient groups in which fludarabine is contra-indicated include those with a history of autoimmune haemolytic anaemia and the elderly with co-morbidities. In summary, although CLL therapy has evolved significantly over the decades, the leukaemia remains incurable, and clinical management problems remain. Recent advances in our knowledge of the biology of CLL have however revealed novel therapeutic targets, investigation of which forms the basis for this thesis.

### **1.3 Overview of CLL biology**

#### **1.3.1 Historical understanding of CLL biology**

CLL has been historically considered a leukaemia characterised by a relentless accumulation of long-lived, functionally incompetent lymphocytes that escape apoptosis. In 1967, Dameshek described CLL as follows:

“The continued increase in lymphocytes of a similar type year after year suggest an increased proliferation of these cells, but a number of studies, including very low levels of RNA synthesis, and the failure to detect evidence of increased DNA replication and mitotic activity suggest that accumulation of poorly reactive lymphocytes, rather than increased proliferation, may be fundamental to the disease. It is likely that the lifespan of the small lymphocytes of the disorder may be considerably lengthened with the consequence that they remain and accumulate in lymph nodes, spleen, bone marrow, liver and blood” (73).

Dameshek proposed that the morphology of malignant lymphocytes, resembling small resting lymphocytes, and the non-responsiveness of CLL cells to mitogenic stimulation, supported this view (73). With the advent of FCM, this view was perpetuated by the analysis of CLL cell RNA and DNA content, which established definitively that over 99% of circulating CLL cells were in G<sub>0</sub> or early G<sub>1</sub> phases of cell cycle (103). Moreover, the demonstration that the prototype anti-apoptotic protein Bcl-2 is consistently over-expressed in CLL cells (104), demonstrated a mechanism by which CLL cells may evade apoptosis.

### 1.3.2 Current understanding of CLL biology

The traditional understanding of CLL biology has been challenged over the last decade by a number of lines of evidence, which have transformed the conventional view, and established that CLL represents a far more dynamic malignant process than previously considered. Several groups have reported evidence of clonal evolution of CLL cells, identified by repeated analysis of cytogenetic abnormalities (105, 106), and demonstration of oligoclonality of IgV<sub>H</sub> genes (107, 108), which would be acquired through proliferation. The observations that telomere regions in CLL lymphocytes are uniformly shorter than those of normal B cells, are shorter in unmutated CLL than mutated CLL (109), and that telomere length shows an inverse correlation with advancing disease (110, 111), suggest that the rate of proliferation of the malignant clone may be higher than previously thought. This has now been confirmed by elegant *in vivo* studies in CLL patients. Messmer *et al.* used a an *in vivo* cell labelling technique in which patients drank deuterated water (<sup>2</sup>H<sub>2</sub>O) for 12 weeks, followed by analysis of <sup>2</sup>H incorporation into CLL cell DNA (112). This study confirmed significant rates of renewal CLL cells within the clone, with cell 'birth rates' ranging from 0.1 to over 1% of the total clone size per day. Patients with CLL birth rates of greater than 0.35% of the clone per day were significantly more likely to have progressive clinical disease than those with lower rates. Foci of proliferating CLL cells have been demonstrated histologically within patient LN biopsies, termed proliferation centres (PC) (113). In contrast to normal GCs, proliferating CLL cells lack CD10 and Bcl-6 expression, and express Bcl-2 (114), however CLL PCs are similar to GCs in that FDCs and T lymphocytes are seen interspersed with the malignant clone (113). Using *in vitro* co-culture models, heterogeneous levels of CLL cell proliferation have been observed, with proliferation more marked in ZAP-70 positive and progressive CLL cases (115, 116), highlighting the importance of proliferation, in addition to accumulation, in the progression of CLL. Importantly, the mathematical models employed by Messmer *et al.* calculated significant CLL cell death rates, demonstrating that CLL cells are not as refractory to apoptosis as initially believed (112).

While elements of the traditional model of CLL have been validated over time, in that there is undoubtedly an accumulative component to the disease, this circulating pool has been established to be populated by proliferating cells within the BM and LN. The evidence of significant clonal turnover in CLL confirms that

the malignant cells are not fundamentally resistant to apoptosis, but rather suggests that CLL cells may need to compete for survival signals. A number of lines of evidence suggest this is the case, and these are discussed in detail below.

#### **1.4 The role of antigen in the pathogenesis of CLL**

Although the cell of origin of CLL remains uncertain, a wealth of studies over the last decade analysing the surface Ig expressed by CLL cells has led to progress in this field. Prior to the analysis of Ig gene mutation status, a widely-held view was that CLL most likely arises from malignant transformation of a marginal-zone (MZ) B lymphocyte, based on the similarity of these cells to murine CD5<sup>+</sup> B1 B cells (117). The identification of subgroups of CLL patients with different prognoses, based on IgV<sub>H</sub> mutation status, raised the possibility that CLL may encompass two separate but related malignancies, with unmutated CLL arising from a pre-GC naïve B cell, and mutated CLL arising from an antigen-experienced post-GC memory B lymphocyte (38). However, this view has been challenged by the observation that all CLL cells express cell-surface proteins consistent with activation through the BCR, including CD23, CD25, CD69, and CD71, with reduced expression of CD22, and CD79b, although differences in expression levels of CD69 and CD71 between mutational subgroups suggested differences in time since antigen exposure (118). In addition, all CLL cells express a wide range of genes consistent with antigenic stimulation (119, 120). Furthermore, the universal gene expression signature of CLL cells most resembles that of normal memory B cells, rather than naïve or GC subtypes (120).

Further evidence that CLL cells have encountered antigen comes from the observation that CLL cells express a very restricted set of Ig genes compared to normal B lymphocytes, with one study demonstrating frequent use of V<sub>H</sub>4-34, V<sub>H</sub>3-07, and V<sub>H</sub>1-69 genes (35). On meta-analysis, a significant over-representation of V<sub>H</sub>1, and under-representation of V<sub>H</sub>3 genes compared to normal CD5<sup>+</sup> B lymphocytes was reported (35). Studies of V<sub>H</sub>1-69 gene usage in healthy individuals over 75 years of age found no increased use of this allele, arguing against the CLL-associated repertoire simply reflecting normal age-related changes in the Ig repertoire (121). Furthermore, V<sub>H</sub>1-69 expressing CLL cells were noted particularly use specific D<sub>H</sub> and J<sub>H</sub> gene segments, that significantly differ from those used by normal B cells (122). This group also identified that the V<sub>H</sub> gene third complementarity determining region (CDR3) in these cases was significantly longer than that of normal B cells. CDR regions are specific

hypervariable regions of the  $V_H$  and  $V_L$  chain genes which associate to form the antigen binding site at the tip of the antibody molecule (1), thus conservation in the expression of these gene segments strongly implicates interaction with specific antigen. Studies of  $V_H3-21$  expressing CLL cases, frequently associated with mutated Ig genes, identified the use of a conserved short CDR3 gene segment in this subgroup (123). In addition, the CDR3 gene segment in a number of  $V_H3-21$  cases associated with particular lambda light chain genes, specifically  $V_{\lambda 2-14}$  and  $J_{\lambda 3}$  genes (123). These Ig molecules formed from the non-random pairing of heavy and light chain genes are referred to as stereotyped. A study of 1220 non-familial CLL cases found that 1.3% of cases expressed a stereotyped unmutated BCR with virtually identical Ig,  $V_H1-69$  with a CDR3 using the second reading frame of  $D3-16$  and  $J_H3$ , in association with the kappa light chain gene  $A27$  (124). Several groups have now reported over one hundred CLL-associated stereotyped BCRs, with a reported incidence of BCR stereotypy in over 20% of all cases (125-128). Patient subgroup analysis in these studies revealed BCR stereotypy to be significantly more frequent in unmutated CLL (around 40%) than mutated CLL (around 10%), suggesting a link with prognosis. Recurrent amino acid changes have been characterised in the  $V_H$  genes of CLL patients with stereotyped BCRs, particularly in cases expressing  $V_H3-21$  and  $V_H4-34$  genes (128), providing evidence for stereotypy in SHM patterns in addition to Ig gene usage. Stereotyped amino acid changes have also been identified in light chain genes in CLL cases expressing stereotyped BCRs, particularly those expressing  $V_H3-21/V_L3-21$  and  $V_H4-34/V_L2-30$  subgroups (129). The functional significance of stereotyped BCRs in CLL is underscored by the observation that the expression of a stereotyped  $V_H3-21$  BCR is a negative prognostic marker, independent of Ig mutational status (123, 130). In addition, the expression of a stereotyped BCR has been associated with an increased risk of transformation of CLL to high-grade lymphoma (131).

Although CLL cells are now recognised to have arisen from antigen-experienced B lymphocytes, a number of unresolved issues remain. Intense research continues into determining the nature of the antigen(s) recognised by the BCR of CLL cells. Since the late 1980s, it has been recognised that CLL B cells may secrete antibodies with auto-reactive specificity, capable of binding human Ig, or single- or double-stranded DNA (132, 133). With the advent of Ig mutational analysis, it was established that the majority (around 80%) of unmutated CLL cases produce antibodies that demonstrate poly-reactivity to a number of auto-antigens, while

poly-reactivity was observed in only 15% of mutated CLL (134). Recent studies using phage libraries to screen for potential ligands of CLL cell antibodies confirmed significant differences between mutational subsets; antibodies produced by unmutated CLL cells demonstrated low-affinity, low-specificity interactions on screening, while mutated CLL cell antibodies demonstrated more selective higher-affinity interactions, consistent with SHM (135). These data remain consistent with different antigenic encounters and/or cell of origin of the mutational subgroups. However, Herve *et al.* went on to revert the antibodies of mutated CLL cells to their germline sequences, and demonstrated the majority of these to regain poly- and auto-reactivity, suggesting that both unmutated and mutated CLL arises from auto-reactive B cells, raising the possibility of a common cell of origin (134). Recent studies of antibodies expressed by CLL cells from both mutational subgroups, with or without stereotyped BCRs, have identified common antibody reactivity to a number of self antigens, predominantly cytoskeletal proteins (vimentin, filamin B, and colifin-1), cardiolipin, and oxidised low-density lipoprotein (136, 137). These antigens are exposed on cell membranes during cellular apoptosis, and both groups demonstrated CLL antibodies to bind apoptotic B and T cell lines cells *in vitro*. Furthermore, the BCR of one stereotyped unmutated V<sub>H</sub>1-69 CLL subset was shown to bind non-muscle myosin heavy chain IIA (MYHIIA), which is also exposed on the surface of apoptotic cells (138).

In addition to auto-antigens, a number of CLL antibodies have also been demonstrated to exhibit specificity for bacterial antigens including streptococcus pneumoniae polysaccharides (136). It is interesting to note that a 2.5 fold relative risk of CLL has been reported in individuals who have had three or more episodes of pneumonia (139). In addition, in some cases of CLL lacking expression of a stereotyped BCR, there is evidence of antigenic stimulation by bacterial superantigens. Superantigens are able to bind IgV regions outwith CDR regions, thus are less restricted by IgV region sequence (140). In a recent study of mutated CLL cases which use the V<sub>H</sub>3-23 gene, in which stereotypy has not been described, the vast majority expressed conserved binding sites for the staphylococcus aureus protein A (SpA) superantigen (141). Of note, this group demonstrated mutated V<sub>H</sub>3-23 gene use to be an independent poor prognostic marker within the mutated CLL cohort as a whole.

These data have led to the hypothesis that both mutated and unmutated CLL may arise from a common population of B cells which produce low-avidity, poly-

reactive, “natural antibodies” that may participate in a housekeeping function to remove apoptotic cells, and contribute to the initial stages of the adaptive immune response to foreign pathogens (17, 136). In support of this hypothesis is the recent finding that naïve B cells expressing identical stereotyped V<sub>H</sub>1-69 BCRs to those found in CLL have been demonstrated in the peripheral blood of healthy individuals (142). The currently considered candidate normal counterparts of CLL cells include CD5<sup>+</sup> B-1 lymphocytes or MZ B cells, both of which express BCRs with specificity for both self and bacterial antigens (17). Although mutated CLL may yet arise from a B cell which has transited through a GC and undergone SHM in a T cell dependent process, it is also possible that both mutational groups may arise from MZ B cells without a GC reaction. MZ B cells may be activated to differentiate to plasma cells or memory B cells in a T cell-independent manner, in a process which may or may not result in SHM (17).

It is interesting to note that a population of circulating IgM<sup>+</sup>, IgD<sup>+</sup>, CD27<sup>+</sup> B cells, termed ‘IgM memory cells’ have been identified in peripheral blood, thought to be the circulating counterpart of MZ B cells, and have been demonstrated to undergo SHM through a T-cell independent process (143). Of note, the human IgM memory B cell compartment is enriched in V<sub>H</sub>3 expressing cells, with some demonstrating SpA reactivity (144). In a recent study 94.7% of IgM memory B cells in normal individuals were found to contain SHM consistent with antigen encounter, and to display markedly less self-reactivity than naïve B cells (144). The authors proposed that a third checkpoint for B cell tolerance exists between naïve and memory IgM B cell compartments, prior to SHM, in order to prevent the possibility of rapid expansion of potentially autoreactive IgM memory cells (144). It is tempting to speculate that subversion of such a tolerogenic process may lead to the potential expansion of somatically mutated antigen-experienced IgM expressing B cells, and potentially represent a cell of origin of some mutated CLL cases. Some interesting observations from V<sub>H</sub>4-34 expressing cells support such a hypothesis. The V<sub>H</sub>4-34 gene is commonly used by CLL cells (35), most frequently the mutated subset, with 79% of cases in one study showing evidence of SHM, and is associated with indolent disease (128). Of note, the germline V<sub>H</sub>4-34 gene encodes auto-reactive antibodies which recognise the N-acetylglucosamine (NAL) antigenic determinant of the I/i blood group antigen and has features of anti-DNA binding antibodies (128). In healthy individuals, V<sub>H</sub>4-34 expressing B cells are present in appreciable numbers, however V<sub>H</sub>4-34

antibodies are not seen, leading to the suggestion that SHM and possibly additional tolerance measures must occur to enable these cells to remain in the circulating B cell pool (145). It is interesting to note that while V<sub>H</sub>4-34 cases show evidence of SHM predicted to negate anti-DNA reactivity, amino acid residues for the I blood group antigen remain conserved, suggesting these CLL cells may still be capable of stimulation by auto- or exogenous antigens (128). Of note, a recent study demonstrated significant intraclonal diversity in some mutated V<sub>H</sub>4-34 expressing CLL cases, which suggests ongoing antigenic stimulation (146).

Whatever the precise cell of origin of CLL cells, the emerging model suggests that an initiating mutation occurs at an early point in an auto-reactive B cell that favours clonal expansion on antigen encounter (17). The subsequent course of events leading to leukaemic transformation has been proposed to be shaped depending on whether SHM occurs, and this model is presented in Figure 1.4. In the absence of IgV<sub>H</sub> gene mutations, antigen-driven clonal expansion may continue, raising the probability of a leukaemia initiating mutation being acquired, leading to unmutated CLL. SHM may either result in increased BCR affinity for antigen leading to anergy, or reduced binding specificity leading to clonal ignorance. The role of antigenic stimulation in inducing leukaemic transformation in mutated CLL, and in the progression of CLL after leukaemic transformation remains under investigation. An emerging hypothesis suggests that the progressive course of unmutated CLL, and some mutated CLL cases, may be determined by the ability of CLL cells to continue to be stimulated by antigenic exposure (134, 145). This hypothesis, and the combined data implicating antigenic stimulation in the pathogenesis of CLL has led to significant research into BCR signal transduction in CLL cells. These data are presented in Section 1.6, preceded by an overview of BCR signal transduction in normal B lymphocytes.

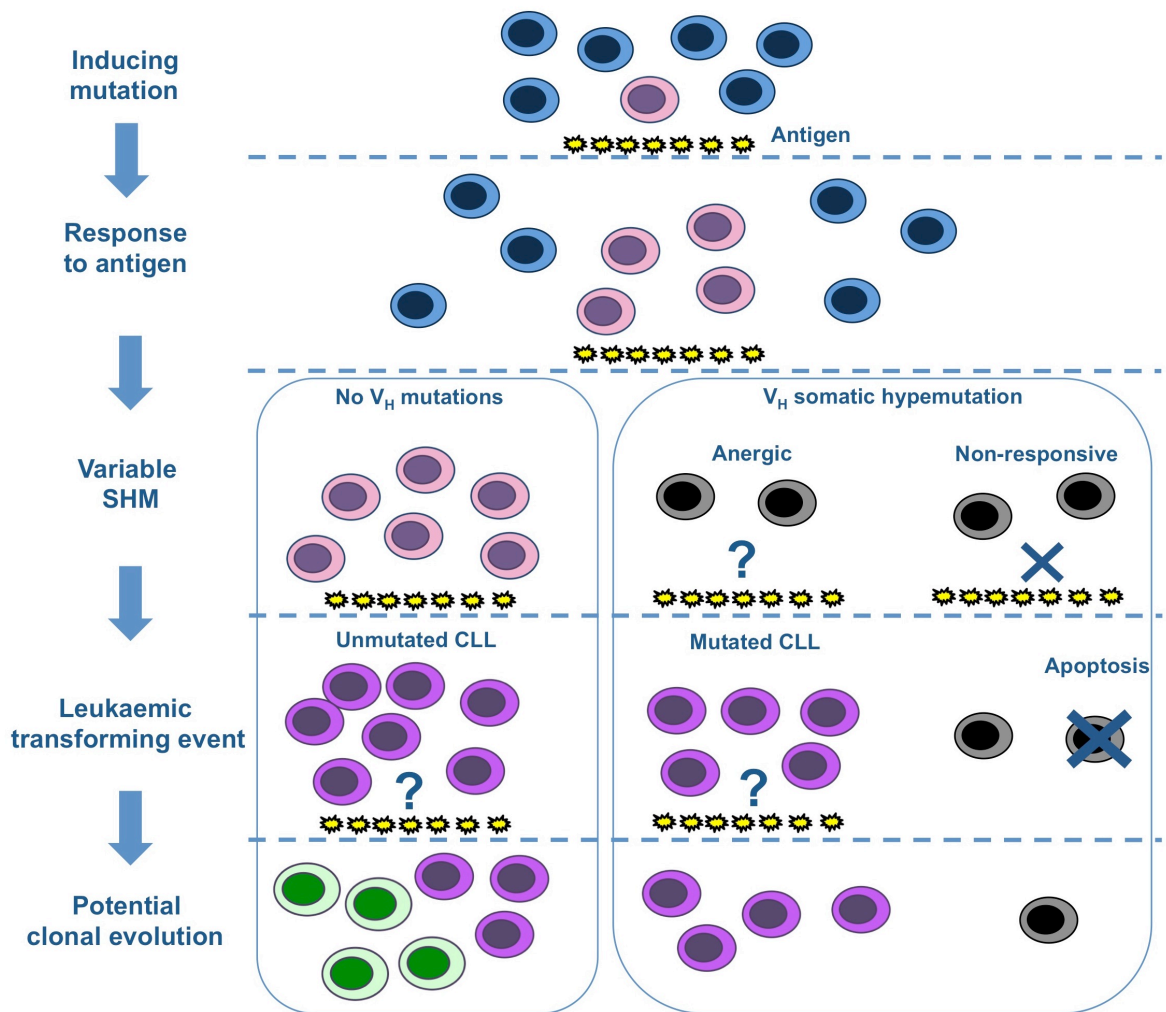


**Figure 1.4 Proposed model of antigen stimulation in the pathogenesis of CLL, adapted from Chiorazzi (17)**

This model suggests that within the normal B lymphocyte population (blue cells) a predisposing lesion occurs within a single cell (pink cell), providing it with a proliferative advantage in response to antigen (yellow). Cells which have undergone SHM are shown in grey. This model proposes that additional genomic aberrations are required for transformation to CLL (purple cells). Stages where the continued role of antigenic stimulation has yet to be fully determined are indicated by blue question marks. With continued proliferation CLL cells may acquire further genetic lesions (for example 13q, 11q, or 17p deletion) in the process of clonal evolution (green cells), largely confined to unmutated CLL.

## 1.5 B cell receptor signal transduction

### 1.5.1 Early events following BCR engagement by antigen

As outlined in Section 1.1.1, the BCR consists of membrane Ig, non-covalently associated with ITAM-containing Ig $\alpha$  and Ig $\beta$  chains. Antigens presented to the BCR may be soluble or associated with cell membranes. Current evidence suggests the most relevant mechanism of BCR stimulation *in vivo* is through antigen associated with membranes of FDCs and macrophages, which can retain significant amounts of antigen on the cell surface bound to Fc and complement receptors (147-149). Following B cell engagement by membrane-bound antigen, many BCR units are redistributed within the cell membrane to cluster at the site of antigen binding (150). This process is dependent on signalling through the BCR, and involves extensive cytoskeletal reorganisation, involving an initial phase of B cell cytoplasmic spreading across the antigen-presenting cell membrane, followed by a phase of cytoplasmic retraction, as shown diagrammatically in Figure 1.5 (151). In addition to increasing antigen density, cytoskeletal reorganisation greatly increases the recruitment of kinases involved in proximal BCR signal transduction and co-receptors such as CD19 to the BCR cluster, forming the microsignalosome (147, 152). This clustering of the BCR occurs predominantly within specialised lipid-rich membrane areas termed 'lipid-rafts', which also facilitate association of key signalling components (153).

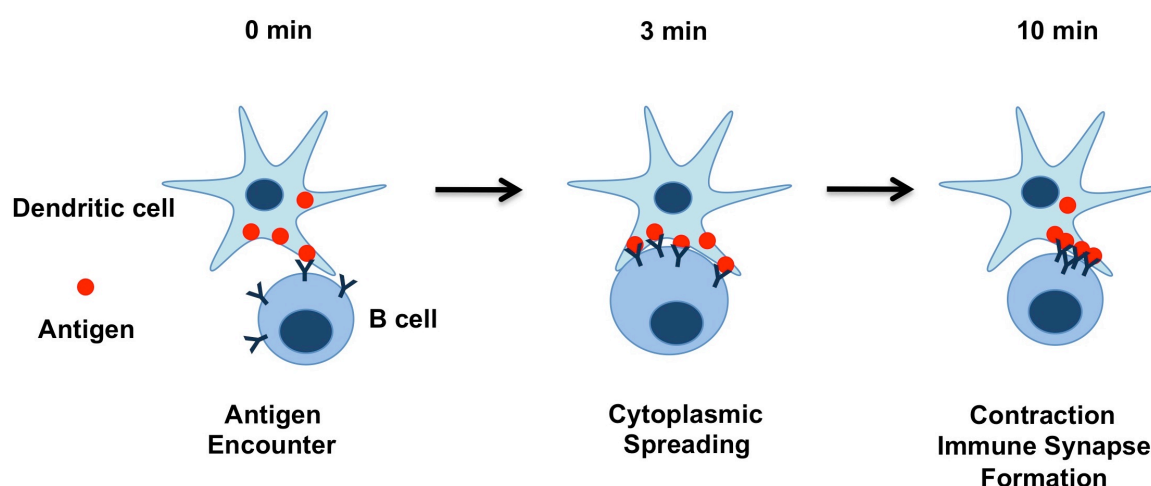


**Figure 1.5 B cell cytoplasmic spreading and contraction response on antigen stimulation**

## 1.5.2 Signal transduction

A schematic overview of BCR signal transduction is shown in Figure 1.6.

Following antigen engagement of the BCR, the Src family of non-receptor tyrosine kinases, in particular Lyn, Fyn, Blk, or Lck, phosphorylate ITAM regions of the Ig $\alpha$  and Ig $\beta$  chains (154, 155). Each ITAM sequence contains two tyrosine residues, and double phosphorylation of both ITAMs allows the recruitment and activation of spleen tyrosine kinase (Syk), which binds to the ITAM sequences via its Src homology 2 (SH2) domains (154). Activated Syk phosphorylates the B cell linker protein (BLNK), which acts as an adaptor molecule, allowing the assembly of a multi-protein complex, including the TEC-family tyrosine kinase Bruton's tyrosine kinase (Btk), phospholipase C $\gamma$ 2 (PLC $\gamma$ 2), and the VAV family of Rho GTPases (3, 156). Concurrently, Lyn phosphorylates the BCR co-receptor CD19, resulting in the recruitment of the enzyme phosphatidylinositol-3-kinase (PI-3K). PI-3K in turn phosphorylates phosphatidylinositol-4,5-bisphosphate (PIP $_2$ ) to convert it to phosphatidylinositol-3,4,5-triphosphate (PIP $_3$ ) (155). PIP $_3$  results in membrane localisation of Btk and PLC $\gamma$ 2, enabling them to bind BLNK through their pleckstrin-homology (PH) domains (157). PIP $_3$  also recruits another adaptor protein, B lymphocyte adaptor molecule of 32 kDa (Bam32), which further tethers PLC $\gamma$ 2 to the plasma membrane. Btk and Syk can then effectively phosphorylate and activate PLC $\gamma$ 2, which converts PI(4,5)P $_2$  to inositol triphosphate I(1,4,5)P $_3$  and diacylglycerol (DAG). I(1,4,5)P $_3$  formation results in the release of calcium from intra-cellular stores, and activation of extra-cellular calcium channels (155). The magnitude and duration of flux in cytoplasmic calcium concentration controls activation of the transcription factors nuclear factor of activated T cells (NFAT), activated directly through calcium-calmodulin complexes, and nuclear factor kappa-light-chain enhancer of activated B cells (NF- $\kappa$ B), activated indirectly through Ca $^{2+}$ -dependent activation of atypical protein kinase C (PKC) isoforms ( $\zeta$  and  $\iota/\lambda$ ) (158, 159). DAG meanwhile activates classical PKC isoforms ( $\alpha$ ,  $\beta$ , and  $\gamma$ ) which in turn activated mitogen activated protein kinases (MAPK) (160). MAPK are also activated through the activation of Vav, and the adaptor complex Grb2/SOS, which associate with phosphorylated BLNK. Key downstream signalling pathways are described in further detail below.

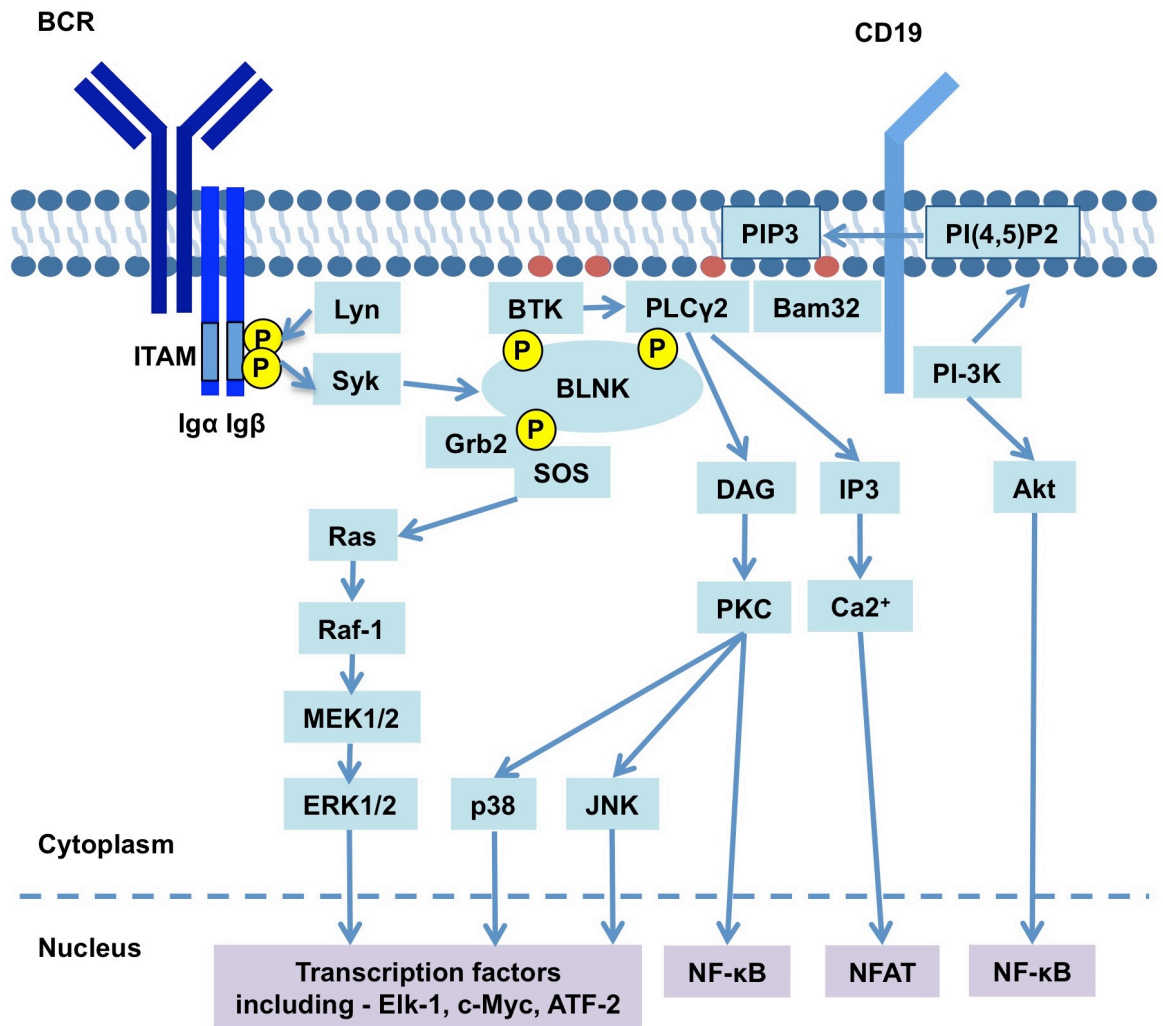


**Figure 1.6 An overview of the B cell antigen receptor signalling pathway**

### 1.5.2.1 MAPK signalling pathway

There are three main classes of MAPK; c-Jun NH<sub>2</sub>-terminal kinase (JNK) family, the p38 MAPK family, and the extra-cellular signal-related kinase (ERK) family (161). MAPK are serine-threonine protein kinases which control a wide range of biological effects, and are essential for normal haemopoiesis. The ERK pathway predominantly mediates anti-apoptotic and mitogenic gene expression in response to cytokines and growth factors. The p38 and JNK MAPKs are activated by stress and growth factors, and control predominantly apoptosis and cell-cycle progression (161). MAPK require dual phosphorylation on tyrosine and threonine residues for activity, and phosphorylation on these residues is controlled by a complex series of regulatory kinases, outlined in Figure 1.7. MAPK kinases (MAPKKs or MEKs) may phosphorylate MAPK on both tyrosine and threonine residues. Specificity is achieved in MAPK activation as specific MEKs

phosphorylate specific MAPK; in outline, MEKs 1 and 2 phosphorylate ERK, MEKs 3, 4, and 6 phosphorylate p38, and MEKs 4 and 7 activate JNK. MEKs are in turn regulated by the activity of MAPK kinase kinases (MAPKKKs), which are a family of serine kinases. MAPKKKs are furthermore activated by small G proteins, including Ras for the ERK pathway, and Rho proteins for the p38 and JNK pathways (161). The transcription factors regulated by MAPK include Elk-1 and c-myc by ERK, c-Jun and ATF-2 by JNK, and ATF-2 and MAX by p38 MAPK, and the functional outcome of activation is dependent on the developmental stage of the B cell (155).

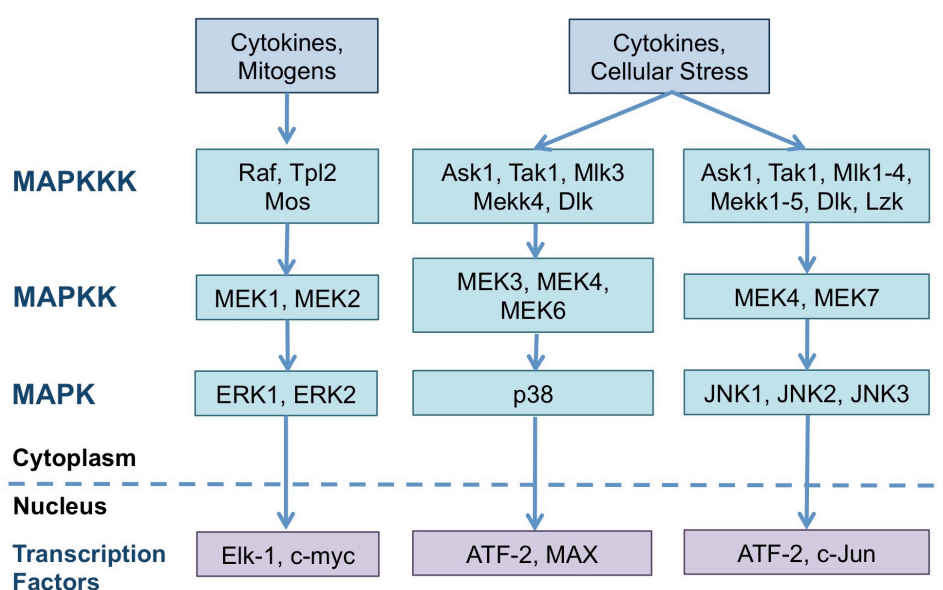


**Figure 1.7 Regulation of MAPK activation**

### 1.5.2.2 PI-3K/Akt signalling pathway

There are four classes of PI-3K, named I<sub>A</sub>, I<sub>B</sub>, II, and III, differentiated by structural and substrate specificity characteristics (162). Class I<sub>A</sub> PI-3K is involved in signalling downstream of the BCR. This class of PI-3K are heterodimers of a regulatory subunit (p85 $\alpha$ , p85 $\beta$ , p55 $\alpha$ , p50 $\alpha$ , or p55 $\gamma$ ) and a p110 catalytic subunit (p110 $\alpha$ , p110 $\beta$ , or p110 $\delta$ ) (162). The p85 regulatory PI-3K subunit associates with phosphorylated CD19, via its' SH2 domains, and this in turn activates the catalytic p110 subunit (155). In addition to converting PI(4,5)P<sub>2</sub> to PIP<sub>3</sub> following BCR activation, PI-3K also recruits the serine/threonine kinase Akt (protein kinase B) to the lipid membrane (163). A conformational change in Akt allows full activation through phosphorylation on Thr<sup>308</sup> (catalysed by PDK1) and Ser<sup>473</sup>, resulting in the release of active Akt from the membrane to exert cytoplasmic effects (155, 164).

Key signalling targets of Akt are shown in Figure 1.8. Akt phosphorylates the pro-apoptotic Bcl-2 family protein Bad, preventing it from interacting with anti-apoptotic Bcl-x<sub>L</sub>, resulting in a net anti-apoptotic effect (165). Akt also regulates a number of nuclear transcription factors, including E2F, NF-κB, Ca<sup>2+</sup>/cAMP response element binding protein (CREB), and forkhead transcription factors (155). Akt negative regulation of forkhead transcription factors results in the degradation of additional pro-apoptotic proteins, including Fas-ligand and Bim (155). Akt also directly phosphorylates and inactivates caspase 9, an effector of the intrinsic apoptotic pathway (166, 167). PI-3K/Akt signalling following BCR stimulation also results in phosphorylation of components of the mammalian target of rapamycin (mTOR) complex, which in turn phosphorylates the p70 s6 kinase (168). P70 s6 kinase phosphorylates the s6 protein, resulting in protein synthesis (169). In summary, PI-3K/Akt targets following BCR signalling broadly prevent apoptosis, and promote cell cycle progression.

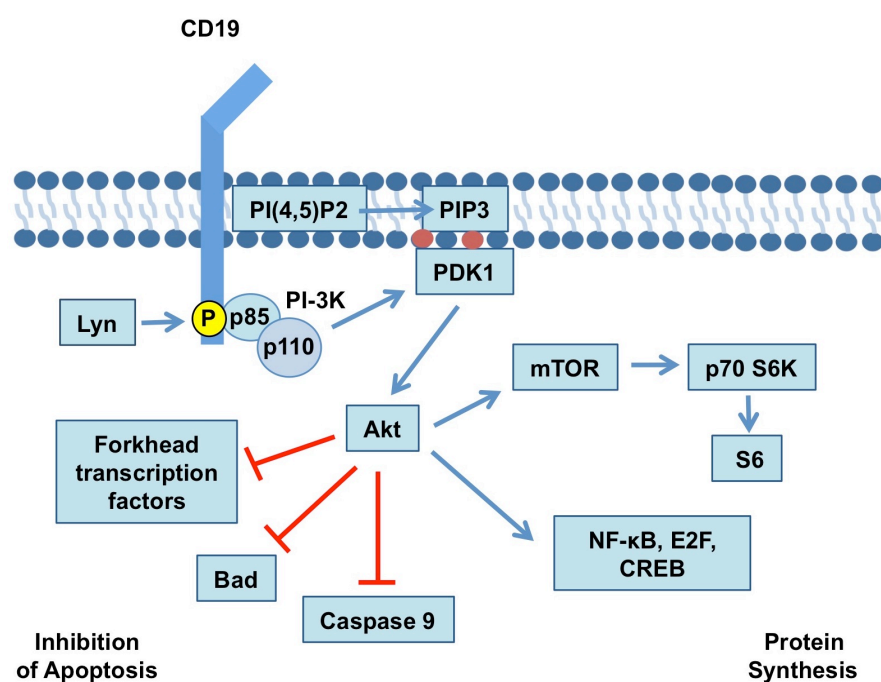


**Figure 1.8 An outline of the PI-3K/Akt signalling pathway**

### 1.5.2.3 NF-κB signalling

The NF-κB family of transcription factors comprises NF-κB1 (p50), NF-κB2 (p52) RelA (p65), RelB, and c-Rel, which bind to DNA as heterodimers (170). NF-κB heterodimers are held within the cytoplasm in the resting state, through interaction with inhibitory IκB proteins. On activating stimuli such as BCR stimulation, IκB is phosphorylated by IκB kinases, which target IκB for proteasomal degradation, and

allow NF- $\kappa$ B heterodimers to translocate to the nucleus and direct gene expression (170). Activity of NF- $\kappa$ B transcription factors is essential for the survival and function of mature B cells (171), and following BCR engagement, NF- $\kappa$ B increases the expression of anti-apoptotic Bcl-2 family proteins, including Bcl-2, Bcl-x<sub>L</sub>, and A1, and cell-cycle related proteins including cyclin D2 (3).

### **1.5.3 Tonic BCR signalling**

As outlined in Section 1.1.1, expression of a functional pre-BCR or BCR is essential for normal lymphocyte development. In addition, it is now understood that mature B cells also depend on expression of a functional BCR for survival, as conditional ablation of BCR expression results in rapid B cell apoptosis (172, 173), suggesting that a basal level of signalling may occur independently of antigen. Three models for the generation of antigen-independent 'tonic' signals through the BCR complex have been proposed (174). The homeotypic model proposes that a basal level of signalling may occur due to a degree of self-aggregation of pre-B and B cell receptors, while the lipid raft model suggests that basal signals may be determined by the fraction of membrane-associated BCR complexes within these specialised lipid-rich membrane domains. The currently favoured model of tonic signalling is the equilibrium model, which states that the level of basal signal transduction results from a dynamic balance of activities of Src family kinases capable of phosphorylating ITAMs, and the activity of negative regulatory tyrosine phosphatases, including SH2-associated protein-1 (SHP-1), which is activated by the BCR co-receptor CD22 (174). This model is supported by a study showing that mice lacking the Src family kinases Blk, Fyn, and Lyn are deficient in pre-BCR function (175). An indication that the tyrosine kinase c-Abl may participate in tonic signalling in B cells came from a study in Abelson murine leukaemia virus transformed cell lines, which exhibit maturation arrest at the pre-B cell stage (176). In these cells, inhibition of c-Abl activity with the ATP-competitive tyrosine kinase inhibitor (TKI) imatinib induced expression of RAG-1 and RAG-2, and allowed Ig light chain rearrangement to occur (176), confirming c-Abl to block cellular differentiation, which may be relevant to leukaemogenesis. Notably, a similar role for c-Abl kinase, in conjunction with ERK MAPK, in the repression of RAG gene transcription has also been identified in T lymphocytes (177).

## 1.6 BCR signalling in CLL cells

### 1.6.1 BCR signal transduction in CLL cells

All CLL cases are characterised by low surface Ig expression, usually IgM and IgD, usually expressed on mature, antigen-experienced B cells (178), therefore it may be supposed that the ability of CLL cells to signal through the BCR is limited. However, it has long been appreciated that a subset of CLL cells show evidence of activation following *in vitro* BCR stimulation (179, 180). Shortly after the appreciation of the prognostic impact of IgV<sub>H</sub> mutational status, came the realisation that the response of CLL cells to BCR ligation correlated significantly with IgV<sub>H</sub> mutational status, with 80% of unmutated CLL cases responding and only 20% of mutated CLL cases responding in one series (181). Further evidence that ongoing signalling through the BCR may be involved in the progression of CLL after leukaemic transformation comes from analysis of CLL gene expression signatures. Despite a broadly similar gene expression profile between Ig mutational subtypes, of the several hundred differentially expressed genes, several genes expressed in the unmutated subgroup are involved in mitogenic BCR signalling, leading the authors to speculate that these cases may continually respond to (auto)-antigen *in vivo* (119).

Although Allsup *et al.* identified that a cut-off of less than 5% difference from germline IgV<sub>H</sub> sequence was more predictive of BCR signalling competency than the conventional 2% variation from germline sequence, some unmutated cells were again non-responsive and a few mutated CLL cases were responsive to IgM stimulation, confirming that additional regulation of BCR signal transduction exists in CLL (182). In this study, differences in the level of surface IgM between samples did not account for the observed differences in signalling. Expression of ZAP-70 has been demonstrated to correlate with the phosphorylation of Syk following BCR ligation in CLL cells (183). Although ZAP-70 expression largely correlated with Ig mutational status, mutated CLL cells expressing ZAP-70 also showed enhanced Syk phosphorylation following BCR stimulation (183). This group also demonstrated that ZAP-70 becomes tyrosine phosphorylated and associates with the BCR following stimulation, suggesting an active role in BCR signalling, analogous to its' role in T lymphocytes. Further studies in which ZAP-70 negative CLL cells were transfected with either wild-type or mutated ZAP-70 constructs identified that enhancement of BCR signalling by ZAP-70 is dependent

on the integrity of the SH2 region, but not the kinase domain, suggesting that ZAP-70 acts as an adaptor protein regulating BCR signalling in CLL cells (184), which may well account for the negative prognostic impact of ZAP-70 expression. However, Deglesne *et al.* reported a number of ZAP-70 expressing CLL cases to be non-responsive to BCR stimulation, and some ZAP-70 positive cases showing little response to BCR ligation, suggesting yet further regulation exists (185). An association between CD38 expression in CLL cells and an intact  $Ca^{2+}$  flux in response to BCR ligation has been described (186), and CD38 was proposed to be a receptor which may prolong signalling generated through the BCR, however this has not been demonstrated in a recent study (187). Furthermore, expression of the proto-oncogene T-cell leukaemia 1 (Tcl-1), a positive regulator of Akt activation, in CLL cells has been reported to correlate with increased signalling response and metabolic activity following BCR stimulation (188). Of note, high Tcl-1 expression was an independent predictor for short PFS in this study. In contrast to these proteins that promote BCR signal transduction in CLL cells, over-expression of protein kinase C $\beta$ II (PKC $\beta$ II) has been shown to negatively regulate  $Ca^{2+}$  flux following BCR stimulation, proposed to maintain BCR signalling below the level that may trigger apoptosis following encounter with antigen (189). The observation that high PKC $\beta$ II expression in CLL patient samples correlated with both a high white cell count, and advanced stage of disease (189), indicates that the regulation of BCR signalling by PKC $\beta$ II is functionally relevant *in vivo*.

According to the model of CLL outlined in Figure 1.4, the majority of mutated CLL cells are predicted to persist as anergic or unresponsive B cells. Analysis of CLL cells in which poor  $Ca^{2+}$  flux was observed following IgM stimulation *in vitro* revealed defective Syk phosphorylation despite normal Syk expression, suggesting altered regulation of proximal components of the BCR signalling pathway (190). Allsup *et al.* compared CD79a phosphorylation on BCR stimulation between Ig mutational subgroups of CLL; while in unmutated CLL cells CD79a was phosphorylated on BCR stimulation, CD79a was constitutively phosphorylated in mutated CLL cells, suggesting previous antigenic stimulation (182). Moreover, in BCR non-responsive CLL cells from both mutational subgroups, the BCR was prevented from translocating to lipid rafts following IgM stimulation, through a mechanism involving Src kinases, a similar phenomenon to that observed in non-malignant anergic B lymphocytes (182). In murine B lymphocytes, an anergic tolerised state is molecularly characterised by constitutive

ERK activation and nuclear NF-AT localisation (191). It is of great interest therefore that 49% (25/51) of CLL samples in one study showed evidence of constitutive ERK phosphorylation and NF-AT activity in the absence of Akt phosphorylation (191). The same subset of CLL samples were also significantly less responsive to *in vitro* BCR stimulation compared to those lacking constitutive ERK phosphorylation, leading the authors to conclude that the molecular features observed also reflect an anergic state (191). The anergic molecular phenotype significantly correlated with an early stage of disease at patient diagnosis, but no associations with other clinical or biological parameters (including IgV<sub>H</sub> mutational status) were identified (191). Another study of the signalling response to BCR stimulation with soluble anti-IgM antibodies has suggested that all CLL cells may have signalling features reminiscent of anergic B cells (192). In this study, incomplete MAPK activation following BCR stimulation was observed; phosphorylation of ERK occurred in 100% of unmutated and 75% of mutated CLL samples, while JNK or p38 phosphorylation was rarely observed (192). However, stimulation of CLL cells with immobilised anti-IgM antibodies resulted in more sustained activation of ERK and Akt in both subgroups (192). As B cell stimulation by immobilised anti-IgM antibodies has been proposed to model T-independent antigenic stimulation, the authors concluded that T-dependent and T-independent antigens may induce different signalling responses in CLL cells. Murine anergic B lymphocytes require continuous BCR engagement by antigen to retain tolerance, and regain responsiveness to antigen stimulation on antigen removal (193). Of interest, CLL cells initially unresponsive to *in vitro* BCR stimulation regain surface IgM expression and BCR-responsiveness following *in vitro* culture, strengthening the case that CLL cells encounter antigen *in vivo* (187).

In order to investigate the functional consequences of BCR signal transduction observed in CLL cells, a number of groups have assessed the effect of BCR stimulation on CLL cell survival and proliferation. One of the first studies was that of Bernal *et al.*, who stimulated CLL cells *in vitro* with F(ab')<sub>2</sub> antibody fragments to human IgM, which resulted in a significant reduction in spontaneous apoptosis, associated with activation of NF- $\kappa$ B, and increased expression of anti-apoptotic proteins including Bcl-2 and Mcl-1 (194). These pro-survival effects were completely blocked by the PI-3K inhibitor LY294002, implicating PI-3K as the predominant mediator of anti-apoptotic signalling (194). Many other groups have since confirmed the anti-apoptotic effect of prolonged BCR stimulation of CLL cells

*in vitro*, either using soluble F(ab')<sub>2</sub> anti-IgM fragments or anti-IgM antibodies immobilised on beads or tissue culture plates (182, 185, 192, 195). Two of these groups observed a pro-survival effect on stimulation with immobilised anti-IgM only, while soluble anti-IgM resulted in increased spontaneous apoptosis (185, 192). Introduction of constitutively active Akt into primary CLL cells recapitulated the anti-apoptotic profile of Bcl-2 proteins observed on BCR stimulation, with up-regulation of Bcl-x<sub>L</sub>, XIAP, and Mcl-1 (196). Furthermore, this group demonstrated down-regulation of Mcl-1 using siRNA blocked the anti-apoptotic effect of prolonged BCR stimulation and induced apoptosis. While transfection of CLL cells with constitutively active MEK2 led to up-regulation of XIAP, no significant increase in viability was observed, leading the authors to conclude that Akt-mediated Mcl-1 up-regulation is the major anti-apoptotic signalling pathway downstream of the BCR in CLL cells (196). Of note, immobilised anti-IgM stimulation of CLL cells significantly reduced the level of apoptosis observed on fludarabine treatment *in vitro*, and correlated with retained Mcl-1 expression and reduced poly ADP ribose polymerase (PARP) cleavage (192). High Mcl-1 expression in freshly isolated peripheral blood CLL cells has been shown to significantly predict for a reduced likelihood of achieving a CR following chemotherapy (chlorambucil or fludarabine) (197), suggesting that this signalling pathway may play a role in chemoresistance *in vivo*.

The demonstration that clonal evolution, characterised by the acquisition of new chromosomal abnormalities on FISH, predominantly occurs in unmutated CLL cases (198), suggests that BCR signalling may drive leukaemic cell proliferation. Although *in vitro* studies have failed to demonstrate S-phase cell cycle entry or cell division following anti-IgM stimulation of CLL cells (185, 186), Deglesne *et al.* reported BCR responsive CLL cells to increase in size and metabolic activity, with concurrent up-regulation of cyclin D2 and the cyclin-dependent kinase (cdk) 4. Despite changes in expression of genes involved in cell cycle entry, expression of the cell cycle inhibitor p27<sup>kip1</sup> remained high in all cases, leading the authors to suggest that the ability of CLL cells to respond to antigenic stimulation *in vivo* is likely to prime them for proliferation on the receipt of further costimulation from T cells (CD154 or IL-4) or stromal cells (185). In this study, 84% of the patients whose CLL cells responded to BCR stimulation *in vitro* showed evidence of progressive disease, measured by LDT or Binet stage B or C disease, while all BCR unresponsive cases were stable stage A patients. These data have been

corroborated by the results of a recent gene expression study in CLL cells following BCR stimulation. In unmutated CLL cells only, BCR crosslinking led to up-regulation of several genes involved in signal transduction (including MAPK pathway genes), and cell cycle progression (including *cdk4*) (199). Furthermore, this group demonstrated IgM stimulation of these unmutated CLL samples to induce a 2.7-fold increase in the percentage of cells in G<sub>1</sub> after 24 hr of stimulation (199).

Collectively, these data strongly implicate a role for BCR signal transduction in response to antigenic stimulation in the maintenance and progression of CLL, identifying BCR signal transduction as a rational novel therapeutic target. In addition, the data linking BCR signalling to chemoresistance *in vitro* suggests that BCR stimulation may play a role in *in vivo* chemoresistance.

### **1.6.2 Evidence for dysregulated tonic BCR signalling in CLL**

In addition to the evidence that antigen-induced BCR signal transduction is central to CLL pathogenesis, recent research has identified that tyrosine kinases involved in BCR signal transduction are over-expressed and constitutively active in CLL, namely Lyn and c-Abl, raising the possibility that dysregulated antigen-independent signals downstream of the BCR also contribute to CLL pathogenesis.

#### **1.6.2.1 Lyn kinase**

Lyn is a member of the Src kinase family, which comprises Lyn, Hck, Blk, Src, Fyn, Lck, Yrk, Yes, and Fgr (200). Lyn is the predominant Src kinase expressed in normal B lymphocytes, and exists in two functionally-identical isoforms, of 53 and 56 kDa (201). In addition to promoting proximal BCR signal transduction, Lyn is believed to also exert a negative regulatory effect on signalling, as Lyn<sup>-/-</sup> mice develop B cell hyper-reactivity and autoimmune glomerulonephritis (202). All Src kinases are structurally conserved, containing three SH domains, of which the C terminal SH1 domain is responsible for the kinase activity (200). The structure of Lyn kinase is shown in Figure 1.9. Lyn activity is regulated by phosphorylation of the C terminal Tyr<sup>507</sup>. Tyr<sup>507</sup> phosphorylation by Csk retains Lyn in an inactive conformation, in which the C terminal associates with the SH2 domain. Dephosphorylation of Tyr<sup>507</sup> by CD45 releases the C terminal from SH2 domain, and allows autophosphorylation of Tyr<sup>396</sup> in the kinase domain to occur, resulting in kinase activation (200).

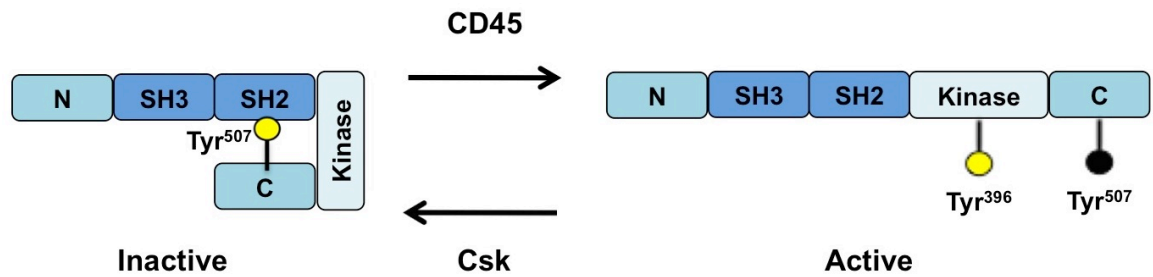


**Figure 1.9 Diagram of the regulation of Lyn kinase activity**

Lyn has been reported to be uniformly over-expressed 2.5-5 fold at the protein level in CLL cells, while expression of other Src kinases including Src, Fyn, Fgr, and Lck were expressed at levels comparable to normal B lymphocytes (203). Kinase assays confirmed Lyn to be constitutively active, with little increase in activity following BCR stimulation (203). The mechanism for Lyn over-expression in CLL remains to be determined, however down-regulation of microRNA-337-5p has been proposed as a potential factor (204). A potential mechanism for constitutive Lyn activity has been proposed to be due to the level of Lyn expressed exceeding the level of inhibitory Csk kinase (203). In addition to expression within the plasma membrane, Contri *et al.* demonstrated Lyn to be abnormally located within the cytoplasm of CLL cells (203). A potential role for Lyn in CLL pathogenesis was suggested by the demonstration that in a screen of kinase inhibitors, only Src kinase inhibitors such as PP2 reduced the global tyrosine phosphorylation characteristic of CLL cells, and induced apoptosis (203).

Lyn has also been implicated as an oncogenic kinase in a number of other haematopoietic malignancies. In acute myeloid leukaemia (AML), Lyn is constitutively active, and abnormally located within the plasma membrane and cytoplasm, and associated with an increase in global tyrosine phosphorylation (205). Similarly to CLL, the tyrosine phosphorylation pattern was inhibited by PP2, and moreover, specific Lyn inhibition using siRNA significantly reduced the colony forming potential of primary AML cells (205). Lyn kinase activity is also well established as a mechanism of resistance to imatinib in CML and Philadelphia-chromosome positive acute lymphoblastic leukaemia (ALL) (206, 207). A novel TEL-Lyn fusion gene has recently been reported in primary myelofibrosis (208). Lyn has also been implicated in the pathogenesis of lymphoid malignancies. In B-cell non-Hodgkin's lymphomas, Lyn associates with a Cbp/PAG adaptor protein within lipid rafts, to form a signalosome linking Lyn to Signal Transducer and

Activator of Transcription (STAT)-3 (209). Src inhibitors dissociated the Lyn/Cbp/PAG complex, inhibited proliferation, and induced apoptosis in NHL cell lines (209).

### **1.6.2.2 c-Abl kinase**

c-Abl is a homologue of the v-Abl oncogene encoded by the Abelson murine leukaemia virus (210). An essential role for c-Abl in normal lymphopoiesis has been established following the observation that mice homozygous for inactivating c-Abl mutations have severe B and T lymphopenia and thymic and splenic atrophy (210). Following BCR stimulation, c-Abl phosphorylates the BCR co-receptor CD19, ultimately resulting in PI-3K activation (211). Additionally, c-Abl has been implicated in tonic BCR signalling as described in Section 1.5.3.

The 1b splice variant of c-Abl has been demonstrated to be heterogeneously over-expressed in CLL, and constitutively active (212). Furthermore, significant associations were observed between high c-Abl protein expression and, unmutated IgV<sub>H</sub> genes, ZAP-70 expression, Binet stage B or C disease, and a high circulating white cell count (212). In addition, inhibition of c-Abl using imatinib induced apoptosis, with the sensitivity of CLL cells to imatinib-induced apoptosis correlating positively with c-Abl expression. The induction of apoptosis correlated with the inhibition of NF- $\kappa$ B activity, suggesting a molecular mechanism for apoptosis (212). Moreover, imatinib also sensitised CLL cells to chlorambucil *in vitro* (213).

Although further work is required to fully determine the roles of dysregulated Lyn and c-Abl kinases in CLL, these combined data further support inhibition of BCR signal transduction as an attractive novel therapeutic approach in CLL.

## **1.7 The role of the microenvironment in CLL**

Increasingly, it is being appreciated that few malignant disorders are defined by truly autonomous neoplastic cells, rather, most cancers depend, to varying extents, on a wide array of accessory cells within the tumour microenvironment (214). In haematopoietic malignancies, including acute leukaemias and CML, the BM microenvironment is exploited by a subpopulation of the leukaemic clone which have acquired the properties of self-renewal (215). Such leukaemia stem cells (LSCs) within the microenvironmental niche may escape chemotherapy, and lead to disease relapse. The issue of whether LSCs exist in CLL remains an area under active investigation, however, it is now firmly established that CLL cells,

similar to many other B cell malignancies, retain the dependence of normal B lymphocytes on a number of interactions with the BM and LN microenvironment (216). The importance of the microenvironment CLL is underscored by the observation that CLL cells undergo variable rates of spontaneous apoptosis on *in vitro* culture (217). In addition, the extent and pattern of BM infiltration in CLL has prognostic value (218). Although the normal BM and LN microenvironments differ in composition and function, supporting normal B lymphocyte development and differentiation in response to antigen respectively (216), both tissue compartments are sites of CLL cell proliferation (219). On examination of BM and LN biopsies from CLL patients, a proportion of malignant lymphocytes are located within PC, in close association with a number of accessory cells, including stromal cells, dendritic cells, T lymphocytes, and macrophages (219). It is within such PCs that CLL cell interaction with antigen is proposed to occur (145). The close association of CLL cells within this specialised microenvironment also brings the malignant cells into contact with a number of cell associated and secreted factors which promote CLL cell survival and proliferation. A summary of the key interactions between CLL cells and microenvironmental stimuli are shown in Figure 1.10, and described in detail below. It is becoming increasingly appreciated that the interaction of CLL cells with the microenvironment is a dynamic two-way process, in which the malignant lymphocytes play a key role both in recruiting supporting cells and directing expression of favourable signalling proteins by accessory cells.

### **1.7.1 The role of stromal cells in CLL**

Co-culture of CLL cells with primary human BM-derived stromal cells has been demonstrated to significantly reduce apoptosis of CLL cells *in vitro*, and can maintain CLL cell viability for several weeks (220). The protective effect of stromal co-culture is largely dependent on direct contact between CLL and stromal cells, as it was not observed on CLL cell culture in transwell inserts above stromal cells, or with stromal cell conditioned medium (220, 221). In addition to stromal cells, CLL cell survival *in vitro* can also be increased by co-culture with a dendritic cell line (222). Many secreted cytokines including IL-2, IL-4, IL-10, vascular endothelial growth factor (VEGF), and interferon (IFN)  $-\alpha$  and  $-\gamma$  are known to support CLL cell viability *in vitro*, and culture of CLL cells in transwells above primary BM cultures provided a degree of protection from apoptosis, less so than direct contact, suggesting that secreted cytokines also contribute to promoting CLL cell survival (223).

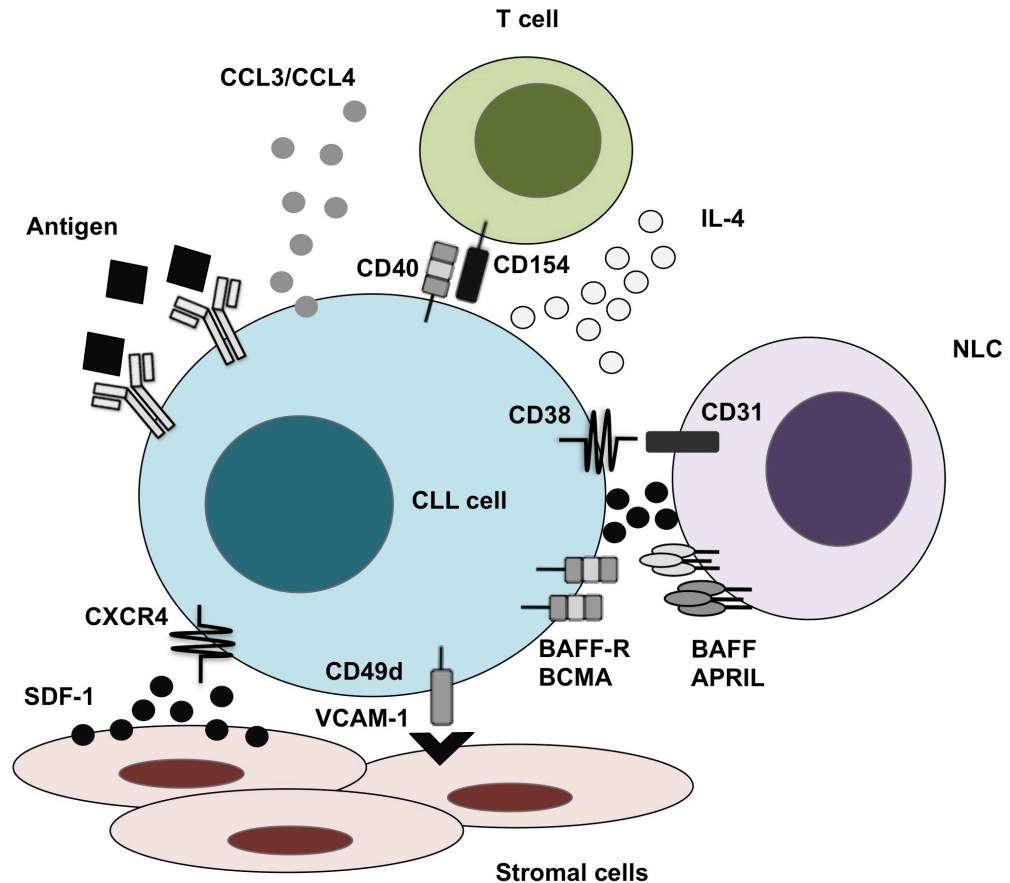


**Figure 1.10 Key interactions between CLL cells and the microenvironment**

Adhesion to BM stromal cells has been shown to induce resistance to chemotherapy in a number of haematological malignancies, including ALL (224), CML (225), and multiple myeloma (226). Stromal cell co-culture *in vitro* has been demonstrated to significantly protect CLL cells from apoptosis induced by hydrocortisone (220), chlorambucil (223), and fludarabine (227). These studies raise the possibility that chemoresistant CLL cells located within stromal-rich microenvironments in the BM and possibly LN may be responsible for the persistence of MRD and eventual relapse. In support of this, in studies assessing MRD using sensitive FCM techniques, patients with detectable MRD in the peripheral blood all had greater than 5% BM involvement (228). It is now clear that a multitude of inter-related signalling pathways are involved in stromal-mediated protection of CLL cells from apoptosis, and the key pathways are described in detail below.

### 1.7.1.1 SDF-1/CXCR4 axis

Stromal cell-derived factor-1 (SDF-1; CXCL12), is a member of the CXC chemokine family, with a number of essential functions including the retention of haematopoietic progenitor cells within the bone marrow, and homing of mature lymphocytes to secondary lymphoid organs (229). SDF-1 has been demonstrated to play a major role in attraction and retention of CLL cells to stromal microenvironments (230). SDF-1 is predominantly expressed by BM and LN fibroblasts, and although a number of splice variants have been identified, SDF-1 $\alpha$  is the main secreted form (231). SDF-1 may be secreted to stimulate cells in a cell-free manner, however SDF-1 has been well characterised to bind glycosaminoglycans in cell membranes such as heparan sulphate, and it is the latter immobilised form that is believed to account for biologically relevant signalling *in vivo* (232). The sole receptor for SDF-1 is CXCR4, a 352 amino acid G protein linked receptor (231), and an overview of CXCR4 signalling is shown in Figure 1.11. Binding of SDF-1 to CXCR4 activates the PI-3K/Akt, NF- $\kappa$ B, MEK/ERK, and Janus kinase (JAK)/STAT pathways (233, 234). In addition, Src kinases including Src, Lyn, and Fyn are phosphorylated (231, 235), and regulate activation of downstream kinases including focal adhesion kinase (FAK) (233). FAK has an important role in regulating cytoskeletal reorganisation and cell migration, through phosphorylation of downstream kinases including paxillin and p130<sup>CAS</sup> (236). A positive feedback loop exists between activated Src and FAK in which both increase the activating phosphorylation of the other (236). Termination of CXCR4 signalling is largely dependent upon SDF-1-induced internalisation of CXCR4, in a mechanism dependent upon PKC (231).

CXCR4 signalling is essential for retention of developing B lymphocyte progenitors within the BM (237), as evidenced by defective B but not T lymphopoiesis in mice lacking SDF-1 or CXCR4 (238). The mechanism by which SDF-1 retains haematopoietic progenitors within the BM involves activation of  $\beta$ 1 integrins (239). Mature B lymphocytes also express CXCR4, and although some *in vitro* studies have shown only naïve and memory B cells are responsive to SDF-1 stimulation (240), there is evidence to suggest that dynamic regulation of CXCR4 signalling is central to the transit of activated B cells through the GC (9).

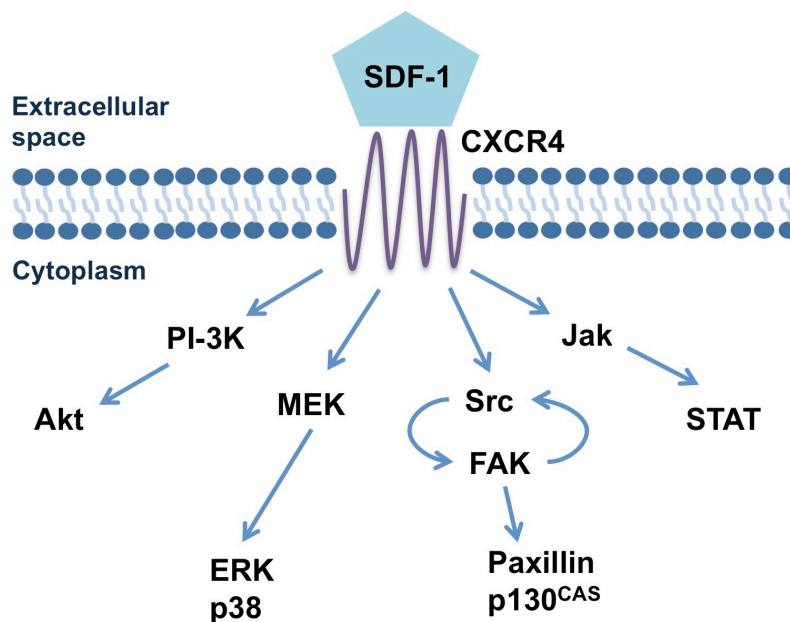


**Figure 1.11 CXCR4 signalling pathway**

CLL cells express high levels of surface CXCR4, around four-fold that of normal B lymphocytes (241). CXCR4 receptors are functional in CLL cells, as evidenced by induction of ERK phosphorylation, calcium mobilisation and actin polymerisation following SDF-1 stimulation, and migration toward SDF-1 in transwell culture experiments (230, 241). In addition, culture of CLL cells with the SDF-1-expressing murine BM stromal cell line M2-10B4 resulted in spontaneous migration of over five percent of CLL cells beneath the stromal cell layer (pseudoemperipolesis), which was confirmed to be dependent on SDF-1/CXCR4 interaction as it was inhibited by anti-CXCR4 antibodies (230). Moreover, culture of CLL cells *in vitro* with recombinant SDF-1 significantly reduced spontaneous apoptosis rates, demonstrating that SDF-1 exerts a pro-survival effect (242). Small molecule inhibitors of CXCR4 have been shown to inhibit SDF-1 signalling in CLL cells, and resensitise CLL cells co-cultured with stromal cells to chemotherapy (393).

### 1.7.1.2 Integrins

Integrins are key cell surface receptors which mediate attachment of cells to endothelial and stromal cells, and integrin function is central to co-ordinating the immune response to infection (243). Integrins are each composed of an  $\alpha$  and  $\beta$  chain heterodimer (243). CLL cells frequently express  $\beta$ 1 (CD29),  $\beta$ 2 (CD18) chains, with variable expression of  $\alpha$ 3 (CD49c),  $\alpha$ 4 (CD49d), and  $\alpha$ 5 (CD49e)

(244). Key integrins which may be expressed by CLL cells include Very Late Antigen-4 (VLA-4;  $\alpha 4\beta 1$ ), which binds vascular cell adhesion molecule-1 (VCAM-1) and fibronectin, and Lymphocyte Function-associated Antigen-1 (LFA-1;  $\alpha L\beta 2$ ), which interacts with intercellular adhesion molecules (ICAMs) (243, 245). In addition to expressing integrins, CLL cells may also express the integrin ligands ICAM-1 (CD54), ICAM-2, and ICAM-3 (245). Adhesion of CLL cells to stromal cells, and associated protection from apoptosis, has been demonstrated to involve both  $\beta 1$  and  $\beta 2$  integrins (221). Notably, an association between  $\beta$ -integrin expression and poor prognostic subsets has been reported (246). CLL cells have been reported to bind to GCs of tonsillar sections through interaction of VLA-4 with VCAM-1 (247). In addition, *in vitro* adhesion of CLL cells expressing VLA-4 to fibronectin increases expression of Bcl-2 and Bcl-x<sub>L</sub>, and inhibits both spontaneous and fludarabine-induced apoptosis (248, 249). Recently, culture of CLL cells with primary BM stromal cells has been shown to induce up-regulation of CD49d and CD54, suggesting that initial interactions between CLL cells and stromal cells may modulate the microenvironment in such a way as to favour retention of CLL cells (115). Pseudoemperipolesis of CLL cells into a stromal cell layer in response to SDF-1 has been shown to induce up-regulation of CD49d on the CLL cell surface, highlighting co-operation between chemokine and integrin signalling in the retention of CLL cells within tissues (230). Several studies have demonstrated that CD49d expression is an independent adverse prognostic indicator in CLL (250-252), implicating integrin-mediated adhesion as an important factor in both disease progression and possibly chemoresistance.

### **1.7.1.3 Angiogenic cytokines**

CLL cells have been shown to constitutively express angiogenic cytokines including VEGF, basic fibroblast growth factor (bFGF), and the negative regulator thrombospondin 1 (TSP-1), in addition to the VEGF receptor (253), raising the possibility of autocrine VEGF signalling in CLL cells. In addition to basal autocrine VEGF signalling, there is evidence to suggest that CLL cell interaction with BM stromal elements may alter cytokine expression in favour of a pro-angiogenic state. Kay *et al.* demonstrated that CLL cell co-culture with primary BM cultures resulted in a significant increase in pro-angiogenic bFGF, with a reduction in anti-angiogenic TSP-1 (223). In this study, co-culture resulted in a reduced level of secreted VEGF. These results contrast with a more recent report, in which direct

co-culture of CLL cells with the stromal cell line M2-10B4 resulted in a significant increase in VEGF secretion compared to that observed on CLL culture in transwells above stromal cells (254). VEGF stimulation of CLL cells results in induction of Mcl-1 and XIAP, and protects cells against apoptosis on chlorambucil treatment (255). Therefore, in addition to stimulating angiogenesis, stromal-induced VEGF expression may also contribute to cell adhesion-mediated chemoresistance in CLL. In support of this hypothesis, high serum VEGF levels have been significantly correlated with Mcl-1 expression in CLL cells (256), and also correlate with risk of progression in stage A CLL (257).

### **1.7.2 Nurse-like cells**

Cells capable of differentiating *in vitro* into large, adherent cells which support CLL cell survival have been identified in the blood of CLL patients, and are referred to as nurse-like cells (NLC) (242). FISH analysis has confirmed that NLCs do not arise from the CLL clone (242). Phenotypically, NLCs resemble BM stromal cells, expressing vimentin and STRO-1 (242), but also express surface CD45, CD14, and CD68, leading to the conclusion that NLCs differentiate from haematopoietic precursors related to the monocytic lineage (258). It has been proposed that NLC may differentiate within extramedullary lymphoid compartments to both attract and support the survival of CLL cells within the lymphoid microenvironment (242). In agreement with this hypothesis, CD14<sup>+</sup> splenocytes isolated from CLL patients demonstrated a phenotype consistent with NLCs, and differentiated rapidly *in vitro* into cells with a NLC morphology (258). NLCs have been shown express SDF-1, and maintain viability of CLL cells through activation of ERK-MAPK (242). In addition, it is now appreciated that NLCs regulate CLL cell survival via a number of additional signalling pathways, which are described below.

#### **1.7.2.1 BAFF and APRIL**

NLCs also express both B cell activation factor (BAFF, also known as BLyS) and a proliferation-inducing ligand (APRIL), members of the tumour necrosis factor (TNF) family of ligands (259). BAFF may bind BAFF receptor (BAFF-R), and both BAFF and APRIL can additionally interact with the receptors B-cell maturation antigen (BCMA) and transmembrane activator and calcium modulator and cyclophilin ligand-interactor (TACI) (260). BAFF and APRIL regulate B lymphocyte development, notably BAFF over-expression leads to B cell proliferation and autoimmunity in mouse models (260), while APRIL transgenic mice develop a B-1

lymphoproliferative disorder (261). The receptors for BAFF and APRIL are expressed on CLL cells, as they are on normal B lymphocytes (262, 263). Furthermore, these studies and others have confirmed that BAFF and APRIL protect CLL cells from spontaneous and drug-induced apoptosis *in vitro*, in a mechanism involving activation of NF- $\kappa$ B (259). Unlike the signalling observed in normal B lymphocytes, BAFF and APRIL activate the canonical NF- $\kappa$ B pathway in CLL cells (264). Co-culture of CLL cells with NLC in the presence of soluble BCMA significantly inhibited the protective effects of NLCs, confirming the contribution of BAFF and APRIL signalling to the anti-apoptotic effect of NLC co-culture (259).

Also in contrast to normal B lymphocytes, CLL cells themselves variably express BAFF and APRIL, raising the possibility of autocrine survival signalling in addition to paracrine stimulation from NLCs (262, 263). Of note, high serum levels of APRIL, and to a lesser extent BAFF, have been identified as negative prognostic indicators of survival in CLL (265, 266). Moreover, serum BAFF levels have recently been reported to be elevated in cases of familial CLL compared to sporadic CLL, suggesting a role in CLL pathogenesis (267).

#### **1.7.2.2 CD31/CD38 axis**

NLCs have been demonstrated to express high levels of CD31, the ligand for CD38 (268). CD38 is expressed by normal lymphocytes, and associates with the BCR and TCR in B and T lymphocytes respectively (269). CD38 expressing CLL cells are induced to proliferate on co-culture with murine fibroblasts transfected to express CD31 (268). Further investigation by this group of the mechanism responsible for this observation revealed that CD38/CD31 interaction results in co-ordinated up-regulation of the survival receptor CD100 and down-regulation of the inhibitory receptor CD72 on the CLL cell surface. Deaglio *et al.* also demonstrated NLCs to express significant plexin-B1, the ligand for CD100 (268), strengthening the hypothesis that interaction of CD38<sup>+</sup> CLL cells with CD31<sup>+</sup>/plexin-B1<sup>+</sup> NLCs is mechanistically linked to the aggressive disease course of this patient subgroup.

#### **1.7.3 T lymphocytes in CLL**

Over the last decade, accumulating evidence has amassed to confirm that there is significant dysregulation of T lymphocyte function in CLL, and it has been proposed to underlie clinical features of CLL, including hypogammaglobulinaemia

and autoimmune haemolytic anaemia (270). While normal B lymphocyte numbers progressively fall during the course of CLL, circulating T lymphocyte counts, both CD4<sup>+</sup> and CD8<sup>+</sup> subsets, are significantly elevated above normal ranges (270), and demonstrate oligoclonality (271). The contribution of direct antigenic stimulation of the TCR by CLL cells in driving the expansion of T lymphocytes remains uncertain. The CD4<sup>+</sup> T cells in the peripheral blood of CLL patients are CD45<sup>RO</sup> positive, suggesting antigen exposure, however lack additional activation markers such as CD69 and HLA-DR (272). A significant association between an increased frequency of activated CD4<sup>+</sup> lymphocytes expressing the activation marker CD54 and disease progression has been reported, however, a corresponding decrease in expression of the T cell co-receptor CD28 was seen, again suggesting incomplete T cell activation (273). CLL cells are poor antigen presenting cells, in part due to low expression of surface T cell co-stimulatory molecules CD80 and CD86 (274). Moreover, impaired immune synapse formation is observed between CLL cells and autologous CD4<sup>+</sup> and CD8<sup>+</sup> T lymphocytes, and in addition, CLL cells have been demonstrated to induce defects in immune synapse formation on contact with allogeneic T lymphocytes from healthy donors (275). These observations may explain the difficulties in generating autologous T-cell responses in the pre-clinical development of immunotherapy in CLL (276).

*In vitro* CD40 stimulation of CLL cells has been shown to increase expression of CD80 and CD86 (274), and allow induction of T cell proliferation (276), however the available evidence suggests that T lymphocytes may favour the expansion of the malignant CLL clone rather than promote eradication. Co-culture of CLL cells with CD4<sup>+</sup> T lymphocytes has been demonstrated to increase CLL cell survival *in vitro*, mediated at least partly through IL-4 signalling (277). In addition, the observation that T lymphocyte telomeres are significantly shorter in patients with ZAP-70<sup>+</sup>/CD38<sup>+</sup> progressive CLL compared to those with stable disease suggests a pathologic role for T lymphocytes in the clinical progression of CLL (278). Within LN and BM PCs, a large number of T lymphocytes are seen interspersed with the CLL cells (219, 279). The T cells are predominantly CD4<sup>+</sup> T cells (280), many of which express CD154 (279). Adding weight to the argument that T cells promote proliferation of CLL cells, a recent study demonstrated that within PCs in primary CLL patient LN samples, Ki67<sup>+</sup> CLL cells were significantly more likely to be directly associated with an adjacent CD4<sup>+</sup> T cell than Ki67<sup>-</sup> CLL cells (281). T cells

from CLL patients with progressive disease have been demonstrated to show increased spontaneous and induced secretion of many cytokines, including IL-2, IL-4, and TNF $\alpha$  (282). Of note, with advancing stage CLL, the predominant CD4<sup>+</sup> T cell subset shifts from a T helper 1 (Th<sub>1</sub>) to IL-4-producing Th<sub>2</sub> population (283). The shift in CD4<sup>+</sup> repertoire has been demonstrated to be driven by the CLL clone itself, as co-culture of CLL cells with allogeneic CD4<sup>+</sup> T lymphocytes led to down-regulation of T cell p38- and JNK-MAPK activity, required for Th<sub>1</sub> differentiation (284). Further supporting the case that CD4<sup>+</sup> T cells promote CLL progression, the percentage of peripheral blood CD4<sup>+</sup> memory T lymphocytes in the CD4<sup>+</sup> T cell pool has been reported to be significantly greater in unmutated as compared to mutated CLL, and was shown to be an independent predictor for short treatment-free survival on multivariate analysis (277).

### **1.7.3.1 CD40 signalling in CLL**

CD40 is a 45 kDa member of the TNF receptor superfamily, expressed on normal and malignant B cells, monocytes, and dendritic cells, and has a key role in promoting effective antigen presentation to T lymphocytes (285). CD154 is one of the main co-stimulatory molecules expressed by activated CD4<sup>+</sup> T cells, and CD40 stimulation of B lymphocytes leads to up-regulation of MHC II and the T cell co-stimulatory molecules CD80 and CD86 (285). Upon stimulation, CD40 clusters within lipid rafts and associates with TNF receptor-associated factor proteins (TRAFs), that mediate the recruitment and activation of several signalling kinases, including PI-3K, PLC $\gamma$ , ERK-, p38-, and JNK-MAPK (286). A schematic representation of downstream signalling pathways is shown in Figure 1.12. Activation of NF- $\kappa$ B leads to increased transcription of Bcl-2 family anti-apoptotic genes, including Bcl-x<sub>L</sub> and A1. In addition to promoting cellular survival, CD40 signalling also promotes proliferation, through increasing expression of cyclin-D dependent kinases cdk4 and cdk6, at the same time as decreasing expression of the cell cycle inhibitory kinase p27<sup>kip1</sup> (286).

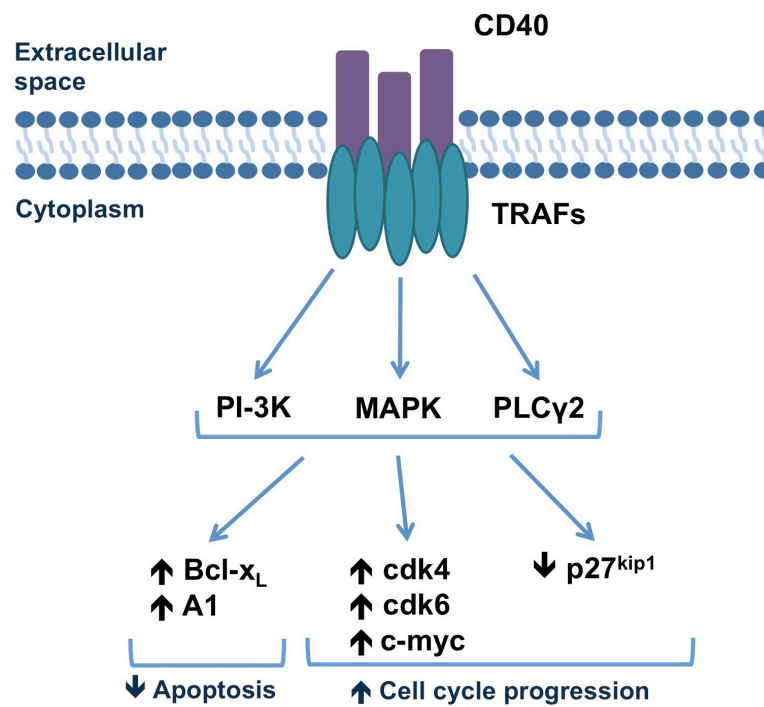


**Figure 1.12 Overview of CD40 signalling**

CLL cells variably express both CD40 and CD154, raising the possibility of yet another autocrine signalling pathway (287), in addition to paracrine signalling through interaction with adjacent CD154-expressing T lymphocytes within the PC. CD40 stimulation of CLL cells *in vitro* inhibits spontaneous apoptosis (288). The anti-apoptotic effect of CD40 stimulation has been demonstrated to involve NF-κB activation (288), resulting in up-regulation of the anti-apoptotic Bcl-2 family proteins Mcl-1, Bcl-x<sub>L</sub>, and Bfl-1 (289, 290). Although alterations in pro-apoptotic Bcl-2 family proteins also occur following CD154 stimulation of CLL cells, in particular increased expression of Bid (290, 291), and down-regulation of Noxa (292), the balance of Bcl-2 proteins favours cell survival. Furthermore, the Fas-antagonist Flip is up-regulated on CD154 stimulation of CLL cells (289), and CD154-stimulated CLL cells have been shown to be resistant to Fas ligand-induced apoptosis (290). In addition to maintaining CLL cell survival, CD40 signalling has been shown in many studies to induce proliferation of CLL cells *in vitro* (293, 294). CD40 signalling also contributes to chemoresistance in CLL, as CD154 stimulation significantly reduces the sensitivity of CLL cells to apoptosis on treatment with fludarabine *in vitro* (289, 290).

Another example of CLL cells shaping the microenvironment comes from the observation that *in vitro* CD154 stimulation induces CLL cells to express CCL17

and CCL22, and secrete CCL22, a potent CD4<sup>+</sup> T lymphocyte chemoattractant, which binds the receptor CCR4 on activated T cells (279). Culture supernatants from CD154 stimulated CLL cells stimulated migration of CD4<sup>+</sup>CD154<sup>+</sup> T lymphocytes in transwell assays (279), suggesting that CD40 stimulated CLL cells within PCs may actively recruit additional T lymphocytes, which in turn could promote survival and proliferation of a larger CLL clone.

### 1.7.3.2 IL-4 signalling in CLL

Binding of IL-4 to the IL-4 receptor on normal B lymphocytes leads to activation of JAK kinases, which recruit signalling components to the receptor, including STAT proteins and insulin-receptor substrate 1 (IRS-1) and IRS-2 (295), as shown in Figure 1.13. IRS-1 and -2 recruit the p85 subunit of PI-3K, which activates Akt, and STAT homodimers translocate to the nucleus to direct gene transcription. IL-4 signalling prevents apoptosis of B cells through stabilisation of Bcl-2, protection from Fas-induced apoptosis (295).

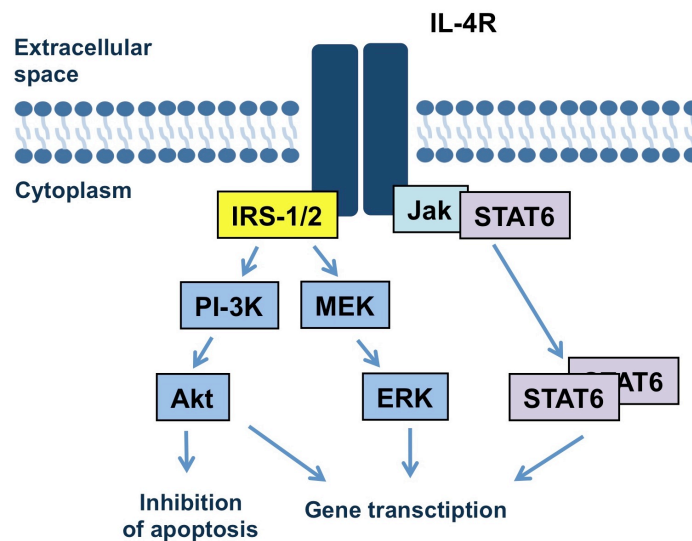


**Figure 1.13 Overview of IL-4 signalling**

CLL cells express higher levels of IL-4 receptors than normal B cells (296), and correspondingly, T lymphocytes isolated from CLL patients secrete greater amounts of IL-4 in response to phytohaemagglutinin (PHA) than T cells from healthy donors (297). IL-4 receptors are functional on CLL cells, as IL-4 stimulation has been shown to induce STAT1, STAT5, and STAT6 activation (295), in addition to phosphorylation of PKC and Akt (298). *In vitro* culture of CLL cells with IL-4 reduces spontaneous apoptosis (296); this pro-survival effect was

blocked on incubation with IL-4 and a blocking antibody to IL-4R (299). Akin to normal B lymphocytes, IL-4 stimulated CLL cells are resistant to Fas-mediated apoptosis (298). In addition, CLL cells stimulated with IL-4 *in vitro* were significantly less sensitive to the apoptotic effects of dexamethasone and fludarabine, through a PI-3K dependent mechanism (300). IL-4 represents yet another potential autocrine signalling pathway in CLL, as CLL cells also express IL-4 (299).

## **1.8 Potential novel therapeutic strategies based on knowledge of CLL biology**

The identification of numerous signalling pathways that govern CLL cell survival, proliferation, and chemoresistance *in vitro* have provided translational researchers with a wealth of novel targets against which to design therapeutic agents, as evidenced by the wealth of targeted small molecule inhibitors and monoclonal antibodies currently in pre-clinical development or phase I/II clinical trials (301). However, the multitude of potential targets also raises the problem of identifying the key, non-redundant, signalling pathways to which the malignant cells are 'addicted'. Given the heterogeneity of CLL, these pathways may differ between prognostic groups, and furthermore, in the knowledge that CLL cells circulate between blood and lymphoid tissues, may also differ depending on the anatomical location of cells within individual patients. To be informative, future translational studies must address the efficacy of potential novel therapeutic agents not only on CLL cells themselves, but also on malignant cells within the context of the supportive microenvironment. While targeted chemotherapy remains a goal, the question remains as to whether in the context of the CLL microenvironment single targeted therapies will be sufficient to induce CLL cell apoptosis, or whether combinations of targeted agents may be necessary to induce apoptosis directly, or overcome resistance to conventional chemotherapy. This project aims to address these issues, utilising investigational agents based on advances in CLL biology.

### **1.8.1 Rationale for investigation of the Src/c-Abl TKI dasatinib**

As outlined in Section 1.6, both basal and stimulated signalling through the BCR is heavily implicated in the pathogenesis of CLL, therefore inhibition of BCR signal transduction is a rational novel therapeutic approach. In view of the data demonstrating that inhibition of either c-Abl or Src kinases induces apoptosis of

CLL cells *in vitro* (203, 212), we were interested to examine the anti-leukaemic effects of dual Src/c-Abl TKIs in CLL.

Dasatinib (Srycel™ formerly BMS-354825, Figure 1.14) is a potent dual Src and c-Abl TKI, developed by the pharmaceutical company Bristol-Myers Squibb, for the treatment of CML. CML is characterised by a reciprocal translocation between chromosomes 9 and 22, creating the Philadelphia chromosome, a product of which is the fusion protein Bcr-Abl, a constitutively active tyrosine kinase (302). The Bcr-Abl TKI imatinib revolutionised the treatment of CML, however some patients are resistant to therapy due to Src-family kinase activity (206). Dasatinib was selected for further investigation from a panel of thiazole-based dual Src/Abl kinase inhibitors on the basis of potency and favourable pharmacokinetic and pharmacodynamic profile *in vivo* on pre-clinical testing (303), and the chemical structure is shown in Figure 1.14.

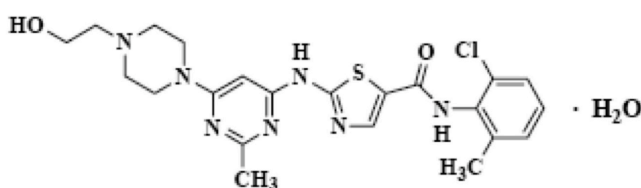


**Figure 1.14 The chemical structure of dasatinib**

Dasatinib binds with subnanomolar affinity to the ATP-binding site of Bcr-Abl (and wild-type c-Abl) with a 325-fold greater affinity than imatinib (303). Part of the greater potency of dasatinib for binding to Bcr-Abl is due to the ability of dasatinib to bind to both active and inactive conformations of the kinase (304). An  $IC_{50}$  below 1 nM was also observed for dasatinib binding to all Src-family tyrosine kinases assessed, including c-Src, Lck, and Yes (303). In this study, dasatinib also bound c-kit ( $IC_{50}$  5nM), platelet-derived growth factor receptor  $\beta$  (PDGFR $\beta$ ;  $IC_{50}$  28 nM), and VEGF receptor (VEGFR;  $IC_{50}$  2000 M). Recent studies have identified additional significant kinase targets for dasatinib, including the Tec family kinases Btk ( $IC_{50}$  5 nM) and Tec ( $IC_{50}$  297 nM), which are essential for normal antigen receptor signalling in B and T lymphocytes (305). Chemical proteomic approaches using CML cell lines and primary cells have now identified over thirty kinase targets of dasatinib (306, 307). Dasatinib has been extensively shown to exert potent antitumour activity in xenograft mouse models of CML, using the

K562 cell line (303, 308). In these studies dasatinib was administered once or twice daily, with similar efficacy.

Pharmacokinetic and pharmacodynamic studies in mouse models informed dasatinib dosing in early clinical trials, with dasatinib used as a dose of 140 mg daily, either as a once daily dose, or twice-daily split dose (308). Dasatinib used at these doses induced significant haematological and cytogenetic responses in CML patients resistant or refractory to imatinib (309). Dasatinib was approved by the United States FDA in 2006 for the treatment of CML and Philadelphia chromosome positive ALL (310). The pivotal phase II study of dasatinib 70 mg twice daily in imatinib-resistant or intolerant patients with chronic phase CML reported 90% patients to achieve complete haematological remission, and 52% major cytogenetic remission (310). Side effects noted included headache, diarrhoea, peripheral oedema, and pleural effusions, which were rarely severe, however grade 3 to 4 cytopenias were frequent, specifically, neutropenia (49%), thrombocytopenia (47%), and anaemia (22%). A subsequent dose and scheduling trial demonstrated a dose of 100 mg once daily to be as efficacious as 70 mg twice-daily, and to significantly reduce the incidence of side effects, including pleural effusion (311). The incidence of grade 3 to 4 neutropenia fell from 42 to 33%, and thrombocytopenia from 37 to 22%, and 100 mg once daily dosing is now standard practice in CML. In addition to inducing apoptosis of CML cells, dasatinib has been demonstrated to induce apoptosis of lung cancer and head and neck cancer cell lines (312, 313).

### **1.8.2 The rationale for inhibition of Bcl-2 family proteins in CLL**

Apoptosis, or programmed cell death, is central to normal tissue homeostasis. Normal regulation of apoptosis plays a major role in prevention of autoimmunity and malignancy, and also describes the mechanism of cell death induced by the majority of chemotherapeutic agents (314). There are two main routes to apoptosis; the extrinsic pathway is activated by the binding of cell surface 'death receptors', while the intrinsic pathway is generally activated by intracellular stress due to cytotoxic agents, radiation, or lack of growth factor stimulation (315). Both pathways lead to activation of a succession of cysteine proteases termed caspases, of which initiator caspases sequentially activate effector caspases that sequentially cleave essential intracellular proteins. The two apoptotic pathways are outlined in Figure 1.15.

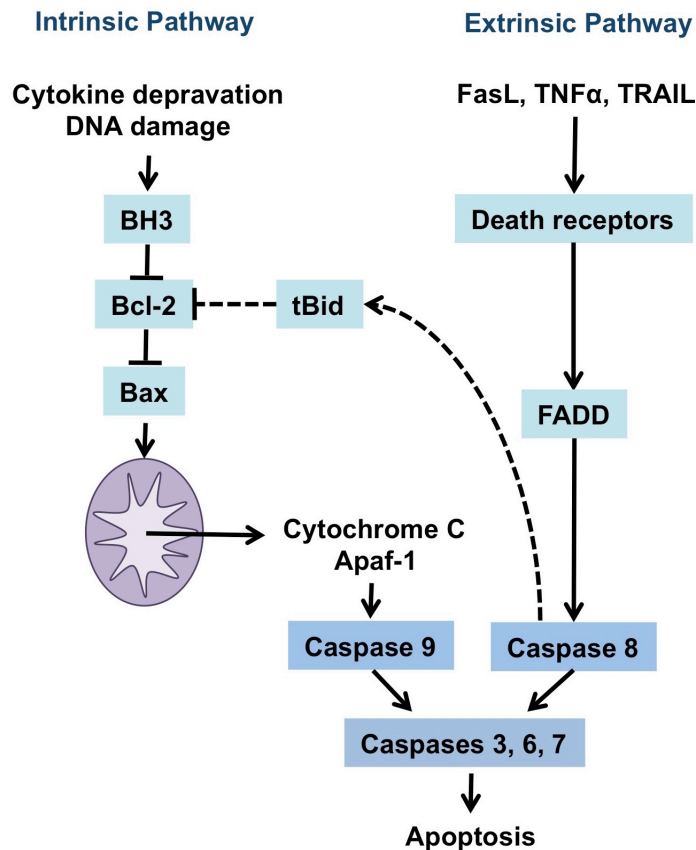


**Figure 1.15 Outline of intrinsic and extrinsic apoptotic pathways**

The extrinsic pathway is activated on engagement of the TNF-family receptor Fas (CD95) or TNF-related apoptosis-inducing ligand (TRAIL) receptors on the cell surface, recruiting Fas-associated death domain (FADD), leading to activation of caspase 8. In outline, the intrinsic pathway is activated by the release of cytochrome c from the mitochondrial intermembrane space. Cytoplasmic cytochrome c induces a structural change in the apoptosis protease activating factor-1 (Apaf-1), which can then bind pro-caspase 9 via caspase recruitment domains (CARDs), leading to formation termed the apoptosome complex, which activates caspase 9 (315). Bcl-2 family proteins are central to the regulation of this pathway by controlling the integrity of the mitochondrial membrane. Activated caspase 8 or 9 then activate the effector caspases, caspases 3, 6, and 7, which effect DNA and protein degradation (315). Although largely independent, cross-activation of the intrinsic pathway by external pathway apoptotic signals can occur, as caspase 8 cleaves Bid to its' pro-apoptotic form, truncated Bid (tBid), which then antagonises anti-apoptotic Bcl-2 proteins (315).

As the Bcl-2 family of proteins are implicated in the intrinsic resistance of CLL cells to chemotherapy, and in resistance induced by external signals from the

microenvironment, this pathway has received much interest as a novel therapeutic target in CLL. The Bcl-2 family of proteins comprises three groups of proteins, the pro-apoptotic members Bax and Bak, the anti-apoptotic group including Bcl-2, Bcl-x<sub>L</sub>, Mcl-1, Bcl-w, Bcl-2A1, and Bcl-B, and the final group of small proteins containing only the third Bcl-2 homology domain (BH3) in common with the others, which comprises Bim, Bad, Bid, Bik, Noxa, Puma, Bmf, and Hrk (316). Upon activation, Bax and Bak form oligomeric pores in the outer mitochondrial membrane, resulting in cytochrome c release (316). This process is accompanied by a reduction in mitochondrial inner membrane potential (MMP) (317). Two opposing models concerning the control of Bak and Bax activity continue to be debated (318, 319). The indirect activation model states that anti-apoptotic Bcl-2 proteins bind Bak and Bax, preventing their oligomerisation. In this model, BH3 proteins may activate apoptosis by competing with Bak and Bax for binding to anti-apoptotic Bcl-2 proteins, resulting in any displaced Bak and Bax becoming free to heterodimerise. The alternative direct activation model proposes that Bak and Bax require direct activation, by interaction with BH3 proteins, and proposes that the main role of anti-apoptotic Bcl-2 proteins may be to sequester such BH3 'activators' (including Bim, tBid, and Puma). This model suggests apoptosis may be initiated on displacement of these activator BH3 proteins by 'sensitiser' BH3 proteins including Bad (314).

The observation that a high Bcl-2/Bax ratio correlated with resistance to chemotherapy-induced apoptosis of CLL cells *in vitro* (320), led to investigation of the effect of specific inhibition of Bcl-2 with siRNA. Down-regulation of Bcl-2 using antisense RNA in CLL cells *in vitro* led to increased apoptosis (321), and chemosensitised CLL cells to chlorambucil (322). Phase I and II trials of oblimersen sodium, a clinical-grade Bcl-2 antisense oligonucleotide, in fludarabine-refractory patients however proved disappointing with partial responses seen in only two of twenty-six evaluable patients (323). More recently, a phase III randomised controlled trial of fludarabine and cyclophosphamide, with or without oblimersen, reported an increase in CR rate from 8 to 17%, and a significant increase in PFS and OS with the addition of oblimersen in heavily pre-treated patients (324).

One proposed explanation for the limited results observed with targeted Bcl-2 down-regulation was that the approach may in fact be too narrowly targeted, given the demonstration that in addition to Bcl-2, Mcl-1 and Bcl-x<sub>L</sub> are induced by a

number of microenvironmental stimuli and implicated in chemoresistance. Several small molecule inhibitors have subsequently been identified and developed which are structurally similar to the BH3-only Bcl-2 proteins, termed 'BH3 mimetics', which are able to compete with native BH3 proteins and/or Bax and Bak for binding to several anti-apoptotic Bcl-2 proteins (325, 326). The BH3-mimetic ABT-737 binds Bcl-2, Bcl-x<sub>L</sub>, and Bcl-w, and induces apoptosis of CLL cells at low nanomolar concentrations *in vitro* (327, 328). ABT-737 induces significantly less apoptosis of CLL cells co-cultured with stromal cells (329), leading to the conclusion that even agents demonstrated to have potent apoptosis-inducing effects *in vitro* may need to be studied in combination with agents targeting non-overlapping survival pathways.

### **1.8.3 Rationale for inhibition of heat shock protein 90**

Heat shock proteins function as chaperone proteins, regulating the stability of client proteins through direct association. Heat shock protein 90 (HSP90) exists in two conformations, a resting state with low ATPase activity, which is the predominant form found in normal cells, however on ATP-binding HSP90 undergoes a conformational change to become highly active and able to form multi-protein complexes (330). In an ATP-bound state, HSP90 may interact with a number of potential client proteins, including growth factor receptors (eg, VEGFR), proteins involved in survival signalling pathways (eg, Src kinases, Akt and Raf-1), and cell cycle control (eg, survivin, cdk2, and cdk4) (330). HSP90 is over-expressed in CLL cells compared to normal B cells, with expression level correlating with advanced disease (331). Recently, ZAP-70 was shown to be a novel conditional HSP90 client protein within CLL cells (332). Although ZAP-70 positive and negative CLL cells express similar amounts of HSP90, only in ZAP-70 positive cases has HSP90 been found in the highly active ATP-bound conformation (332).

The prototype HSP90 inhibitor is the ansamycin antibiotic geldanamycin (GA), which competes with ATP for the ATP-binding domain of HSP90 (333). GA has limited therapeutic potential due to frequent hepatotoxicity and poor stability (333). Analogues of GA have been developed, including 17-allylamino derivative (17-AAG), and the more potent and orally bioavailable 17-desmethoxy-17-N,N-dimethylaminoethylamino-geldanamycin (17-DMAG), and are currently undergoing investigation in a number of cancers, including haematological malignancies (330,

333). GA has been demonstrated to induce apoptosis of CLL cells *in vitro*, and sensitise CLL cells to chemotherapy and rituximab (334, 335). Notably, HSP90 inhibition with 17-AAG has been demonstrated to lead to degradation of ZAP-70 and impair BCR signal transduction in CLL cells (332). In this study, a significant linear relationship was observed between ZAP-70 expression and apoptosis induced by 17-AAG (and similar greater response in unmutated compared to mutated CLL), suggesting HSP90 inhibition may be of particular benefit to high-risk patients (332). Of note, a recent study also reported that GA down-regulated mutated p53 whilst up-regulating wild-type p53 (336).

The effects of HSP90 inhibitors on CLL cells exposed to microenvironmental stimuli have not been investigated. In view of this class of inhibitors potentially inhibiting a number of pro-survival signalling pathways, and reducing ZAP-70 expression, HSP90 inhibitors are attractive agents to study in combination with agents aimed at targeting BCR signalling.

## 1.9 Aims and objectives

The primary aim of this project was to thoroughly investigate the potential of the Src/c-Abl TKI dasatinib as a novel therapeutic agent for the treatment of CLL, both as a single agent, and in rationally designed combination strategies. In addition, the effect of dasatinib on BCR signal transduction was assessed.

Experiments were designed to address the following specific aims:

- i. To assess the ability of dasatinib to induce apoptosis of CLL cells *in vitro*, and determine whether response correlates with established prognostic parameters.
- ii. To investigate whether dasatinib exhibits synergy with established chemotherapeutic agents fludarabine and chlorambucil, and also with BH3-mimetic Bcl-2 inhibitors and the HSP-90 inhibitor 17-DMAG.
- iii. To establish whether dasatinib inhibits B cell antigen receptor signalling in CLL cells.
- iv. To test dasatinib, alone and in promising combinations, in stromal co-culture models which reproduce signalling networks encountered in the microenvironment.

**Chapter 2:**  
**Materials and Methods**

## **2.1 Cells and Reagents**

Addresses of suppliers of the materials and reagents used during this project are listed in Table 2.1

### **2.1.1 CLL patient samples**

Peripheral blood samples were obtained after written informed consent with the approval of the Local Research and Ethics Committee, from patients with a clinically confirmed diagnosis of B cell CLL. Samples were accepted from patients at all points of the disease course, with the only exclusion being patients that had received chemotherapy for CLL within the preceding three months. Linked clinical data on clinical stage (Binet), treatment history, ZAP-70 expression, and cytogenetic abnormalities by FISH where available were stored. Details of the samples collected are listed in Table 2.2.

### **2.1.2 Normal blood samples**

Buffy coat components from normal healthy blood donors were obtained from the Scottish National Blood Transfusion Service, with approval of the organisation's ethical review committee. Buffy coat components contain a high concentration of leucocytes and platelets, and were used as a source of normal B lymphocytes for experiments (see Section 2.2.6). Buffy coat components were received 24 hr after bleeding of the donor, once results of routine virology screening were available.

### **2.1.3 Drugs and Inhibitors**

Details of the stock concentrations, diluents, and storage conditions of all drugs and inhibitors used are listed in Table 2.3. The chemotherapeutic drugs chlorambucil and fludarabine were purchased from Sigma Aldrich Ltd. Further details of the properties of individual inhibitors are detailed below.

PP2 is an ATP-competitive inhibitor of all Src family kinases, while the related inhibitor PP3 has no Src kinase inhibitory activity, and is a recommended negative control for PP2. Both PP2 and PP3 were purchased from Merck Chemicals Ltd. Dasatinib was initially supplied by Bristol-Myers Squibb under a Materials Transfer Agreement, and later purchased from LC Laboratories. Imatinib mesylate was also purchased from LC Laboratories.

Bcl-2 inhibitor I, Bcl-2 inhibitor III, the HSP90 inhibitor 17-DMAG, PI-3K and MAPK inhibitors were all obtained from Merck Chemicals Ltd. Bcl-2 inhibitor I comprises a mixture of two tautomers, which compete with Bak BH3 peptide for binding to

both Bcl-2 ( $IC_{50} = 10 \mu\text{M}$ ) and Bcl-x<sub>L</sub> ( $IC_{50} = 7 \mu\text{M}$ ) (325). Bcl-2 inhibitor III (EM20-25) binds Bcl-2, leading to disruption of interaction of Bcl-2 with Bax (337). 17-DMAG is a potent ATP-competitive HSP-90 inhibitor ( $IC_{50} = 51 \text{ nM}$  for HSP-90 $\alpha$ ).

LY294002 is a selective PI-3K inhibitor ( $IC_{50} = 1.4 \mu\text{M}$ ), which binds the ATP-binding site of the enzyme. PD98059 is a cell-permeable MEK kinase inhibitor, with an  $IC_{50}$  of  $4 \mu\text{M}$  for MEK1. SB203580 is an inhibitor of p38 MAPK ( $IC_{50} = 34 \text{ nM}$  *in vitro*,  $600 \text{ nM}$  in cells), with little inhibition of JNK and p42 MAP kinase. Insolution™ JNK inhibitor II is a selective, reversible JNK inhibitor ( $IC_{50} = 40 \text{ nM}$  for JNK-1 and JNK-2, and  $90 \text{ nM}$  for JNK-3).

The pan-caspase inhibitor Z-Val-Ala-DL-Asp(OMe)-fluoromethylketone (Z-VAD-fmk) was purchased from Bachem. Z-VAD-fmk was used at a final concentration of  $25 \mu\text{M}$ , and was added to CLL cells 2 hours prior to the addition of dasatinib, to allow full caspase inhibition prior to drug treatment.

#### **2.1.4 Chemokines and cytokines**

Recombinant human SDF-1 $\alpha$  (CXCL12) was purchased from R&D Systems as a lyophilised powder. The powder was reconstituted at  $10 \mu\text{g/ml}$  in phosphate buffered saline (PBS) supplemented with 0.1% bovine serum albumin (BSA) and stored at  $-20^{\circ}\text{C}$ . Recombinant human IL-4 was purchased from Peprotech EC Ltd. as a lyophilised powder, which was reconstituted to  $10 \mu\text{g/ml}$  in sterile water and stored at  $-20^{\circ}\text{C}$  until required.

#### **2.1.5 Antibodies**

Biotinylated mouse anti-human IgM, and purified mouse IgG1  $\kappa$  isotype control were purchased from BD Biosciences. Goat F(ab')<sub>2</sub> fragments to human IgM were purchased from MP Biomedicals as a lyophilised powder, which was reconstituted with distilled water to a final antibody concentration of  $3.5 \text{ mg/ml}$ , and stored at  $4^{\circ}\text{C}$  until used.

All antibodies used in FCM were purchased from BD Biosciences, and are listed in Table 2.4. Antibodies used for western blotting are detailed in Table 2.5.

## **2.2 Tissue culture**

All procedures were performed using sterile technique in a laminar air flow hood. All tissue culture consumables (tissue culture plates, tubes, and pipettes) were

purchased from Fisher Scientific U.K. or Greiner Bio-One Ltd. unless otherwise stated.

### **2.2.1 Purification of CLL cells from patient samples**

CLL cells were isolated from whole blood using Rosettesep™ human B cell enrichment cocktail (StemCell Technologies), following manufacturers' instructions as follows. Rosettesep™ was added to whole blood at 50 µl/ml and incubated at room temperature (RT) for 20 min. The blood was then diluted with an equal volume of sterile PBS, layered onto Histopaque®-1077 density separation medium (Sigma Aldrich Ltd.), and centrifuged at 850 g for 20 min. The cells at the Histopaque®:plasma interface were removed and washed twice in sterile PBS by centrifugation at 300 g for 5 min. CLL cell separation efficiency was assessed by FCM, using the following fluorochrome conjugated antibodies - CD19-FITC, CD5-PE, and CD23-APC, as described in Section 2.3.1. The CD19<sup>+</sup>/CD5<sup>+</sup> population was over 95% in all cases, and a representative example of purification is shown in Figure 2.1. Prior to cryopreservation,  $2 \times 10^7$  cells were transferred to a fresh tube for preparation of protein lysates.

### **2.2.2 Cell counting using a haemocytometer**

To determine cell counts prior to cryopreservation of cells and when setting up experiments, cells were counted using the trypan blue exclusion method. Briefly, trypan blue (Sigma Aldrich Ltd.) was diluted 1:10 (v/v) in PBS to a working stock. Cells were diluted in trypan blue solution to enable at least 100 viable cells (able to exclude trypan blue dye) to be counted over two 1 mm<sup>2</sup> squares of a haemocytometer chamber (Hawksley). The absolute cell count was determined by multiplying the number of cells per mm<sup>2</sup> by first the dilution factor from the starting cell concentration, then multiplying again by 10<sup>4</sup> to determine the cell count per ml.

### **2.2.3 Cryopreservation of cells**

CLL cells were prepared as above, then resuspended in freezing media (90% fetal bovine serum (FBS; Invitrogen Ltd.) and 10% dimethylsulphoxide (DMSO)) at a concentration of  $2-4 \times 10^7$  cells/ml. The resulting cell suspension was transferred to 2 ml cryovials (Greiner BioOne Ltd.) in 1 ml aliquots. Cryovials were frozen slowly at around 1°C per hour by transferring to polystyrene containers and placing in a freezer at -80°C overnight. Cryovials were subsequently transferred to a -150°C freezer for long-term storage.

#### **2.2.4 Recovery of cryopreserved samples**

Cells were thawed at 37°C by suspending the cryovial in a waterbath, with gentle agitation, until the ice crystals had melted, then transferred to a 15 ml sterile tube. To ensure slow rehydration of cells, and removal of cell debris, 10 ml 'DAMP' solution (DNAse I 10000 units/L (Stemcell Technologies), MgCl<sub>2</sub> 2.5 mM, trisodium citrate 16 mM (both Sigma Aldrich Ltd.), 1% Human Serum Albumin (SNBTS) in PBS) was added dropwise over 20 min, with gentle agitation, and then centrifuged at 300 g for 5 min.

#### **2.2.5 Culture of CLL cells**

Following recovery, CLL cells were washed once in 10 ml RPMI-1640 containing 10% FBS, 50 U/ml penicillin, 50 µg/ml streptomycin, and 2 mM L-glutamine (Invitrogen Ltd.) (complete media), resuspended in 10 ml complete media and incubated overnight in a 25 cm<sup>2</sup> flask in a humidified atmosphere containing 5% CO<sub>2</sub> prior to treatment. Unless otherwise specified, CLL cells were cultured at 1 x 10<sup>6</sup>/ml in complete media during experiments.

#### **2.2.6 Isolation of B lymphocytes from buffy coats**

##### **2.2.6.1 Mononuclear cell preparation**

The individual buffy coats (approximately 50 ml) were diluted with an equal volume of sterile PBS. The diluted sample was divided into 25 ml aliquots, which were layered over 15 ml Histopaque<sup>®</sup>-1077 density separation medium in a 50 ml Leucosep<sup>®</sup> tube (Greiner Bio-One Ltd.) and centrifuged at 400 g for 20 min. The mononuclear cell (MNC) layer was transferred using a Pasteur pipette to a 15 ml sterile tube, and washed twice with PBS by centrifugation (300 g for 5 min). MNCs were sometimes cryopreserved at this stage for later B cell selection.

##### **2.2.6.2 CD19 selection using magnetic cell sorting**

This protocol was used to enrich B lymphocytes from buffy coat MNC preparations. The mononuclear cell sample was diluted in MACS buffer (PBS supplemented with 2mM EDTA and 0.5% BSA (both Sigma Aldrich Ltd.)) at 4°C. Cells were counted using a haemocytometer, and 1 x 10<sup>8</sup> cells were transferred to a fresh tube and washed in MACS buffer by centrifugation at 300 g for 10 min. Cells were resuspended in 800 µl MACS buffer, following which 200 µl (20 µl per 1 x 10<sup>7</sup> cells) human CD19 MicroBeads (Miltenyi Biotec) were then added, and cells incubated at 4°C for 15 min. After incubation, cells were washed in 10 ml

MACS buffer as above, and resuspended in 3 ml MACS buffer prior to magnetic separation. Concurrently, an LS positive selection column (Miltenyi Biotech) was prepared by inserting the column into a MidiMACS<sup>®</sup> magnet (Miltenyi Biotech) and rinsing with 3 ml MACS buffer. The labelled cell suspension was then added to the column, followed by three washes each with 3 ml MACS buffer to remove trapped unlabelled cells. The flow-through solution was retained for later analysis. Next, the column was removed from the magnet and transferred to a fresh 15 ml collection tube. The cells were removed from the column by adding 5 ml MACS buffer to the column and flushing briskly with the plunger supplied. Cells were washed twice in MACS buffer (300 g for 5 min) then resuspended in 10 ml complete medium, counted, and cultured in a 25 cm<sup>2</sup> tissue culture flask overnight. In each case, to confirm the efficacy of CD19<sup>+</sup> enrichment, samples of the cell suspension before and after MACS separation were stained with anti-CD19 PE. A typical FCM plot is shown in Figure 2.2.

## **2.2.7 Cell Lines**

### **2.2.7.1 NT-L and CD154L cells**

Mouse fibroblast L-cells (NT-L) and L-cells stably transfected with CD154 (CD40 ligand; CD154L cells) were a gift of Professor J. Gordon (University of Birmingham, UK). Both cell lines were maintained in complete medium at 37°C in a humidified atmosphere containing 5% CO<sub>2</sub>. Every 3-5 days, when the cell density approached confluency, cells were detached from the plate with trypsin, final concentration 0.05% in PBS (Invitrogen Ltd.), washed and re-cultured at a 1/10 dilution. Expression of CD154 by CD154L cells was confirmed by FCM (Fig. 2.3).

### **2.2.7.2 M2-10B4 cells**

The murine fibroblast cell line M2-10B4 was sourced from stocks held within our laboratory. M2-10B4 cells are known to express SDF-1 (230) This cell line was maintained in complete medium as above.

### **2.2.7.3 Ramos cells**

The Burkitt lymphoma cell line Ramos was a kind gift of Professor M. Harnett (University of Glasgow, UK). Ramos cells were maintained in complete media, with 4/5 media change every 72 hr to maintain an optimal cell density.

#### **2.2.7.4 HT29 cells**

The colon carcinoma cell line HT29, which is known to express high levels of constitutively phosphorylated Src and FAK kinases, was a gift of Dr. V. Brunton (University of Edinburgh, UK). HT29 cells were cultured in Dulbecco's Modified Eagle Medium (DMEM; Invitrogen, U.K.), supplemented with 10% FBS, 50 U/ml penicillin, 50 µg/ml streptomycin, and 2 mM L-glutamine.

#### **2.2.8 CLL cell stimulation**

##### **2.2.8.1 Short term BCR stimulation using biotinylated anti-IgM**

CLL cells were incubated in RPMI-1640 containing 0.5% BSA for 2 hr prior to BCR stimulation. Cells ( $3 \times 10^6$ /condition) were incubated in 1.5 ml eppendorf tubes at 4°C in 100 µl 0.5% BSA media supplemented with 10 µg/ml biotinylated anti-IgM ± 100 nM dasatinib for 30 min. Cells were then washed in 1 ml ice-cold PBS and resuspended in 100 µl 0.5% BSA media ± 100 nM dasatinib as appropriate. For stimulated cells, 100 µl avidin (Sigma Aldrich) at a concentration of 50 µg/ml was added (final concentration 25 µg/ml), and cells incubated at 37°C in a waterbath for 10 or 30 min. Avidin was not added to unstimulated control cells. At the end of incubation times, tubes were placed on ice and 1 ml PBS supplemented with PhosStop Phosphatase Inhibitor Cocktail Tablets (Roche Diagnostics Ltd.) was added. Cells were pelleted by centrifugation (600 g for 5 min) and protein lysates prepared.

##### **2.2.8.2 Long term BCR stimulation with anti-IgM F(ab')<sub>2</sub> fragments**

The addition of soluble anti-IgM F(ab')<sub>2</sub> fragments to culture media has been widely employed to mimic continuous antigen exposure of CLL cells *in vitro* (192, 195). CLL cells were incubated in complete medium and treated as follows: untreated control, 100 nM dasatinib; 10 µg/ml anti-IgM F(ab')<sub>2</sub> fragments, or; both dasatinib and anti-IgM F(ab')<sub>2</sub> fragments. After 48 hr culture, cells were harvested and an aliquot of one-tenth of the cells assessed for viability using Annexin V/VIprobe, and the remainder used to prepare protein lysates.

##### **2.2.8.3 Long term BCR stimulation with immobilised anti-IgM**

Anti-IgM antibodies immobilised on tissue culture plates or microbeads has been proposed to allow more persistent BCR stimulation of CLL cells *in vitro* than soluble anti-IgM due to both higher ligand valency and the prevention of BCR downregulation, and suggested as a model for T cell-independent antigenic

stimulation (192). Therefore, in some experiments, the effects of BCR stimulation with soluble or immobilised anti-IgM were compared. On the day prior to the experiment, wells of a 24-well tissue culture plate were incubated with 1 ml biotinylated anti-IgM (10 µg/ml) or 10 µg/ml purified isotype control (both in PBS) for 3 hr at 37°C. This incubation period enabled the antibody to adhere to the tissue culture plate. Following this, wells were incubated with complete media for 15 min as a blocking solution to prevent non-specific binding of CLL cells to tissue culture plastic, and washed a further two times with 1 ml complete media, then stored at 4°C overnight. The following day, CLL cells ( $2 \times 10^6$ /ml) were added to the plates with or without 100 nM dasatinib, and cells incubated for 48 hr. Following this, an aliquot of one-tenth of the cells was analysed by FCM for Annexin V/Viaprobe, and the remainder used to prepare a protein lysate.

#### **2.2.8.4 Short-term stimulation with SDF-1**

CLL cells were incubated in RPMI-1640 supplemented with 0.5% BSA for 2 hr prior to the assay. Cells were then plated at  $3 \times 10^6$  cells/ml in 0.5% BSA media with or without 100 nM dasatinib in wells of a 48 well tissue culture plate. Cells were then either untreated, or incubated with 100 ng/ml SDF-1 for 3 or 10 min at 37°C. Cells were then transferred to 1.5 ml eppendorf tubes, pelleted by centrifugation (600 g for 3 min), and washed in 1 ml PBS containing 1 µM microcystin LR (BioMol), prior to preparation of protein lysates for western blotting.

#### **2.2.8.5 Long term SDF-1 stimulation**

CLL cells were incubated in complete medium with or without 100 nM dasatinib for 30 min prior to the addition of 100 ng/ml SDF-1. Following 48 hr culture, cells were harvested for viability assessment using Annexin V/Viaprobe FCM.

#### **2.2.8.6 Co-culture with stromal cells**

Prior to use in co-culture experiments, stromal cells were irradiated to prevent proliferation during the culture period. Briefly, NT-L cells and CD154L cells were grown to near confluency, harvested with trypsin, and pelleted by centrifugation in a 15 ml sterile tube after washing in complete media. The cell pellets were irradiated to 30 Gy using an X-RAD 225 cabinet irradiator (RPS Services Limited), and cryopreserved in 90% FBS/ 10% DMSO. On the day prior to the beginning of the experiment, stromal cells were thawed using DAMP, as described in Section 2.2.4, and counted using a haemocytometer. To ensure consistency in co-culture conditions between experiments, stromal cells were plated at constant densities as

follows:  $1 \times 10^4$  cells/well in 96 well plates;  $4 \times 10^4$  cells/well in 48-well plates; and  $1 \times 10^5$  cells/well in 12 or 24 well plates. Stromal cells were allowed to adhere to the tissue culture plate for at least 6 hr, following which the media was removed and replaced with media containing CLL cells at  $1 \times 10^6$ /ml. When CLL cells were co-cultured with CD154L cells, complete media was supplemented with 10 ng/ml IL-4. CLL cells were co-cultured overnight (approximately 12 hr) prior to drug treatments. On the day of experiments, CLL cells were treated as described whilst remaining in co-culture for the duration of the experiment. At the end of experiments, CLL cells were detached from the stromal cell layer by pipetting. Adequate harvesting of CLL cells was confirmed by microscopy of the culture plate. Counting of the harvested cells using a haemocytometer confirmed that stromal cell contamination of CLL cells was consistently less than 1%.

#### **2.2.8.7 Co-culture with soluble CD154 and IL-4**

CLL cells were incubated in 1 ml complete media at  $3 \times 10^6$ /ml in the presence or absence of the drug treatments to be tested for 30 min prior to the addition of CD154 and IL-4. Concurrently, recombinant CD154 was mixed with Enhancer for Ligands (both Axxora (UK) Ltd.) for 30 min. The mixture was then added to the cell suspension at final concentrations of 100 ng/ml for CD154 and 1  $\mu$ g/ml Enhancer for Ligands, in addition to 10 ng/ml IL-4. Following 2 or 48 hr incubation, cells were harvested for FCM or protein lysate preparation.

#### **2.2.9 CLL cell proliferation assay**

##### **2.2.9.1 CFSE staining of CLL cells**

Carboxyfluorescein diacetate succinimidyl ester (CFSE) is an intracellular dye which has been used to monitor lymphocyte proliferation (338). CFSE is taken up into the cell cytoplasm where esterases remove acetate groups, which retains the dye within the cell cytoplasm, where it may become covalently coupled to intracellular molecules via its' succinimidyl groups. As cells divide, the CFSE (and hence fluorescence) halves, allowing assessment of several cell divisions by FCM, recording in the FL-1 channel of a flow cytometer. CFSE was obtained from Invitrogen Ltd., and stored in aliquots of 5 mM in DMSO at  $-20^\circ\text{C}$ .

CLL cells were stained with CFSE immediately after recovery from frozen. Following rehydration with DAMP, cells ( $3-5 \times 10^7$ ) were washed twice in PBS, and resuspended in 10 ml PBS supplemented with 5% FBS. One tenth (1 ml) of the cell solution was removed and placed in culture in a 25 ml flask in complete media

to be used for unstained controls. The remainder of the cells were pelleted by centrifugation (300 g for 5 min) and resuspended in 5 ml PBS / 5% FBS. To this, CFSE was added to a final concentration of 1  $\mu$ M, cells were thoroughly mixed by pipetting, and incubated at 37°C in a waterbath for 8 min. The cells were then removed and 50 ml of ice-cold quenching solution (PBS supplemented with 20% FBS) was added immediately. Cells were centrifuged (300 g for 10 min), and washed once more in PBS / 5% FBS. Cells were then resuspended in 10 ml complete media and incubated overnight in a 25 ml flask at 37°C.

### **2.2.9.2 12 day 154L/IL-4 co-culture**

This co-culture experiment was designed to assess the effect of dasatinib on proliferation of CLL cells in 154L/IL-4 co-culture over a 12 day period, assessing proliferation at days 0, 3, 6, 9, and 12. For each time point, four wells containing  $1 \times 10^5$  CD154L cells were prepared as described (20 wells in total; Section 2.2.8.6). To three of these,  $5 \times 10^5$  CFSE stained CLL cells were added in 1 ml complete media supplemented with 10 ng/ml IL-4, and an aliquot of unstained CLL cells from the same sample added to the fourth well. One well containing CFSE-stained CLL cells was left as an untreated control, the second treated with 100 nM dasatinib, and the third treated with 50 ng/ml colcemid (Invitrogen Ltd.). Cells were incubated at 37°C in a humidified atmosphere. Media and drugs were replaced every 72 hr as follows – supernatant media and cells were aspirated into sterile tubes and centrifuged at 300 g for 5 min. During this time, 500  $\mu$ l fresh complete media plus IL-4 was pipetted into the stroma-containing wells to prevent drying of the wells. The pelleted cells were resuspended in 500  $\mu$ l fresh complete media plus IL-4, transferred back to the original well, and drugs added fresh at the original concentrations above. At day 6 of co-culture  $0.5 \times 10^5$  fresh CD154L cells were added per well, to compensate for a degree of stromal cell death throughout the culture. To harvest cells for analysis at appropriate time points, supernatant media was transferred to a 5 ml FACS tube. The stromal layer was then detached by incubation with trypsin for 2 min, and also transferred to the FACS tube. Cells were then analysed by FCM as described in Section 2.3.9.

## **2.3 Flow cytometry**

### **2.3.1 Assessment of surface antigen expression**

Cells were harvested and washed in FACS buffer (HBSS supplemented with 1% BSA and 0.05% sodium azide (Sigma Aldrich Ltd.)) prior to FCM analysis. Cells

were then incubated with fluorochrome-conjugated antibodies diluted as indicated in Table 2.4 in 100  $\mu$ l FACS buffer at 4°C in the dark for 30 min. Appropriate isotype controls were included in all experiments. Cells were then washed twice in FACS buffer, and resuspended in FACS buffer prior to analysis. When assessing CLL cell purity following processing, propidium iodide (PI) at a final concentration of 25  $\mu$ g/ml was added at this stage to exclude dead cells from analysis in some cases. As PI exclusion gating correlated well with results obtained gating on forward-scatter (FSC) and side-scatter (SSC), subsequent analysis was performed gating cells on FSC/SSC only. FCM analysis was performed using either a FACSCalibur, or FACSCanto II flow cytometer (both BD Biosciences). Unless otherwise stated, 10,000 events were recorded per sample. Data was acquired using BD FACSDiva (BD Biosciences) software, and analysed using BD FACSDiva or FlowJo (Tree Star, Inc.) software.

### **2.3.2 Analysis of intracellular proteins**

Caspase 3 activation was measured by intracellular FCM using an antibody to the active form of caspase 3 (BD Biosciences). Following treatments as indicated, CLL cells ( $1-5 \times 10^5$  cells) were washed in ice-cold PBS in 5 ml FACS tubes. Cells were resuspended in 150  $\mu$ l Fixation/Permeabilisation solution (BD Biosciences) and incubated at 4°C for 20 min. Cells were washed in 2 ml BD Perm/Wash™ buffer (BD Biosciences), then incubated with anti-active caspase 3 antibody, or rabbit IgG isotype control antibody (5  $\mu$ l per test, both BD Biosciences) in Perm/Wash™ buffer at 4°C for 30 min. Cells were washed in Perm/Wash™ buffer, then analysed. Cells with a fluorescence intensity greater than that of the isotype-matched control were considered positive, as shown in Figure 2.4.

### **2.3.3 Measurement of Syk<sup>Y348</sup> phosphorylation by intracellular phosphospecific flow cytometry**

CLL cells were incubated in RPMI containing 0.5% BSA for 2 hr prior to the experiment.  $2 \times 10^6$  cells were transferred to each 5 ml FACS tube and washed in PBS. Cells were resuspended in 100  $\mu$ l media containing 10  $\mu$ g/ml biotinylated anti-IgM  $\pm$  100 nM dasatinib, and incubated for 30 min on ice. Cells were then washed in PBS and resuspended in media with or without 100 nM dasatinib (100  $\mu$ l for samples to be stimulated with avidin, and 200  $\mu$ l for controls). To IgM stimulated samples, 100  $\mu$ l avidin solution was added to achieve a final concentration of 25  $\mu$ g/ml, and tubes incubated at 37°C in a waterbath for 10 min.

At the end of the experiment, 200  $\mu$ l of pre-warmed 3.6% formaldehyde (Sigma Aldrich) in PBS (final concentration 1.8%) was added to each tube in order to fix the cells, and incubated at RT for 10 min. Tubes were then centrifuged (300 g for 5 min) and cell pellets resuspended in 1 ml ice-cold 100% methanol (Sigma Aldrich), vortexed briefly, and incubated on ice for 15 min. Cells were then pelleted and washed in 1x BD Perm/Wash<sup>TM</sup> buffer, then stained with anti-Syk<sup>Y348</sup>-PE or PE-labelled isotype control antibody at a 1/20 dilution in Perm/Wash<sup>TM</sup> buffer. Cells were washed twice in Perm/Wash<sup>TM</sup> buffer, and resuspended in 500  $\mu$ l Perm/Wash<sup>TM</sup> buffer for FCM analysis. Cells were live-gated by FSC/SSC, and 10,000 events recorded per sample, and the PE-channel mean fluorescence intensity (MFI) recorded.

#### **2.3.4 Annexin V / Viaprobe Staining**

Following treatments, CLL cells ( $1-5 \times 10^5$ ) were washed once in ice-cold PBS, and resuspended in 100  $\mu$ l 1x Annexin V binding buffer (BD Biosciences) containing 3  $\mu$ l Annexin V-FITC and 3  $\mu$ l Viaprobe (both BD Biosciences) per test, and incubated at RT for 15 min in the dark. The reaction was terminated by adding 400  $\mu$ l Annexin V binding buffer, and cells analysed on a FACS Canto II flow cytometer. Tubes containing unstained cells, or Annexin V or Viaprobe single-stained cells were recorded to set FSC/SSC voltages and set compensation. Annexin V<sup>-</sup>/Viaprobe<sup>-</sup> cells were considered viable, and Annexin V<sup>+</sup>/Viaprobe<sup>-</sup> cells considered early apoptotic, as demonstrated in Figure 2.5.

#### **2.3.5 Assessment of Mitochondrial Membrane Potential**

As described in Section 1.8.2, loss of MMP is a key early event in apoptosis, controlled by the Bcl-2 family of proteins. A number of methods have been developed to quantitate MMP within cells, as a marker of apoptosis, reviewed in (317). In this study, MMP was measured using the lipophilic cationic indicator tetramethylrhodaminemethylester (TMRM) (Invitrogen Molecular Probes), which exhibits fluorescence in the FL-2 channel on a flow cytometer. In viable cells with an normal MMP, TMRM accumulates in the mitochondrial intermembrane space, leading to high recorded fluorescence. On loss of mitochondrial membrane integrity, the ability of TMRM to accumulate is lost, resulting in a marked decrease in measurable fluorescence (317).

TMRM stock solution (10 mM) was prepared in DMSO and stored at -20°C.

Following treatments as indicated, CLL cells ( $1-10 \times 10^5$ ) were stained with 150

nM TMRM in PBS, incubated at 37°C for 15 min, then placed on ice. Analysis by FCM was then performed within 10 min. For each sample, 10,000 ungated events were recorded, and fluorescence analysed in the FL-2 channel. As CLL cells undergo a degree of spontaneous apoptosis *in vitro* (Figs. 2.4 and 2.5), cells with high and low fluorescence were observed in all samples analysed. During analysis, consistent gates were set on FL-2 fluorescence in order to compare treated and control cells within each experiment.

### **2.3.6 Chemotaxis assay**

In this assay, the ability of CLL cells to migrate along an SDF-1 concentration gradient through a polycarbonate membrane was assessed. CLL cells were cultured in RPMI-1640 supplemented with 0.5% BSA for 2 hr prior to the assay, and this media was used throughout. A total of  $5 \times 10^5$  CLL cells in 100  $\mu$ l 0.5% BSA media was plated into round-bottomed 96 well plates. Cells were either untreated, or treated with 1, 10, or 100 nM dasatinib for 30 min. Additionally, cells were treated with 10  $\mu$ g/ml of the CXCR4 antagonist AMD3100 as a positive control expected to inhibit chemotaxis toward SDF-1. All treatments were performed in duplicate wells. After pre-incubation with drugs, the 100  $\mu$ l cell suspension was transferred to the upper chamber of a 6.5 mm diameter transwell culture insert (Costar) with a pore-size 5  $\mu$ m. The transwell inserts were then placed into wells containing 600  $\mu$ l media supplemented with 150 ng/ml SDF-1. Transwells containing untreated CLL cells placed above media containing no SDF-1 were included as a negative control to account for non-specific migration. The transwell chamber plates were incubated at 37°C in 5% CO<sub>2</sub> for 4 hr. Following this, transwell inserts were removed and the media in the lower chamber mixed thoroughly by pipetting. From each well, three 150  $\mu$ l aliquots were directly transferred to 5 ml FACS tubes for analysis. Transmigrated cells were assessed by counting the number of acquired events recorded on high flow for 30 s.

### **2.3.7 Actin polymerisation assay**

CLL cells were incubated in RPMI-1640 supplemented with 0.5% BSA for 2 hr prior to the assay, and this media used in all steps throughout. CLL cells were plated at  $2 \times 10^6$  cells/ml in wells of a 24 well plate, and treated as follows: untreated; 100 nM dasatinib; 40  $\mu$ g/ml AMD3100, or; both 100 nM dasatinib and 40  $\mu$ g/ml AMD3100 for 30 min. Before addition of SDF-1, 100  $\mu$ l aliquots were removed from each well and transferred to 5 ml FACS tubes containing 250  $\mu$ l BD

Fix/Perm solution. SDF-1 was then added to wells at 100 ng/ml, and 100  $\mu$ l aliquots from each well removed into BD Fix/Perm solution as above at the following time points, 15, 60, 300, and 600 s. At the end of the experiment, tubes were incubated at 4°C for 20 min to fix and permeabilise the cells. Cells were then washed in 2 ml Perm/Wash™ buffer and stained with Alexa Fluor® 488-conjugated phalloidin (Invitrogen Ltd.) at a 1/100 dilution in Perm/Wash™ buffer at 4°C for 10 min. Cells were again washed and resuspended in Perm/Wash™ buffer prior to FACS analysis. Data were acquired on a FACSCanto II flow cytometer, gated on live lymphocytes by FSC/SSC, recording fluorescence in the FITC channel from 10,000 gated events.

### **2.3.8 Pseudoemperipolesis assay**

This assay assesses the ability of CLL cells to spontaneously migrate beneath a layer of stromal cells (pseudoemperipolesis). Firstly, tissue culture plates were coated with collagen I (Invitrogen Ltd.) at 50  $\mu$ g/ml in PBS supplemented with 0.02 M acetic acid (Sigma Aldrich Ltd.) for 1 hr at RT, followed by washing three times with PBS. Two days prior to the assay, M2-10B4 cells in complete media were plated at  $1.5 \times 10^5$  cells/well in a collagen-coated 24-well tissue culture plate. The cells were cultured for 48 hr until the cells were confluent. On the day of the assay, CLL cells were plated at  $2 \times 10^6$  cells/ml in a fresh 24-well plate (8 wells). Cells in three wells were treated with 100 nM dasatinib for 30 min. Following this, supernatant media was removed from 6 wells containing M2-10B4 cells, and 1 ml of CLL cells (from 3 untreated wells and 3 dasatinib-treated wells) were transferred onto stromal containing wells. The plate was cultured at 37°C in 5% CO<sub>2</sub> for 5 hr, then each well was washed thoroughly three times with complete media. To ensure the adequacy of the washing process, 1 ml CLL cells was added to a further stromal layer, incubated 5 min, and thereafter washed and treated as other wells. An additional well containing stroma only was also washed and analysed, as a negative control. After washing, wells were analysed and photographed using phase-contrast microscopy, to document pseudoemperipolesis and ensure complete removal of non-migrated cells. CLL cells which have migrated beneath the stromal layer appear dark and non-refractile, in contrast to cells above the stromal layer (230), as shown in Figure 2.6. The stromal cell layer was detached by incubating wells with 1 ml trypsin at 37°C for 1 min, harvested by pipetting into 5 ml FACS tubes, and washed in PBS. To an additional tube, 100  $\mu$ l of the input CLL cell suspension was added, as a positive control and allow enumeration of

transmigrated cells. Each cell pellet was stained with anti-CD19 APC at 4°C for 20 min, washed twice in FACS buffer, then resuspended in 500 µl FACS buffer for flow cytometric analysis. Cells were analysed using a FACSCanto II flow cytometer, and FSC and SSC voltages set so that both lymphocytes and stromal cells were visible and clearly separated. Gates were set around the location of the lymphocyte population, and on this gate cells were further gated on CD19<sup>+</sup> events to exclude stromal cell debris from the count. Using this gating strategy, samples were counted, in triplicate, by recording the number of positive events obtained by accumulating on high flow for 30 s. To quantitate pseudoemperipolesis, the count recorded in each test sample was determined as a percentage of the input cell count (10 x the recorded input cell count to allow for dilution factor). Negative control samples containing stromal cells alone, or CLL cells washed after 5 min consistently gave values of less than 0.05% migrated cells, confirming minimal background counts.

### **2.3.9 FACS for CFSE proliferation experiments**

#### **2.3.9.1 Cell counting by flow cytometry**

CLL cells co-cultured in the 12-day 154L/IL-4 proliferation co-culture model (as described in Section 2.2.9) were transferred to FACS tubes, washed in PBS, and then incubated with an anti-CD19 APC-conjugated antibody for 30 min at 4°C. Cells were subsequently washed in FACS buffer (300 g for 5 min), and each cell pellet resuspended in 450 µl FACS buffer. To each tube, 50 µl CountBright™ absolute counting beads (Invitrogen Ltd.), warmed to RT and vortexed, was added and samples mixed thoroughly. CountBright™ beads are a suspension of microspheres of known concentration which are FSC<sup>low</sup>/SSC<sup>high</sup> and have high fluorescence across wavelengths up to 635 nm, allowing determination of accurate cell counts by FCM. Data was acquired on a FACSCanto II flow cytometer, using FSC/SSC voltages set to allow clear identification of both the CLL cell and counting bead populations. CountBright™ beads were gated first on FSC/SSC, and further on high fluorescence in the FL-5 (APC-Cy7) channel, to exclude non-bead events falling into the size-gated population. CLL cells were differentiated from stromal cells by gating first on FSC/SSC, and furthermore on CD19 expression. An example of the gating strategy used is shown in Figure 2.7. For each sample, 5000 bead events were acquired, and the number of recorded CLL cell events noted. From these data, the CLL cell concentration (cells/µl) was

calculated using Equation 2.1, where A = number of cell events, B = number of bead events, C = assigned bead count of the lot (beads/50  $\mu$ l), and D = volume of the sample. As the sample volume was 500  $\mu$ l, the cell concentration/  $\mu$ l was multiplied by 500 to give the absolute cell count.

$$\frac{A}{B} \times \frac{C}{D} = \text{concentration of cells}/\mu\text{l}$$

**Equation 2.1 Equation to determine cell number by FCM**

**2.3.9.2 Analysis of cell division using CFSE**

After assessment of cell counts, each sample was further analysed by FCM to assess cell division using the method of CFSE dilution. CLL cells were again identified by gating on FSC/SSC then CD19 expression and 10, 000 gated events recorded per sample. First, the colcemid control tube was recorded; as cells in this tube were inhibited from undergoing cell division, the FL-1 MFI was taken as the MFI of the undivided cell population. As the CFSE dye is split equally on cell division, each daughter cell will have half the fluorescence of the parent cell. The gate to encompass cells that had divided once was set by including an area with approximately half the MFI of the undivided population. Gates to include cells in subsequent cell divisions were set similarly, as shown in Figure 2.8. This allowed the determination of the percentage of total CLL cells within each cell division.

**2.3.9.3 Calculation of percentage recovery of input cells**

This analysis was performed in order to determine the percentage of the starting cell population that could be accounted for given the total cell count and number of cell divisions, in order to assess whether net cell death had occurred during the culture period. At each time point, the absolute number of cells in each division was calculated by dividing the total cell count by the percentage of cells within the cell division. The cell recovery number was then calculated for each sample using Equation 2.2, where R = recovery number,  $n_0$  = number of undivided cells,  $n_1$  = number of cells in division 2,  $n_3$  = number of cells in division 3 and so on.

$$R = n_0 + \frac{n_1}{2} + \frac{n_2}{4} + \frac{n_3}{8} \dots$$

**Equation 2.2 Equation to calculate cell recovery**

The recovery number of each sample was then expressed as a percentage of the input cell number at day 0, as assessed by FCM, to calculate the recovery percentage.

#### **2.4 Assessment of calcium flux following BCR stimulation by fluorescence spectrophotometry**

Calcium flux following BCR stimulation was measured using Fura-2 AM. Fura-2 AM is a cell permeable fluorescent calcium indicator (339). Following uptake into the cell, the AM ester groups of Fura-2 are hydrolysed by non-specific esterases, which renders Fura-2 membrane-impermeant, therefore trapped within the cytoplasm, in a similar way to CFSE. On binding intracellular calcium the fluorescent excitation wavelength of Fura-2 shortens. This property allows the calculation of calcium concentration  $[Ca^{2+}]$  from the ratio of the dye's fluorescence intensities ( $F_1$  and  $F_2$ ), measured at 510 nm using two excitation wavelengths ( $\lambda_1$  and  $\lambda_2$ ; 340 and 380 nm) as described in (339), using Equation 2.3, where  $K_d$  represents the dissociation constant of Fura-2,  $Q$  the ratio of  $F_{min}$  to  $F_{max}$  at  $\lambda_2$ ,  $R$  represents the fluorescence intensity ratio  $F_{\lambda_1}/F_{\lambda_2}$ .

$$[Ca^{2+}] = K_d Q \frac{(R - R_{min})}{(R_{max} - R)}$$

#### **Equation 2.3 Equation to calculate calcium concentration**

Fura-2 AM was prepared as a 2.5 mM stock solution in DMSO and stored at -20 °C until use. CLL cells were incubated in RPMI-1640 containing 0.5% BSA for 2 hr prior to experiments. Cells were then pelleted and re-suspended at  $5 \times 10^6$ /ml in HEPES  $Ca^{2+}$ -supplemented buffer (145 mM NaCl, 5 mM KCl, 1 mM  $MgSO_4$ , 1 mM  $CaCl_2$ , 10 mM HEPES, 0.18% glucose, and 0.2% BSA, adjusted to pH 7.4). Fura-2 AM was added to the cell suspension at a final concentration of 1  $\mu$ M, and cells incubated at 37°C for 30 min in the dark. Cells were washed twice in 5 ml buffer, then re-suspended in buffer containing 10  $\mu$ g/ml biotinylated anti-IgM with or without 100 nM dasatinib for a further 30 min at 4°C. After washing as before, cells were re-suspended at  $2 \times 10^6$ /ml in buffer. Calcium flux was measured using a Hitachi F-7000 Fluorescence Spectrophotometer (Hitachi High Technologies America, Inc.). For each recording, 1.5 ml of the cell suspension was transferred to the fluorimeter cuvette and allowed to warm to 37°C for 3 min, with continuous

stirring, prior to data acquisition. Fluorescence was measured at 340 and 380 nm every 1.7s during recording, to detect calcium-bound and calcium-free Fura-2 respectively. After recording basal fluorescence, 50  $\mu$ l of a 250  $\mu$ M avidin stock was injected into the cuvette to crosslink bound surface IgM, and recording continued for up to 300 s. At this time, 50  $\mu$ l 1% Triton was injected to lyse cells in order to determine an  $R_{\max}$ , following which 50  $\mu$ l 0.5 M EDTA was injected to give  $R_{\min}$ , and  $[Ca^{2+}]$  at each time point calculated by the spectrophotometer software (FL solutions), using Equation 2.3. The  $[Ca^{2+}]$  was then plotted against time for all experimental conditions. Prior to analysis of CLL cells, the experimental protocol was optimised using Ramos B cells, a human mature B cell lymphoma cell line. A representative recording is shown in Figure 2.9.

## **2.5 Assessment of actin polymerisation using confocal fluorescence microscopy**

Multispot microscope slides (C. A. Hendley (Essex) Ltd.) were coated in 0.01% Poly-L-Lysine (Sigma Aldrich) in distilled water for 10 min and allowed to air dry. On the day before the experiment, slides were coated with anti-IgM or isotype control by pipetting 30  $\mu$ l of PBS containing either 10  $\mu$ g/ml biotinylated anti-IgM or 10  $\mu$ g/ml IgG1  $\kappa$  isotype control onto each spot and incubating at 4°C overnight. On the day of experiment, antibody solution was aspirated from the slides which were then blocked with complete media for 30 min. Meanwhile, CLL cells were counted using Trypan blue exclusion and diluted to  $5 \times 10^5$  per ml, then treated  $\pm$  100 nM dasatinib for 30 min at 37°C. Following this, 30  $\mu$ l of control or dasatinib treated cells was transferred to spots coated with anti-IgM or isotype control, and the slides incubated at 37°C for 30 min in a humidified chamber. Media was then aspirated from slides using a tissue, and 30  $\mu$ l of 3.7% formaldehyde (Sigma Aldrich Ltd.) in PBS was added per spot and slides incubated at RT for 15 min to fix cells. Slides were washed twice in PBS in a Coplin jar (5 min), lightly dried, then 30  $\mu$ l 0.5% Triton (Sigma Aldrich Ltd.) in PBS was added per spot for 10 min to permeabilise the cells. Excess liquid was aspirated, and slides incubated with 5% BSA in PBS for 30 min at room temperature to block non-specific staining. Spots were then incubated with 30  $\mu$ l Alexa Flour<sup>®</sup> 488 phalloidin at a 1/200 dilution in PBS containing 1% BSA for 30 min at 4°C in the dark. A slide was left unstained as a negative control. Slides were washed twice in PBS then once in distilled water and left to air-dry in the dark before mounting. Slides were mounted

with Vectashield® mounting medium for fluorescence with DAPI (Vector Laboratories Ltd.) and incubated at 4°C for 20 min prior to assessment. Slides were viewed and photographed using an AxioImager M1 fluorescence microscope (Carl Zeiss Ltd.) and images analysed using AxioVision 5.2 software (Carl Zeiss Ltd.). To quantitate the percentage of cells with evidence of spreading following BCR stimulation, 200 cells from each sample were viewed and scored either positive or negative.

## **2.6 Western Blotting**

### **2.6.1 Cell Lysate Preparation**

Following treatments described, cells were pelleted and washed twice in cold PBS (300 g for 5 min), then resuspended in lysis buffer containing 1% NP-40, 10% glycerol, 20 mM Tris (pH 7.5), and 137 mM NaCl (all Sigma Aldrich Ltd.) supplemented with Complete Protease Inhibitor Cocktail and PhosStop phosphatase inhibitor tablets (both Roche Diagnostics Ltd.) at a volume of  $1 \times 10^6$  cells per 10  $\mu$ l buffer. Cells were mixed by pipetting and incubated on ice for 20 min. Following incubation, cell lysates were clarified by centrifugation at 10,000 g for 10 min. Lysates were subsequently stored at -20°C prior to electrophoretic separation.

### **2.6.2 Protein Quantification**

Protein concentration in lysates was determined using the bicinchoninic acid (BCA) method (Pierce). The manufacturers instructions were modified as follows to allow quantitation of the small volumes of protein lysate (20-40  $\mu$ l total) obtained from CLL samples. BSA protein standards of the following concentrations were prepared in sterile water: 2000, 1500, 1000, 750, 500, 250, 125, 25, and 0  $\mu$ g/ml and stored at -20°C until required. For each assay, the kit solutions A and B were first mixed at a ratio of 50:1, and 100  $\mu$ l of the resulting solution pipetted per well into a 96-well flat-bottomed tissue culture plate. To this, 2  $\mu$ l of protein standard or test lysate was added per well. Protein standards were assayed in duplicate and test samples once due to the small sample volume. The plate was incubated at 37°C for 30 min and then absorbance read at 562 nm on a Spectramax M5 plate reader (MDS Analytical Technologies). SoftMax Pro 5.2 software (MDS Analytical Technologies) was used to generate a standard curve and calculate protein concentration of test samples.

### **2.6.3 Sodium dodecyl sulphate-polyacrylamide gel electrophoresis (SDS-PAGE) and transfer**

Protein electrophoresis was carried out using the Invitrogen Xcell SureLock™ Mini cell system with NuPAGE® Novex® pre-cast 4-12% Bis-Tris gels and buffers all obtained from Invitrogen Ltd. Equal amounts of protein (typically 10-30 µg) were diluted with 4 x NUPAGE LDS sample buffer (10 % (w/v) Glycerol, 1.7% (w/v) Tris-Base, 1.7% Tris-HCl, 2% (w/v) lithium dodecyl sulfate (LDL), 0.15% (w/v) EDTA, 0.019% Serva Blue G250 and 0.063% Phenol Red (pH 8.5)), 10 x NuPAGE reducing agent with distilled H<sub>2</sub>O to an equal appropriate final volume. Samples were then heated to 70°C for 10 min in a waterbath, then centrifuged briefly. Samples were loaded on the gel alongside 5 µl SeeBlue® Plus2 Pre-Stained Standard (Invitrogen Ltd.) and resolved by running at 80V for 15 min, then 150V for 60 minutes with NuPAGE MOPS running buffer (50 mM 3-(N-morpholino) propane sulfonic acid (MOPS), 50 mM Tris-Base, 3.5 mM SDS and 1.0 mM EDTA (pH 7.7)), supplemented with NuPAGE antioxidant. Gels were subsequently transferred to polyvinylidene fluoride (PVDF) membranes (Bio-Rad Laboratories) as follows. 20 x NuPAGE transfer buffer (25 mM Bicine, 25 mM Bis-Tris, 1.0 mM EDTA, 50 µM Chlorobutanol (pH 7.2)) was diluted with dH<sub>2</sub>O and supplemented with 20% (v/v) methanol (Sigma Aldrich Ltd.) and NuPAGE antioxidant. The PVDF membrane was then activated by incubation in 100% methanol for 30 sec, rinsed briefly in dH<sub>2</sub>O, and immersed in transfer buffer until required. Gel/membrane sandwiches were assembled using 1.0 mm gel blotting paper (Whatman plc), and electrophoretic transfer performed using the Invitrogen XCell II™ Blot Module and sponges, as per manufacturer's instructions, running at 30 V for 70 min.

### **2.6.4 Immunolabelling and detection**

After transfer, PVDF membranes were washed for 5 min in Tris buffered saline (TBS; 0.5 M NaCl and 20 mM Tris pH 7.5) supplemented with 0.1% (v/v) Tween-20 (TBS-T) then blocked for 1 hr with 5% non-fat milk in TBS-T. Membranes were incubated with primary antibodies as listed in Table 2.5 overnight at 4°C on a roller at the indicated dilution. Primary antibodies were diluted in 5% BSA in TBS-T or 5% non-fat dried milk in TBS-T as per the manufacturer's advice. Membranes were subsequently washed three times (15 min per wash) in TBS-T, and incubated with the appropriate species horseradish peroxidase (HRP)-conjugated

secondary antibody in 1% BSA in TBS-T for 1 hr at RT. Following this, membranes were washed four times (15 min per wash) in TBS-T, and immunodetection performed using the Immun-Star™ Western C™ HRP chemiluminescent kit and Molecular Imager® ChemiDoc™ XRS system (Bio-Rad Laboratories).

For detection of phosphotyrosine only, the following protocol was used. Membranes were blocked for overnight in TBS supplemented with 5% BSA, 1% ovalbumin, and 0.05% sodium azide (all Sigma Aldrich). Membranes were then incubated overnight at RT with clone 4G10 anti-phosphotyrosine antibody at a 1:10,000 dilution in blocking solution. Immunoblots were then washed (4 x 15 min) in TBS supplemented with 0.05% NP-40, and incubated with HRP-conjugated anti-mouse secondary antibody at a dilution of 1:10,000 in a 1:5 dilution of the blocking solution in TBS for 1 hr at RT. Membranes were washed (4 x 15 min) in TBS plus 0.05% NP-40, then developed by chemiluminescence as above.

### **2.6.5 Membrane stripping and re-probing**

Stripping of the PVDF membranes was often required prior to detection of the next protein. Following detection of phospho-proteins, membranes were always stripped prior to detection of the total protein. 10 x Re-Blot™ Plus Strong antibody stripping solution (Millipore) was diluted in deionised water, and each membrane incubated in 10 ml 1 x stripping solution for 15-30 min at RT. Membranes were washed in TBS-T twice, then re-blocked in 5% milk/TBS-T for 1 hr prior to incubation with the next primary antibody.

## **2.7 Quantitative PCR**

### **2.7.1 RNA extraction**

Cell lines (M2-10B4, NT-L, and CD154-L) were harvested, washed in ice-cold PBS, and pelleted by centrifugation at 500 g for 3 min at 4°C prior to RNA extraction. RNA extraction was then performed using the RNA-Easy mini kit according to manufacturer's instructions (Qiagen). RNA was stored diluted in RNase free H<sub>2</sub>O at -80°C. RNA concentration was determined using a NanoDrop spectrophotometer (Labtech International Ltd.).

### **2.7.2 Reverse Transcription PCR**

cDNA was prepared from 1 µg RNA using the High-Capacity cDNA Reverse Transcription Kit (Applied Biosystems). RNA samples were prepared to a

concentration of 1 µg per 10 µl in nuclease-free H<sub>2</sub>O, heated to 65°C for 10 min, then placed on ice. To 10 µl of diluted RNA, 10 µl of a pre-prepared 2 x reverse transcription mastermix (in nuclease-free H<sub>2</sub>O) was added, to give a final concentration of 1 x RT-buffer, 4 mM dNTP mix, 1 x RT random primers, and 2.5 IU/ml MultiScribe reverse transcriptase. For each reaction, 10 µl master mix was added to a PCR tube containing 1 µg RNA. The reaction mixture was heated to 37°C in a Mastercycler™ PCR machine (Eppendorf UK Ltd.) for 2 hr. The reaction was then heated to 85°C for 5 sec to denature the reverse transcriptase, then cooled to 4°C. The resulting cDNA samples were stored at -20°C.

### **2.7.3 TaqMan® Real-Time PCR**

Quantitative PCR was performed using a TaqMan® Gene Expression Assay (Applied Biosystems), as follows. The TaqMan® Gene Expression Assay probes were mouse SDF-1 with a FAM reporter, and mouse GAPDH with a VIC-MGB reporter. In a MicroAmp™ Optical 96-well reaction plate (Applied Biosystems) a total volume of 25 µl/reaction was prepared, containing 1 x TaqMan® Gene Expression Mastermix (AmpliTaq Gold® DNA Polymerase (Ultra Pure), Uracil-DNA glycosylase, dNTPs with deoxyuridine triphosphate, ROX™ Passive Reference, in addition to optimised buffer components), 1 x TaqMan® Gene Expression Assay, 1 µl cDNA diluted in nuclease-free water. For each sample, each gene was assayed in quadruplicate, and a negative control containing nuclease-free water in place of cDNA was included. Plate wells were capped and the plate centrifuged briefly. The plate was inserted into an Applied Biosystems 7900 Fast Real-Time PCR System thermal cycler, and programmed to complete 40 cycles as follows: 50°C for 2 min, 95°C for 10 min, 95°C for 15 sec, and 60°C for 1 min. Reactions were analysed using Sequence Detections Systems software version 2.3 (Applied Biosystems). For each sample, the cycle threshold (Ct) was determined for both GAPDH and SDF-1. Results for each sample were expressed as the delta Ct ( $\Delta$ CT; SDF-1 Ct minus GAPDH Ct).

## **2.8 Statistical Analysis**

### **2.8.1 Software used for statistical analysis**

Results are shown as mean  $\pm$  SEM. Statistical analysis was performed using GraphPad Prism 4 software (GraphPad Software Inc.), using the Students unpaired t-test to compare groups. The Wilcoxon Signed Ranks test was used to

analyse experiments in which data of treated groups were expressed relative to the untreated controls (set to 100%).

### **2.8.2 Statistical analysis of data generated in drug combination experiments**

To assess whether the effect of dasatinib in combination with other chemotherapeutic agents or novel inhibitors was synergistic, additive, or antagonistic, data from drug combination experiments was analysed using Calcsyn<sup>®</sup> software (Version 2.0; Biosoft), which uses the mathematical model developed by Chou (340). In these experiments, CLL cells at  $1 \times 10^6$ /ml were treated with increasing concentrations of single drugs or drug combinations at a fixed ratio, as demonstrated in Figure 2.10. Following 24 hr of treatment, cells were harvested and apoptosis assessed by Annexin V/Viaprobe staining by FCM. For each drug treatment, the percentage of cells remaining viable (Annexin V<sup>-</sup>/Viaprobe<sup>-</sup>) relative to the untreated control was calculated (viable %). The viable percentage was converted to the fraction affected ( $f_a$ ) using Equation 2.4.

$$f_a = 1 - \frac{\text{viable}\%}{100}$$

#### **Equation 2.4 Equation to calculate the fraction affected for synergy experiments**

The fraction affected for each drug treatment was entered into a Calcsyn<sup>®</sup> software worksheet, allowing analysis of the data as follows. The software generated dose and effect curves for each drug treatment, which were further related using the median-effect equation of Chou (Equation 2.5 (340)), where D is the dose of drug,  $D_m$  the median effect dose (or LD<sub>50</sub>),  $f_u$  the fraction unaffected ( $1 - f_a$ ), and m an exponent signifying the sigmoidicity of the dose-effect curve.

$$\frac{f_a}{f_u} = \left( \frac{D}{D_m} \right)^m$$

#### **Equation 2.5 Median effect equation**

A linear relationship between dose and effect was constructed by the software by plotting  $x = \log(D)$  against  $y = \log(f_a/f_u)$ , based on the logarithmic form of the median effect equation (Equation 2.6)

$$\text{Log}\left(\frac{f_a}{f_u}\right) = m\log(D) - m\log(D_m)$$

**Equation 2.6 Logarithmic expression of the median effect equation used to construct median effect plots**

For each drug treatment, a linear correlation coefficient (r) was calculated by the software, which depicted the conformity of the data to the median-effect plot. Experiments in which  $r > 0.90$  were accepted for analysis. Synergy or antagonism of drug pairings was calculated by the software computing the combination index (CI). The CI equation is based on the multiple drug-effect equation of Chou and Talalay (Equation 2.7 (340)),  $(D_x)_1$  is the concentration of drug 1 causing x% inhibition, and  $(D_x)_2$  the concentration of drug 2 causing x% inhibition.

$$CI = \frac{(D)_1}{(D_x)_1} + \frac{(D)_2}{(D_x)_2}$$

**Equation 2.7 Combination index equation**

A CI of 1 indicates that the drug pairing has an additive effect,  $CI < 1$  indicates synergy (more than additive effect), and  $CI > 1$  indicates an antagonistic effect. The degree of synergism or antagonism has been graded as shown in Table 2.6. The software plots the calculated CIs on an isobologram plot, illustrated in Figure 2.11.

**Table 2.1 Suppliers addresses**

<b>Company</b>	<b>Address</b>
Applied Biosystems	Lingley House, 120 Birchwood Boulevard, Warrington, WA3 7QH, UK
Axxora (UK) Ltd.	P.O. Box 6757 Bingham, Nottingham NG13 8LS, UK
Bachem	Hegenheimer Strasse 5 79576 Weil am Rhein Germany
BD Biosciences	The Danby Building, Edmund Halley Road, Oxford Science Park, OX4 4DQ, Oxford, UK
BioMol c/o Enzo Life Sciences Ltd.	Palatine House, Matford Court, Exeter, EX2 8NL, UK
Bio-Rad Laboratories	Bio-Rad House, Maxted Road, Hemel Hempstead, HP2-7DX, UK
Biosoft	PO Box 1013, Great Shelford, Cambridge, CB22 5WQ, UK
Bristol-Myers Squibb	Route 206, Provinceline Road, P.O. Box 4000 Princeton, New Jersey, 08543, US
C. A. Hendley (Essex) Ltd.	Oakwood Hill Industrial Estate, Oakwood Hill, Loughton, Essex, IG10 3TZ, UK
Cell Signaling Technology c/o New England Biolabs	75-77 Knowl Piece, Wilbury Way, Hitchin, Herts SG4 0TY, UK
Costar c/o Fisher Scientific UK	Bishop Meadow Road, Loughborough, LE 1 5RG Leicestershire, UK
Eppendorf UK Ltd.	Endurance House, Vision Park, Chivers Way, Histon, Cambridge, CB24 9ZR, UK
Fisher Scientific UK	Bishop Meadow Road, Loughborough, LE 1 5RG Leicestershire, UK
Greiner Bio-One Ltd.	Unit 5, Stroudwater Business Park, Brunel Way Stonehouse, Gloucestershire, GL103SX, U.K.
GraphPad Software Inc.	2236 Avenida de la Playa, La Jolla, CA 92037, US
Hawksley	Marlborough Road, Lancing Business Park, Lancing, Sussex, BN15 8TN, UK
Invitrogen Ltd. Part of Life Technologies	Invitrogen Ltd, 3 Fountain Drive, Inchinnan Business Park, Paisley, UK
Labtech International Ltd.	Acorn House, The Broyle, Ringmer, East Sussex, BN8 5NN, UK
LC Laboratories	165 New Boston Street Woburn, MA 01801
MDS Analytical Technologies (GB) Limited	660 - 665 Eskdale Road, Winnersh Triangle, Wokingham, Berkshire, RG41 5TS, UK

Merck Chemicals Ltd.	Boulevard Industrial Park, Padge Road, Beeston, Nottingham, NG9 2JR, UK
Millipore (U.K.) Limited	Suite 3 & 5, Building 6, Croxley Green Business Park, Watford, WD18 8YH
Miltenyi Biotech	Almac House, Church Lane, Bisley, Surrey, GU24 9DR, UK
MP Biomedicals	Wellington House, East Road, Cambridge, UK
PeptoTech EC Ltd.	PeptoTech House, 29 Margravine Road, London W6 8LL, UK
Pierce, c/o Perbio Science UK Ltd.	Unit 9, Atley Way, North Nelson Industrial Estate, Cramlington, Northumberland, NE23 1WA, UK
R&D Systems	R&D Systems Europe Ltd., 19 Barton Lane, Abingdon Science Park, Abingdon, OX14 3NB, UK
Roche Diagnostics Ltd.	Charles Avenue, Burgess Hill, RH15 9RY, UK
RPS Services Limited	Unit 1A, The Cottage, 100 Royston Road, Byfleet, Surrey, KT14 7NY, UK
Sigma Aldrich Ltd.	The Old Brickyard, New Rd, Gillingham, Dorset, SP8 4XT, UK
Tree Star, Inc.	340 A Street #101, Ashland, OR 97520, US
Vector Laboratories Inc.	3, Accent Park, Bakewell Road, Orton Southgate, Peterborough, PE2 6XS, UK
Whatman plc	Springfield Mill, James Whatman Way, Maidstone, Kent, ME14 2LE, UK
Carl Zeiss Ltd.	15 - 20 Woodfield Road , Welwyn Garden City, Hertfordshire, AL7 1JQ, UK

**Table 2.2 Details of CLL samples stored**

Sample Number	Age	Sex	Binet Stage*	Treated	ZAP-70 Status	FISH
1	58	M	A	no	n/a	n/a
2	51	M	A	no	neg	nil
3	56	F	A	no	neg	n/a
4	57	F	A	no	neg	n/a
5	69	M	A	no	neg	13q-
6	71	M	C	no	neg	n/a
7	74	M	C	yes	pos	11q-
8	60	F	A	no	neg	11q-
9	67	F	B	yes	neg	n/a
10	71	M	A	no	n/a	n/a
11	52	M	A	no	neg	11q- and +12
12	60	F	A	no	neg	13q-
13	77	M	A	no	neg	13q-
14	63	M	C	yes	pos	17q-
15	48	F	A	no	pos	nil
16	77	F	A	yes	pos	nil
17	79	M	A	no	n/a	n/a
18	62	F	B	Yes	pos	11q-
19	72	M	A	Yes	n/a	n/a
20	80	M	A	No	n/a	n/a
21	66	F	C	Yes	pos	nil
22	77	F	A	Yes	n/a	n/a
23	80	F	A	No	n/a	n/a
24	81	F	B	Yes	pos	13q-
25	66	M	A	No	n/a	n/a
26	69	M	A	Yes	pos	13q-
27	88	F	C	Yes	n/a	n/a
28	70	F	A	No	pos	17p-
29	73	M	C	Yes	pos	nil
30	68	M	A	No	n/a	n/a
31	76	M	A	No	n/a	n/a
32	66	F	B + C	No	pos	nil
33	88	M	A	No	n/a	n/a
34	65	M	B	Yes	pos	11q-
35	69	M	A	No	pos	11q-
36	76	M	A	Yes	pos	11q-
37	69	F	A	No	n/a	n/a
38	67	M	B	Yes	pos	nil
39	75	M	A	Yes	n/a	n/a
40	85	F	A	No	n/a	n/a
41	60	M	A	No	neg	nil
42	75	F	B	Yes	n/a	n/a
43	94	M	A	No	n/a	n/a
44	64	F	A	No	neg	nil
45	79	M	B	Yes	pos	13q-

Sample Number	Age	Sex	Binet Stage	Treated	ZAP-70 Status	FISH
46	53	F	A	No	pos	nil
47	59	M	B	No	neg	+12
48	78	F	A	No	n/a	n/a
49†	--	--	--	--	--	--
50	62	M	C	Yes	pos	nil
51	77	M	A + C	No	neg	nil
52	79	F	B	Yes	neg	11q-
53	84	F	A	No	n/a	n/a
54	55	F	A	No	neg	nil
55	78	F	A	No	n/a	n/a
56	92	F	A + C	No	n/a	n/a
57	73	M	C	No	pos	nil
58	66	M	A	No	n/a	n/a
59	87	F	A	No	neg	n/a
60	60	F	A	No	pos	nil
61	76	M	C	Yes	n/a	n/a
62	84	F	A	Yes	n/a	n/a
63	64	M	A	No	n/a	n/a
64	65	M	C	Yes	neg	nil
65	70	F	C	Yes	neg	nil
66	79	F	A	Yes	n/a	n/a
67	71	M	A	No	pos	nil
68	59	F	C	Yes	pos	nil
69	45	M	A	Yes	pos	nil
70	75	F	C	No	neg	nil
71	63	M	A	No	n/a	n/a
72	52	F	A	No	pos	nil
73	76	F	A	Yes	pos	nil
74	71	F	A	Yes	neg	nil
75	76	M	C	No	n/a	n/a
76	52	F	A	No	pos	6q-
77	63	M	A	No	neg	nil

neg = ZAP-70 negative, pos = ZAP-70 positive

n/a = Not available

nil = No abnormality detected by FISH

Chromosomal deletions are indicated by (-) and trisomy denoted by (+)

\* Where more than one stage is listed, this denotes separate samples collected at different stages of disease

† This patient was found to have an alternative diagnosis following cell storage

**Table 2.3 Details of inhibitor preparation and storage**

<b>Inhibitor</b>	<b>MW*</b>	<b>Stock Concentration</b>	<b>Diluent</b>	<b>Storage Temperature</b>
AMD3100	794.5	10 mg/ml	H <sub>2</sub> O	-20°C
Bcl-2 inhibitor I	300.3	5 mM	DMSO	-20°C
Bcl-2 inhibitor III	376.7	5 mM	DMSO	-20°C
Chlorambucil	304.2	100 mM	DMSO	-20°C
Dasatinib	488	20 mM	DMSO	-20°C
17-DMAG	653.2	1 mM	H <sub>2</sub> O	-20°C
Fludarabine	285.2	5 mM	DMSO	-20°C
Imatinib	589.7	100 mM	DMSO	4°C
JNK inhibitor II	220.2	50 mM	DMSO	-20°C
LY294002	307.4	10 mM	DMSO	-20°C
PD98059	267.3	50 mM	DMSO	-20°C
PP2	301.8	5 mM	DMSO	4°C
PP3	211.2	5 mM	DMSO	4°C
SB203580	377.4	10 mM	DMSO	-20°C
Z-VAD-fmk	467.5	25 mM	DMSO	-20°C

\* molecular weight

**Table 2.4 Antibodies used for FCM**

Description	Reactivity	Clone	Format	Isotype
CD19	Human	HIB19	FITC	IgG <sub>1</sub> κ
CD19	Human	HIB19	PE	IgG <sub>1</sub> κ
CD19	Human	HIB19	APC	IgG <sub>1</sub> κ
CD5	Human	UCHT2	PE	IgG <sub>1</sub> κ
CD23	Human	M-L233	APC	IgG <sub>1</sub> κ
Caspase 3 (active form)	Human	C92-605	PE	IgG <sub>1</sub> κ
Syk (Tyr <sup>348</sup> )	Human	I120-722	PE	IgG <sub>1</sub> κ
Isotype control	Human	MOPC-21	FITC	IgG <sub>1</sub> κ
Isotype control	Human	MOPC-21	PE	IgG <sub>1</sub> κ
Isotype control	Human	MOPC-21	APC	IgG <sub>1</sub> κ

**Table 2.5 Antibodies used for western blotting**

Specificity*	Species	Dilution	Manufacturer
Akt	rabbit	1:1000	Cell Signaling
p-Akt (Thr <sup>308</sup> )	rabbit	1:1000	Cell Signaling
Bcl-2	mouse	1:1000	Cell Signaling
Bcl-x <sub>L</sub>	rabbit	1:2000	BD Biosciences
Bim	rabbit	1:1000	Cell Signaling
β tubulin	rabbit	1:1000	Cell Signaling
Caspase 9	rabbit	1:1000	Cell Signaling
ERK1/2	rabbit	1:1000	Cell Signaling
p-ERK1/2 (Thr <sup>202</sup> /Tyr <sup>204</sup> )	rabbit	1:1000	Cell Signaling
p-FAK (Tyr <sup>576</sup> /Tyr <sup>577</sup> )	rabbit	1:1000	Cell Signaling
GAPDH	rabbit	1:1000	Cell Signaling
HSP90	mouse	1:2000	R&D Systems
IκBα	rabbit	1:1000	Cell Signaling
p-IκBα (Ser <sup>32/36</sup> )	mouse	1:1000	Cell Signaling
Lyn	rabbit	1:1000	Cell Signaling
p-Lyn (Tyr <sup>396</sup> )	rabbit	1:5000	Epitomics
Mcl-1	rabbit	1:1000	Cell Signaling
PARP	rabbit	1:1000	Cell Signaling
p70 s6 kinase	rabbit	1:1000	Cell Signaling
p-p70 s6 kinase (Thr <sup>389</sup> )	rabbit	1:1000	Cell Signaling
SAPK/JNK	rabbit	1:1000	Cell Signaling
p-SAPK/JNK (Thr <sup>183</sup> /Tyr <sup>185</sup> )	mouse	1:500	Cell Signaling
Src	mouse	1:1000	Cell Signaling
p-Src Family (Tyr <sup>416</sup> )	rabbit	1:1000	Cell Signaling
p-Syk (Tyr <sup>352</sup> )	rabbit	1:1000	Cell Signaling
Survivin	rabbit	1:1000	Cell Signaling
p-Tyrosine (clone 4G10)	mouse	1:10,000	Millipore
Anti-rabbit IgG, HRP-linked antibody	goat	1:5000	Cell Signaling
Anti-mouse IgG, HRP-linked antibody	horse	1:5000	Cell Signaling

\* p denotes antibody specificity for the phosphorylated form of the indicated protein. The specific phosphorylation site(s) are denoted in brackets.

**Table 2.6 Definitions of drug synergism and antagonism**

<b>Range of CI</b>	<b>Description</b>	<b>Symbol</b>
< 0.1	Very strong synergism	+++++
0.1-0.3	Strong synergism	++++
0.3-0.7	Synergism	+++
0.7-0.85	Moderate synergism	++
0.85-0.9	Slight synergism	+
0.9-1.1	Nearly additive	±
1.1-1.2	Slight antagonism	-
1.2-1.45	Moderate antagonism	--
1.45-3.3	Antagonism	---
3.3-10	Strong antagonism	----
>10	Very strong antagonism	-----

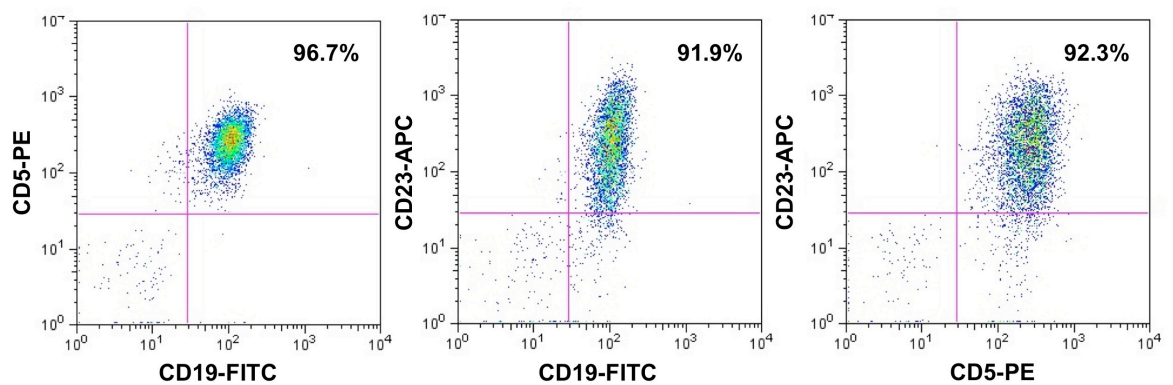


**Figure 2.1 FCM plot of a representative CLL patient sample following Rosettesep™ purification**

A whole blood sample from a CLL patient (CLL 41) was processed using Rosettesep™ negative selection, as described in Section 2.2.1. Following purification, FCM was performed as described in Section 2.3.1 to assess the percentage of CLL cells obtained. Dot plots are live-gated on FSC/SSC, and the percentage of cells dual-staining for the antigen combinations as indicated is shown in the top-right corner.

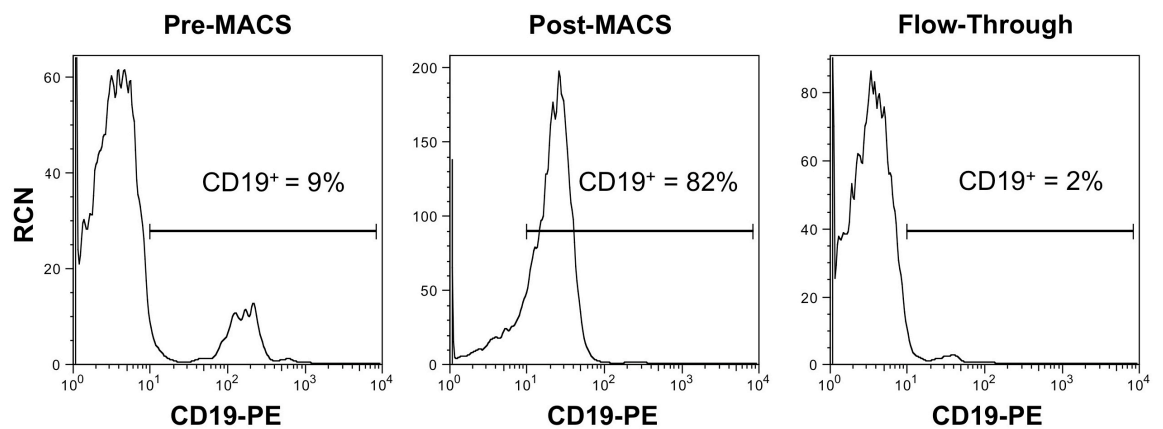


**Figure 2.2 Enrichment of B lymphocytes from buffy coat using MACS sorting.**

Normal B lymphocytes were isolated from a buffy coat using Histopaque and MACS sorting. The figure demonstrates the typical efficiency of B cell enrichment. Histograms have been live-gated on FSC/SSC, and show relative cell number (RCN) against CD19-PE staining.

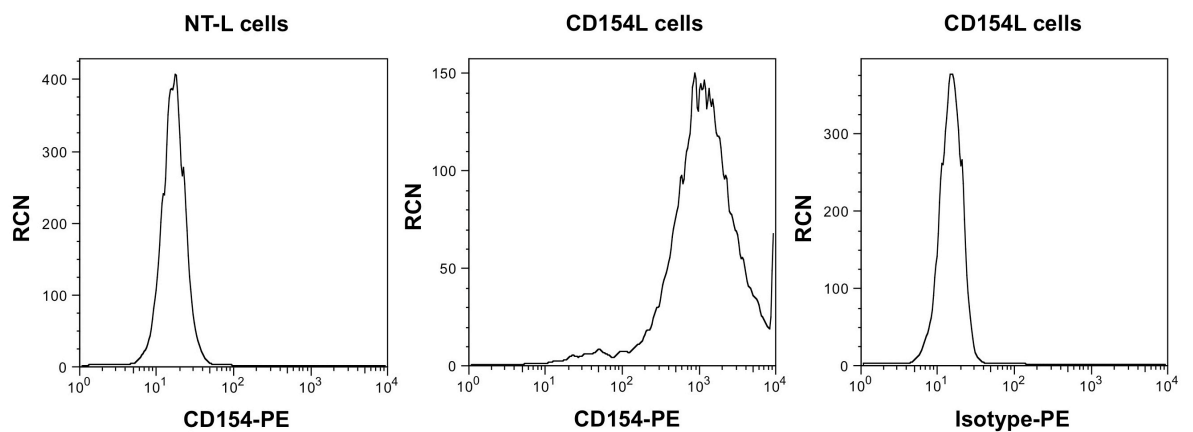


**Figure 2.3 Confirmation of CD154 expression on CD154L cells by FCM**

NT-L cells and CD154L cells were stained with a PE-conjugated antibody specific for CD154 prior to FCM. CD154L cells were also stained with an PE-conjugated isotype control antibody. Cells were live-gated on FSC/SSC, and the histograms show RCN against PE fluorescence.

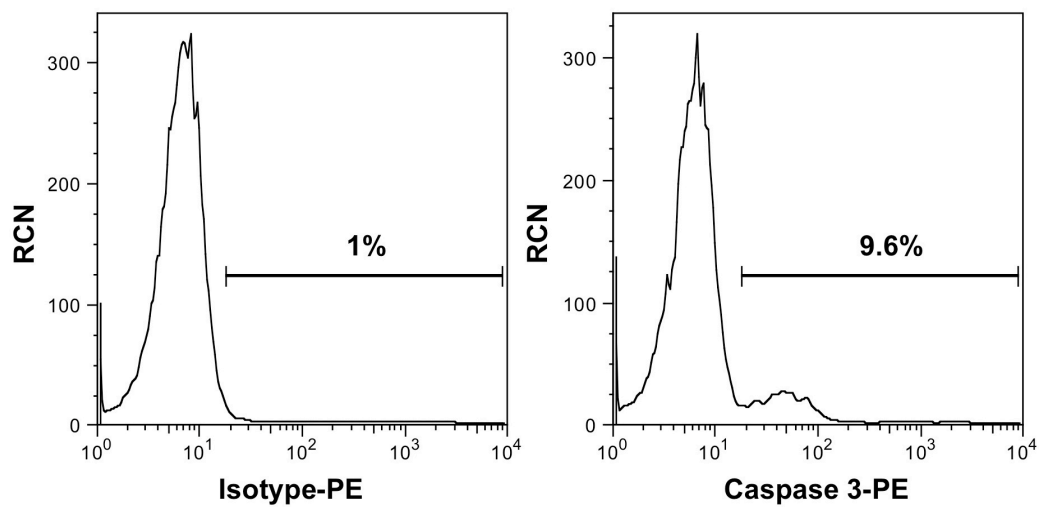


**Figure 2.4 Gating strategy used to determine percentage of CLL cells containing activated caspase 3**

CLL cells were analysed for caspase 3 activation as described in Section 2.3.2. Cells were not gated on FSC/SSC. Following FCM, cells were analysed by creating a gate which included not more than 1% of cells stained with the isotype control antibody. This gate was then applied to histograms of untreated or dasatinib-treated cells to calculate the percentage of total cells containing activated caspase 3.

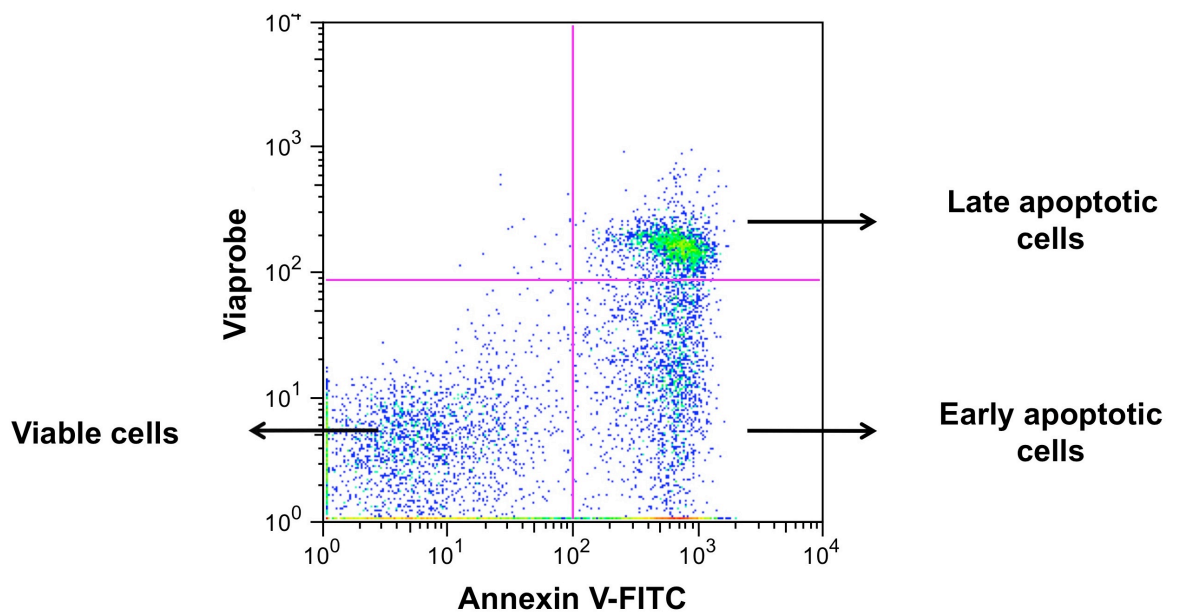


**Figure 2.5 Example of gating strategy used to assess apoptosis in CLL cells stained with Annexin V and Viaprobe**

CLL cells were stained with Annexin V-FITC and Viaprobe as described in Section 2.3.4. The dot plot above shows a CLL sample stained following 24 hr in culture in complete media. In experiments, quadrant gates as shown were set in order to quantify the percentages of viable (Annexin V<sup>-</sup>/Viaprobe<sup>-</sup>), early (Annexin V<sup>+</sup>/Viaprobe<sup>-</sup>), and late (Annexin V<sup>+</sup>/Viaprobe<sup>+</sup>) apoptotic cells.

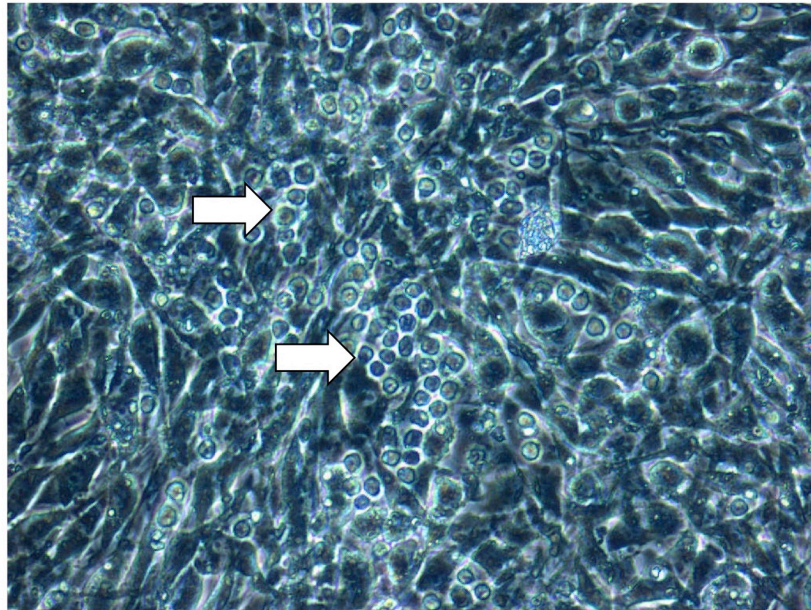


**Figure 2.6 Pseudoemperipolesis of CLL cells beneath M2-10B4 stromal cells**

CLL cells from one patient sample (CLL 64) were co-cultured on a prepared M2-10B4 stromal cell layer for 5 hr. Non-migrated cells were washed by washing wells three times with media, and the stromal cell layer photographed. The white arrows indicate CLL cells which demonstrate pseudoemperipolesis into the stromal cell layer, identified by their non-refractile appearance. Cells were subsequently collected and analysed by FCM as described in Section 2.3.8.

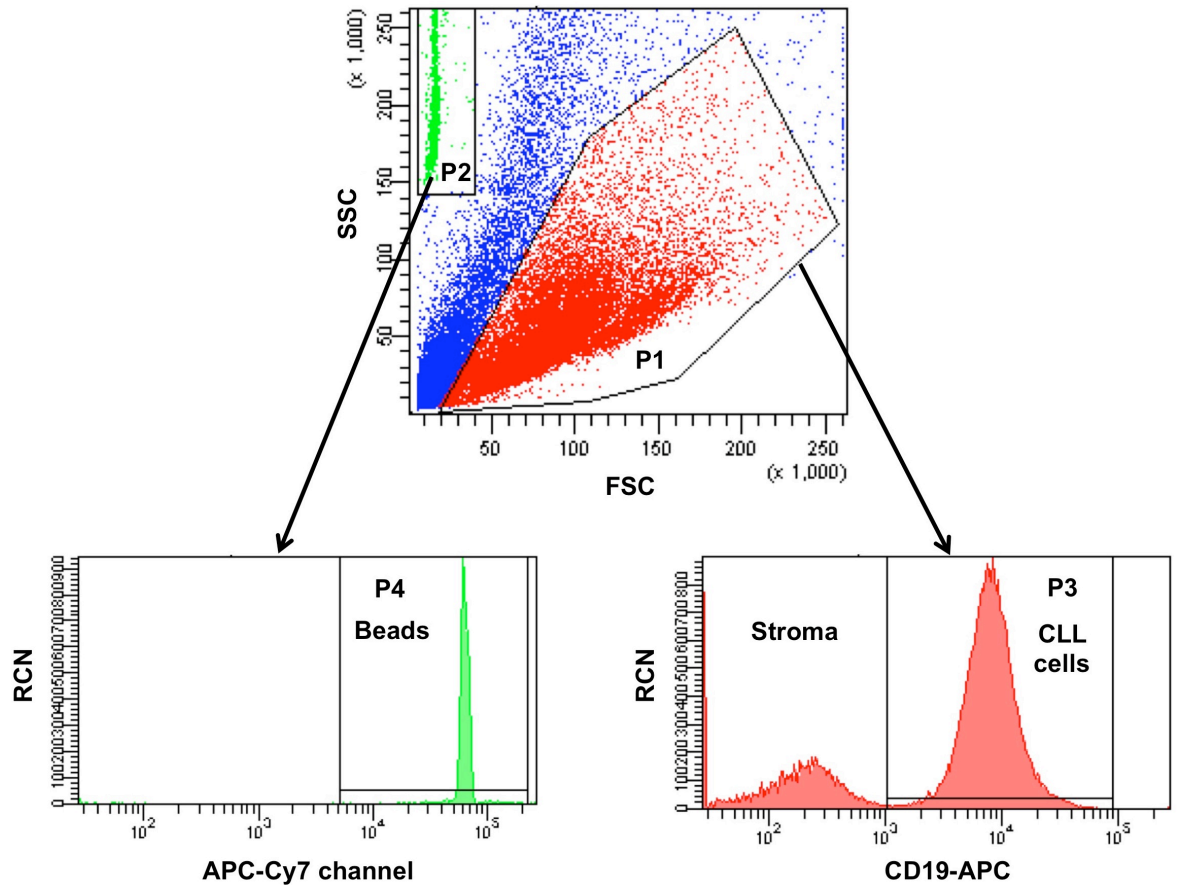
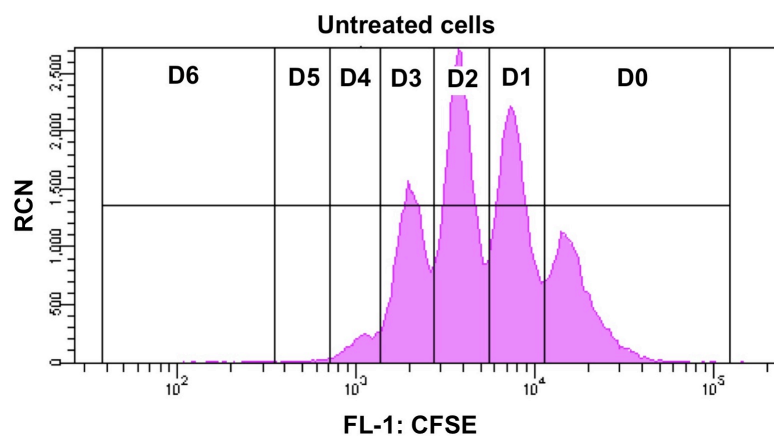
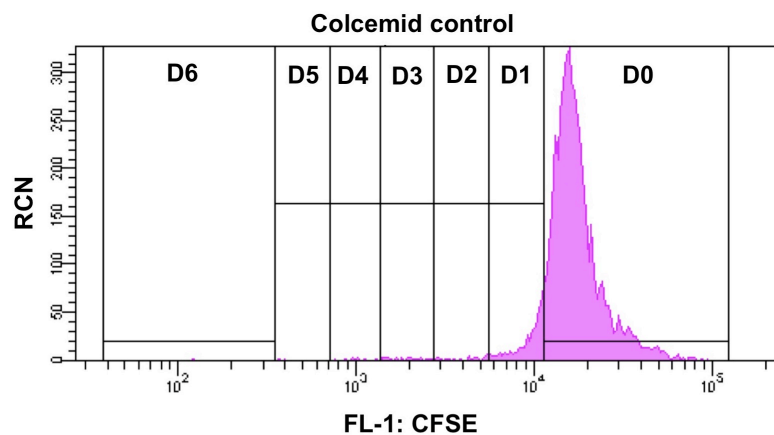


**Figure 2.7 Gating strategy used to perform CLL cell counts using CountBright™ beads**

To count CLL cells cultured in the 12-day proliferation assay by FCM, cells were treated as described in Section 1.3.9.1. In summary, cells were stained with an anti-CD19 APC-conjugated antibody, then CountBright™ beads were added prior to FCM. The dot plot shows gates set around the proliferating CLL cell (P1) and counting bead (P2) populations. As the counting beads fluoresce highly in all channels, the P2 gate was further gated on APC-Cy7 fluorescence (P4) to exclude any stromal cells falling into the gated population. The P1 gate was further gated on CD19 expression, again to exclude stromal cells falling into the size-gated population. Following the setting of gates, acquisition was started to record 5000 bead events (P4). The number of P3 events recorded during the period of acquisition was taken as the CLL cell count, for calculation of cell number using Equation 2.1.



**Untreated cells**

Gate	MFI	% of cells
D0	18,160	18.6
D1	7,798	28
D2	3,896	32
D3	2,036	18.3
D4	1,086	2.8
D5	577	0.2
D6	243	0

**Figure 2.8 Gating strategy used to assess CLL proliferation using CFSE**

The two histogram plots show the analysis of colcemid-treated (upper) and untreated (lower) CLL cells from one sample following six days of culture in the 154L/IL-4 proliferation assay. The MFI of colcemid-treated cells was used in order to set gates to delineate cells within successive cell divisions, as described in Section 1.3.9.2 and demonstrated in the table above. The table also indicates the percentage of total CLL cells within each division; **D0** represents undivided cells, **D1** cells in division 1, and so on.

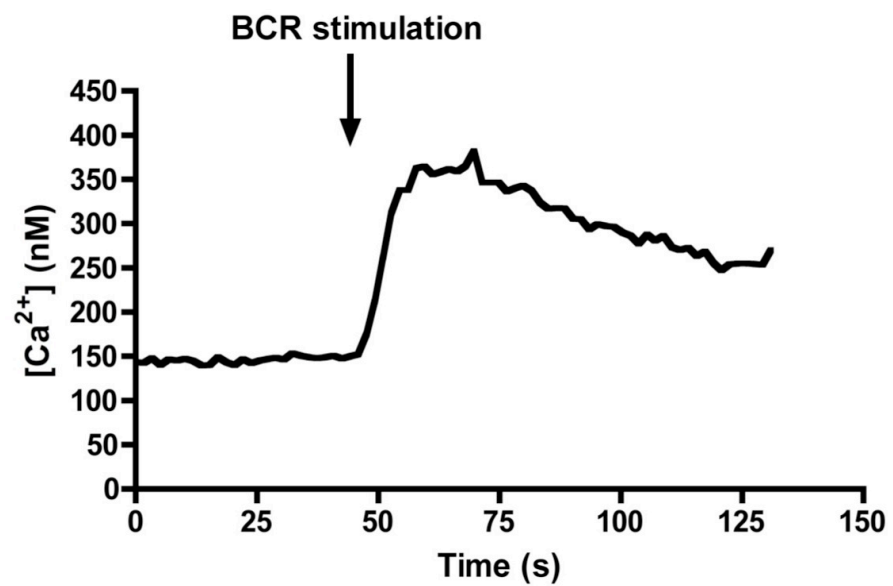


**Figure 2.9 Example of the determination of calcium flux following BCR crosslinking in Ramos B cells by fluorescence spectrophotometry**

Ramos B cells were loaded with 1  $\mu$ M Fura-2 as described in Section 2.4. Cells were then incubated with 10  $\mu$ g/ml biotinylated anti-IgM for 30 min prior to BCR stimulation. Cells were transferred to the spectrophotometer cuvette; basal calcium concentration was recorded for 40 sec, followed by BCR crosslinking by injection of avidin into the cell suspension (arrowed). Data were recorded for a total of 130 sec. The graph shows the change in  $[Ca^{2+}]$  over time in a representative experiment.

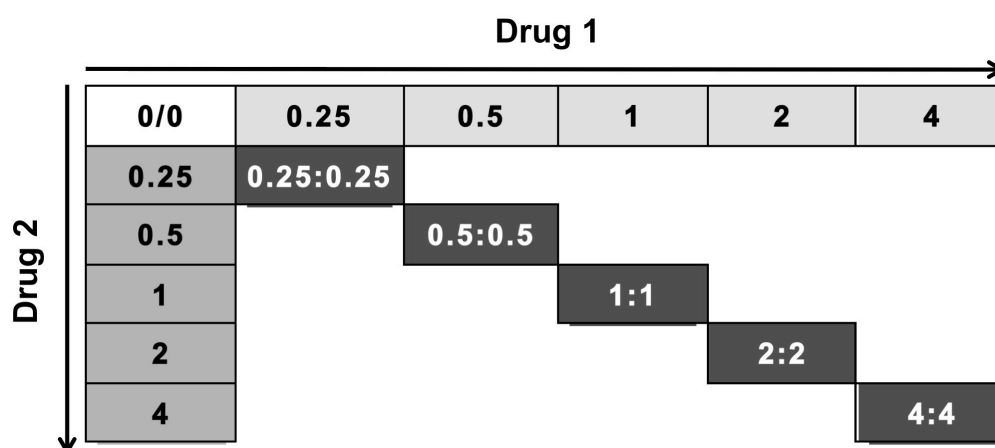


**Figure 2.10 Illustration of the constant ratio combination design of drug synergy experiments**

The numbers in this Figure refer to the multiple or fraction of the determined  $EC_{50}$ , with 1 representing the  $EC_{50}$  concentration. Drug combination treatments (diagonal) were planned using drugs at their equipotency ratio ( $EC_{50}$  of each drug), and multiples or fractions thereof. This approach maintained a constant drug ratio in combination treatments, which allowed data analysis with Calcsyn<sup>®</sup> software as described in Section 2.8.2.

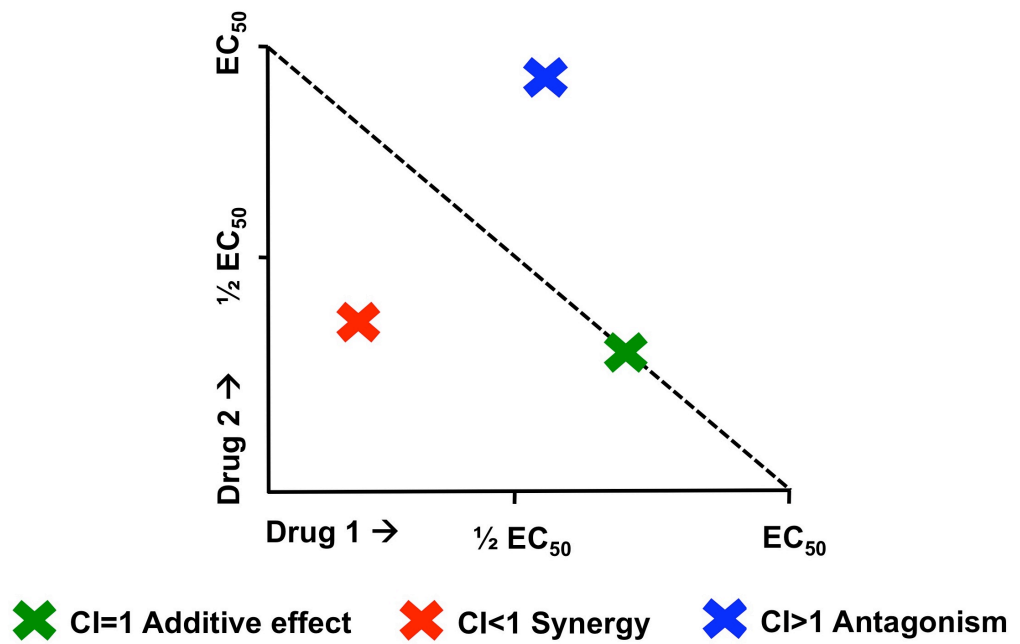


**Figure 2.11 Classical isobologram and illustration of synergistic or antagonistic effects.**

The graph illustrates the principle of the isobologram plot, in which the dotted line is representative of concentrations of drug 1 and drug 2 required to produce an additive effect ( $CI=1$ ). Points to the left of the line indicate synergy ( $CI<1$ ) and above and to the right indicate antagonism ( $CI>1$ ).

### **Chapter 3:**

**Dasatinib induces apoptosis of CLL cells *in vitro*, and shows synergy with established and novel chemotherapeutic agents.**

### **3.1 Introduction**

The rationale for investigating dual Src/c-Abl TKI in CLL stems from the fact that inhibition of Src kinases or c-Abl singly induces a degree of apoptosis of CLL cells *in vitro*, raising the possibility that dual Src and c-Abl kinase inhibition may be a more effective therapeutic approach. In this Chapter, the ability of dasatinib to induce apoptosis of primary CLL cells is assessed, with the following specific objectives.

### **3.2 Aims and Objectives**

To investigate the ability of dasatinib to induce apoptosis of CLL cells *in vitro*, the specific aims of this chapter were:

- i. To test the ability of the Src/c-Abl TKI dasatinib to induce apoptosis of CLL cells *in vitro*;
- ii. To assess whether the apoptotic response to dasatinib varies between prognostic groups;
- iii. To determine the mechanism of apoptosis triggered by dasatinib;
- iv. To establish whether dasatinib causes preferential apoptosis of CLL cells compared to normal B lymphocytes;
- v. To investigate whether dasatinib exhibits synergy with established current chemotherapeutic agents, and with novel Bcl-2 and HSP90 inhibitors.

### 3.3 Results

#### 3.3.1 The Src/c-Abl TKI dasatinib induces apoptosis of CLL cells *in vitro*.

In order to test the hypothesis that dual Src/c-Abl TKI would be an appropriate investigational treatment for CLL, preliminary experiments were performed to confirm over-expression of Lyn and c-Abl kinases in CLL cells. The expression of Lyn and c-Abl kinases in cell lysates prepared from normal B lymphocytes and CLL cells was assessed by immunoblotting, and is shown in Figure 3.1. Both c-Abl and Lyn are seen to be over-expressed in CLL samples compared to normal lymphocytes. This was confirmed using densitometry, with Lyn expression ranging from 2-3.5 fold that of normal B lymphocytes, and c-Abl over-expression ranging from 1.7-3.4 fold. In order to confirm that inhibition of Src kinases could induce apoptosis, primary CLL cells were incubated *in vitro* with increasing concentrations of the Src-family kinase inhibitor PP2 (1-10  $\mu\text{M}$ ), or the negative control compound PP3, which has no Src kinase inhibitory activity. Following a 48 hr incubation, apoptosis was assessed by FCM using Annexin V/Viaprobe staining. As can be seen in Figure 3.2A, PP2 increased the percentage of early apoptotic cells in a concentration-dependent manner. Figure 3.2B shows the  $\text{IC}_{50}$  for PP2 in CLL cells at 48 hr to be in the region of 7  $\mu\text{M}$ , similar to the value of 10  $\mu\text{M}$  reported previously by Contri *et al.* (203). Data is expressed as the percentage of viable cells relative to the control in individual experiments, as this allows for comparison between samples which show variable rates of spontaneous apoptosis on culture *in vitro*. To directly compare PP2, imatinib, and dasatinib, CLL patient samples were incubated with each of the inhibitors for 48 hr, following which apoptosis was assessed by FCM. As the project aimed to be translational to the clinic, emphasis was placed on comparing clinically achievable concentrations of imatinib and dasatinib. Pharmacokinetic studies conducted in patients treated with TKIs for CML have determined the maximum tolerated plasma concentration ( $C_{\text{max}}$ ) of standard dose imatinib (400 mg) to be in the region of 4  $\mu\text{M}$  (213) with a mean trough concentration of approximately 1  $\mu\text{M}$  (341). Similar studies of CML patients treated with dasatinib have determined a  $C_{\text{max}}$  of 129 nM (342). Therefore, CLL cells were treated with imatinib (1 and 10  $\mu\text{M}$ ), PP2 (1, 3, 6, and 10  $\mu\text{M}$ ), or dasatinib (1, 10, 100, and 300 nM) for 48 hr, followed by assessment of apoptosis by FCM (Fig. 3.3). While 10  $\mu\text{M}$  imatinib only achieved a modest level of apoptosis (mean cell viability 80.4% of untreated control), dasatinib induced a greater level of apoptosis at clinically achievable

concentrations (100 nM resulting in a mean cell viability of 55.8% relative to control), confirming dasatinib to be worthy of further investigation.

To determine the optimal time point to assess apoptosis following dasatinib treatment, CLL cells from three different samples were treated with increasing concentrations of dasatinib and apoptosis assessed at 24, 48, and 72 hr of incubation. Apoptosis was observed after 24 hr of exposure (Fig. 3.4), with a slight increase at the later time points which did not reach statistical significance. On the basis of these preliminary data, 48 hr of dasatinib treatment was selected for analysis of apoptosis in a larger group of patient samples. Results from the assessment of dasatinib exposure in 18 different CLL samples are shown in Fig. 3.5. Whilst dasatinib rarely resulted in apoptosis of over 50% of cells relative to untreated controls, the half-maximal effect concentration ( $EC_{50}$ ) concentration is in the region of 10 to 30 nM, which is consistent with the known  $EC_{50}$ s of dasatinib for Src and c-Abl kinases. In addition, the degree of apoptosis observed on dasatinib treatment reaches a peak at 100 nM, with a plateau in response at greater concentrations. In view of this, 100 nM dasatinib was selected for use in all further experiments unless otherwise stated.

### **3.3.2 Dasatinib-induced apoptosis is independent of established prognostic factors.**

To assess whether the level of apoptosis achieved with dasatinib correlated with established prognostic factors, a panel of 28 CLL patient samples were treated in the presence or absence of 100 nM dasatinib for 48 hr, followed by assessment of apoptosis. Although the mean reduction in viability was 33.7% ( $p < 0.001$ ), significant inter-patient variability was observed, with a standard deviation of 17.9% (Fig. 3.6). The percentage reduction in viability following 48 hr treatment with 100 nM dasatinib for each individual sample was next correlated with ZAP-70 status (Fig. 3.7A), Binet clinical stage (Fig. 3.7B), and FISH cytogenetic abnormalities (Fig. 3.7C). No significant correlation was seen between the level of response to dasatinib and any of these prognostic factors. Significantly, CLL cells harbouring deletions of chromosomes 11q or 17p responded similarly to other cases, demonstrating that dasatinib induced apoptosis is not p53 dependent. As our CLL samples were obtained from both untreated and previously treated patients, it is possible that effects of previous chemotherapy may have confounded the results. However, when the data were correlated with patient treatment history (Fig. 3.7D), no significant difference was observed between treated and untreated

patients. In addition, no correlation was observed between the rate of spontaneous *in vitro* apoptosis and sensitivity to dasatinib.

### **3.3.3 Dasatinib-induced apoptosis in CLL cells is caspase-dependent.**

Although measurement of the binding of Annexin V to exposed phosphatidylserine on the cell surface is a well established method for the assessment of apoptosis in B lymphocytes (343), loss of phospholipid asymmetry is an early event in the pathway of apoptosis which occurs prior to DNA fragmentation. Indeed, a study investigating apoptosis following crosslinking of surface immunoglobulin in the B cell lymphoma cell line BCL<sub>1</sub>3B3 have demonstrated that Annexin V binding cells can remain viable following cessation of stimulation, confirming that membrane asymmetry occurs prior to commitment to apoptosis (344). In addition, assessment of Annexin V/Viaprobe staining gives no information on the pathway of apoptosis triggered within the cell. Therefore, to assess whether analysis of Annexin V binding by FCM is reflective of the percentage of CLL cells committed to apoptosis, and to investigate the apoptotic mechanism triggered by dasatinib, CLL cells were treated with and without 100 nM dasatinib for 48 hr, followed by simultaneous assessment of a number of measures of apoptosis by FCM. Aliquots of cells were stained with either Annexin V/Viaprobe, with TMRM to assess MMP, or a PE-conjugated antibody specific for the activated form of caspase 3.

In Figure 3.8A, it can be seen that in addition to increasing the percentage of cells which bind Annexin V, dasatinib also leads to loss of MMP, and activation of caspase 3. Data generated from assessment of three CLL patient samples demonstrated that the percentage of cells which bind Annexin V following dasatinib treatment is very similar to the percentages of cells which lose MMP and show caspase 3 activation (Fig 3.8B), confirming that at this time point, Annexin V staining does accurately reflect the percentage of CLL cells committed to apoptosis.

Although the execution of cell death by apoptosis is conventionally considered to be carried out exclusively by the action of effector caspases 3, 6, and 7, it is becoming increasingly recognised that apoptosis may occur through caspase-independent pathways, executed by the release of alternate proteases from mitochondria or lysosomes (345, 346). To determine whether apoptosis induced by dasatinib is entirely caspase dependent, CLL cells were treated with the pan-

caspase inhibitor Z-VAD-fmk 2 hr prior to treatment with and without dasatinib for up to 48 hr. In Figure 3.9A, Z-VAD-fmk is seen to slightly reduce the level of spontaneous apoptosis, and completely inhibit apoptosis induced by dasatinib. At 48 hr (Fig. 3.9B), Z-VAD-fmk treatment is seen to slightly increase apoptosis, suggesting a degree of toxicity, which is likely to explain why Z-VAD-fmk fails to completely prevent apoptosis induced by dasatinib at this time point. These data confirm that dasatinib-induced apoptosis of CLL cells is caspase-dependent.

As loss of MMP and caspase 3 activation may be triggered by both the extrinsic and intrinsic pathways of apoptosis (315), western blotting was used to assess the cleavage of initiator pro-caspases 8 and 9 in CLL cells treated with dasatinib. CLL cells were treated with increasing concentrations of dasatinib for 48 hr, followed by assessment of apoptosis using Annexin V/VI probe staining, and assessment of caspase 8, caspase 9, and PARP by immunoblotting. With increasing concentrations of dasatinib, the increase of apoptotic cells assessed by FCM was accompanied by increased cleavage of full-length 116 kDa PARP to the 89 kDa fragment, confirming apoptosis (Fig. 3.10). Alongside this, a decrease in the levels of pro-caspase 8 and pro-caspase 9 was observed, although no cleaved active caspase fragments were observed. As caspase activation is an early event in apoptosis, 48 hr may be too late a time point to fully assess caspase activation. Therefore, to assess caspase activation at earlier time points, CLL cells from one patient were treated with 100 nM dasatinib for time points up to 24 hr, and caspases were again assessed by Western blotting. Prior to 12 hr of treatment, both pro-caspase 8 and pro-caspase 9 cleavage products were detectable, and preceded the complete cleavage of PARP (Fig 3.11). These data suggest that dasatinib may induce apoptosis through both the extrinsic and intrinsic pathways. Experiments assessing the effect of specific caspase inhibitors on apoptosis induced by dasatinib would clarify the relative contribution of both pathways.

### **3.3.4 Duration of dasatinib exposure required to induce apoptosis of CLL cells *in vitro*.**

In performing translational assessment of novel therapeutic agents, an important consideration is the length of exposure time required to commit cells to apoptosis. In CML cells, incubation with 100 nM dasatinib for 4 hr followed by drug washout is sufficient to induce a degree of apoptosis, measured at 72 hr (347). To determine the length of dasatinib exposure required to induce apoptosis in CLL cells, cells were treated with 100 nM dasatinib for 2, 4, 8, 12, and 24 hr, followed by drug

washout, and culture in complete medium for a total of 48 hr. Untreated cells, and cells treated continuously with 100 nM dasatinib for 48 hr were also included as indicated (Fig. 3.12). A degree of apoptosis was observed after as little as 2 hr of dasatinib exposure, with little difference observed between 2 and 24 hr incubation (Fig 3.12), suggesting that a degree of dasatinib-induced apoptosis is induced on short-term exposure. As a greater level of apoptosis was observed on continuous drug exposure, a sustained target inhibition may be required for maximum effect.

### **3.3.5 Dasatinib also induces a degree of apoptosis in normal B lymphocytes.**

Although cytopenias due to generalised myelosuppression are common in patients with CML treated with dasatinib (309), the question remains as to whether dasatinib shows a selective toxic effect towards CLL cells as opposed to normal mature B lymphocytes. To address this issue, normal B lymphocytes were isolated from 'buffy coat' components from blood donations using CD19 positive magnetic selection. Following separation, cells were treated with increasing concentrations of dasatinib, and apoptosis was assessed at 24 and 48 hr. At 24 hr, dasatinib reduced the mean cell viability from 58 to 43% (n=3; Fig. 3.13). Normal B lymphocytes did not survive well on *in vitro* culture, compared with CLL cells, as has been reported by others (221), with a mean cell viability at 48 hr of just 33%, making formal comparison between CLL cells and normal B cells difficult at this time point.

### **3.3.6 Bcl-2 inhibitors and HSP90 inhibitors induce apoptosis of CLL cells *in vitro*.**

Results thus far indicate that dasatinib alone induces apoptosis of less than fifty percent of CLL cells, therefore this agent may be best utilised in combination strategies. Therefore, the next phase of investigation focussed on the assessment of drugs which may enhance apoptosis with dasatinib, followed by studies to assess the efficacy of dasatinib in combination with both novel agents and established chemotherapeutic agents.

As outlined in Section 1.8.2, small molecule Bcl-2 inhibitors show much promise in CLL as novel therapeutic agents in CLL. In addition to dysregulated tyrosine kinases which provide survival signals to CLL cells, the apoptotic machinery is also dysregulated, with high level expression of anti-apoptotic Bcl-2. Therefore, combining a TKI such as dasatinib with an agent capable of redressing the

balance of apoptosis-regulatory proteins within CLL cells is a rational novel therapeutic approach.

The efficacy of two BH3-mimetic Bcl-2 inhibitors to induce apoptosis of CLL cells was first assessed in order to determine appropriate drug concentrations to study in combination with dasatinib. CLL cells were treated with increasing concentrations of Bcl-2 inhibitor I and Bcl-2 inhibitor III (both 0-10  $\mu\text{M}$ ) for 24 and 48 hr, followed by assessment of apoptosis using Annexin V/VI probe staining. Both inhibitors induced concentration-dependent apoptosis of CLL cells, and representative experiments are shown in Figure 3.14. The mean  $\pm$  SEM  $\text{IC}_{50}$  of Bcl-2 inhibitor I was  $4.6 \pm 0.2 \mu\text{M}$  at 24 hr, and  $4.3 \pm 0.3 \mu\text{M}$  at 48 hr ( $n=5$ ). The mean  $\pm$  SEM  $\text{IC}_{50}$  for Bcl-2 inhibitor III was  $4.9 \pm 0.3 \mu\text{M}$ , and at 48 hr was  $3.6 \pm 0.4 \mu\text{M}$  ( $n=5$ ). As Bcl-2 inhibitor I induced a more consistent response in CLL cells, and binds both Bcl-2 and Bcl-x<sub>L</sub> (325), it was selected for further study in combination studies.

The rationale for investigating dasatinib in combination with HSP90 inhibitors stems from the knowledge that in CLL cells, in addition to increased membrane-associated Lyn kinase, around 30% of total Lyn is located within the cytoplasm (203), where it has been proposed to exert an anti-apoptotic effect. The catalytic domain of cytoplasmic Lyn has been demonstrated to be associated with HSP90, maintaining Lyn in an active conformation, preventing degradation of the protein by the proteasome (348). HSP90-associated Lyn forms part of a multi-molecular complex, in which Lyn engages additional proteins including haematopoietic lineage cell-specific protein-1 (HS1) and SH2-domain-containing tyrosine phosphatase (SHP-1L) through its SH3 domains (348). HS1 is phosphorylated on BCR stimulation, and phosphorylated HS1 has been identified as a poor prognostic feature in CLL (349). Treatment of CLL cells with the HSP90 inhibitors geldanamycin or 17-AAG resulted in the dissociation of Lyn from HSP90, in a timescale correlating with reversal of the global increase in tyrosine phosphorylation, and induction of apoptosis (348). Used in combination, dasatinib and HSP90 inhibitors may result in a synergistic effect due to simultaneous targeting of Lyn kinase activity and the cytoplasmic HSP90 complex which prevents Lyn degradation.

To confirm that 17-DMAG induces apoptosis of CLL cells *in vitro*, cells were treated with increasing concentrations of 17-DMAG (0.01-3  $\mu\text{M}$ ) for 24 and 48 hr,

followed by assessment of apoptosis. Results from a total of five experiments are shown in Fig 3.15. Similar to a previous report (332), 17-DMAG induced apoptosis of CLL cells at sub-micromolar concentrations, with an  $IC_{50}$  at 48 hr in the region of 0.2  $\mu$ M.

### **3.3.7 Dasatinib exhibits synergy with fludarabine, chlorambucil, and novel therapeutic agents *in vitro*.**

Synergy between two drugs describes the situation in which the combination results in a more than additive effect on the target or cell viability (340). In addition to increasing the desired toxic effect on malignant cells, synergy between agents may prove advantageous in allowing lower concentrations of each individual drug to be used to achieve a desired effect, in order to avoid toxicity to normal cells. We investigated whether dasatinib exhibited synergy in combination with the current standard chemotherapeutic agents chlorambucil and fludarabine, and also with the novel Bcl-2 and HSP90 inhibitors.

Calculusyn software, based on the method of Chou and Talalay(340), was used to assess drug synergy, as described in detail in Section 2.8.2. For all drug combination experiments, the diagonal constant ratio combination experimental design was used, in which cells are treated with serial dilutions of drugs alone, and in combination at multiples and dilutions of their equipotency ratio. Published  $IC_{50}$ s for chlorambucil in CLL cells range from 5-80  $\mu$ M (213), and fludarabine from 0.4-20  $\mu$ M (350). The concentrations of dasatinib used in all cases were 6.25, 12.5, 25, 50, and 100 nM. Concentrations of fludarabine used were 1.25, 2.5, 5, 10, and 20  $\mu$ M (200:1 ratio to dasatinib), and of chlorambucil used were 3.13, 6.25, 12.5, 25, and 50  $\mu$ M (500:1 ratio to dasatinib). Bcl-2 inhibitor I was used at 0.5, 1, 2, 4, and 8  $\mu$ M (80:1 ratio to dasatinib), and 17-DMAG was used at 62.5, 125, 250, 500, and 1000 nM (10:1 ratio to dasatinib).

In all combination experiments, CLL cells were treated with drugs alone and in combination for 24 hr, followed by assessment of apoptosis by Annexin V/VIprobe using FCM. Data generated for each drug treatment was expressed as the fraction affected using Equation 2.4, following which Calculusyn<sup>®</sup> software was used to calculate CIs. A representative example of the graphs generated by the software for an experiment assessing dasatinib in combination with fludarabine is given in Figure 3.16, which shows the dose response curves for each individual drug and the combination (Fig. 3.16A), the median effect plot of each dose

response curve calculated from the dose-response curve using Equation 2.6 (Fig. 3.16B), and the classical isobologram, on which the EC<sub>50</sub>, EC<sub>75</sub>, and EC<sub>90</sub> isobolograms are shown (Fig. 3.16C). In the example shown, the EC<sub>50</sub> CI is 0.23, EC<sub>75</sub> CI 0.34, and EC<sub>90</sub> CI 0.58 (r=0.90). The EC<sub>50</sub> CI's for five individual samples in which dasatinib was assessed in combination with each of the four drugs are shown in Figure 3.17, with a summary in Table 3.1. Dasatinib exhibited synergy with all four drugs tested, most notably with fludarabine, with a mean EC<sub>50</sub> CI of 0.29 (strong synergy). The mean EC<sub>50</sub> CIs for dasatinib in combination with chlorambucil, Bcl-2 inhibitor I, and 17-DMAG were 0.62, 0.76, and 0.48 respectively. In conclusion, although dasatinib exhibits modest apoptosis as a single agent, the demonstrated synergy with both established and novel chemotherapeutic agents confirm that dasatinib may be an attractive drug in combination studies.

### 3.4 Discussion

We have demonstrated that the dual Src/c-Abl TKI dasatinib induces apoptosis of CLL cells *in vitro* at clinically achievable concentrations, and is significantly more potent than the Abl inhibitor imatinib. As dasatinib is now appreciated to inhibit a significant number of tyrosine kinases, this raises the question of the chief targets of the anti-leukaemic effects of the drug in CLL cells. The EC<sub>50</sub> of dasatinib in CLL cells of 10-30 nM is consistent with the known inhibitory concentrations of dasatinib for Src and c-Abl kinases. As dasatinib and PP2 inhibit all Src family kinases, it is possible that inhibition of Src kinases other than Lyn may be involved in the induction of apoptosis. Although expression of the Src kinases Lck and Fgr has been reported in CLL (351, 352), Contri *et al.* compared expression of the Src kinases Lyn, Src, Fyn, Fgr, and Lck at the protein level in ten CLL samples, and demonstrated Lyn to be the predominantly expressed Src kinase in all cases (203). Although specific inhibition of individual Src kinases using antisense RNA would help to establish the relative contributions of each to the increase in basal global tyrosine phosphorylation in CLL cells, recent evidence strongly implicates Lyn to be the predominant kinase involved. Cytoplasmic Lyn is associated with HSP90, and disruption of this complex using the HSP90 inhibitor geldanamycin inhibited the tyrosine phosphorylation pattern and induced apoptosis (348). The c-Abl kinase inhibitors imatinib and nilotinib have been shown to have little effect on the global tyrosine phosphorylation pattern in CLL cells (353). Of note, Lyn knockdown with siRNA in a B cell lymphoma cell line significantly inhibited proliferation (354).

As outlined in Section 1.6.2.2, c-Abl expression was reported to correlate with adverse prognostic features in CLL. Moreover, the capacity of unmutated CLL or ZAP-70 positive cases to signal through the BCR led to great interest in investigation of dual Src/c-Abl TKIs as novel agents to preferentially target BCR-mediated survival signals key to the biology of high-risk patient groups. In view of this, the anti-leukaemic effects of dasatinib in CLL cells *in vitro* have now been assessed by a number of groups in addition to the present study (350, 353, 355, 356). In keeping with our study, Veldurthy *et al.* reported dasatinib as a single agent capable of inducing apoptosis of CLL cells, but to rarely reach an IC<sub>50</sub>, despite high drug concentrations. This group also reported CLL cells with unmutated IgV<sub>H</sub> genes (or expressing ZAP-70) to be significantly more sensitive to dasatinib than those with mutated IgV<sub>H</sub> genes or lacking ZAP-70 expression (353).

In our study, although mutational status of our CLL patient samples was not available, no significant difference in the level of apoptosis induced by dasatinib was observed between ZAP-70 positive and negative CLL cells. In comparing the two studies, a number of variables require consideration. Both studies used CLL samples obtained from some patients who had received previous treatment. As may be expected, in our study, more ZAP-70 patients had received prior treatment than ZAP-70 negative patients (8 of 14 compared to 4 of 14 respectively), however as we observed no significant difference in response between treated and untreated groups, it is unlikely that this significantly biased our results. It is possible that the different findings between the studies may be partly explained by the difference in dasatinib concentrations used, 5  $\mu$ M was used by Veldurthy *et al.*, compared to 100 nM used in our experiments. As the IC<sub>50</sub>s of dasatinib for c-Abl and Src kinases are in the low nanomolar range (303), these kinases will be adequately inhibited using a concentration of 100 nM, supported by our data showing a mean EC<sub>50</sub> concentration of 10-30 nM for dasatinib. At a concentration of 5  $\mu$ M, dasatinib is predicted to inhibit additional tyrosine kinases, including MEK (IC<sub>50</sub> = 1.7  $\mu$ M) and VEGFR-2 (IC<sub>50</sub> > 2  $\mu$ M) (303), raising the possibility of 'off-target' inhibition of additional kinases which may vary in activity between mutated and unmutated CLL. In support of this hypothesis, a recent study found that a significant difference in the level of apoptosis on dasatinib treatment between IgV<sub>H</sub> mutational subgroups (greater in unmutated than mutated CLL) was only observed at concentrations of dasatinib of 10  $\mu$ M and above, whilst levels of cell death were similar between mutational subgroups on treatment with 100 nM dasatinib (357). Moreover, another published study, using 100 nM dasatinib, reported no significant associations between level of apoptotic response and Rai stage, mutational status or ZAP-70 expression (350).

As Lyn over-expression, constitutive activity, and association with the cytoplasmic multi-protein complex involving HSP90, are features common to both IgV<sub>H</sub> mutational subgroups (203, 348), the pro-apoptotic effect of Src kinase inhibition by dasatinib should be equal between mutational groups. A recent case report of a patient with CML treated with dasatinib, who had co-existent ZAP-70 negative CLL, achieved NCI-WG criteria for partial remission (PR)(22) of CLL whilst on therapy (358). Although an isolated case, this suggests that further clinical investigation of dasatinib should not be limited to those with ZAP-70 positive or unmutated CLL.

The role of c-Abl signalling in CLL, and the effect of TKIs on c-Abl signalling in CLL requires further clarification. In a study of 26 CLL patient samples, a significant association between basal c-Abl expression and the level of apoptosis induced by treatment with 10  $\mu$ M imatinib for 72 hr has been reported (212), leading to the conclusion that CLL cells expressing high levels of constitutively active c-Abl are dependent on c-Abl signalling for survival. It was therefore surprising that CLL cells expressing high levels of c-Abl have been reported to be significantly less sensitive to dasatinib than those with low c-Abl expression (350). This study suggested that CLL cell sensitivity to dasatinib is dependent on inhibition of c-Abl downstream pathways, however both groups demonstrated that in CLL cells expressing high levels of c-Abl, significant inhibition of the downstream kinase Dok could be achieved by TKI treatment. Furthermore, using an electrophoretic mobility shift assay, Lin *et al.* confirmed that imatinib inhibits NF- $\kappa$ B transcriptional activity (212). It may be relevant that in the study by Amrein *et al.* the NF- $\kappa$ B-p65 levels were significantly higher in the c-Abl<sup>high</sup> group of samples compared to the c-Abl<sup>low</sup> group (350). Supporting this is the fact that in the three patient samples analysed for NF- $\kappa$ B-p65 (Rel A) expression following treatment with dasatinib, there is a positive correlation between the ability of dasatinib to inhibit Rel A expression and the CLL cell sensitivity to dasatinib. RelA is an independent biomarker of prognosis in CLL (359), and may be regulated by c-Abl-independent pathways such as PI-3K/Akt signalling (360), therefore the sensitivity of CLL cells to dasatinib may in part depend on inhibition of NF- $\kappa$ B activity, and this may explain the apparent contradiction between the two reports.

In addition, CLL cell sensitivity to TKI with imatinib has been reported to correlate positively with expression of the prostate-apoptosis regulatory protein (Par-4) (361). Par-4 has been characterised as a tumour suppressor gene which sensitises cells to both the intrinsic and extrinsic pathways of apoptosis, in addition to negatively regulating survival signalling pathways such as NF- $\kappa$ B (362). In the Jurkat T-lymphocytic cell line, Par-4 increases caspase 8 cleavage following cell exposure to chemotherapeutic agents (363), and sensitise Bcr-Abl positive cells to imatinib (364). Further studies to correlate Par-4 expression, and the effect of dasatinib on NF- $\kappa$ B activity may therefore be informative.

In the present study, no correlation between dasatinib sensitivity and either Binet clinical stage or FISH cytogenetic group was found. Of note, dasatinib induced a comparable level of apoptosis in CLL cells with 17p deletions on FISH to that

observed in other cases, suggesting that dasatinib triggers apoptosis through a p53-independent pathway, as has previously been reported for imatinib in CLL (212). Supporting this conclusion, a high level of apoptosis following dasatinib treatment of a CLL sample with a combined 17p deletion and functional mutation of the remaining allele has been reported in another study (353). In fact, recent evidence suggests that CLL cells with 17p deletion are more sensitive to the pro-apoptotic effect of dasatinib than those with functional p53 (365), suggesting that p53 signal transduction may actually inhibit apoptosis following dasatinib treatment in CLL cells. Following DNA damage, nuclear p53 promotes transcription of a number of genes which promote apoptosis (including Puma and Bax), or cell cycle arrest and repair (p21<sup>CIP1</sup>), whilst cytoplasmic p53 interacts directly with Bcl-2 proteins on the mitochondrial surface (Bcl-2, Bcl-x<sub>L</sub>, and Bax); apoptosis occurs if the capacity of the cell to repair DNA damage is overwhelmed by pro-apoptotic stimuli (366). In CLL cells, inhibition of p53 transcriptional activity using the selective inhibitor pifithrin  $\alpha$  actually augmented the level of apoptosis induced by fludarabine *in vitro* (367). The transcriptional targets mediating the anti-apoptotic effects of p53 in CLL cells remain to be elucidated, although p21<sup>CIP1</sup> may be proposed as a candidate. In preliminary experiments, Amrein *et al.* also demonstrated that pifithrin  $\alpha$  was able to augment apoptosis induced by dasatinib alone in CLL cells with wild-type p53 (365). Collectively, these data suggest that dasatinib may benefit patients with p53 deletion or mutation. A recent case report of a near complete remission in a patient with stage B unmutated CLL with 17p deletion, who was treated with dasatinib for a co-existent gastro-intestinal stromal tumour (368), supports further clinical investigation of dasatinib in this patient group.

Our results confirm that whilst apoptosis induced by dasatinib is p53-independent, it is dependent on caspase activation. Using a concentration of 5  $\mu$ M dasatinib, Veldurthy *et al.* reported dasatinib to induce loss of MMP, cleavage of both initiator caspases 8 and 9, and effector caspases 3, 6, and 7, resulting in PARP cleavage (353). In our study, we also observed cleavage of both caspase 8 and 9, loss of MMP, and PARP cleavage, confirming these features are also seen on treatment of CLL cells with a clinically attainable concentration of dasatinib, and suggesting dasatinib to activate both the extrinsic and intrinsic apoptotic pathways. Cleavage of both caspase 8 and 9 has also been reported on treatment of B-cell lymphoma cell lines with a dual Src/c-Abl TKI (369). Dasatinib decreases expression of the

anti-apoptotic Bcl-2 proteins Mcl-1 and Bcl-x<sub>L</sub> (353), which may explain the mechanism for loss of MMP and caspase 9 activation. It is interesting to note that in human neutrophils, direct phosphorylation of caspase 8 by Lyn has been reported, and shown to extend neutrophil survival (370); whether such an interaction occurs in CLL cells remains to be determined. As caspase 8 can itself activate the mitochondrial apoptotic pathway through the cleavage of Bid (371), caspase 8 activation could be the initiating pro-apoptotic event on dasatinib treatment of CLL cells. The relative contribution of the intrinsic and extrinsic apoptotic pathways in dasatinib-induced apoptosis may be clarified by the use of specific inhibitors of caspase 8 and 9.

In our experiments, normal B lymphocytes isolated from buffy coat components survived poorly on *in vitro* culture, making formal comparison of the effects of dasatinib on normal compared to CLL cells at 48 hr difficult. At 24 hr, a slight concentration-dependent reduction in viability was observed, which did not reach statistical significance. Using the XTT assay to assess cellular respiration, Veldurthy *et al.* reported a significant dose-dependent decrease in metabolic activity in CLL cells treated with dasatinib, whilst peripheral blood mononuclear cells (PBMC) were unaffected at dasatinib concentrations up to 5  $\mu$ M (353). In PBMC preparations, T cells will account for the majority of lymphocytes. T lymphocyte viability has been shown to be unaffected by dasatinib (372). In our studies, B lymphocytes were specifically isolated from PBMC preparations by positive magnetic selection for CD19, therefore the difference in dasatinib effect between the two studies may be explained by the composition of the cell population being assessed. As B lymphocytes are dependent on a basal level of BCR signalling, involving Lyn kinase, there is a possibility that Lyn inhibition may induce apoptosis of normal B lymphocytes by inhibiting tonic signalling (373). The effect of dasatinib on tonic and ligand-induced BCR signalling is addressed in Chapter 4.

Our data show dasatinib to induce modest apoptosis in most CLL samples tested, suggesting its' clinical utility as a single agent may be limited. In a recent phase II clinical trial of dasatinib, dosed as 140 mg once-daily, in 15 patients with refractory or relapsed CLL, NCI-WG-defined PRs were achieved in only two patients, with no CRs (374). We demonstrated dasatinib to exhibit synergy with both established and novel chemotherapeutic agents. Veldurthy *et al.* found the combination of 5  $\mu$ M dasatinib with 5  $\mu$ M fludarabine to result in approximately 50% greater

apoptosis than with either agent alone (353). Whilst encouraging, these data are insufficient for the assessment of synergy between two drugs. We used the established method of Chou and Talalay to assess synergy in drug combinations (340), as described in Section 2.8.2, to calculate CIs. Using this method, the combination of dasatinib and fludarabine was confirmed to be strongly synergistic, with a mean CI of 0.26. Dasatinib in combination with chlorambucil was also synergistic, however less so than with fludarabine. Synergy between dasatinib and both fludarabine and chlorambucil has also been reported by Amrein *et al.*, who used a similar mathematical analysis (350).

There is evidence to suggest that inhibition of c-Abl is central to the ability of dasatinib to sensitise CLL cells to chemotherapeutic agents. Imatinib has previously been reported to sensitise CLL cells to chlorambucil (213). Alkylating agents such as chlorambucil induced apoptosis largely by the introduction of DNA interstrand crosslinks (375), and the CLL cells' ability to repair crosslinked DNA correlated with drug sensitivity (376). Following DNA damage, c-Abl relocates to the cell nucleus (377), where it may promote both DNA repair or apoptosis. Within the nucleus, c-Abl becomes phosphorylated by ATM, and subsequently phosphorylates and activates the p53-related pro-apoptotic kinase p73 (366). Inhibition of c-Abl with imatinib has been shown to inhibit CD154-induced expression of p73 in CLL cells (291). Simultaneously, activated c-Abl also phosphorylates Rad51, an enzyme involved in DNA recombination and repair (378, 379). Phosphorylated Rad51 is able to associate with the related enzyme Rad52, to promote DNA repair. In CLL cells, c-Abl inhibition by imatinib inhibited the increase in phosphorylation of Rad51 induced by chlorambucil, and this mechanism was proposed to account for the sensitisation of CLL cells to chlorambucil by imatinib (213). Amrein *et al.* demonstrated that dasatinib inhibited up-regulation of Rad51 following treatment with chlorambucil or fludarabine, and increased the total level of DNA damage, as assessed by the accumulation of the histone-family protein  $\gamma$ H2AX (350). In this study, dasatinib also inhibited the up-regulation of p53 protein levels on treatment of CLL cells with either chlorambucil or fludarabine. As the mechanism of fludarabine-induced apoptosis also involves the introduction of DNA strand breaks (380), inhibition of DNA repair through c-Abl inhibition may well account for synergy between fludarabine and chlorambucil. Although in the present study, stronger synergy was observed between dasatinib and fludarabine in 4 of 5 cases, Amrein *et al.* reported no significant difference

between the synergy value reported for dasatinib in combination with fludarabine as compared to chlorambucil (350). Analysis of a larger cohort of patient samples is required to draw firm conclusions.

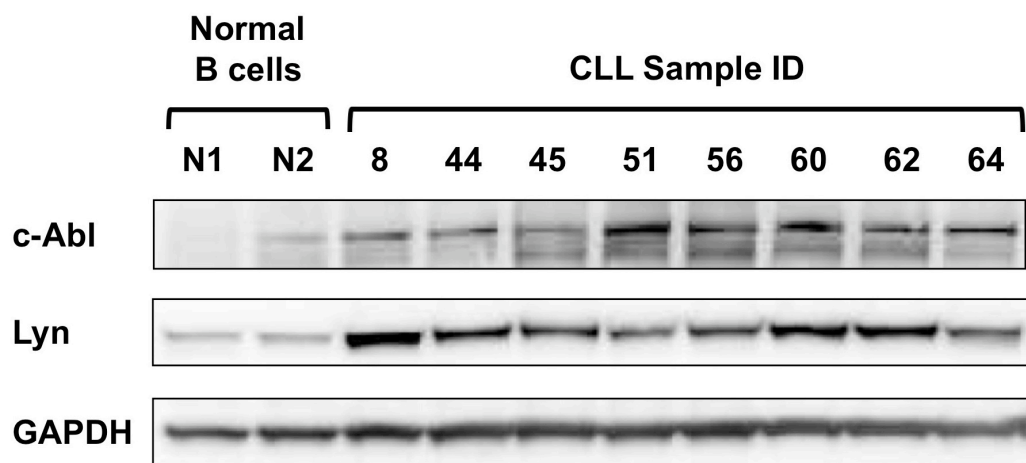
Synergy between dasatinib and either BH3-mimetic Bcl-2 inhibitors or HSP90 inhibitors has not previously been reported in CLL cells. Further work is required to determine the mechanism of synergy in each case. Very recently, the sensitivity of DLBCL cell lines to the Src kinase inhibitor PP2 has been shown to negatively correlate with both Bcl-2 and Bcl-x<sub>L</sub> expression (354). Further analysis of the effect of dasatinib on Bcl-2 family protein expression may aid understanding of the mechanism of synergy with Bcl-2 inhibitor I. The synergy between dasatinib and 17-DMAG may be due to Lyn-specific effects of inhibition of kinase activity by dasatinib combined with increased Lyn degradation following disruption of the cytosolic HSP90/Lyn complex, or may be due to inhibition of additional pro-survival signalling pathways by 17-DMAG.

In summary, these data show dasatinib as an attractive candidate for further investigation in combination strategies. Further experiments will aim to assess the effect of dasatinib on BCR signalling (Chapter 4), and to determine the efficacy of dasatinib combination approaches to induce apoptosis of CLL cells cultured in the presence of additional microenvironmental signals (Chapter 5).

**Table 3.1 Degree of synergy observed in CLL cells treated with dasatinib in combination with established and novel therapeutic agents**

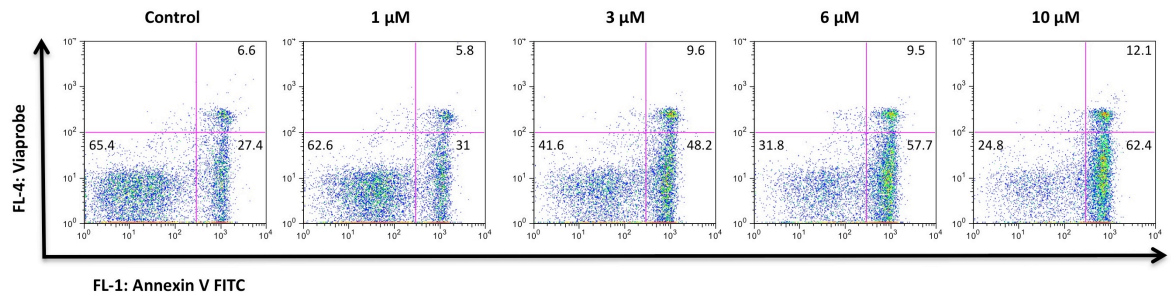
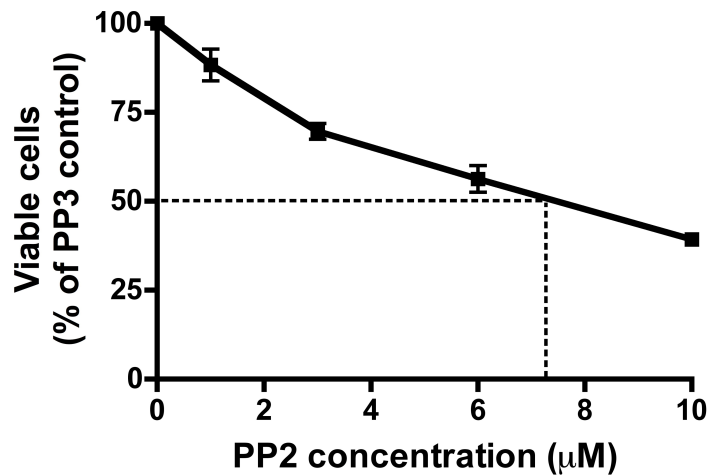
<b>Drug in combination with dasatinib</b>	<b>Ratio of drug to dasatinib</b>	<b>Mean EC<sub>50</sub> CI (SEM)</b>	<b>Degree of Synergy*</b>
Fludarabine	200:1	0.17 (0.11)	++++
Chlorambucil	500:1	0.62 (0.05)	+++
Bcl-2 inhibitor I	80:1	0.76 (0.03)	++
17-DMAG	10:1	0.48 (0.04)	+++

\* Definitions of synergy as described in Table 2.6



**Figure 3.1 Lyn and c-Abl are over-expressed in CLL cells compared to normal B lymphocytes**

Protein lysates were prepared from freshly isolated CLL cells, and from normal B lymphocytes isolated from blood donations using magnetic positive selection for CD19 as described in Section 2.2.6.2. Proteins were separated by gel electrophoresis, followed by immunoblotting for Lyn and c-Abl kinases. GAPDH was included as a protein loading control.

**A****B**

**Figure 3.2 The Src kinase inhibitor PP2 induces apoptosis of CLL cells**

**A** CLL cells were treated with 10 μM PP3 as a negative and vehicle control, and with increasing concentrations of the Src kinase inhibitor PP2 as shown for 48 hr, and apoptosis assessed using Annexin V/Viaprobe staining by FCM. Each condition was performed in triplicate. Dot plots from one replicate are shown, with numbers representing the percentage of total cells in each quadrant. **B** CLL cells from three patients (CLL9, CLL 35, and CLL 44) were treated with 10 μM PP3 or increasing concentrations of PP2 for 48 hr, and apoptosis assessed using Annexin V/Viaprobe staining by FCM. Each experiment was performed in at least duplicate. Results represent the mean ( $\pm$  SEM) viabilities of treated cells, relative to the PP3 negative control.

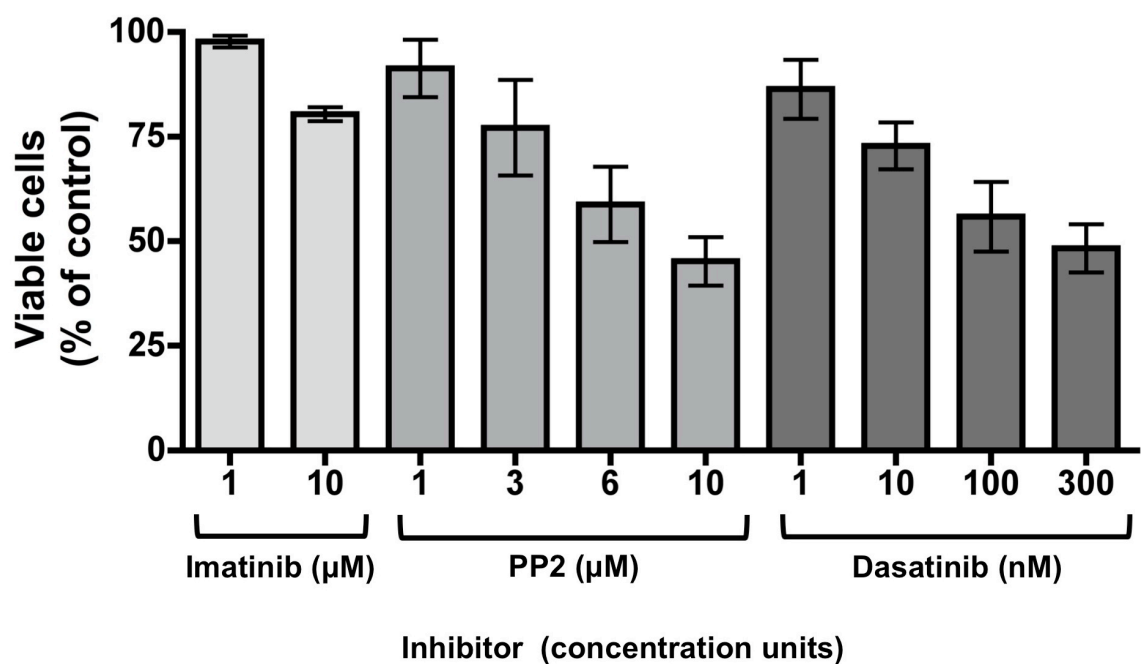
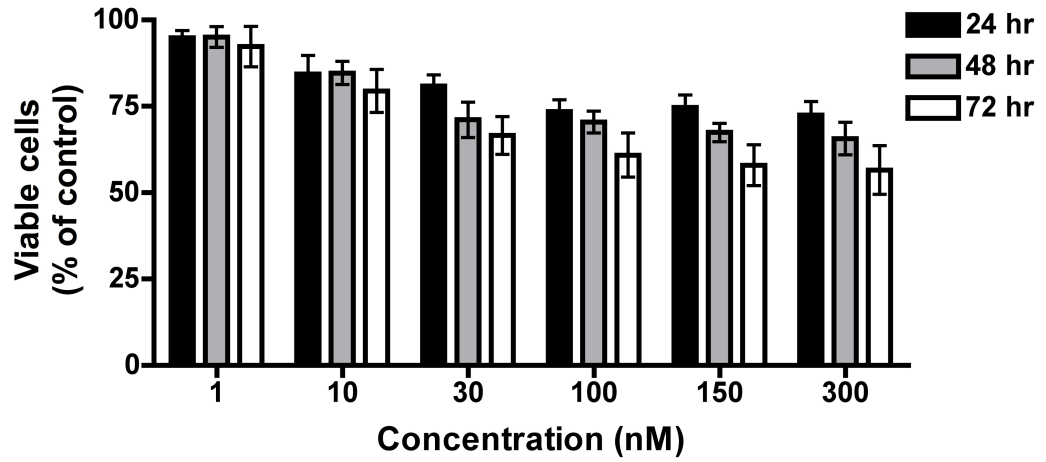


**Figure 3.3 Comparison of imatinib, PP2, and dasatinib on CLL cell viability**  
 CLL cells from three patients (CLL 35, CLL 44, and CLL 51) were treated with increasing concentrations of imatinib, PP2, dasatinib, or vehicle control (DMSO) for 48 hr, followed by assessment of apoptosis by FCM using Annexin V/Viaprobe staining. Results show the mean ( $\pm$  SEM) cell viabilities of treated cells, expressed as a percentage of the vehicle control.

**A**



**B**

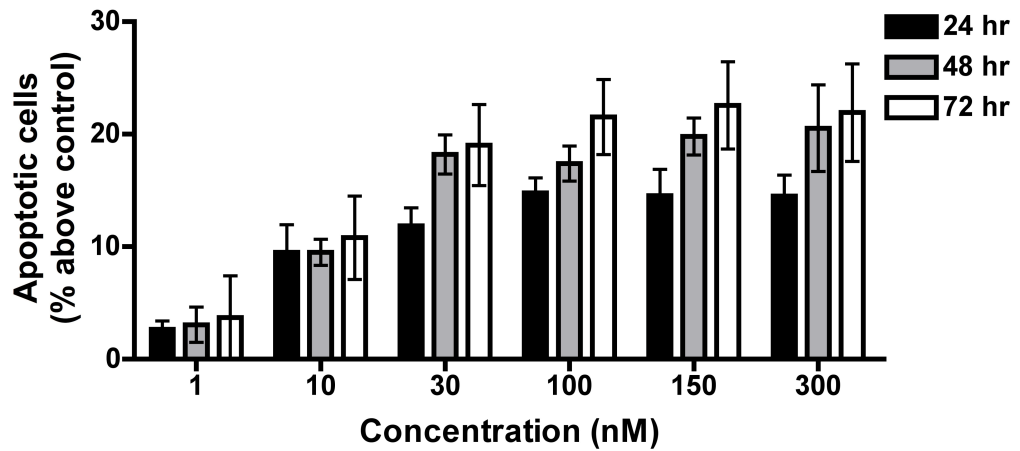
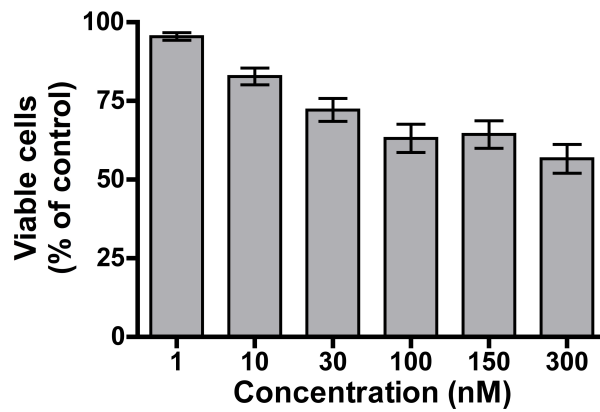


**Figure 3.4 Time course of apoptosis induced by dasatinib in CLL cells**

CLL cells from three patients (CLL 9, CLL 28, and CLL 38) were treated with increasing concentrations of dasatinib as shown, and apoptosis assessed by FCM using Annexin V/Viaprobe at 24, 48, and 72 hr. Each condition was performed in duplicate. Results represent the mean ( $\pm$  SEM) percentage of viable cells **A** or apoptotic, Annexin V<sup>+</sup>/Viaprobe<sup>-</sup>, cells **B** relative to untreated controls.

**A**



**B**

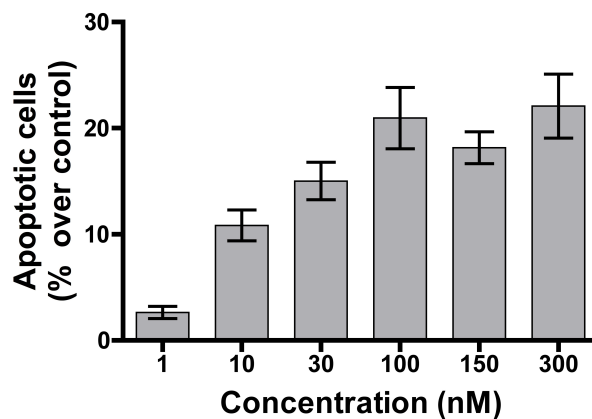
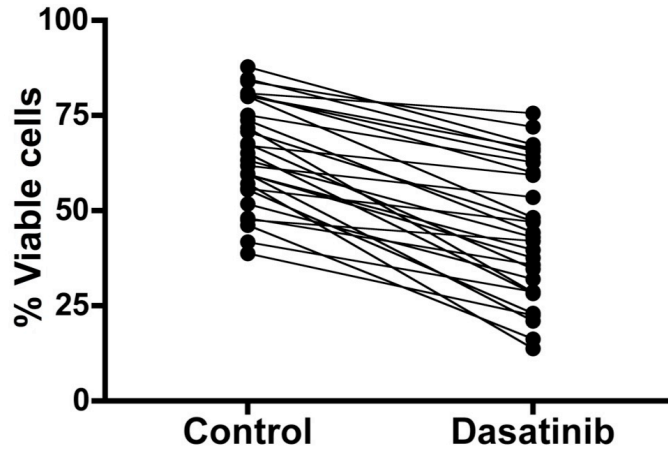


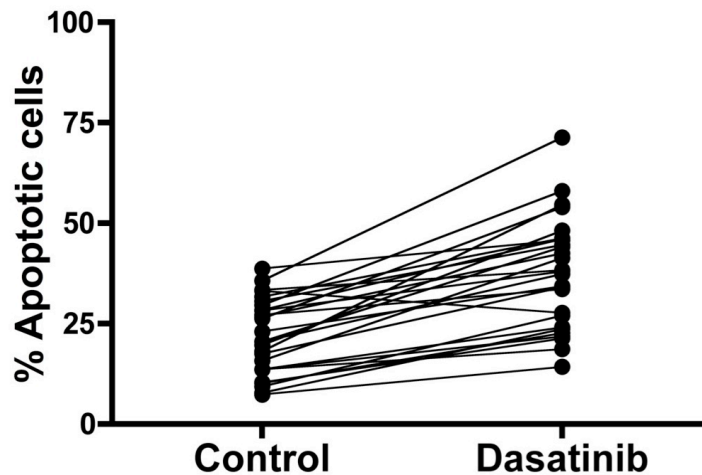
**Figure 3.5 Effect of increasing concentrations of dasatinib on CLL cell viability following 48 hr continuous treatment**

CLL cells from eighteen patients were treated for 48 hr with increasing concentrations of dasatinib, and apoptosis assessed by Annexin V/Viaprobe staining by FCM. Results represent the mean ( $\pm$  SEM) cell viability **A** and apoptosis **B** of treated samples relative to untreated controls. Annexin V<sup>+</sup>/Viaprobe<sup>-</sup> cells were considered apoptotic.

**A**

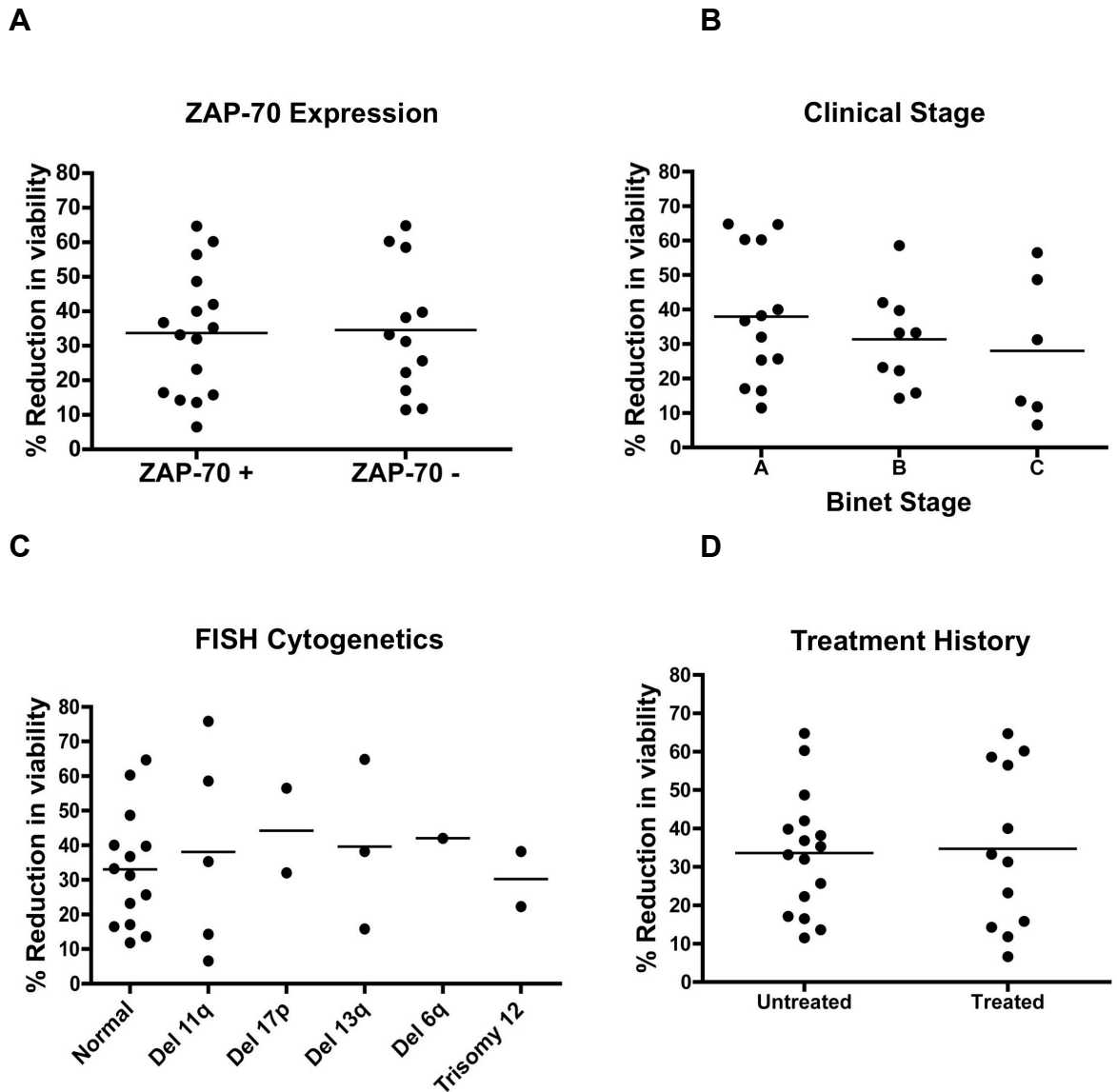


**B**



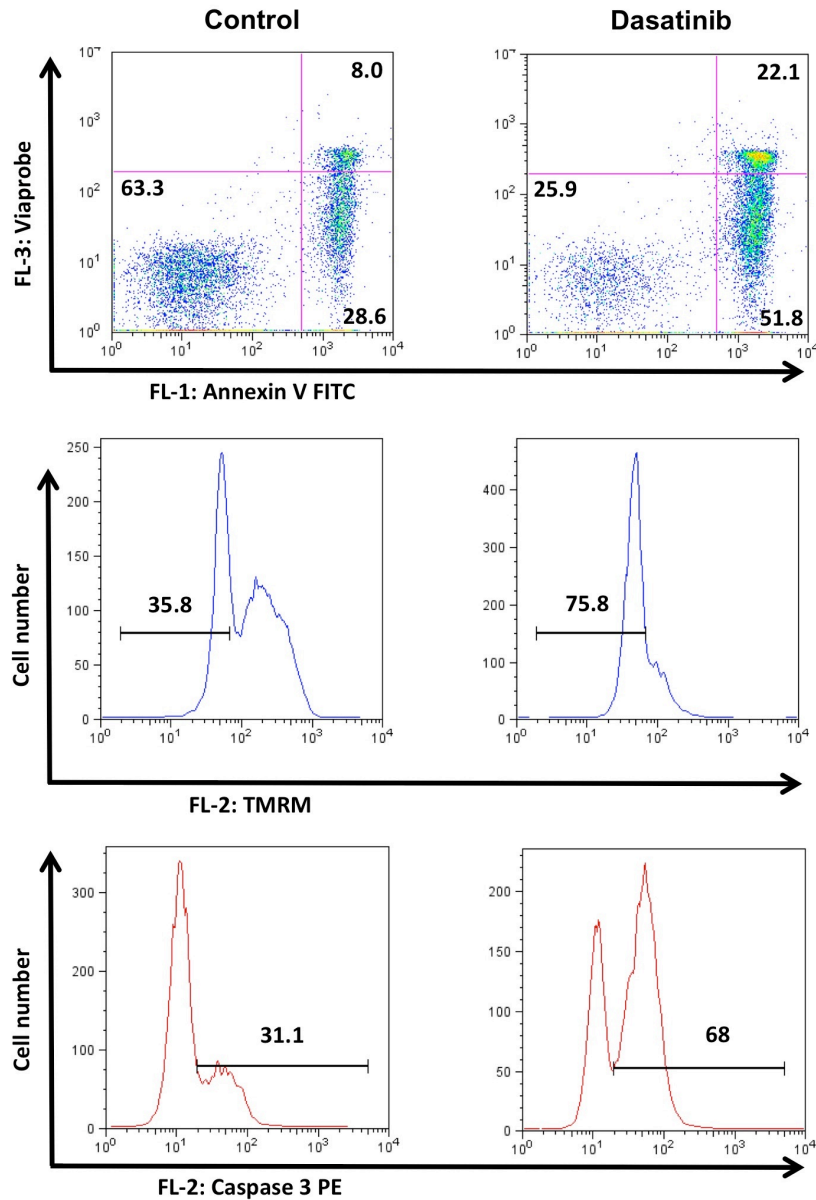
**Figure 3.6 Effect of 48 hr treatment with 100 nM dasatinib on individual CLL sample viability**

CLL cells from 28 patients were treated with 100 nM dasatinib for 48 hr, and apoptosis assessed by Annexin V/Viaprobe staining by FCM. The graphs show the percentage of viable **A** and apoptotic **B** cells in untreated and dasatinib treated samples. Annexin V<sup>+</sup>/Viaprobe<sup>-</sup> cells were considered apoptotic. The interconnecting lines connect paired results from each individual patient sample.



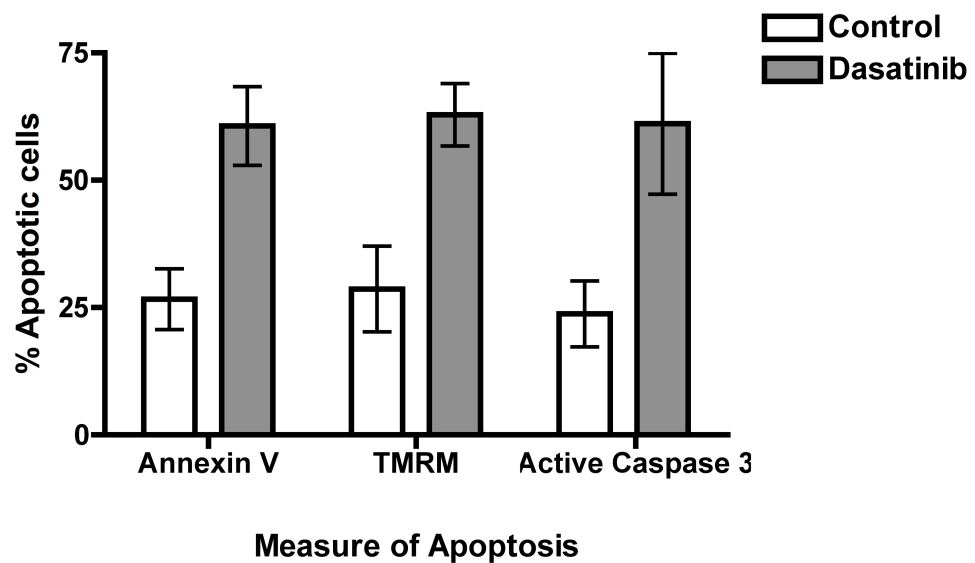
**Figure 3.7 Correlation of dasatinib response to prognostic factors**

The graphs correlate the individual patient sample responses shown in Fig. 3.6 with ZAP-70 expression **A**, Binet clinical stage **B**, and cytogenetic abnormalities detected by FISH **C**. In addition, response was correlated with patient treatment history **D**. Data is expressed for each sample as the percentage reduction in viability observed following 48 hr treatment with 100 nM dasatinib, relative to the untreated control.



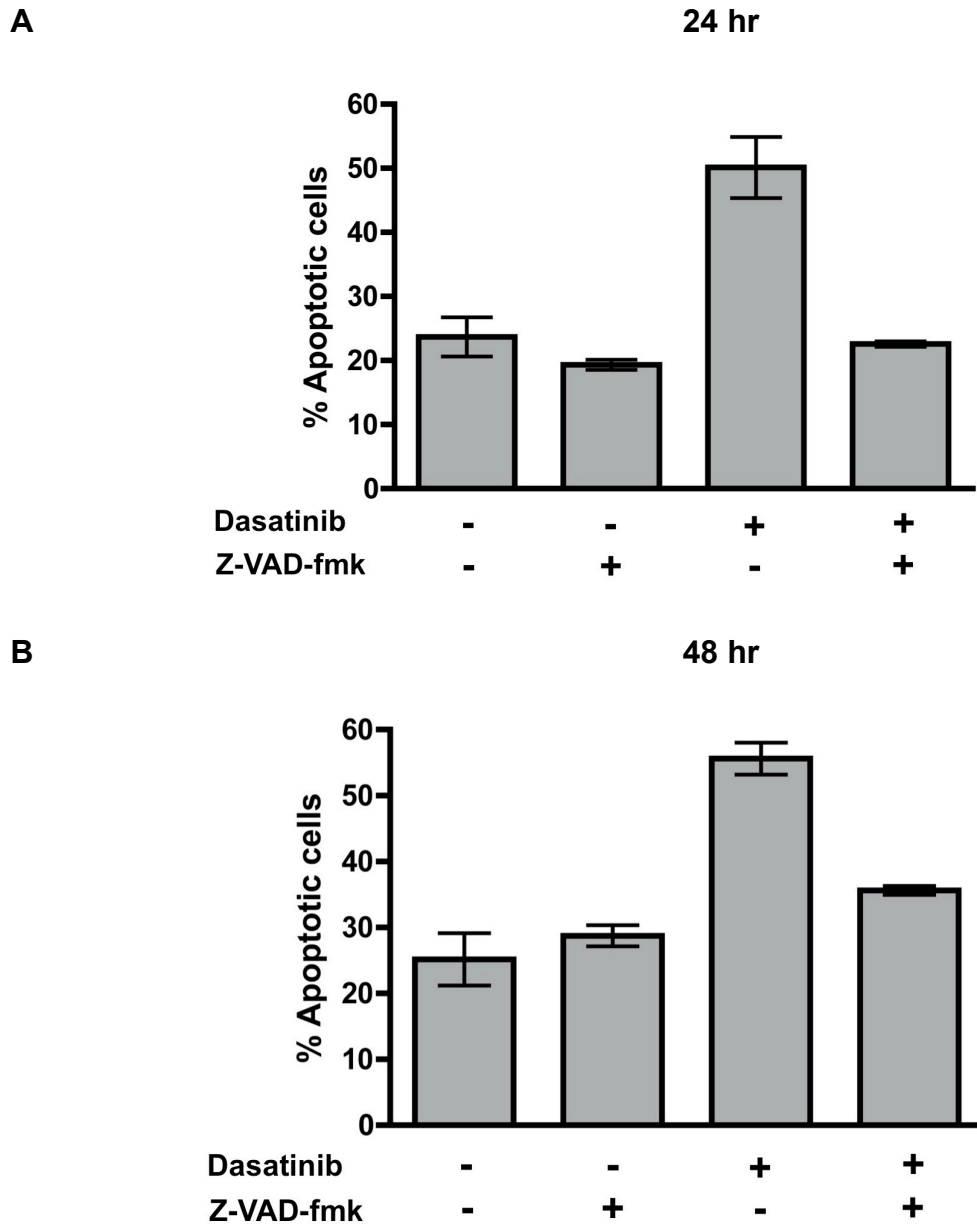
**Figure 3.8A Dasatinib induces loss of MMP and leads to caspase 3 activation.**

CLL cells from one patient (CLL 44) were cultured in the presence and absence of 100 nM dasatinib for 48 hr, then analysed by FCM for Annexin V/Viaprobe staining, for MMP using TMRM, and for caspase 3 activation, as described in Section 2.3. The experiment was performed in triplicate, and representative plots are shown. The numbers shown on the dot plots represent the percentage of cells within each quadrant. The gates on the histograms reflect the percentage of cells which have lost normal MMP (middle), and the percentage of cells in which caspase 3 is in an active conformation (bottom).



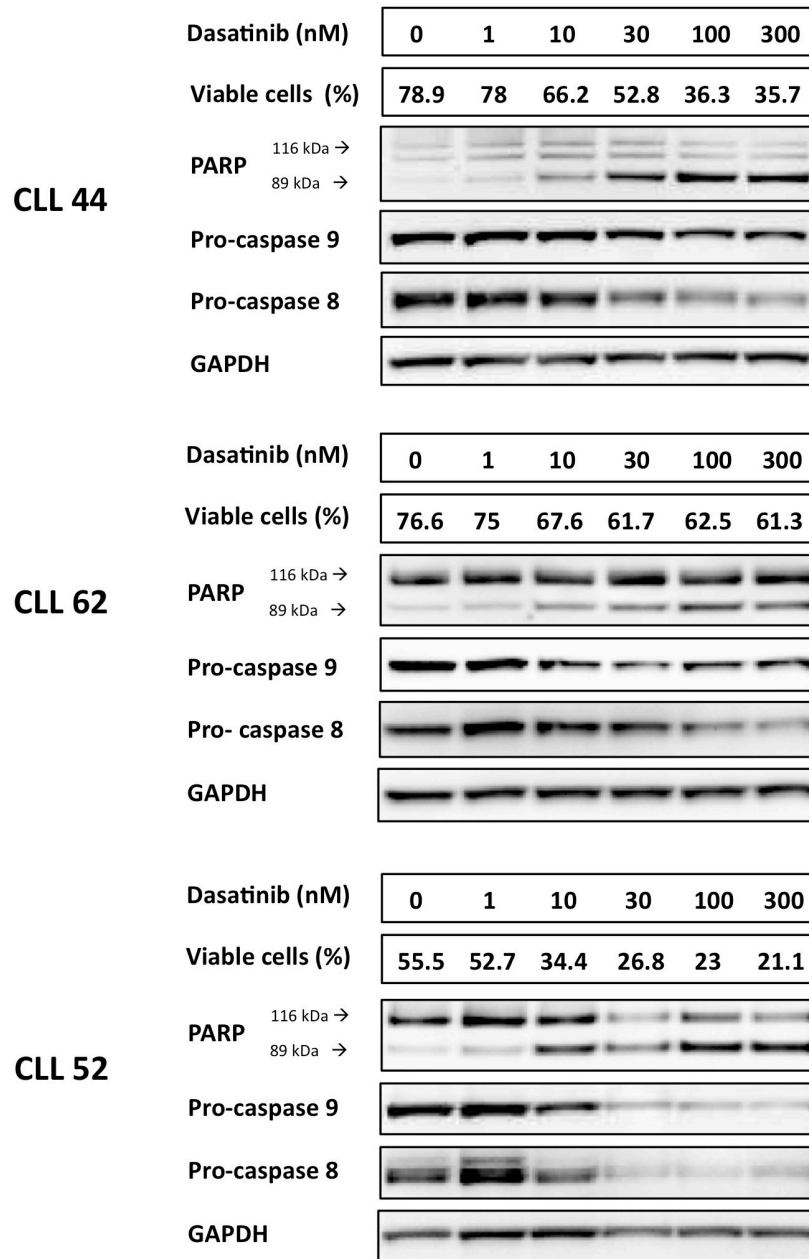
**Figure 3.8B Annexin V positivity correlates with loss of MMP and caspase activation following dasatinib treatment**

The results represent the mean  $\pm$  SEM values obtained from a total of three independent experiments carried out as described in Figure 3.8A. In this analysis, all Annexin V binding cells were considered apoptotic, as were cells which had lost normal MMP, and those which contained activated caspase 3.



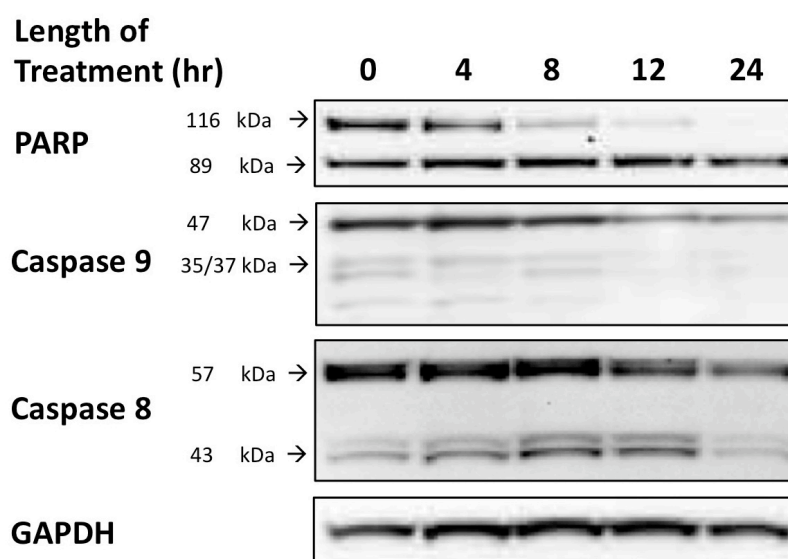
**Figure 3.9 Dasatinib-induced apoptosis is caspase-dependent**

CLL cells from three patients (CLL 12, CLL 44, and CLL 50) were treated with 25  $\mu$ M Z-VAD-fmk for 2 hr prior to treatment with 100 nM dasatinib as indicated. Apoptosis was assessed by Annexin V/Viaprobe staining by FCM at 24 and 48 hr. Annexin V<sup>+</sup>/Viaprobe<sup>-</sup> cells were considered apoptotic. Each condition was performed in triplicate in each patient sample. The results represent the mean ( $\pm$  SEM) percentages of apoptotic cells following treatments as indicated at 24 hr **A** and 48 hr **B**.



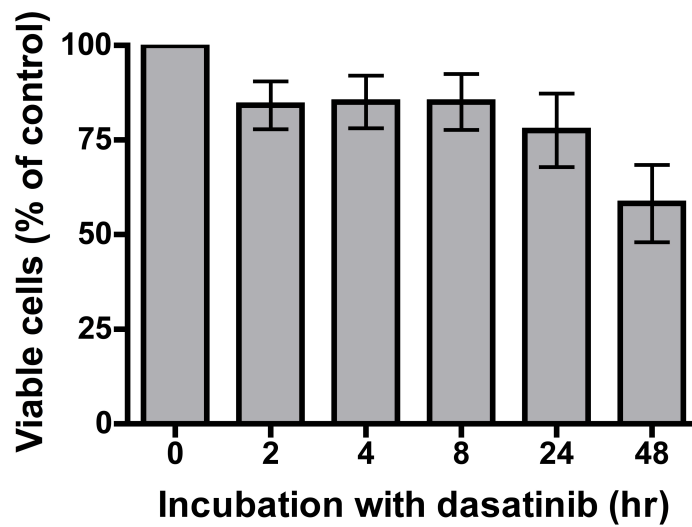
**Figure 3.10 Pro-caspase 8 and pro-caspase 9 are cleaved during dasatinib-induced apoptosis**

CLL cells from three patients were treated with increasing concentrations of dasatinib for 48 hr, then protein lysates prepared for analysis of initiator caspases 8 and 9, and PARP, by western blotting. An aliquot of cells from each condition was also taken for assessment of apoptosis by FCM using Annexin V/Viaprobe staining, and the percentage of viable cells in each treatment condition is shown above the immunoblot.



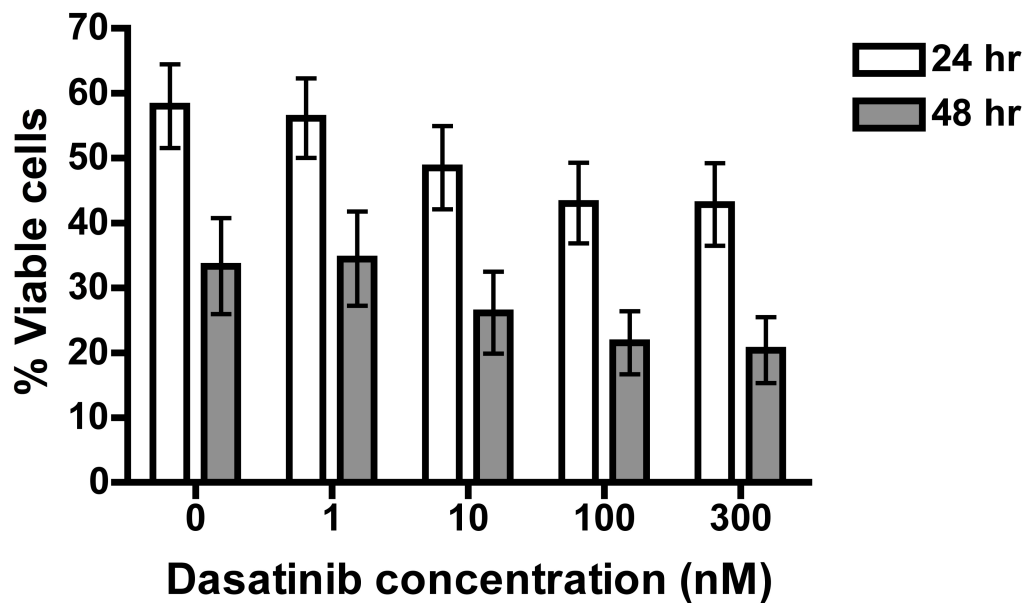
**Figure 3.11 Caspase cleavage occurs within hours of dasatinib treatment**

CLL cells from one patient (CLL 52) were treated with 100 nM dasatinib for 0, 4, 8, 12, and 24 hr, then protein lysates prepared for the assessment of caspase 8, caspase 9, and PARP by western blotting. Cleavage of pro-caspase 9 to active 35 and 37 kDa fragments is seen, as is cleavage of pro-caspase 8 to intermediate 41 and 43 kDa fragments.



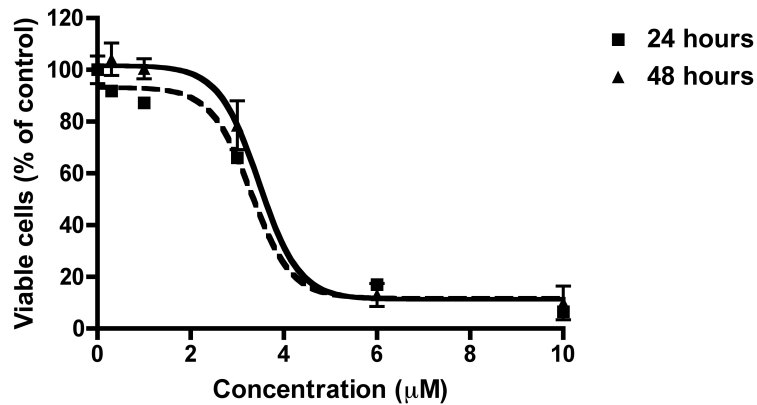
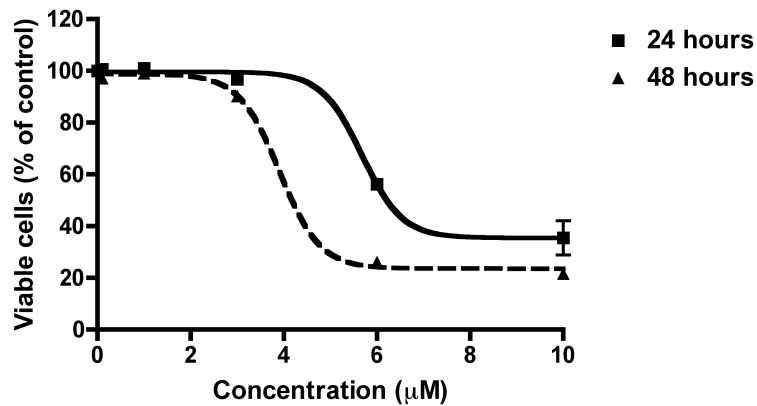
**Figure 3.12 Comparison of fixed-time versus continuous dasatinib exposure on CLL cell viability.**

CLL cells from three patients (CLL 16, CLL 35, and CLL 50) were treated with 100 nM dasatinib for 2, 4, 8, 24, and 48 hours. Following incubation for the relevant time points up to 24 hr, cells were pelleted and washed twice in PBS to remove dasatinib, and resuspended in complete media until 48 hr from the start of the experiment. Cells from all treatment conditions were harvested at 48 hr, and apoptosis assessed by Annexin V/Viaprobe staining.



**Figure 3.13 Dasatinib induces a degree of apoptosis in normal B lymphocytes**

Normal B lymphocytes (n=3) were treated with increasing concentrations of dasatinib for 24 and 48 hr, and apoptosis was assessed by FCM using Annexin V/Viaprobe staining. Each condition was performed in duplicate for each sample. The data are presented as the mean ( $\pm$  SEM) absolute cell viabilities for each condition at both time points.

**A****Bcl-2 inhibitor I****B****Bcl-2 inhibitor III**

**Figure 3.14 Bcl-2 inhibitors induce apoptosis of CLL cells *in vitro***

**A** CLL cells (n=5) were treated with increasing concentrations of Bcl-2 inhibitor I for 24 and 48 hr, and apoptosis assessed by FCM for Annexin V/Viaprobe staining. Each condition in each sample was performed in triplicate. The graph shows results from a representative experiment. Results are expressed as the mean ( $\pm$  SEM) cell viabilities of treated cells relative to the untreated control. **B**

CLL cells (n=5) were treated with increasing concentrations of Bcl-2 inhibitor III for 24 and 48 hr, and apoptosis assessed by FCM for Annexin V/Viaprobe staining. Each condition in each sample was performed in triplicate. The graph shows results from a representative experiment. Results are expressed as the mean ( $\pm$  SEM) cell viabilities of treated cells relative to the untreated control.

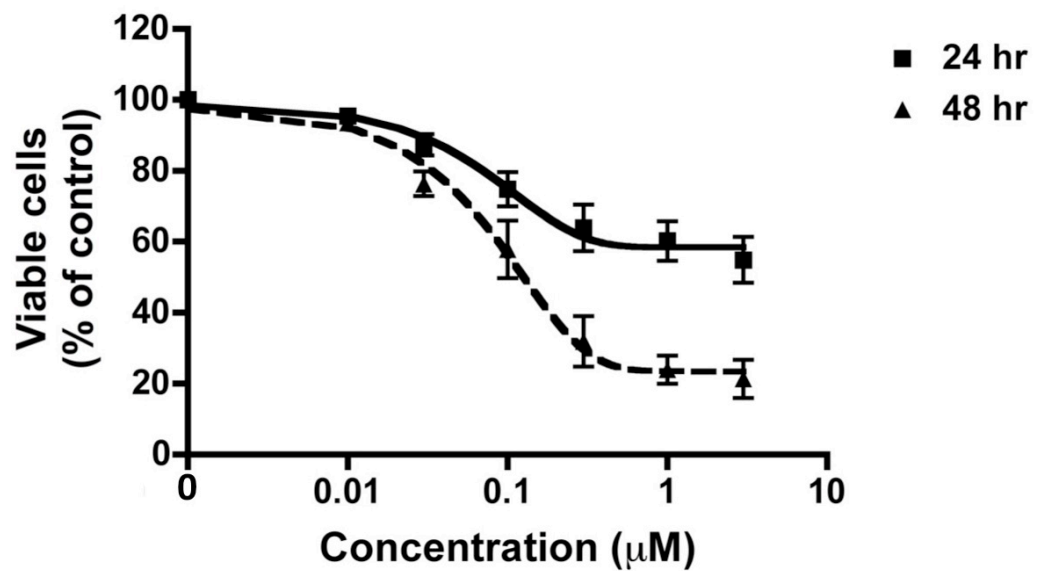


**Figure 3.15** 17-DMAG induces apoptosis of CLL cells *in vitro*.

CLL cells (n=5) were treated with increasing concentrations of 17-DMAG, followed by assessment of apoptosis by Annexin V/Viaprobe FCM at 24 and 48 hr. Results are expressed as the mean ( $\pm$  SEM) cell viabilities, relative to untreated controls.

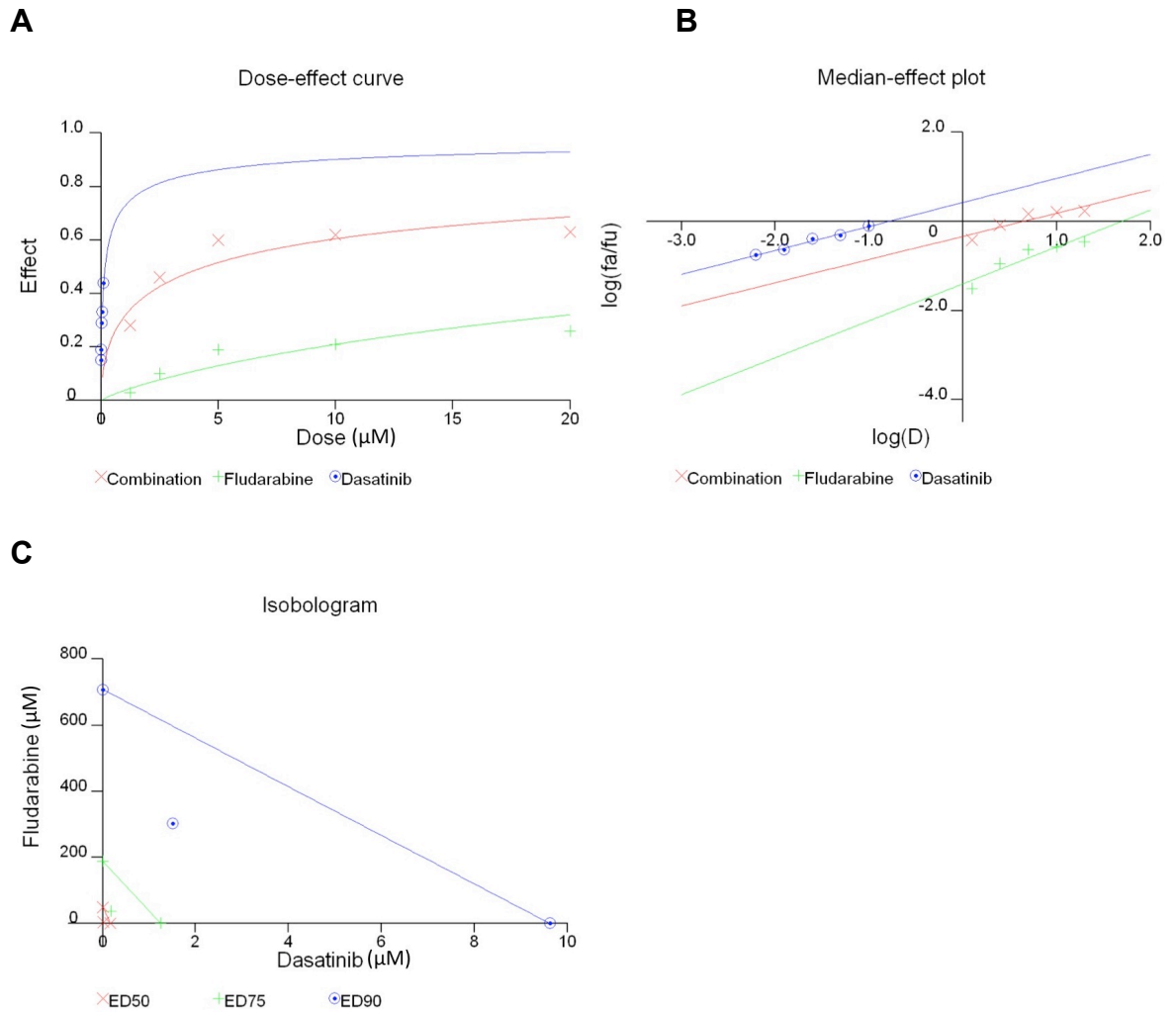


**Figure 3.16 An example of graphs generated by Calcsyn software during analysis of dasatinib combination experiments**

CLL cells were treated with increasing concentrations of dasatinib (6.25, 12.5, 25, 50, and 100 nM), fludarabine (1.25, 2.5, 5, 10, and 20  $\mu\text{M}$ ), or the combination of both at a fixed ratio of 200:1 using the concentrations described for 24 hr, then apoptosis assessed by Annexin V/Viaprobe FCM. For each condition, the reduction in viability relative to the vehicle control was converted to the  $f_a$ , using Equation 2.4 and entered into the Calcsyn<sup>®</sup> software programme, which was used to analyse data as described in Section 2.8.2. **A** The dose-response graph for drugs used singly and in combination, calculated from the  $f_a$  data, is shown. **B** Equations 2.5 and 2.6 enabled the construction of the median effect plot. **C** The  $\text{EC}_{50}$  (ED50),  $\text{EC}_{75}$  (ED75) and  $\text{EC}_{90}$  (ED90) CIs are plotted on the classical isobologram graph.

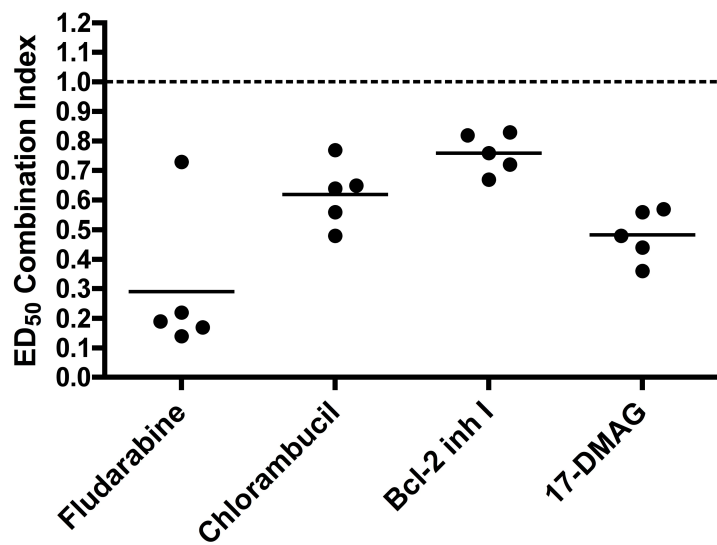


**Figure 3.17 EC<sub>50</sub> combination indices for dasatinib in combination with established and novel agents**

A: The results show the EC<sub>50</sub> CIs for dasatinib in combination with fludarabine, chlorambucil, Bcl-2 inhibitor I, and 17-DMAG. Experiments were performed on 5 CLL samples for each combination, and each black circle represents one experiment.

#### **Chapter 4:**

**Dasatinib inhibits BCR signalling in CLL cells, and reduces CLL cell migration towards SDF-1.**

## 4.1 Introduction

### 4.1.1 Evidence for the therapeutic potential of inhibiting tonic signalling in B cell malignancies

Mature B lymphocytes require continued surface expression of Ig for survival (381), enabling low-level antigen-independent association of kinases such as Lyn and Syk with Ig ITAM sequences, to mediate a degree of tonic signalling (373). *In vitro* studies on B cell lymphoma cells have provided evidence that tonic signalling through the BCR is central to the malignant phenotype. Inhibition of membrane Ig expression by siRNA to Ig $\alpha$  inhibited growth and survival of many B cell lymphoma cell lines (382). Furthermore, this group identified constitutive phosphorylation of Syk in these cell lines, and as downregulation of surface Ig $\alpha$  inhibited phosphorylation of both Syk and the downstream target BLNK, it was concluded that the antiproliferative effect was mediated by inhibition of tonic signalling. In support of this, Syk inhibition with piceatannol also inhibited lymphoma cell line proliferation (382). Constitutive phosphorylation of Syk and BLNK has also been confirmed in primary diffuse large B cell lymphoma (DLBCL) cells in addition to cell lines, and Syk inhibition with the novel Syk inhibitor R406 induced apoptosis in a number of DLBCL cell lines and primary samples (383). Syk inhibition has also been demonstrated to inhibit tumour growth in an E $\mu$ -MYC mouse model of B cell lymphoma (384), and trials of Syk inhibition in B cell lymphoma are ongoing. Notably, dasatinib has also been reported to inhibit Syk and PLC $\gamma$ 2 phosphorylation in DLBCL cell lines, and induce apoptosis (385).

With the evidence linking tonic BCR signalling to the malignant phenotype of B cell lymphoma, the question has been raised as to whether tonic BCR signalling also occurs in CLL. Although CLL cells express low levels of surface membrane Ig (22), kinases involved in tonic BCR signalling, including Lyn and c-Abl, are overexpressed and constitutively active in CLL (203, 212). Although inhibition of either kinase has been shown to induce apoptosis of CLL cells *in vitro*, the effects of inhibitor on downstream BCR signalling kinases has not been previously reported. Such investigation is important to aid our understanding of the role of tonic signalling in CLL.

#### 4.1.2 The link between BCR signal transduction and migration of B lymphocytes

In normal B lymphocytes, BCR stimulation results in PKC-dependent internalisation of the chemokine receptor CXCR4, resulting in impaired migration toward SDF-1 (386). Inhibition of chemotaxis following BCR signalling has been proposed as a mechanism involved in the egress of pre-B cells from stromal cell niches following successful IgH gene rearrangement (386). Alteration of chemokine responsiveness following antigen stimulation of mature B lymphocytes is also believed to facilitate sequential interaction with T lymphocytes, followed by transit to B cell follicles within LN (387).

The influence of BCR stimulation on CLL cell chemotaxis has been recently investigated (195, 388). Vlad *et al.* observed that BCR stimulation of CLL cells resulted in a variable degree of internalisation of surface CXCR4, and noted impaired chemotaxis toward SDF-1 in those with reduced CXCR4 expression (388). Of significance, this group identified a significant association between the level of CXCR4 internalisation following BCR stimulation, adverse prognostic features, and shorter PFS, leading the authors to propose that CXCR4 down-regulation may promote CLL cell retention within an antigen rich microenvironment where the cells are likely to encounter additional proliferative signals (388).

Quiroga *et al.* also observed that BCR stimulation of CLL cells lead to internalisation of CXCR4 (195). However, in contrast to the previous study, this group reported that BCR stimulation increased CLL cell migration towards SDF-1. In the latter case, chemotaxis experiments were performed following 48 hr incubation with and without anti-IgM, and as the authors also demonstrated incubation with anti-IgM to significantly increase CLL cell viability at 48 hr compared to culture in media alone, this difference in starting cell viability may have influenced results in subsequent chemotaxis assays. It is therefore possible that in this study the higher rate of chemotaxis observed following BCR stimulation may result from the significantly higher viability of this cell population, which would explain the apparent contradiction with previous studies performed in normal and malignant B cells. We were therefore interested in determining whether novel therapeutic agents targeting BCR signal transduction may have wider effects on CLL cell chemotaxis and homing to the microenvironment.

## 4.2 Aims and Objectives

As outlined in Chapter 3, apoptosis induced by dasatinib in CLL cells *in vitro* did not correlate with prognostic factors such as clinical stage IgV<sub>H</sub> mutation status, or ZAP-70 expression. As dasatinib targets Lyn and c-Abl, key kinases associated with proximal BCR signalling, we hypothesised that dasatinib sensitivity may be determined by its' effects on BCR-mediated signal transduction. As the capacity to signal through the BCR is highly associated with adverse prognostic features in CLL, the effect of dasatinib on signalling following crosslinking of surface IgM was assessed.

The specific aims of this chapter were to:

- i. Investigate whether dasatinib alters basal levels of BCR signal transduction, and whether this correlates with apoptotic response;
- ii. Establish if dasatinib is able to inhibit BCR signalling induced by crosslinking of surface IgM;
- iii. Determine whether dasatinib inhibits the pro-survival effect of prolonged BCR crosslinking *in vitro*;
- iv. Assess the effect of dasatinib on CXCR4 expression following BCR crosslinking;
- v. Study CXCR4 signal transduction in CLL cells following SDF-1 stimulation in the presence or absence of dasatinib;
- vi. Investigate whether dasatinib alters CLL cell chemotaxis toward SDF-1.

## 4.3 Results

### 4.3.1 Dasatinib inhibits tonic BCR signalling in CLL cells.

As tonic BCR signalling is largely dependent on ITAM phosphorylation by Src family kinases, assessment of phosphorylation levels of the downstream kinase Syk can be performed as a measure of tonic signalling. Key sites of Syk phosphorylation following association with phosphorylated ITAMs include Tyr<sup>348</sup> and Tyr<sup>352</sup>, followed by auto-phosphorylation of Tyr<sup>525</sup> and Tyr<sup>526</sup>, located in the activation loop (389). Recently, the method of single-cell phospho-FCM has been described as a sensitive method to assess low-level phosphorylation of Syk, BLNK, and PLC $\gamma$ , as measures of tonic BCR signalling, in DLBCL cell lines (383, 385). In order to assess the level of tonic BCR signalling in CLL cells, phospho-specific FCM using an antibody that recognises phosphorylated Syk<sup>Y348</sup> was used, following treatment of CLL cells with or without dasatinib. Representative FCM histograms from one patient are shown in Figure 4.1A. In unstimulated untreated cells, the level of Syk phosphorylation is clearly greater than the isotype control, suggesting a degree of tonic BCR signalling. Addition of dasatinib reduces the level of Syk phosphorylation in unstimulated cells (Fig. 4.1A). In addition, the effect of dasatinib on Syk phosphorylation following ligation of CLL cell surface IgM was also assessed. Stimulation of the BCR *in vivo* involves clustering and crosslinking of many molecules of surface Ig by antigen (150). To mimic such BCR crosslinking *in vitro*, cells were incubated with a biotinylated anti-IgM antibody, followed by crosslinking of antibody with avidin. This experimental approach has been previously described to induce effective pre-T cell receptor signalling *in vitro* (390). Following BCR stimulation, Syk phosphorylation in untreated cells increased, whilst a minimal increase in MFI occurred in dasatinib-treated cells (Fig. 4.1A). Combined results from experiments on 17 patient samples are shown in Fig 4.1B. Dasatinib significantly inhibited the basal level of Syk phosphorylation ( $p < 0.0001$ ) as determined by assessing the MFI of each sample, confirming inhibition of tonic BCR signalling. A significant increase in the level of Syk<sup>Y348</sup> phosphorylation was observed on BCR stimulation in untreated cells ( $p = 0.004$ ), which was also inhibited by dasatinib, suggesting that dasatinib may also inhibit antigen-dependent BCR signalling.

### 4.3.2 CLL sensitivity to dasatinib correlates with basal Syk phosphorylation.

Dasatinib has been investigated as a targeted therapy to BCR signal transduction in DLBCL cell lines, which also over-express Src kinases (385). In this study, variable levels of anti-proliferative activity were observed following dasatinib treatment, despite full Src kinase inhibition in all cases, prompting the authors to search for additional determinants of drug sensitivity. The ability of dasatinib to inhibit phosphorylation of Syk and PLC $\gamma$ 2 on BCR stimulation correlated with drug sensitivity, demonstrating that inhibition of components of the BCR signal transduction cascade is central to the anti-neoplastic effect of dasatinib in DLBCL cells. Unfortunately, the effect of dasatinib on basal levels of Syk and PLC $\gamma$ 2 phosphorylation was not assessed, precluding formal analysis of drug effects on tonic signalling (385). Syk has also recently been reported to be over-expressed in CLL cells (391). In view of these data, we hypothesised that the variable CLL cell sensitivity to dasatinib (described in Chapter 3, Fig. 3.6) may be determined by the ability of the drug to inhibit Syk-dependent tonic BCR signalling in individual cases. To investigate this, the MFI of Syk<sup>Y348</sup> phosphorylation in unstimulated cells treated with or without dasatinib was correlated with the percentage reduction in viability of the same sample on 48 hr treatment with dasatinib (Fig. 4.2). A significant inverse linear relationship was observed between the basal level of Syk<sup>Y348</sup> phosphorylation and dasatinib sensitivity, in that samples with high basal Syk<sup>Y348</sup> phosphorylation were less sensitive to dasatinib (Fig. 4.2A). Importantly, a similar significant linear correlation was observed between the remaining level of Syk<sup>Y348</sup> phosphorylation following 30 min treatment with dasatinib and the level of apoptosis achieved on 48 hr treatment (Fig. 4.2B), supporting the hypothesis that failure to fully inhibit Syk phosphorylation correlates with dasatinib resistance. To assess whether dasatinib sensitivity also correlated with the ability to respond to BCR stimulation in individual samples, the magnitude of Syk<sup>Y348</sup> increase, defined as the MFI ratio of stimulated to unstimulated untreated cells, was correlated with dasatinib sensitivity, however no association was observed (data not shown). These data suggest that dasatinib sensitivity in CLL cells is indeed determined by inhibition of tonic BCR signalling, and raise the possibility that in CLL cells poorly responsive to dasatinib, Syk may be activated independently of Src kinases and transmit survival signals.

To further validate this hypothesis, phosphorylation of both Lyn and Syk was assessed by western blotting in CLL cells treated with or without dasatinib. Eight samples, in which Syk phosphorylation had been assessed by FCM, were chosen to reflect the spectrum of apoptotic response observed on dasatinib treatment. Cells were treated with or without 100 nM dasatinib for 30 min, followed by assessment of phosphorylated and total Lyn and Syk in cell lysates by western blotting (Fig. 4.3). Using this approach, 100 nM dasatinib completely inhibited Lyn<sup>Y396</sup> phosphorylation in all samples as expected. However, Syk<sup>Y352</sup> phosphorylation was also completely inhibited in all CLL samples, regardless of apoptotic response to dasatinib. This may reflect the lower sensitivity of immunoblotting as compared to phospho-FCM. Immunoblotting is advantageous in that total levels of protein expression can be compared between samples. Densitometry was performed on the blots shown in Figure 4.3, to correlate levels of both Lyn and Syk expression with dasatinib sensitivity. A similar analysis was performed in order to correlate the ratio of phosphorylated Syk or Lyn to total protein expression with dasatinib response. A significant inverse linear relationship between Syk expression and dasatinib sensitivity was observed (Fig. 4.4A), consistent with the results obtained by phospho-FCM. However, although not reaching significance, a trend toward increasing dasatinib sensitivity with increasing percentage of Syk phosphorylation was observed (Fig. 4.4B). This seems incongruous with the preceding data, however when viewed in combination with Fig. 4.4A, it can be seen that in this small sample group, the cells with the highest percentage of Syk phosphorylation express the lowest absolute levels of Syk. Viewed together, these data suggest that high expression of Syk results in a higher absolute level of phosphorylated Syk, even though a lower percentage of the total cellular Syk is phosphorylated. No significant associations were seen between the percentage of phosphorylated Lyn, or total Lyn, and dasatinib sensitivity (Fig. 4.4C+D). In summary, these data support the hypothesis that dasatinib sensitivity is related to activity of components of the BCR signalling cascade, and a potential model for signalling in dasatinib sensitive and resistant cells is discussed in Section 4.4.

### **4.3.3 Dasatinib inhibits signalling induced by BCR ligation in CLL cells.**

As detailed in Section 1.5.2, following antigen engagement of the BCR, proximal signalling events downstream of Syk phosphorylation include the recruitment of several adaptor proteins, leading to release of calcium from intracellular stores,

and activation of the PI-3K and MAPK signalling pathways. The fluorescent calcium indicator Fura-2 AM was used to measure calcium flux following BCR stimulation, as described in Chapter 2.4. In order to crosslink the BCR after a stable basal fluorescence had been recorded, the avidin was injected directly into the spectrophotometer cuvette. BCR stimulation resulted in an increase in cytoplasmic calcium concentration of 1.5-2 fold in untreated cells from all three samples assessed, whilst dasatinib-treated cells showed minimal calcium flux (Fig. 4.5), confirming that dasatinib was able to inhibit this key proximal step in BCR signal transduction.

Activation of BCR downstream kinases following IgM crosslinking was assessed by western blotting. CLL cells were incubated in the presence or absence of 100 nM dasatinib for 30 min prior to BCR stimulation, and protein lysates prepared from unstimulated cells, or after 10 or 30 min stimulation. Representative immunoblots from four independent experiments are shown in Figure 4.6. In untreated cells, BCR stimulation resulted in Akt and ERK phosphorylation in both ZAP-70 positive (Fig. 4.6A) and ZAP-70 negative (Fig. 4.6B) CLL samples. The increase in Akt and ERK phosphorylation following BCR crosslinking was completely inhibited by dasatinib in all cases (Fig. 4.6A+B). Phosphorylation of p38 and JNK MAPK following BCR stimulation was assessed in three samples. An increase in p38 phosphorylation on BCR stimulation was observed in untreated cells from all three samples, which was inhibited by dasatinib (Fig. 4.6A+B), however JNK phosphorylation was not observed following BCR stimulation in untreated or dasatinib-treated cells (data not shown). Dasatinib also inhibited phosphorylation of I $\kappa$ B $\alpha$  on BCR stimulation (Fig. 4.6A+B), indicating that dasatinib prevents NF- $\kappa$ B pathway activation following BCR stimulation.

Activation of B lymphocytes through the BCR leads to extensive cytoskeletal reorganisation, in which cytoplasmic spreading and subsequent contraction occur to aggregate antigen into a focal cluster (151). To determine whether dasatinib affects this key process, actin reorganisation following BCR stimulation was assessed by fluorescence microscopy in CLL cells pre-treated with or without 100 nM dasatinib. Of the five CLL samples analysed, cell spreading following BCR stimulation was observed in the untreated cells in four cases, with representative cells shown in Figure 4.7. No cytoplasmic spreading was seen in untreated cells placed onto slides coated with an isotype control antibody. Less cell spreading was observed in dasatinib-treated cells following BCR stimulation (Fig. 4.7). In

order to quantify these observations, in three samples, two hundred cells were counted and scored either positive or negative for cytoplasmic spreading, and the percentage of cells demonstrating cytoplasmic spreading in untreated and dasatinib treated cells from each sample is shown in Fig. 4.7. Combined analysis of all three samples confirmed that dasatinib significantly reduced the percentage of cells able to undergo cytoplasmic spreading in response to BCR stimulation (untreated vs. treated = 66.3% vs. 12.6% respectively;  $p=0.02$ ).

#### **4.3.4 Dasatinib inhibits BCR-mediated up-regulation of Mcl-1 and survival of CLL cells.**

Despite the variable effects on CLL cell survival reported on stimulation with soluble anti-IgM *in vitro*, long-term culture of CLL cells with immobilised anti-IgM increases CLL cell viability *in vitro* (192). To address the functional effect of dasatinib on prolonged BCR stimulation of CLL cells, cells were incubated for 48 hr in the presence or absence of 100 nM dasatinib in each of the following three conditions: complete media alone; complete media in wells coated with 10  $\mu\text{g/ml}$  anti-IgM (immobilised anti-IgM), and; complete media supplemented with 10  $\mu\text{g/ml}$  anti-IgM F(ab')<sub>2</sub> fragments (soluble anti-IgM). At the end of the experiment, cell viability was assessed by Annexin V/VI probe staining by FCM, and protein lysates prepared from the remainder of cells for immunoblotting. The morphology of CLL cells from one representative patient sample cultured for 48 hr are shown (Fig. 4.8). Incubation of untreated CLL cells with soluble anti-IgM visibly increased cell aggregation in suspension, while incubation with immobilised anti-IgM induced the CLL cells to adhere to the antibody-coated surface and increase in size, in keeping with activated B cells. Morphological changes induced by soluble or immobilised anti-IgM were both inhibited by dasatinib in this sample, as was the protective effect of IgM stimulation on cell viability (Fig. 4.8). In Figure 4.9, the mean ( $\pm$  SEM) viabilities of cells treated as described in eleven CLL samples are shown. Incubation of untreated CLL cells with soluble anti-IgM resulted in increased, slightly decreased, or unchanged viability in 63%, 27%, and 10% respectively, with mean viability of 112% relative to unstimulated cells, which did not reach statistical significance. Incubation of untreated CLL cells with immobilised anti-IgM increased cell viability in 82% of samples, resulting in a significant increase in mean cell viability of 116% compared to unstimulated cells ( $p<0.01$ ). Dasatinib completely inhibited the pro-survival effect of prolonged stimulation with either soluble or immobilised anti-IgM, with viabilities of cells

treated with dasatinib in the presence of IgM stimulation similar to that of cells treated with dasatinib in media alone (Fig. 4.9).

The anti-apoptotic effect of prolonged BCR stimulation has been demonstrated to be largely dependent on activation of the PI-3K/Akt pathway, leading to up-regulation of Bcl-x<sub>L</sub>, Mcl-1, and XIAP (196). Using an siRNA approach, Mcl-1 was identified to be the key anti-apoptotic effector (196). Therefore, the effect of dasatinib on Mcl-1 expression following 48 hr BCR stimulation was assessed. Protein lysates prepared and Mcl-1 expression assessed by western blotting. PARP was also assessed as a marker of apoptosis. Fig. 4.10A shows a western blot from one patient sample in which untreated CLL cell viability was increased by incubation with either soluble or immobilised anti-IgM. In this example, Mcl-1 expression increased on BCR stimulation, and notably the extent of Mcl-1 upregulation was greater following stimulation with immobilised anti-IgM than soluble anti-IgM, and correlated with a higher percentage of viable cells following 48 hr immobilised as compared to soluble anti-IgM stimulation. Dasatinib completely inhibited Mcl-1 up-regulation induced by either soluble or immobilised anti-IgM stimulation, with the protein level reduced to that of cells treated with dasatinib in media alone (Fig. 4.10A). To further assess whether changes in Mcl-1 expression correlate with the increase in cell viability on IgM stimulation, densitometry was performed on this immunoblot, and immunoblots from an additional two experiments in which immobilised anti-IgM stimulation protected cells from spontaneous apoptosis (Fig. 4.10B). Combined densitometric analysis confirmed both upregulation of Mcl-1 on immobilised anti-IgM stimulation, and complete inhibition of Mcl-1 up-regulation by dasatinib (Fig. 4.10B). Mcl-1 was not significantly up-regulated by immobilised anti-IgM in one CLL case in which BCR stimulation had no effect on cell viability (data not shown). Soluble anti-IgM stimulation did not consistently up-regulate Mcl-1 expression in untreated cells, correlating with the results in Fig 4.9, showing less overall pro-survival effect on CLL cells. Collectively, these data confirm that inhibition of BCR signal transduction is a functionally relevant novel therapeutic strategy in CLL.

#### **4.3.5 Dasatinib prevents CXCR4 down-regulation on BCR stimulation**

To assess the effect of dasatinib on CXCR4 internalisation following BCR stimulation, CLL cells were pre-treated with or without 100 nM dasatinib then the BCR was crosslinked. The effect of dasatinib on CXCR4 expression following stimulation with SDF-1, or both SDF-1 and immobilised anti-IgM, was also

assessed. Combined results from three independent experiments are shown in Fig. 4.11. In all three samples assessed, IgM crosslinking resulted in down-regulation of CXCR4, which was prevented by dasatinib. SDF-1 treatment also resulted in significant reduction in CXCR4 expression. Of interest, although not reaching statistical significance ( $p=0.07$ ), CXCR4 expression was slightly higher in dasatinib-treated cells following SDF-1 stimulation. Although these results suggest that dasatinib treatment may retain the ability of CLL cells to respond to SDF-1, as Src kinases, including Lyn, are involved in CXCR4 signal transduction (235), the question remains whether dasatinib may also alter CLL cell migration toward SDF-1 through direct effects on CXCR4 signalling.

#### **4.3.6 Dasatinib inhibits Akt phosphorylation on CXCR4 stimulation in CLL cells.**

The effect of dasatinib on key signalling proteins downstream of CXCR4, namely Src kinases, FAK, Akt, and ERK and p38 MAPK, was assessed by Western blotting following SDF-1 stimulation. CLL cells pre-treated with or without dasatinib and then stimulated with SDF-1 as indicated. Protein lysates were also prepared from unstimulated CLL cells, and lysates from the colorectal carcinoma cell line HT29 served as a positive control, as these cells express both constitutively phosphorylated Src and FAK (392). As both Lyn and Src may participate in CXCR4 signal transduction, a primary antibody reactive to all phosphorylated Src family proteins was used for immunoblotting. Figure 4.12A shows a representative immunoblot probed for Src and FAK phosphorylation. In control CLL cells, two bands were detected with molecular weights in keeping with the 53 and 55 kDa isoforms of Lyn, whilst in HT29 cells, a single band at 60 kDa of phospho-Src was detected. No phosphorylation of FAK was observed in control CLL cells either unstimulated or following SDF-1 stimulation. Dasatinib completely inhibited Src family kinase phosphorylation in control and stimulated cells as expected (Fig. 4.12A). The effect of dasatinib on SDF-1-induced phosphorylation of Akt, and ERK and p38 MAPK was also assessed. Immunoblots from experiments on three patient samples are shown in Figure 4.12B. In cells not treated with dasatinib, SDF-1 stimulation consistently induced phosphorylation of Akt and ERK, while variable levels of p38 phosphorylation were observed. The notable effect of dasatinib was complete inhibition of Akt phosphorylation following SDF-1 stimulation, while ERK phosphorylation remained largely unaffected.

These data suggest that Src kinases, most probably Lyn, are required for Akt activation, likely through activation of PI-3K.

#### **4.3.7 Dasatinib inhibits SDF-1-induced actin polymerisation, chemotaxis, and pseudoemperipolesis.**

Experiments were performed to assess the functional consequences of dasatinib on SDF-1 signalling in CLL cells. Stimulation of CLL cells with SDF-1 results in a rapid increase in actin polymerisation (230, 393). Actin polymerisation following SDF-1 stimulation was assessed by FCM, assessing four conditions: media alone; media supplemented with dasatinib; media supplemented with CXCR4 antagonist AMD3100 or; both dasatinib and AMD3100. After removing an aliquot of cells from each well for fixation, SDF-1 was added to each well, and subsequent aliquots removed as indicated. Following fixation and permeabilisation, cells were incubated with phalloidin prior to analysis by FCM. Due to the preferential affinity of phalloidin for polymerised as compared to monomeric actin, an increase in actin polymerisation can be detected by an increase in MFI on FCM. Following SDF-1 stimulation of CLL cells cultured in media alone, a rapid increase in actin polymerisation, to over 200% that of unstimulated cells, was observed (Fig. 4.13). AMD3100 significantly inhibited actin polymerisation compared to control cells, validating the assay methodology. Incubation of cells with dasatinib for 30 min resulted in a small but significant reduction in the basal level of actin polymerisation ( $p=0.03$ ). At 15 s following SDF-1 stimulation, actin polymerisation was also significantly lower in dasatinib treated cells than control cells ( $p=0.02$ ), however at 60 s and thereafter, actin polymerisation was not significantly different between control and dasatinib-treated cells. In summary, dasatinib treated cells exhibit a blunted and delayed actin polymerisation response to SDF-1 as compared to untreated cells. No significant additive effect was observed on the actin polymerisation response to SDF-1 when dasatinib and AMD3100 were used in combination.

A transwell migration assay was used to assess the effect of dasatinib on chemotaxis toward SDF-1. Briefly, CLL cells were incubated with increasing concentrations of dasatinib, with AMD3100, or left untreated as indicated. Cells were then transferred to the upper chamber of a transwell culture insert, suspended in media supplemented with SDF-1, and incubated for 4 hr. At the end of the experiment, cells that had migrated were counted by FCM. In five independent experiments, migration rates between 23 - 43% of the total input cells

were observed, with rates of spontaneous migration toward a lower chamber containing media only less than 0.01% in all cases. While the CXCR4 antagonist AMD3100 inhibited migration relative to control cells, at the dose used, this did not reach significance (Fig. 4.14). Whilst little effect on chemotaxis was seen at a concentration of 1 nM dasatinib, both 10 and 100 nM dasatinib significantly reduced the percentage of cells migrating to the lower chamber (Fig. 4.14).

These results suggest that dasatinib may inhibit CLL migration to and retention in the stromal microenvironment of the BM and LN. To further investigate this possibility, the ability of dasatinib-treated CLL cells to migrate under a layer of SDF-1 expressing stromal cells (pseudoemperipolesis) was assessed. The murine BM fibroblast cell line M2-10B4 has been reported to express SDF-1, and induce pseudoemperipolesis of co-cultured CLL cells (230). The expression of SDF-1 by M2-10B4 cells was assessed by quantitative reverse-transcription PCR (qRT-PCR) prior to use in experiments. M2-10B4 cells, but not NT-L cells (also a murine BM fibroblast cell line), express appreciable levels of SDF-1 mRNA (Fig. 4.15). To assess pseudoemperipolesis, CLL cells were incubated with or without dasatinib, then incubated on a confluent layer of M2-10B4 cells. At the end of the experiment, non-migrated cells were removed by thorough washing, and the stroma containing pseudoemperipolesed cells documented photographically (Fig. 4.16). CLL cells which have undergone pseudoemperipolesis are characterised by a dark, non-refractile appearance (230). The stromal cell layer was then detached using trypsin, and the presence of CLL cells was analysed by FCM. CLL cells were counted by acquiring CD19<sup>+</sup> events on high flow for 30s for each sample, including counting an aliquot from the total starting cell number, in order to calculate the percentage of migrated cells in each sample. In six of the nine samples analysed, at least 1% of control cells migrated into the stromal plane (Fig. 4.17A), with minimal migration observed in the remaining three samples. In the six samples showing evidence of pseudoemperipolesis, dasatinib significantly inhibited the mean percentage of transmigrated cells, from 2.4% to 1% ( $p < 0.02$ ; Fig. 4.17B). Although these percentages are small, the greater than 50% reduction in migratory capacity achieved by dasatinib may have great clinical relevance.

#### **4.3.8 Dasatinib inhibits pro-survival SDF-1 signalling in CLL cells *in vitro*.**

Addition of recombinant SDF-1 to culture media has been demonstrated to partially inhibit spontaneous apoptosis of CLL cells *in vitro*. In view of the partial

inhibition of CXCR4 signalling, the effect of dasatinib on the anti-apoptotic effect of SDF-1 was assessed. CLL cells were pre-treated with dasatinib as indicated, then incubated in the presence or absence of SDF-1 for 48 hr. Co-culture of CLL cells with SDF-1 alone led to a significant increase in cell viability, with a mean viability of 110% compared to cells incubated in media alone ( $p=0.02$ ; Fig. 4.18). Cells incubated in the presence of dasatinib and SDF-1 had a mean viability similar to that of cells treated with dasatinib alone (Fig. 4.18). The observed effects of dasatinib on CLL cell viability in the presence of SDF-1 may also be explained by the demonstrated inhibition of Akt phosphorylation.

#### 4.4 Discussion

Using a sensitive FCM technique, we detected a basal level of Syk<sup>Y348</sup> phosphorylation in CLL cells, suggesting a degree of tonic signalling. As CLL cells were incubated in serum-free media prior to and during the experiment, the basal Syk phosphorylation is unlikely to have been induced by other soluble factors present in the culture medium. In addition to studies performed in DLBCL, there is now significant published evidence to suggest that Syk-dependent tonic BCR signalling is important for CLL cell survival, and a rational therapeutic target in CLL. Gene expression profiling studies in CLL cells have identified over-expression of several additional proteins in addition to Lyn and c-Abl, involved in BCR signal transduction, including Syk, Vav, and PLC $\gamma_2$ , (391). At the protein level, Syk expression in CLL cells was approximately two-fold that of normal B lymphocytes, and Syk expression was significantly higher in unmutated cases compared with mutated cases (391). Moreover, using phosphotyrosine immunoprecipitation followed by Syk immunoblotting, total basal Syk phosphorylation in CLL cells was demonstrated to be around twice that observed in normal B lymphocytes (391). Increased basal Syk phosphorylation in CLL has subsequently been confirmed by other groups. Baudot *et al.* demonstrated basal phosphorylation on both tyrosines Tyr<sup>352</sup>, and Tyr<sup>525/526</sup> in the activation loop (394). Gobessi *et al.* also demonstrated significant basal Syk<sup>Y352</sup> phosphorylation in a large proportion of unselected CLL samples by both immunoblotting and confocal microscopy, however did not observe a difference between mutational groups (395). Evidence to support specific involvement of Syk kinase activity in the survival of CLL cells comes from two studies in which knock-down of Syk by siRNA resulted in apoptosis (394, 395). Syk-dependent tonic signalling has been shown to promote CLL cell survival at least partly through preventing proteasome-mediated degradation of Mcl-1 (394). A number of pharmacological ATP-competitive inhibitors of Syk kinase activity have been developed, including BAY61-3606, R406, and Syk inhibitor II, which have been demonstrated to induce apoptosis of CLL cells *in vitro* (391, 394, 395). Using a fixed concentration of 2.5  $\mu$ M R406, Gobessi *et al.* found no difference in level of apoptosis between mutational or ZAP-70 subgroups, whereas Buchner *et al.* found 4  $\mu$ M R406 to induce significantly greater apoptosis in unmutated or ZAP-70 positive cases. Buchner *et al.* also found a significant positive association between the relative level of Syk expression in a CLL sample and the percentage cytotoxicity achieved

with R406. A phase I/II clinical trial of fostamatinib disodium, an oral pro-drug of the Syk inhibitor R406, in patients with B cell NHL and CLL has recently been reported, with responses seen in six of eleven (55%) patients with relapsed or refractory CLL or small lymphocytic lymphoma, with a median response duration of over 4 months (396).

In DLBCL cell lines, dasatinib inhibited Src kinase phosphorylation in both dasatinib sensitive and resistant cell lines, however the anti-proliferative activity of dasatinib correlated with inhibition of Syk and PLC $\gamma_2$  phosphorylation (385), leading the authors to suggest that Syk and PLC $\gamma_2$  may be clinically useful biomarkers. In our study, the level of Syk<sup>Y348</sup> phosphorylation was predictive of the apoptotic response of CLL samples to treatment with dasatinib, with cells more resistant to dasatinib retaining a higher level of Syk<sup>Y348</sup> phosphorylation despite dasatinib treatment. Recently, this finding has been confirmed by another group (356). Song *et al.* found 128 nM dasatinib to completely inhibit phosphorylation of Lyn, Src, and Hck kinases (assessed by immunoblotting) in all CLL cells assessed *in vitro*, regardless of apoptotic response. However, again using phospho-specific FCM, significant associations were found between the ability of dasatinib to inhibit basal Syk<sup>Y348</sup> and PLC $\gamma_2$ <sup>Y759</sup> phosphorylation and the level of cytotoxicity achieved with dasatinib (356).

These data suggest that Syk activity may not be solely controlled by Lyn activity, and that variable Syk activation by non-Src kinase routes may explain the variable sensitivity of CLL cells to dasatinib treatment. Whilst the consensus holds that Lyn is the predominant kinase responsible for phosphorylation of ITAM tyrosines, leading to recruitment and activation of Syk (155), Syk has been demonstrated to associate with ITAM sequences independently of Lyn (397). The Lyn-independent regulation of tonic Syk phosphorylation in CLL cells remains to be fully determined, however there is evidence to implicate dysregulation of regulatory phosphatases. Recently, phosphorylation of Syk has been shown to be directly controlled by protein tyrosine phosphatase receptor-type O truncated (PTPROt), which has been implicated as a tumour suppressor gene (398). PTPROt overexpression inhibited Syk phosphorylation and downstream BCR signalling on BCR stimulation, and also inhibited proliferation and induced apoptosis in a B cell lymphoma cell line, suggesting a regulatory role in tonic BCR signalling (398). Recently, the PTPROt promoter has been demonstrated to be methylated in up to 82% of patients with CLL, with methylation correlating with reduced expression as

measured by RT-PCR (399). Furthermore, introduction of PTPROt into a non-expressing CLL cell line significantly increased the level of apoptosis achieved by fludarabine (399). This group did not assess Syk phosphorylation following introduction of PTPROt, and this would be of interest to study in primary CLL cells. Very recently, the target tyrosine substrate for PTPROt on Syk has been confirmed as the activating Tyr<sup>352</sup> (400). In our study, the CLL cases with the highest levels of Syk protein expression also had the highest levels of Syk<sup>Y348</sup> phosphorylation, and lowest response to dasatinib. It may be possible that in such cases, the level of Syk protein exceeds the capacity of PTPROt to dephosphorylate it, leading to Lyn-independent constitutive activity, and relative dasatinib resistance. In CLL cells with lower total levels of Syk protein, Syk phosphorylation may be more under the control of Lyn kinase activity, correlating with sensitivity to apoptosis on dasatinib treatment.

The recent *in vitro* and clinical trial data for the Syk inhibitor R406 have led some to propose that Syk inhibitors may be more effective therapeutic agents in CLL than Src/c-Abl kinase inhibitors. However, Buchner *et al.* demonstrated that CLL cases with low level Syk expression were relatively insensitive to Syk inhibitors. Our results suggest that CLL cells with low expression of Syk are dasatinib sensitive. These data suggest that in a subset of CLL cases, Syk-independent survival signalling through Src and/or c-Abl kinases is important in maintaining the malignant clone. A better understanding of the heterogeneity in antigen-independent BCR signalling is central to establishing which patient subgroups may benefit from specific TKIs in CLL. Further experiments using phospho-FCM to analyse the activity of downstream BCR signalling proteins in Syk high and low expressing CLL cells treated with Src or Syk inhibitors may aid this understanding. Also, further experiments to assess whether synergy is observed between dasatinib and Syk inhibitors may clarify whether dasatinib resistance is due to Syk kinase activity.

BCR stimulation using our avidin-biotin crosslinking method resulted in calcium release, and phosphorylation of downstream kinases in both ZAP-70 positive and negative cases. Little increase in Akt phosphorylation was observed in one ZAP-70 negative case, consistent with a previous study which identified phosphorylation of Akt and ERK in all unmutated and 75% of mutated CLL cells on BCR stimulation (192). Previously, MAPK activation following BCR stimulation has been reported to be incomplete, with infrequent activation of JNK and

decrease in phosphorylation of p38 MAPK (192). In our study, an increase in p38 phosphorylation was observed in all cases, whereas we did not detect JNK phosphorylation in any of the samples analysed. The differences observed may reflect the different experimental techniques employed, as it is reasonable to suggest that crosslinking the BCR with an avidin-biotin method may result in a greater stimulus than the previously reported methods. Of note, the Syk inhibitor R406 has also been confirmed to inhibit intracellular calcium flux, and prevent Akt and ERK phosphorylation following BCR stimulation of CLL cells (195).

In addition to inhibiting BCR signalling in the short term, dasatinib inhibited up-regulation of Mcl-1 on sustained BCR stimulation, and abrogated the anti-apoptotic effect of continued BCR signalling *in vitro*. Studies using specific Mcl-1 siRNA have confirmed that Mcl-1 is key to the anti-apoptotic effect of prolonged BCR stimulation of CLL cells *in vitro* (196). Consistent with the reported findings of Petlickovski *et al.*, we observed immobilised anti-IgM stimulation, but not soluble anti-IgM stimulation to lead to significant up-regulation of Mcl-1 in CLL cells (192). Although dasatinib has previously been reported to induce apoptosis through down-regulation of Mcl-1 expression in unstimulated CLL cells (353), to our knowledge, the present work is the first study to demonstrate dasatinib to inhibit the up-regulation of Mcl-1 following prolonged crosslinking of surface IgM. Of interest, although not reaching statistical significance ( $p=0.11$ ), the mean viability of cells incubated with immobilised anti-IgM and dasatinib was 51.9% of control, compared to 64.5% of control for CLL cells treated with dasatinib in media alone, suggesting that CLL cells may be more sensitive to dasatinib in the presence of BCR stimulation. Scheduling experiments in which CLL cells are stimulated by crosslinking of surface IgM prior to the addition of dasatinib would help to further address this question. Notably, the Syk inhibitor R406 has also been reported to inhibit the pro-survival effect of prolonged BCR stimulation *in vitro* (195, 395), also blocking Mcl-1 up-regulation (395). These studies suggest that whilst Src/c-Abl and Syk inhibitors appear to exert variable effects on tonic BCR signals and viability of unstimulated CLL cells, both classes of inhibitor consistently inhibit pro-survival signalling induced by active crosslinking of the BCR.

In agreement with previous reports, IgM stimulation resulted in a reduction of surface CXCR4 expression on the surface of CLL cells (195, 388). Consistent with the evidence that dasatinib inhibits BCR signalling, dasatinib blocked the downregulation of CXCR4 following IgM crosslinking. Again, similar to dasatinib,

Syk inhibition with R406 has also been shown to prevent internalisation of CXCR4 on BCR stimulation (195). Dasatinib did not change CXCR4 expression in unstimulated CLL cells, and following SDF-1 stimulation, downregulation of surface CXCR4 was slightly less in dasatinib treated cells, suggesting a role for tyrosine kinases in CXCR4 internalisation. Despite this, dasatinib inhibited actin polymerisation and chemotaxis in response to SDF-1, and reduced pseudoemperipolesis of CLL cells on the stromal cell line M2-10B4, similar to the findings reported following treatment of CLL cells with small molecule antagonists of CXCR4. Together, these results imply that dasatinib inhibits signalling downstream of the CXCR4 receptor.

Dasatinib has been extensively investigated as a novel therapeutic agent which may inhibit metastasis of solid organ malignancies through inhibition of Src and FAK signalling pathways. Prostate cancer cell lines express constitutively active Lyn and Src kinases, and inhibition of Src kinase activity by dasatinib resulted in a reduction in phosphorylation of the downstream kinases FAK and p130<sup>CAS</sup>, with no effect on ERK or Akt phosphorylation (313). Inhibition of FAK and p130<sup>CAS</sup> was associated with reduced migration in wound healing assays. In head and neck squamous cell carcinoma and non-small cell lung cancer cell lines, dasatinib also inhibited spontaneous migration, with consistent inhibition of phosphorylation of FAK, p130<sup>CAS</sup>, and paxillin, and variable effects on Akt and MAPK (312). Moreover, similar findings have been reported in a number of other malignancies, including colon carcinoma (392), sarcoma (401), mesothelioma (402), and melanoma (403). Although FAK has been demonstrated to be expressed in a number of B cell malignancies, including CLL (404), the level of basal and induced FAK phosphorylation in CLL cells has not previously been studied. In the present study, we failed to detect phosphorylated Src or FAK by immunoblotting in either unstimulated cells, or following SDF-1 stimulation. Preliminary experiments similarly failed to detect paxillin and p130<sup>CAS</sup> following stimulation. Immunoprecipitation of total FAK followed by phosphotyrosine immunoblotting may allow more sensitive detection of low levels of FAK phosphorylation, however this approach was limited by the cell numbers required to perform such analysis. Alternatively, it may be that FAK is not activated to any extent on SDF-1 stimulation, and alternative pathways are responsible for mediating CLL chemotaxis to SDF-1. In normal B lymphocytes, FAK phosphorylation following CXCR4 engagement is developmentally regulated by at least two mechanisms.

Firstly, as progenitor B lymphocytes mature, expression of the GTP-ase activating protein regulator of G protein signalling 1 (RGS1) increases, and reduces FAK recruitment to the CXCR4 signalosome on SDF-1 stimulation (405). In addition, suppressor of cytokine signalling 3 (SOCS3) expression has been demonstrated to increase as B lymphocytes reach maturity, resulting in FAK ubiquitination and proteasomal degradation on CXCR4 engagement, preventing efficient CXCR4-FAK signalling (406). Although expression of RGS1 and SOCS3 has not been examined in CLL cells, it is possible that failure to detect FAK phosphorylation on SDF-1 stimulation of CLL cells reflects the normal insensitivity of mature B lymphocytes to FAK activation. In any case, our data suggest that migration of CLL cells toward SDF-1 is likely to be regulated by pathways other than the Src/FAK axis.

Using the pan phospho-Src antibody, bands at 53 and 56 kDa were observed by immunoblotting in unstimulated and SDF-1 stimulated CLL cells, likely to represent mainly phosphorylated Lyn kinase, and these were completely inhibited by dasatinib. Both Lyn and Fyn phosphorylation have been observed following SDF-1 stimulation of Jurkat T cells and CD34<sup>+</sup> haematopoietic progenitor cells (235, 407). Furthermore, a specific role for Lyn in SDF-1-induced chemotaxis of haematopoietic cells has been proposed on the basis of experiments performed in Lyn knock-out mice. In transwell assays, migration of BM mononuclear cells from Lyn<sup>-/-</sup> mice towards SDF-1 was impaired by over 75 percent compared to wild type cells (407). To further confirm that impaired chemotaxis was a specific effect of deficiency of Lyn, siRNA knock-down of Lyn was performed in primary CD34<sup>+</sup> haematopoietic progenitor cells, and cell lines including HL-60; such specific Lyn knock-down significantly inhibited cell migration 3 to 7 fold compared with that observed in control siRNA-treated cells (408).

We found dasatinib specifically inhibited phosphorylation of Akt following SDF-1 stimulation of CLL cells, suggesting inhibition of PI-3K activity. There is now evidence in many haematopoietic cell types that Lyn kinase activates PI-3K on CXCR4 stimulation. Both Lyn and Fyn kinases interact directly with the p85 subunit of PI-3K through their SH3 domains in a B cell lymphoma cell line (409), and similar interactions have also been described in chemokine stimulated neutrophils (410). In SDF-1-stimulated HL-60 cells, Lyn immunoprecipitates were found to contain active PI-3K, confirming a functional interaction between these two kinases (407). Our results suggest that Lyn may similarly regulate PI-3K

activity in CLL cells, however immunoprecipitation experiments are needed to confirm whether the regulation occurs through direct interaction.

A number of recent studies implicate PI-3K signalling in chemotaxis toward SDF-1 in haematopoietic cells. Selective PI-3K inhibition with the inhibitors LY290024 or Wortmannin inhibited SDF-1-induced migration in progenitor B lymphocytes (233), whilst murine B lymphocytes containing a mutation of a phosphatase resulting in increased Akt activation exhibited increased chemotaxis toward SDF-1 (411). In addition in CLL cells, Burger *et al.* reported that the PI-3K inhibitor wortmannin partially inhibited the migration of CLL cells toward SDF-1 in transwell assays, whereas the MEK inhibitor PD98059 had no significant effect (230). A very recent study demonstrated that specific inhibition of the p110 $\alpha$  subunit of PI-3K using the novel inhibitors PIK-90 and PI-103 resulted in inhibition of SDF-1 induced actin polymerisation, chemotaxis and pseudoemperipolesis (412). Interestingly, Niedermeier *et al.* noted that pre-treatment of CLL cells with PI-3K inhibitors reduced the level of basal F-actin measured by FCM, similar to our observations with dasatinib. In conclusion, these studies support the hypothesis that inhibition of PI-3K by dasatinib is responsible for the anti-migratory effects observed.

Although both CML and CLL cells express constitutively phosphorylated Lyn kinase, the effects on basal and induced cell motility differ. In CML cells, Bcr/Abl interacts with Lyn kinase, resulting in constitutive activity of the PI-3K cascade (407). In this study, Bcr/Abl positive CML cells showed high rates of spontaneous migration in transwell experiments toward media alone, comparable to rates seen when SDF-1 was added to the lower chamber (407). This mechanism has been proposed to be involved in the release of CML cells from BM. Although CLL cells also express constitutively active Lyn, we observed little spontaneous migration in transwell experiments, and a significant increase in migration of CLL cells towards media supplemented with SDF-1, suggesting that a constitutive association of Lyn with PI-3K is unlikely to be present in CLL cells.

Although chemotaxis toward SDF-1 was significantly inhibited by 10 and 100 nM dasatinib, inhibition of chemotaxis was not complete with migration of CLL cells in the presence of dasatinib remaining over 50% that of controls. In our experiments, the CXCR4 antagonist AMD3100 was also unable to inhibit chemotaxis by over 50% of controls. In our transwell experiments, the concentration of SDF-1 used is likely to be supra-physiological, and also CLL exposure to SDF-1 is continuous, as compared to the likely brief stimulation likely delivered to circulating CLL cells *in*

*vivo*. An alternative explanation is that multiple signalling pathways downstream of CXCR4 may regulate CLL cell migration towards SDF-1, and not all are inhibited by dasatinib. Of note, in the mouse pro-B cell line BAF3, SDF-1 stimulation increased phosphorylation of Syk, which has also been linked to promoting motility (413). In B cell progenitor ALL cells, phosphorylation of p38 was required for leukaemic cell to BM in an *in vivo* model (414), and p38 phosphorylation in response to SDF-1 stimulation was not inhibited by dasatinib in CLL cells.

Whilst all CLL samples assessed exhibited significant chemotaxis along an SDF-1 gradient in transwell assays, only six of the nine samples assessed in the pseudoemperipolexis assay demonstrated significant levels of migration into the M2-10B4 stromal layer, suggesting that additional factors are required for pseudoemperipolexis to occur. In a study of 116 CLL samples, only 45 showed evidence of pseudoemperipolexis into a BM stromal layer (415). In this study, samples able to migrate into the stromal layer expressed significantly higher levels of CD49d and CD38 than cases with little migratory capacity. CD49d and CD38 have been confirmed to be physically associated within CLL cell membranes, and to provide co-operative survival signals to CLL cells (416). The CD49d/CD38 complex has also been demonstrated to associate with ZAP-70 (417). CD49d and CD38 expression was not assessed in our small sample group, however this would be interesting to examine. CLL cell migration into a stromal plane has been confirmed to lead to chemoresistance *in vitro*, and this mechanism is likely to be responsible in part for the adverse prognostic significance of CD38 and CD49d expression (250).

In addition to regulating cell migration, SDF-1 signalling through CXCR4 can also regulate cell adhesion, which may also influence the ability of CLL cells to be retained within protective LN and BM microenvironments. Chemokine receptor signalling can lead to activation of cellular integrins, in a process termed 'inside-out' signalling (243). In mature lymphocytes, PI-3K has been demonstrated to activate the integrin LFA-1 following stimulation with chemokines including SDF-1, resulting in increased adhesion to ICAM-1 (418). It is reasonable to suggest that the inhibitory effect of dasatinib on PI-3K signalling downstream of CXCR4 may inhibit such inside-out integrin activation, and thus inhibit CLL cell adhesion to ICAM-1 expressing cells. However, Lyn has also been described to exert a negative effect on integrin function following chemokine stimulation in some cell types. In CD34<sup>+</sup> haematopoietic progenitor cells, and HL-60 cells in which Lyn has

been knocked-down by siRNA, SDF-1 stimulation resulted in increased adhesion to BM stromal cells (408). Further investigation revealed that within these cell types, on SDF-1 stimulation, Lyn down-regulates affinity of  $\beta 2$ , but not  $\beta 1$ , integrins, resulting in impaired interaction of the  $\beta 2$ -containing LFA-1 with its' ligand ICAM-1, while interaction of the  $\beta 1$ -containing CD49d with VCAM-1 was not affected (408). Such regulation has been proposed to allow cell migration toward a SDF-1 gradient within the BM stromal microenvironment. The net effect of dasatinib on integrin function in CLL cells, in the presence and absence of SDF-1, may be determined by *in vitro* cell adhesion assays, for example to ICAM-1, VCAM-1, or fibronectin.

In addition to regulating retention of lymphocytes within the BM and LN, chemokines have been implicated in promoting CLL cell entry to LN. The chemokine receptors CXCR4, CCR7, and CXCR5 are highly expressed in CLL cells isolated from patients with extensive nodal disease (419). Both SDF-1 signalling through CXCR4, and the chemokine CCL21 signalling through its receptor CCR7 increase expression and secretion of matrix metallo-protease 9 (MMP-9), which aids CLL cell transendothelial migration (420, 421). In prostate cancer and melanoma cell lines, dasatinib has been demonstrated to reduce secretion of MMP9 and reduce cellular invasion (313, 403). It is reasonable to suggest that dasatinib may interfere with induced MMP-9 expression in CLL cells. However, the observation that SDF-1 and CCL21 induced up-regulation of MMP-9 in CLL cells depends on ERK, rather than PI-3K signalling (421), suggests dasatinib may have no inhibitory effect, however further investigations are required to determine this.

In summary, we have demonstrated that dasatinib exerts variable inhibition on tonic BCR signalling in CLL cells, which correlated with the ability of dasatinib to induce apoptosis of CLL cells *in vitro*. Dasatinib inhibited BCR signalling on crosslinking of surface IgM, and abrogated the pro-survival effect of prolonged IgM stimulation *in vitro*. As a result of inhibiting BCR signalling, CXCR4 receptor expression was unchanged in dasatinib-treated cells in the presence of anti-IgM. Despite this, dasatinib inhibited Akt phosphorylation on CXCR4 stimulation, and inhibited chemotaxis towards SDF-1. Whilst further *in vivo* analyses are required, the collective data suggest that in addition to abrogating BCR signalling, dasatinib both directly and indirectly modulates SDF-1 responsiveness, which may inhibit CLL cell retention in favourable microenvironments in LN and BM.

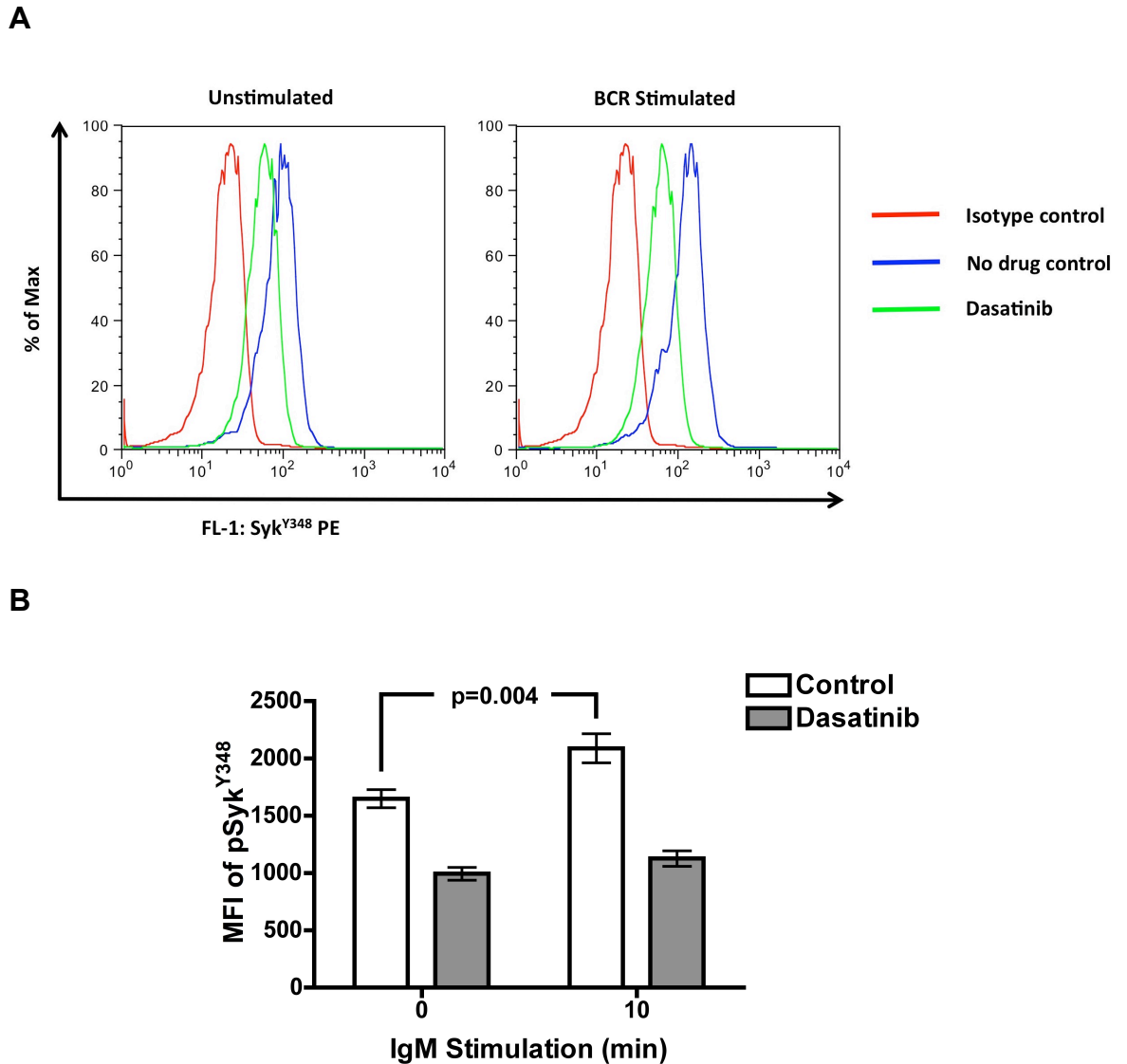
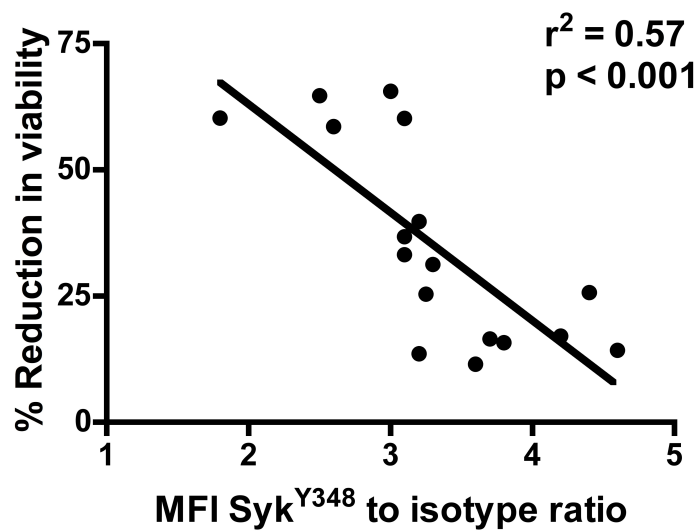


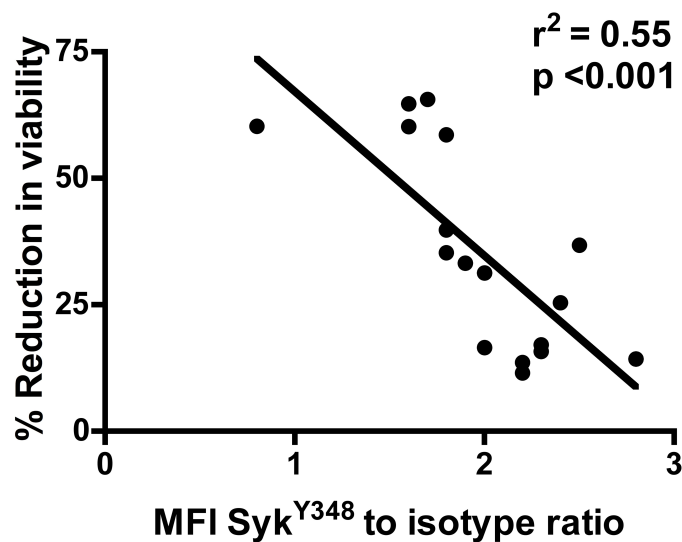
**Figure 4.1 Dasatinib inhibits Syk<sup>Y348</sup> phosphorylation in unstimulated and BCR-stimulated CLL cells**

CLL cells were incubated in RPMI-1640 containing 0.5% BSA for 2 hr prior to the experiment. Cells were then incubated with 10  $\mu$ g/ml biotinylated anti-IgM in the presence and absence of 100 nM dasatinib for 30 min prior to BCR stimulation. Cells were washed, and fixed unstimulated, or following 10 min stimulation with avidin. Syk<sup>Y348</sup> was assessed by intracellular phospho-specific FCM, as described in Section 1.3.3. **A** Histogram plots of unstimulated and stimulated cells from a representative sample (CLL34). **B** The histogram shows the MFI ( $\pm$  SEM) for cells treated as indicated (n=17).

**A**

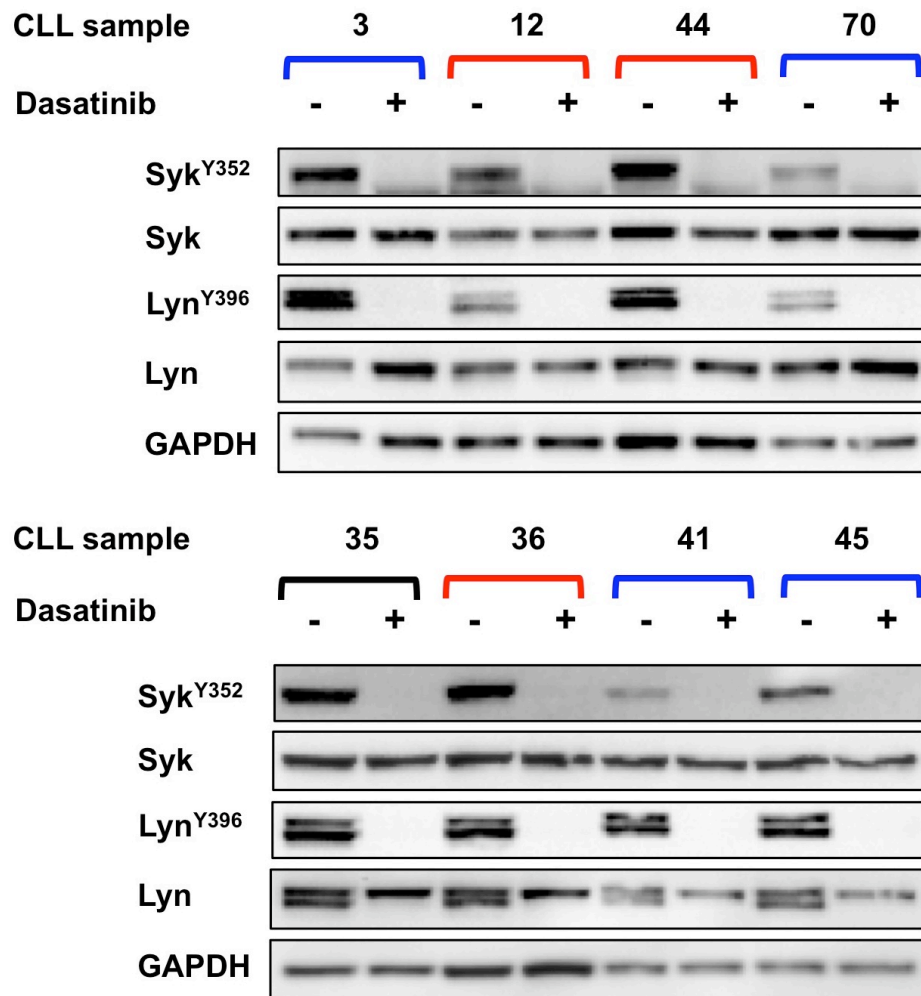


**B**



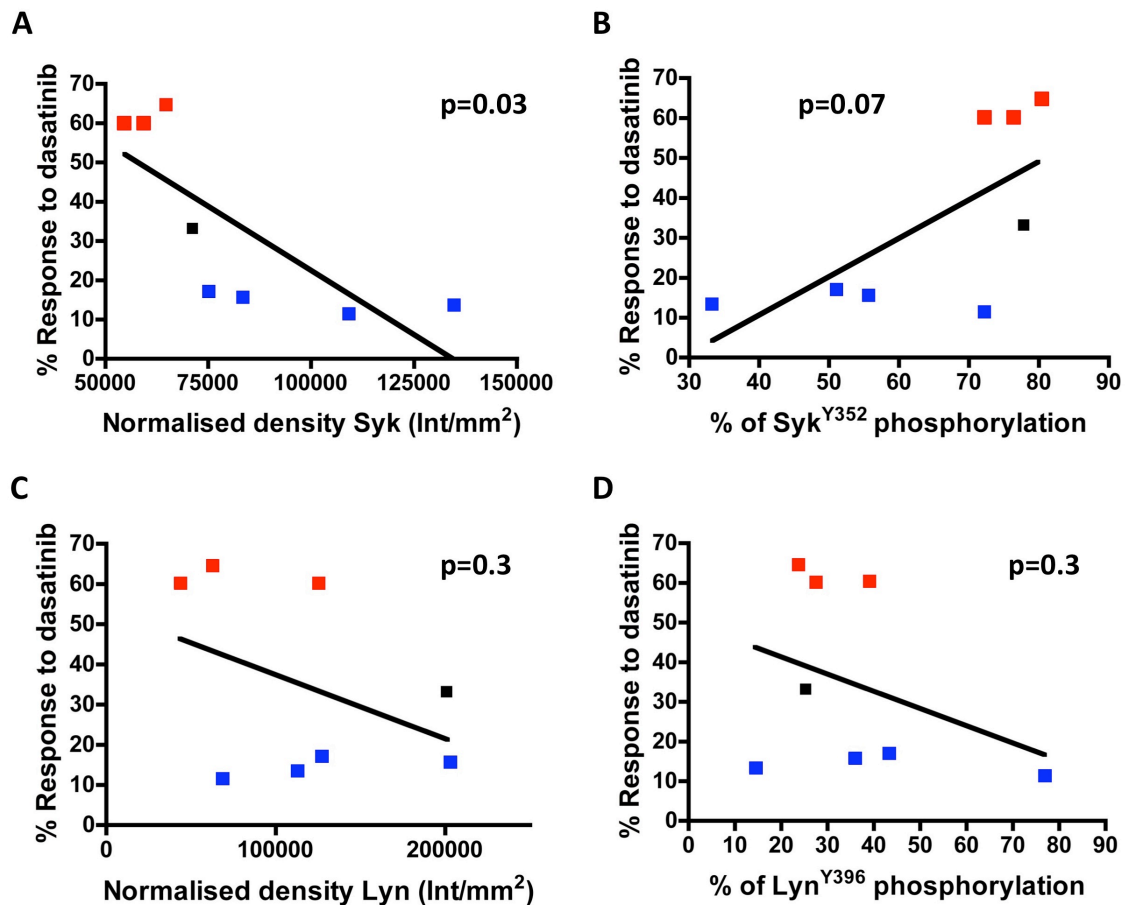
**Figure 4.2 Relationship between Syk<sup>Y348</sup> phosphorylation and apoptosis induced by dasatinib**

**A** Linear regression analysis was performed to relate the basal level of Syk phosphorylation in untreated CLL cells (expressed as the ratio of the measured MFI of the test sample to an isotype matched control; x axis) to the level of apoptosis observed on treatment of the sample with 100 nM dasatinib for 48 hr (y axis) (n=17). **B** Linear regression analysis was performed as described in **A** between the level of Syk phosphorylation following 30 min treatment with 100 nM dasatinib in the same 17 CLL samples.



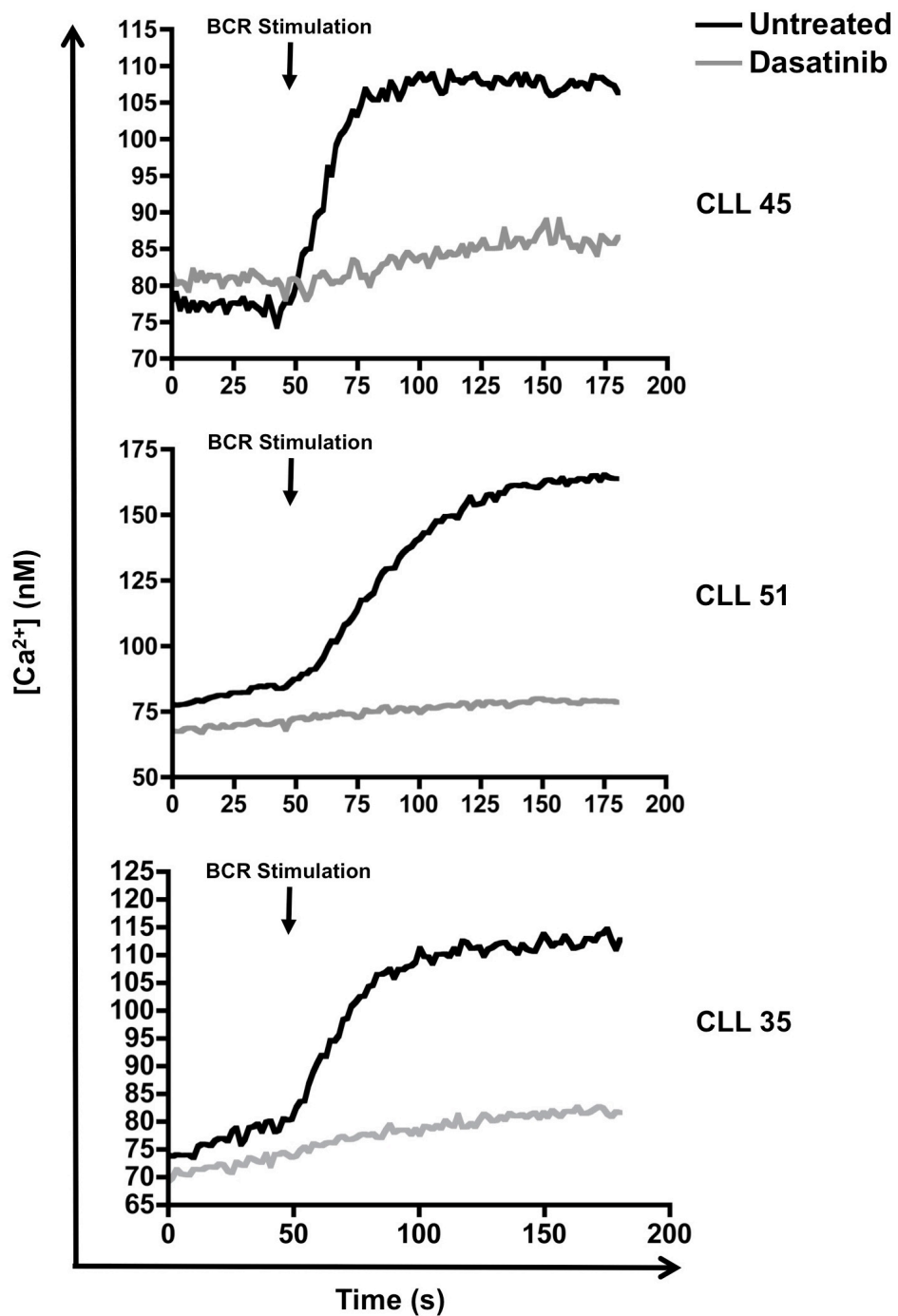
**Figure 4.3 Inhibition of Lyn<sup>Y396</sup> and Syk<sup>Y352</sup> phosphorylation on 30 min treatment with dasatinib**

CLL cells were incubated in RPMI-1640 supplemented with 0.5% BSA for 2hr prior to the experiment. Cells ( $2 \times 10^6$ /ml) were subsequently incubated in the presence and absence of 100 nM dasatinib for 30 min, then protein lysates prepared. Western blotting was performed with antibodies to Syk<sup>Y352</sup>, Syk, Lyn<sup>Y396</sup>, and Lyn, with GAPDH assessed as a protein loading control. CLL samples indicated by red brackets are highly sensitive to dasatinib (over 50% reduction in viability on 48 hr treatment), those described by blue brackets are low responders (less than 20% reduction in viability), and the sample indicated by black brackets was included as an average responder (33% reduction in viability).



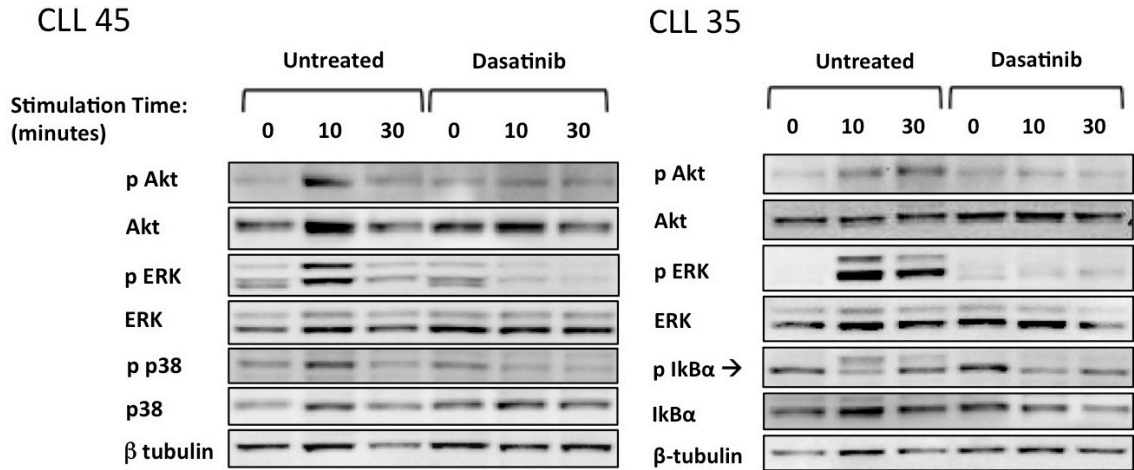
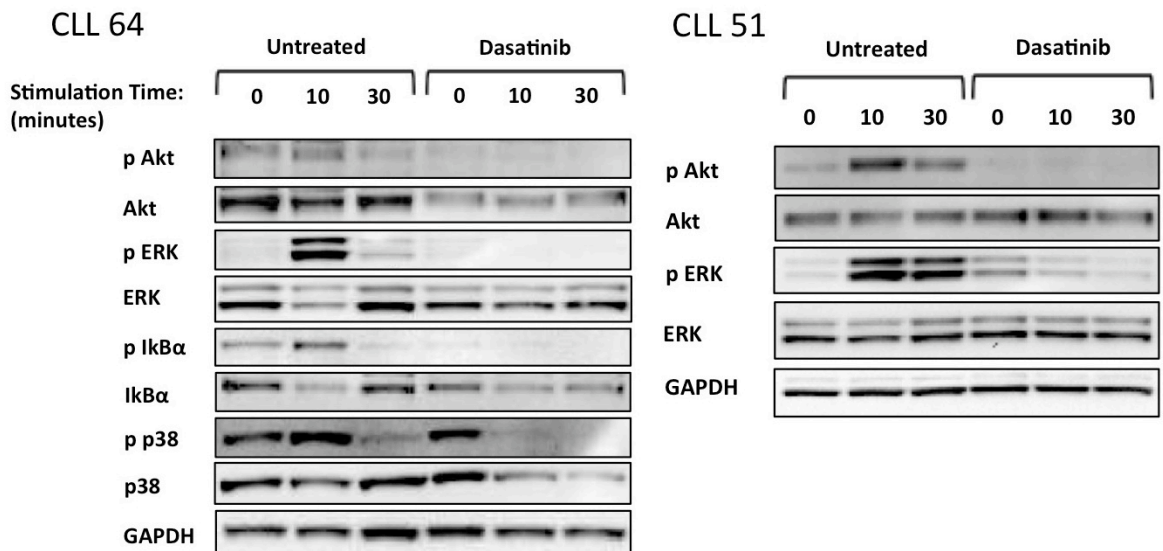
**Figure 4.4 Correlation of levels of total and phosphorylated Syk and Lyn with dasatinib sensitivity**

Densitometry was performed on the control samples from each sample shown in Fig. 4.3, in order to correlate CLL cell response to dasatinib with both the relative basal expression of Syk or Lyn, and also with the ratio of phosphorylated Syk/Lyn to total protein. In each graph the sample points are coloured as in Fig. 4.3, with red squares indicating high, black square indicating moderate, and blue squares indicating low responses to dasatinib. **A** The density (expressed as pixel intensity divided by area in mm<sup>2</sup>) of Syk for each patient sample was normalised to GAPDH to account for differences in protein loading, and plotted on the x axis. The y axis shows the percentage reduction in viability (relative to control) of each sample treated for 48 hr with 100 nM dasatinib. Linear regression analysis was performed to relate the two parameters, and the p value shown. **B** The x axis shows the percentage of total Syk phosphorylated, calculated by dividing the density of phosphorylated Syk by that of total Syk. These values were plotted against dasatinib sensitivity, and linear regression performed as in A. **C** Analysis of total Lyn was carried out as described for Syk in A. **D** Analysis of Lyn phosphorylation was performed as described for Syk in B.



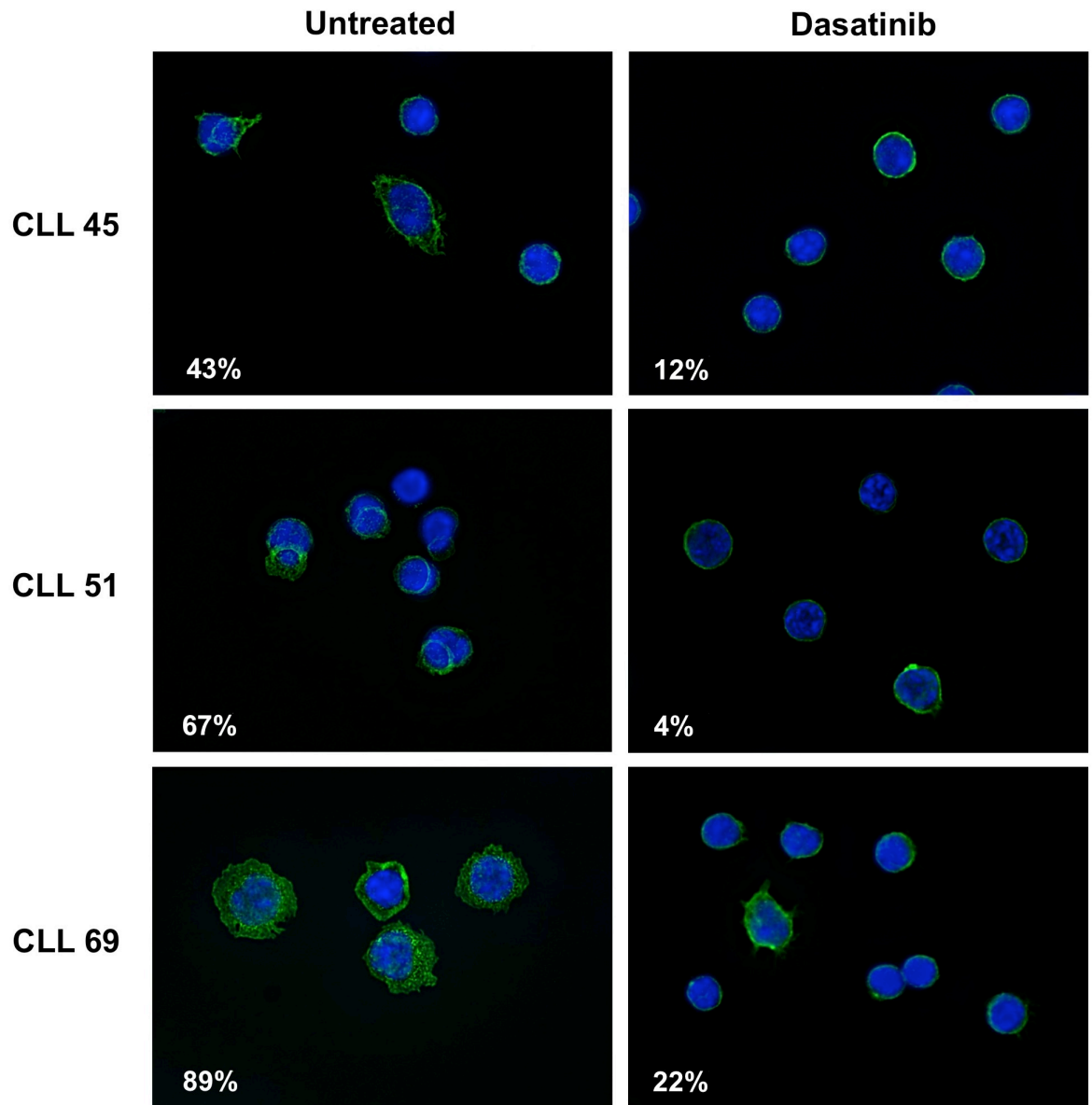
**Figure 4.5 Dasatinib inhibits calcium flux following BCR stimulation in CLL cells**

CLL cells from three patients were incubated with 1  $\mu$ M Fura-2 AM for 30 min at 37°C. Cells were then incubated with 10  $\mu$ g/ml biotinylated anti-IgM with or without 100 nM dasatinib for 30 min prior to BCR stimulation. BCR stimulation with avidin was performed after recording a stable basal reading for 40 s, and the graphs show the change in  $[Ca^{2+}]$  plotted against time. Each condition for each patient sample was recorded in triplicate, and a representative recording from each patient sample shown.

**A****B**

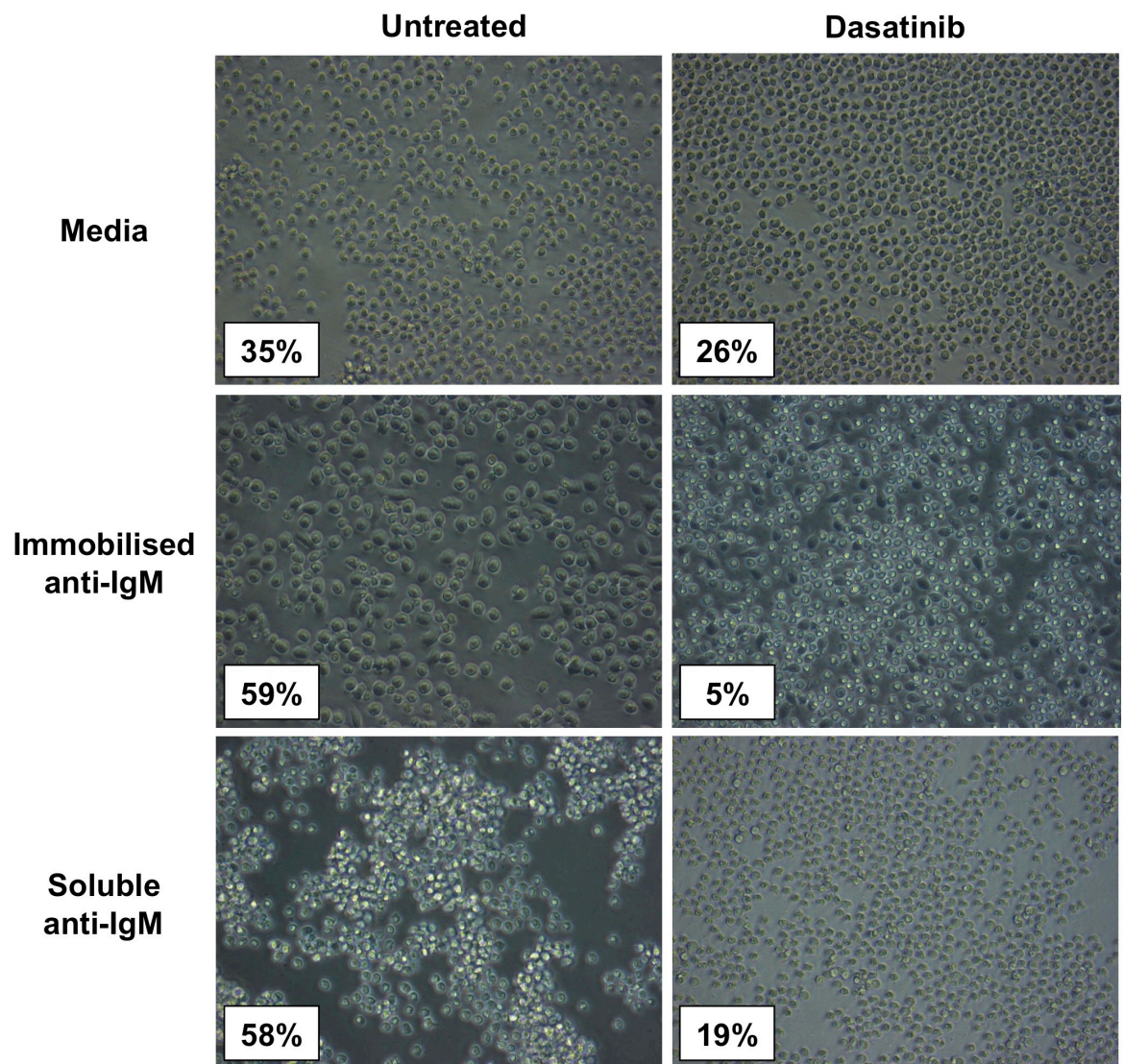
### Figure 4.6 Effect of dasatinib on Akt and MAPK activation following BCR crosslinking

CLL cells were incubated with 10  $\mu\text{g/ml}$  biotinylated anti-IgM in the presence or absence of 100 nM dasatinib for 30 minutes, washed, then lysed unstimulated or following incubation with 25  $\mu\text{g/ml}$  avidin at 37°C for 10 or 30 min. Phosphorylated and total proteins were detected by western blotting. A total of six patient samples were analysed. Akt and ERK phosphorylation were assessed in all samples, and p38 and I $\kappa$ B $\alpha$  phosphorylation each assessed in three samples. Two representative ZAP-70 positive cases are shown in **A**, and two ZAP-70 negative cases in **B**. In the absence of dasatinib, BCR stimulation is seen to induce phosphorylation of ERK and p38 MAPK, Akt, and I $\kappa$ B $\alpha$ , all of which are completely inhibited by dasatinib treatment.



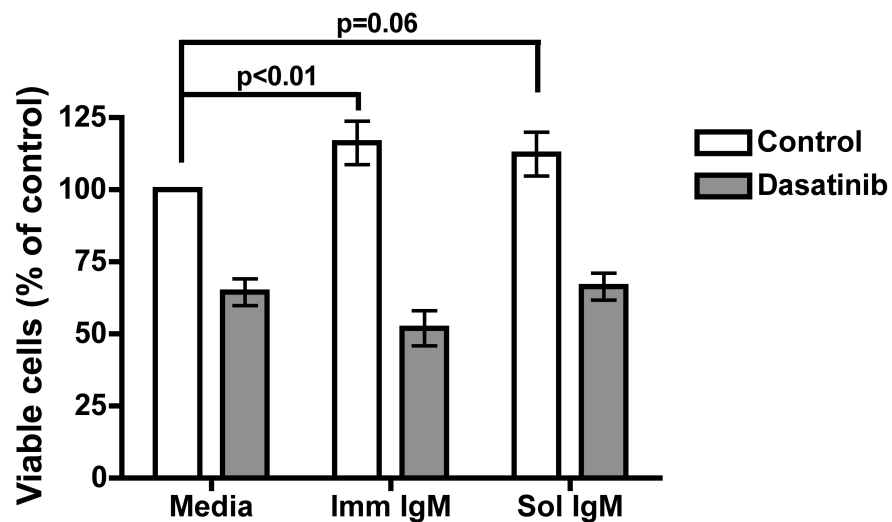
**Figure 4.7 Dasatinib inhibits actin reorganisation following BCR crosslinking**

CLL cells (n=5) were incubated with or without 100 nM dasatinib for 30 min, then transferred to glass slides coated with 10  $\mu\text{g/ml}$  anti-IgM or 10  $\mu\text{g/ml}$  isotype-matched control for a further 30 min at 37°C. Actin was visualised within permeabilised cells by staining with Alexa Fluor 488 phalloidin and nuclei counterstained with DAPI. Representative photographs of dasatinib-treated and control cells from three patients are shown. For each sample, 200 cells were assessed for evidence of cytoplasmic spreading, considered positive or negative. The percentage of positive cells in each sample is shown in the lower left-hand corner.



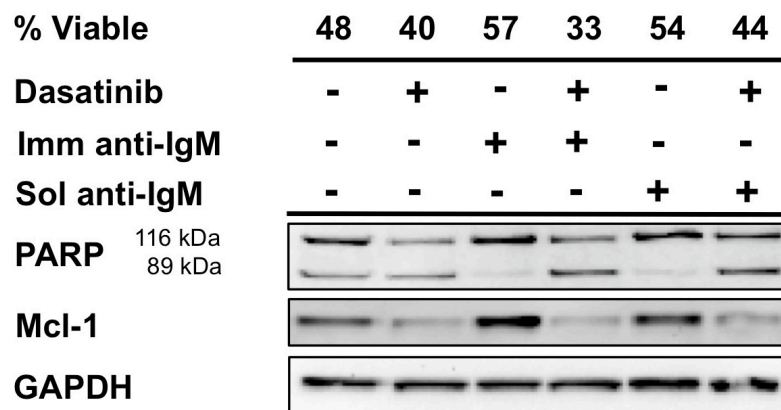
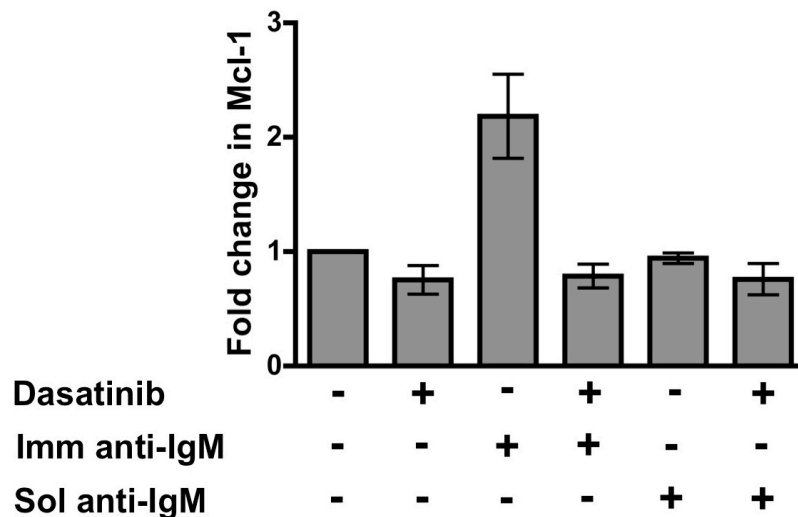
**Figure 4.8 Morphology of CLL cells stimulated with soluble and immobilised anti-IgM in the presence or absence of dasatinib**

CLL cells were cultured either in: complete media alone; wells coated with 10  $\mu\text{g/ml}$  anti-IgM, or; complete media supplemented with 10  $\mu\text{g/ml}$  anti-IgM F(ab')<sub>2</sub> fragments. In addition, cells in each condition were cultured in the presence and absence of 100 nM dasatinib. The photographs show the morphology of one CLL sample (CLL 52) following 48 hr treatment as indicated. The cells were then harvested for assessment of cell viability by FCM staining with Annexin V/VIprobe. The percentages shown in the lower left-hand corner of each photograph represent the cell viabilities of cells cultured in each condition in this patient sample.



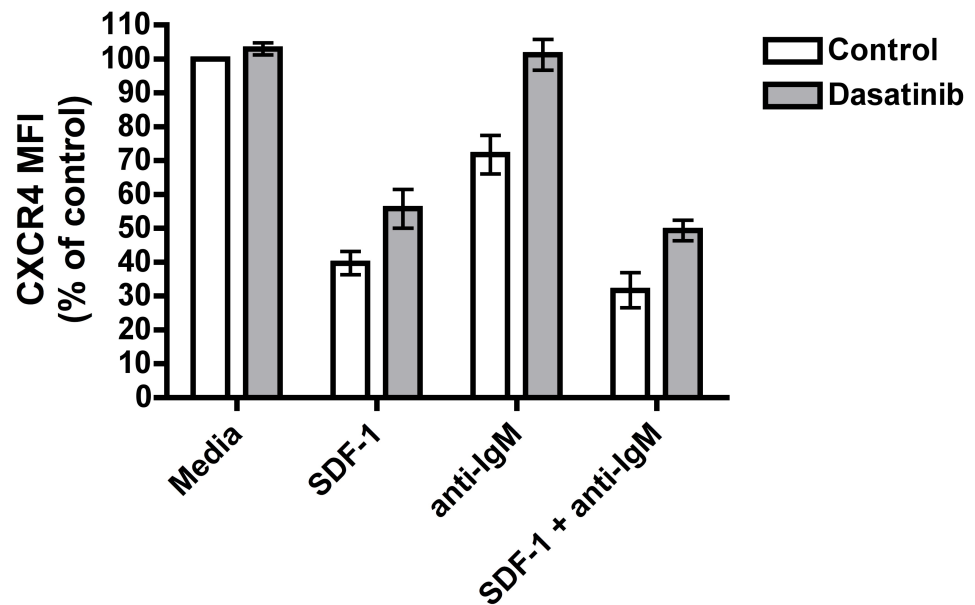
**Figure 4.9 Effect of dasatinib on viability of CLL cells on prolonged BCR stimulation *in vitro***

CLL cells from 11 patient samples were incubated with or without 100 nM dasatinib either in media alone, or with 10  $\mu\text{g/ml}$  soluble or immobilised anti-IgM for 48 hr. Cell viability was assessed by Annexin V/VIprobe by FCM, and is expressed as a percentage of the untreated control for each sample. Both soluble and immobilised anti-IgM increased viability of CLL cells, although this reached statistical significance for immobilised IgM only. Dasatinib completely inhibited the BCR-mediated increase in survival, with viability of cells similar to those treated in media alone.

**A****B**

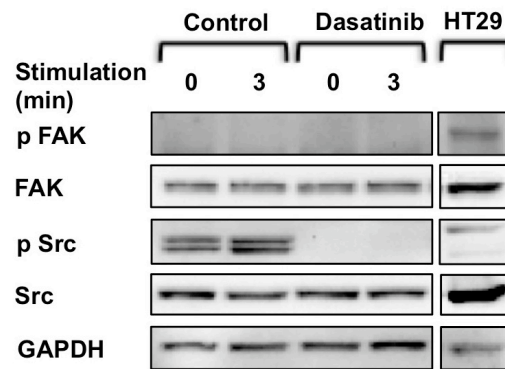
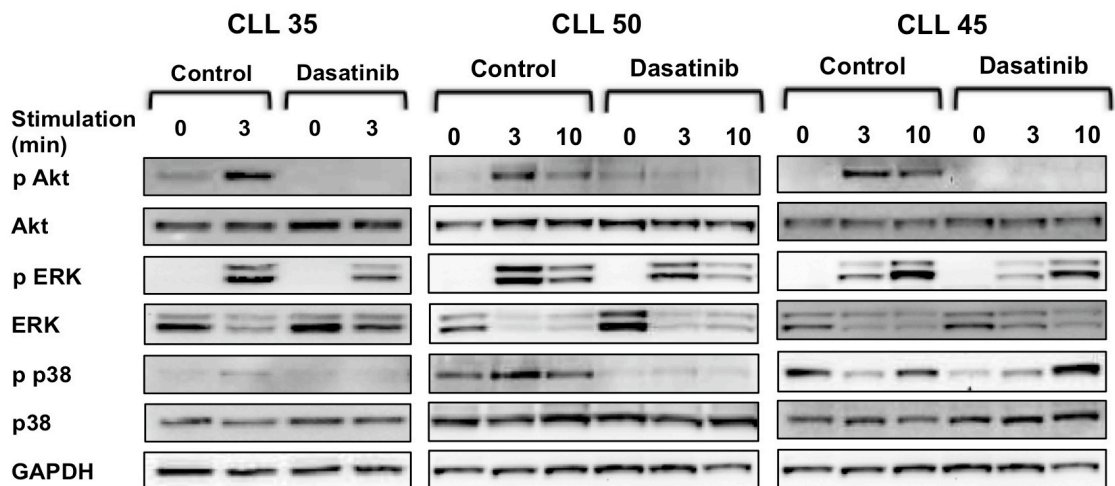
**Figure 4.10 Dasatinib inhibits upregulation of Mcl-1 on prolonged BCR stimulation**

CLL cell lysates from cells incubated with or without 100 nM dasatinib either in media alone, or with 10  $\mu$ g/ml soluble (Sol anti-IgM) or immobilised anti-IgM (Imm anti-IgM) for 48 hr were analysed by western blotting (n=3). **A** An immunoblot from a representative patient sample is shown. The percentage of viable cells measured by Annexin V/VIaprobe FCM is shown above the immunoblot. **B** Densitometry was performed on all three western blots, and the mean ( $\pm$  SEM) fold-change in Mcl-1, relative to untreated cells cultured in media alone, following the indicated treatments is shown.



**Figure 4.11 Dasatinib inhibits down-regulation of CXCR4 expression following BCR stimulation**

CLL cells ( $1 \times 10^6/\text{ml}$ ) were incubated with or without 100 nM dasatinib for 30 min, followed by incubation with 100 ng/ml SDF-1, 10  $\mu\text{g}/\text{ml}$  immobilised anti-IgM, or both, as indicated for a further 4 hr, followed by assessment of CXCR4 surface expression by FCM. Results are expressed as the MFI ( $\pm$  SEM) of each sample expressed as a percentage of the untreated control.

**A****B**

**Figure 4.12 Dasatinib inhibits Akt phosphorylation following SDF-1 stimulation of CLL cells *in vitro***

CLL cells were incubated in RPMI-1640 supplemented with 0.5% BSA for 2 hr prior to experiments. CLL cells ( $3 \times 10^6$ /ml) were incubated with or without 100 nM dasatinib for 30 min. Protein lysates were then prepared from cells either unstimulated, or following 3 or 10 min incubation with 100 ng/ml SDF-1 at 37°C (n=3). **A** Cell lysates prepared following treatments above were analysed by Western blotting for phosphorylated and total Src family kinases and FAK. Unstimulated cell lysates of HT29 cells, known to express phosphorylated FAK, were run alongside as a positive control. A blot from a representative patient is shown. **B** Protein lysates from the same experiments were analysed by western blotting, using the following antibodies, p Akt, Akt, p ERK, ERK, p p38 and p38 kinases, using GAPDH as a loading control.

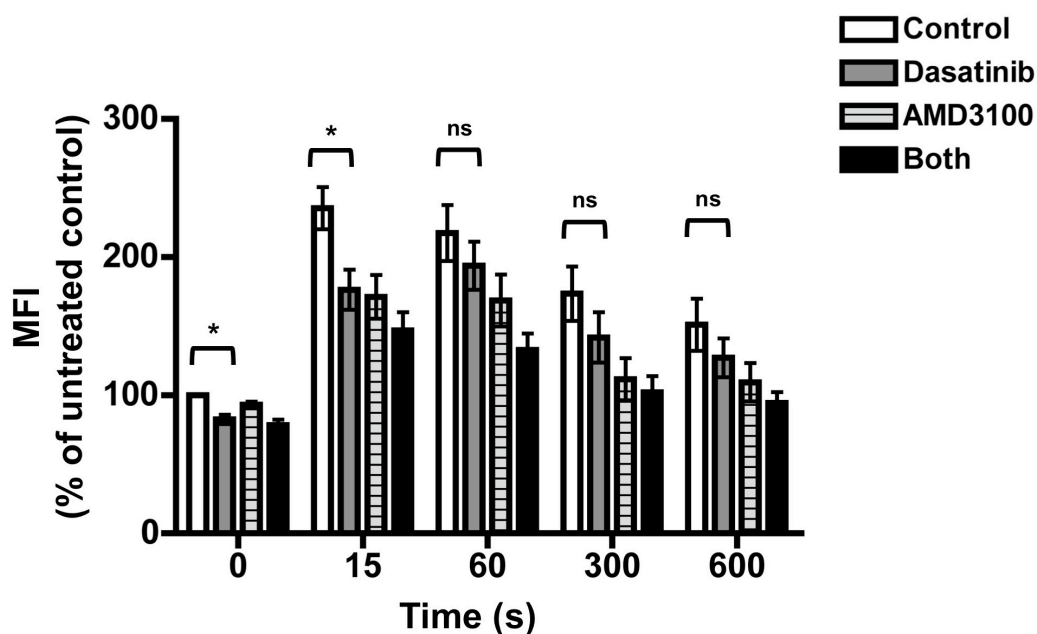


**Figure 4.13 Effect of dasatinib on actin polymerisation following SDF-1 stimulation of CLL cells**

CLL cells were incubated in RPMI-1640 supplemented with 0.5% BSA for 2 hr prior to the experiment. Cells ( $2 \times 10^6$ ) were then incubated for a further 30 min in the following conditions: 0.5% BSA media alone; media containing 100 nM dasatinib; media containing 40  $\mu$ g/ml AMD3100 or; media containing 100 nM dasatinib and 40  $\mu$ g/ml AMD3100. Cells were then stimulated by the addition of 100 ng/ml SDF-1 for 10 minutes. 100  $\mu$ l aliquots from each well were removed pre-stimulation, and at 15, 60, 300, and 600 s after addition of SDF-1, and transferred to tubes containing 250  $\mu$ l BD Fix/Perm solution. Following fixation and permeabilisation, cells were washed then stained with a 1/100 dilution of AlexaFluor® 488-labelled phalloidin for 10 min, and washed twice prior to FCM analysis. The mean fluorescence of each treatment condition was expressed as a percentage of that of the untreated control prior to SDF-1 addition. The graph shows the mean ( $\pm$  SEM) values for five independent experiments on different CLL samples. \* indicates  $p < 0.05$ , and ns denotes not significant.

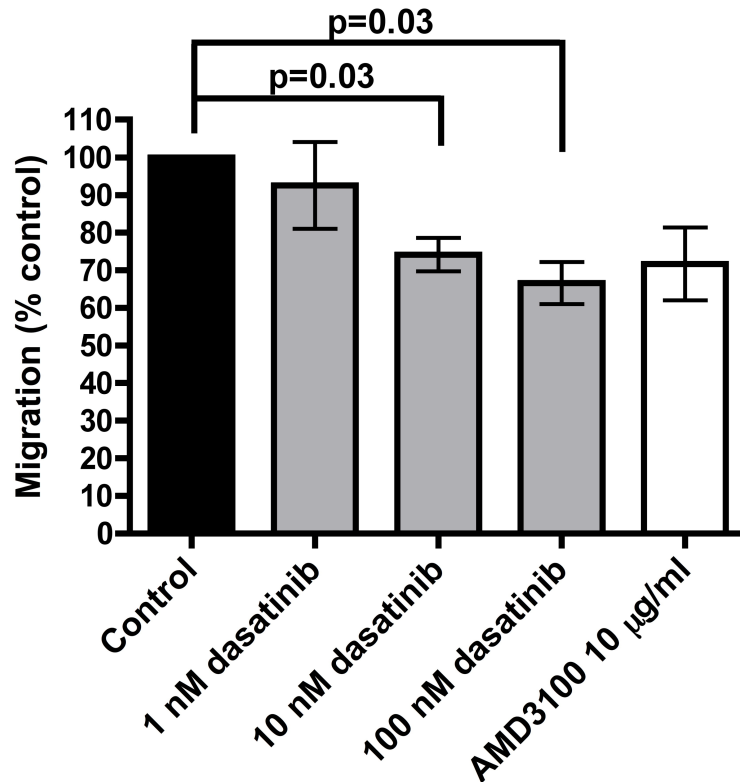


**Figure 4.14 Dasatinib inhibits chemotaxis of CLL cells towards SDF-1**

CLL cells were again incubated in RPMI-1640 supplemented with 0.5% BSA for 2 hr prior to the experiment. Cells ( $5 \times 10^5$ ) in 100  $\mu$ l media were then treated with 1, 10, or 100 nM dasatinib, 10  $\mu$ g/ml AMD3100, or left untreated for a further 30 min. The cells were then transferred to the upper chamber of a 6.5 mm Transwell culture insert, placed into wells containing 600  $\mu$ l media supplemented with 150 ng/ml SDF-1, and incubated for 4 hr at 37°C. Inserts containing untreated CLL cells placed into wells containing media alone were included as a negative control to account for spontaneous migration. For each patient sample, each condition was set up in duplicate wells. After 4 hr incubation, transwells were removed, and three 150  $\mu$ l aliquots removed from the lower chamber for counting by FCM. Cells were counted by recording the number of events acquired on high flow setting for 30 s. Data are expressed as the percentage of migration of treated cells relative to the untreated control, and are the mean ( $\pm$  SEM) of five experiments using different patient samples.

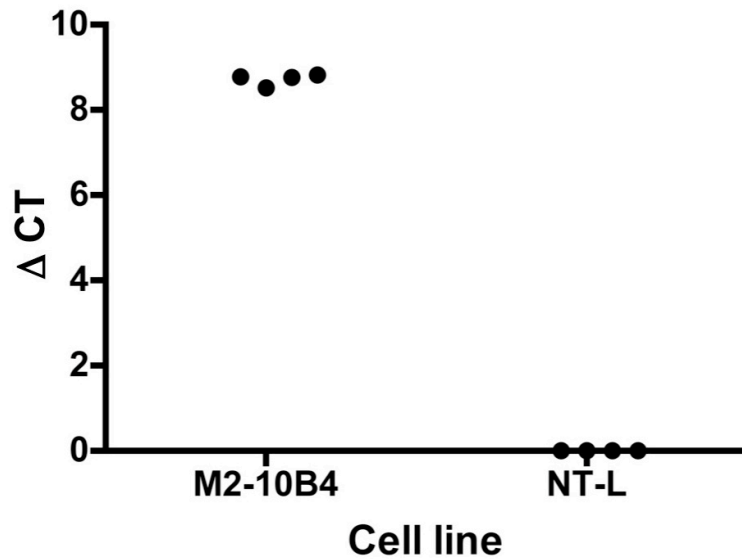
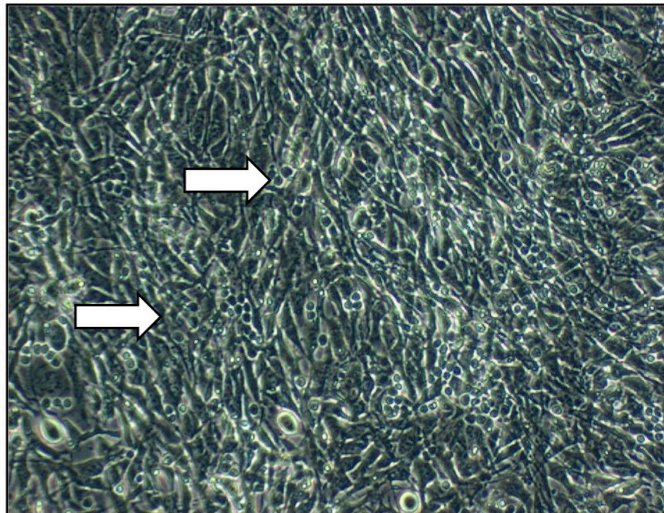


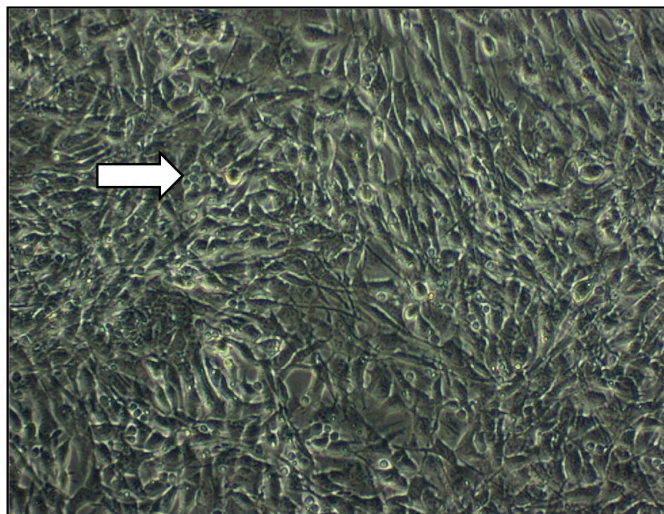
**Figure 4.15 Analysis of SDF-1 RNA expression in the murine BM stromal cell lines M2-10B4 and NT-L**

RNA was prepared from M2-10B4 and NT-L cells, and reverse transcribed to cDNA. Quantitative PCR was performed using TaqMan® Gene Expression Assay probes for SDF-1 and GAPDH, as described in Section 2.7.3. Assays were performed in quadruplicate. Results are expressed as the cycle threshold (CT) of SDF-1 minus the CT of GAPDH, or  $\Delta$ CT. Where the CT of SDF-1 was not reached, the result is expressed as zero.

### Control

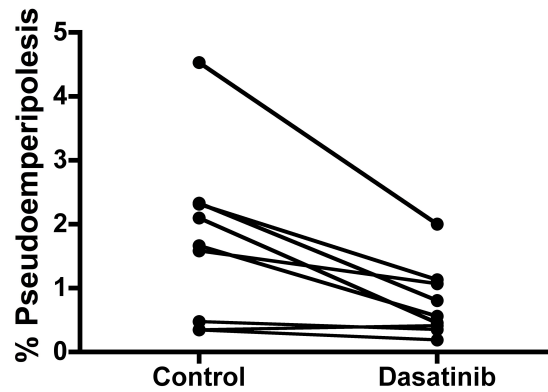
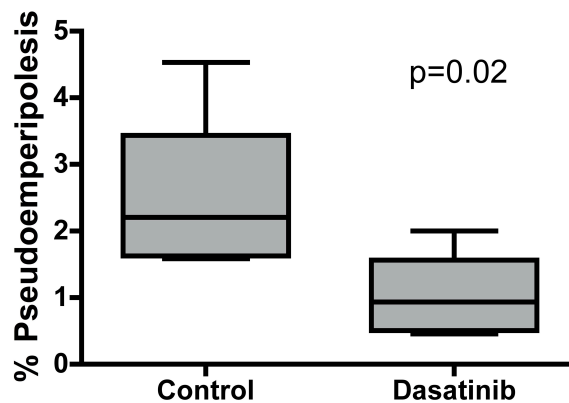


### Dasatinib



**Figure 4.16 Appearance of M2-10B4 stromal cell layers following 5 hr co-culture with CLL cells in the presence or absence of dasatinib**

48 hr prior to the assay, M2-10B4 fibroblasts were plated at  $1.5 \times 10^5$  per well in collagen-coated 24 well tissue culture plates, and allowed to reach confluence. On the day of the experiment, CLL cells ( $2 \times 10^6$ /ml) were pre-treated with 100 nM dasatinib or left untreated, then transferred to stromal-containing wells, and incubated for 5 hr at 37°C. Triplicate wells were set up for each sample. At the end of culture, non-migrated cells were removed by washing three times, and pseudoemperipolesed cells photographed. Cells which have transmigrated into the stromal cell layer lose a refractile appearance on phase-contrast microscopy, and are indicated by white arrows in the photographs from one representative experiment.

**A****B**

**Figure 4.17 Dasatinib inhibits pseudoemperipolesis of CLL cells under M2-10B4 cells**

CLL cells were treated as described in Fig. 4.16. Following removal of non-migrated cells by washing, the stromal cell layer was trypsinised, and stained with an anti-CD19 APC antibody prior to FCM. A 1/10 dilution of the total starting cell population was similarly treated, to allow quantitation of the percentage of migrated cells. Negative controls included a well containing stromal cells only, and a well incubated with CLL cells for 5 min only, to validate the washing steps. Triplicate test wells, and controls were counted by acquiring CD19 positive events on the flow cytometer for 30 s. **A** Each set of points and interconnecting line represent the mean percentage of migrated cells with or without dasatinib in an individual patient sample (n=9). **B** The six samples showing evidence of greater than 1% pseudoemperipolesis in control samples are included in this analysis. The box plots show the median (horizontal line within box) percentage of migrated cells in both groups. The upper and lower borders of the box represent the 75<sup>th</sup> and 25<sup>th</sup> centiles respectively, and the whiskers the highest and lowest values.

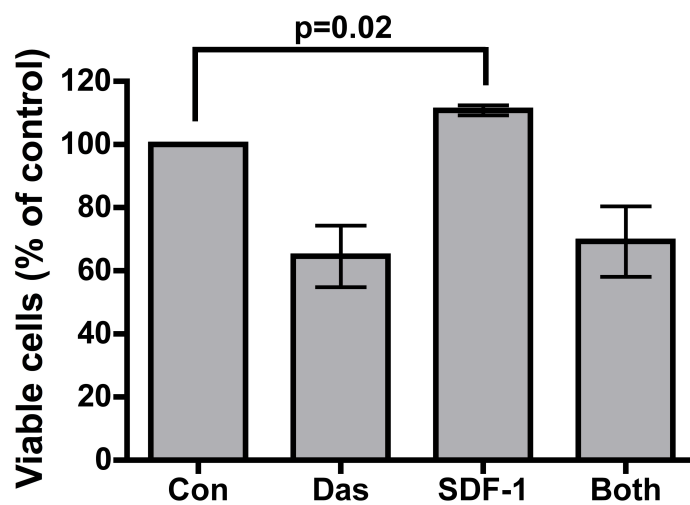


**Figure 4.18 The anti-apoptotic effect of SDF-1 is overcome by dasatinib.**

CLL cells ( $1 \times 10^6$ /ml) were incubated in one of four conditions: complete media (Con); 100 nM dasatinib (Das); 100 ng/ml SDF-1 (SDF-1), or; both Das and SDF-1 for 48 hr, following which apoptosis was assessed by FCM by Annexin V/Viaprobe staining. The graph shows the mean ( $\pm$  SEM) viabilities of cells treated as shown (n=6).

## **Chapter 5:**

**CLL cell co-culture with stromal cells, in the presence or absence of CD154 and IL-4, modulates the anti-leukaemic effects of dasatinib.**

## 5.1 Introduction

### 5.1.1 Modelling the CLL microenvironment *in vitro*

Initial studies investigating the effect of the leukaemic microenvironment on spontaneous and drug-induced apoptosis of CLL cells have employed primary human BM or NLC co-cultures (220, 221, 242). These techniques require invasive collection of patient BM samples and technically demanding tissue culture procedures, and therefore are not readily accessible laboratory models to allow repeated assessment of novel therapeutics. Acknowledgement of the role of the microenvironment in CLL, and the appreciation that *in vitro* chemotherapeutic drug sensitivity often fails to correlate with clinical patient response (197), has led research to focus on developing co-culture systems using stromal cell lines. These models are representative of human primary BM or LN stroma and function as translational models in which to assess novel therapeutic agents. Murine BM fibroblast cell lines, including L cells (NT-L) (116), and M2-10B4 cells (254), have also been demonstrated to protect CLL cells cultured *in vitro* from spontaneous apoptosis. The pro-survival effect of these stromal cell lines, as with primary BM cultures, on CLL cells require cell to cell contact. Co-culture of CLL cells with such stromal cell lines has been proposed to model the peripheral blood CLL cell environment, as cells remain viable, and in G<sub>0</sub>/G<sub>1</sub> phases of cell cycle, akin to circulating CLL cells *in vivo* (116).

CLL cell interactions in peripheral blood are again different from the LN and BM microenvironment, where the association of CLL cells with CD4<sup>+</sup> T lymphocytes drives CLL cell proliferation. Translational assessment of novel therapies in CLL must therefore include assessment of drugs on both non-cycling (blood) and proliferative (tissue) compartments. Co-culture of CLL cells with activated T lymphocytes *in vitro* increased survival and also induced proliferation, dependent on signalling through CD154 and secretion of IL-2 and IL-4 (422). Moreover, co-culture with soluble recombinant CD154 (sCD154) alone induced CLL cell proliferation in 7/18 cases in one study (423), confirming the importance of CD154/CD40 signalling in inducing CLL cell proliferation. In addition, this study noted that co-culture with both sCD154 and IL-4 induced proliferation in 16/18 CLL samples, suggesting the combination of both signalling pathways may drive CLL cell proliferation *in vivo*. CLL cell proliferation on co-culture with murine L fibroblasts bearing an immobilised anti-CD40 monoclonal antibody was also

greatly enhanced by the addition of IL-4 (293), supporting this hypothesis. Synergy between CD154 and IL-4 in inducing up-regulation of cyclin D3 and cyclin E expression, increasing retinoblastoma (Rb) phosphorylation, and down-regulating p27<sup>kip1</sup> has been described (424), which likely explains the molecular mechanism of the observed proliferation. Recently, CLL cell proliferation has been described in a system in which CLL cells were co-cultured with NT-L cells stably transfected to express CD154, in culture media supplemented with recombinant IL-4 (the 154L/IL-4 system) (116). As the level of CLL cell proliferation in this system, as measured by [<sup>3</sup>H]-thymidine incorporation, showed a significant positive correlation with advanced patient clinical stage, the authors suggested that the *in vitro* model may mimic proliferation occurring within PCs *in vivo* (116). CLL cells isolated from patient LN were found to express higher levels of survivin and Bcl-x<sub>L</sub> than those in peripheral blood, and analysis of patient LN by immunohistochemistry confirmed that high expression of both proteins to be localised to CLL cells within PCs (425, 426). Expression of both proteins increased in CLL cells cultured in the 154L/IL-4 system compared to cells cultured on NT-L cells or media alone, strengthening the evidence that this co-culture system simulates the PC microenvironment (426). Increased Mcl-1 expression was also observed on 154L/IL-4 co-culture (426), and high Mcl-1 expression in CLL samples has been found to correlate with *in vivo* chemoresistance (197). Of note, CLL cells cultured in the 154L/IL-4 system were significantly more resistant to fludarabine than those cultured in media alone (426).

It is clear that *in vitro* assessment of chemotherapeutic agents on CLL cells cultured in media alone, many of which are already committed to apoptosis, is unlikely to predict the response of patients to the same treatments. *In vitro* assessment of novel therapeutic approaches remains an important part of pre-clinical drug assessment, and *in vitro* co-culture systems which mimic tissue microenvironments are important in order to achieve this. In this chapter, NT-L and 154L/IL-4 co-culture systems are utilised to assess whether the pro-apoptotic effect of dasatinib, alone or in combination treatments, is modulated by these microenvironmental factors.

## 5.2 Aims and Objectives:

In order to assess how the anti-leukaemic effects of dasatinib are modulated by antigen-independent signals within the microenvironment, the aims of this chapter were to:

- i. Compare the ability of dasatinib to induce apoptosis of CLL cells cultured in media alone to that of cells co-cultured in either the NT-L or 154L/IL-4 system;
- ii. Assess the effect of dasatinib on pro-survival and anti-apoptotic signalling pathways induced by stromal co-culture, in the presence or absence of CD154 and IL-4;
- iii. Investigate whether dasatinib inhibits proliferation of CLL cells co-cultured in the 154L/IL-4 system;
- iv. To determine whether dasatinib retains the ability to chemosensitise CLL cells to established and novel chemotherapeutic agents in NT-L and 154L/IL-4 co-culture.

## 5.3 Results

### 5.3.1 Stromal cell or CD154/IL-4 co-culture greatly reduces apoptosis induced by dasatinib

In order to recapitulate supportive microenvironmental conditions *in vivo*, CLL cells were co-cultured with NT-L cells or the 154L/IL-4 system overnight prior to drug treatments in all co-culture experiments. The effect of 48 hr dasatinib treatment on the viability CLL cells cultured in media alone was compared to that on cells co-cultured with NT-L cells. The mean ( $\pm$  SEM) viabilities of cells treated as described in eight independent experiments are shown in Figure 5.1A. The viability of untreated CLL cells in NT-L co-culture was significantly greater than that of cells cultured in media alone ( $95.9\% \pm 0.7\%$  compared to  $63.9\% \pm 5.3\%$  respectively;  $p < 0.001$ ). However, in addition to a reduction in spontaneous apoptosis, NT-L co-culture led to a significant reduction in the pro-apoptotic effect of dasatinib, with the mean reduction in viability falling from  $35.2\% \pm 2.2\%$  (in cells cultured in media alone) to  $3.9\% \pm 0.4\%$  ( $p < 0.001$ ). 154L/IL-4 system co-culture provided similar protection to CLL cells from apoptosis (Fig. 5.1B). Dasatinib has been described to inhibit global tyrosine phosphorylation in CLL cells cultured *in vitro* (353). In order to assess whether dasatinib retained the ability to inhibit tyrosine phosphorylation in CLL cells in co-culture, cells cultured in media alone, in NT-L or 154L/IL-4 co-culture, were treated with or without dasatinib for 2 hr, followed by western blotting using an antibody specific for phosphotyrosine. A representative immunoblot is shown in Figure 5.2. The predominant tyrosine phosphorylated protein in all three samples assessed corresponded to the molecular weight of Lyn. Dasatinib completely inhibited tyrosine phosphorylation in all three culture conditions, demonstrating that additional signalling pathways are responsible for the protective effects of co-culture.

### 5.3.2 PI-3K/Akt and MAPK activation in NT-L and 154L/IL-4 co-cultured CLL cells abrogates the pro-apoptotic effect of dasatinib

As demonstrated in Chapter 4, dasatinib sensitivity correlated with the ability of the drug to inhibit Syk phosphorylation, key to BCR signal transduction. Veldurthy *et al.* also reported dasatinib-induced apoptosis to correlate with a reduction in both Akt and MAPK phosphorylation (353). As PI-3K and MAPK are activated by a number of cytokine and integrin receptors, implicated in promoting leukaemic cell survival (427), we hypothesised that these signalling pathways may be responsible

for dasatinib resistance in co-culture. Phosphorylation of Akt and MAPKs was assessed by western blotting in CLL cells cultured as follows: in media alone; with NT-L cells, or; in the 154L/IL-4 system. Cells were treated with or without dasatinib for 2 hr prior to preparation of protein lysates, and representative immunoblots from three patient samples are shown in Fig. 5.3. In untreated cells cultured in media alone, basal phosphorylation of Akt was observed in 5/5 cases, of ERK in 2/5 cases, while little or no basal p38, JNK, or p70 s6 kinase phosphorylation was observed in any of the five samples. Dasatinib inhibited basal ERK phosphorylation in 2/2 samples, however basal Akt phosphorylation was inhibited in only 1/5 cases (Fig. 5.3). NT-L or 154L/IL-4 co-culture induced additional ERK phosphorylation in all samples, which was either completely or partially resistant to inhibition with dasatinib. In untreated co-cultured cells, although Akt phosphorylation changed little, phosphorylation of the p70 s6 kinase, a downstream kinase in the PI-3K/Akt signalling pathway (outlined in Section 1.5.2.2) increased in NT-L co-culture, and further increased in 154L/IL-4 co-cultured cells. In either co-culture system, dasatinib caused incomplete, or no inhibition of p70 s6 kinase phosphorylation. In addition, 154L/IL-4, but not NT-L, co-culture significantly increased phosphorylation of p38 and JNK MAPK, which again was not prevented by dasatinib. Collectively, these data show that dasatinib fails to fully inhibit PI-3K/Akt and MAPK activation induced by NT-L or 154L/IL-4 co-culture, suggesting that these signalling pathways may contribute to dasatinib-resistance.

Selective inhibitors of PI-3K and MAPKs were used to investigate this hypothesis, specifically the: PI-3K inhibitor LY294002; MEK1/2 inhibitor PD98059; p38 inhibitor SB203580, and JNK inhibitor II. Initial experiments determined minimum concentrations of 10  $\mu$ M LY294002 and 40  $\mu$ M PD98059 were required to inhibit phosphorylation of Akt and ERK respectively in co-cultured CLL cells (data not shown). In Figure 5.4, representative immunoblots demonstrating that these concentrations of LY294002 and PD98058 selectively inhibit Akt/p70 s6 kinase and ERK phosphorylation respectively in CLL cells co-cultured in the 154L/IL-4 system are shown. In order to investigate whether PI-3K inhibition could resensitise co-cultured CLL cells to dasatinib, cells in NT-L or 154L/IL-4 co-culture were treated with LY294002, dasatinib, or both inhibitors for 48 hr, followed by assessment of apoptosis by FCM. A similar experimental approach was used to assess whether PD98059 could restore dasatinib sensitivity in co-cultured cells. In

NT-L co-culture, both LY294002 and PD98059 significantly increased the degree of apoptosis induced by dasatinib (Fig. 5.5A). Although LY294002 and PD98059 treatment alone reduced the viability of co-cultured CLL cells, the addition of dasatinib significantly increased the pro-apoptotic effect of both inhibitors (Fig. 5.5A). However, in 154L/IL-4 co-culture, neither LY294002 nor PD98059 were able to sensitise CLL cells to dasatinib (Fig. 5.5B). A preliminary experiment found neither 5  $\mu$ M SB203580 nor 50  $\mu$ M JNK inhibitor II to resensitise 154L/IL-4 co-cultured CLL cells to dasatinib (data not shown). In conclusion, these data demonstrate that whilst dasatinib inhibits MAPK and Akt signalling following BCR stimulation, these signalling pathways can be activated by antigen-independent microenvironmental stimuli, and overcome the pro-apoptotic effect of dasatinib.

### **5.3.3 Dasatinib fails to inhibit the up-regulation of anti-apoptotic Bcl-2 family proteins and survivin on 154L/IL-4 co-culture**

As outlined in Section 5.1.1, 154L/IL-4 co-culture up-regulates anti-apoptotic proteins including Mcl-1, Bcl-x<sub>L</sub>, and A1, and the pro-proliferative protein survivin in CLL cells (426). Using western blotting, the effect of 48 hr dasatinib treatment on the expression of Bcl-2 family proteins and survivin was compared between CLL cells cultured in media alone, NT-L co-culture, and 154L/IL-4 co-culture, to further investigate the mechanism of resistance to dasatinib induced by co-culture. A representative immunoblot is shown in Figure 5.6A. Considering untreated CLL cells, while NT-L co-culture little changes expression of any protein assessed, 154L/IL-4 co-culture leads to marked up-regulation of Mcl-1, Bcl-x<sub>L</sub>, and survivin, none of which are inhibited by dasatinib. Densitometric analysis of immunoblots from five experiments confirmed up-regulation of Bcl-x<sub>L</sub> (mean 5.8-fold), Mcl-1 (mean 2.7-fold), and a significant reduction in Bcl-2 expression (mean 0.8-fold) in 154L/IL-4 co-cultured cells as compared to untreated cells cultured in media alone (Fig. 5.6B). None of these changes in protein expression were significantly altered by dasatinib. CD40 stimulation of CLL cells has been reported to lead to down-regulation of the BH3-only Bcl-2 protein Bim, in particular the Bim<sub>EL</sub> isoform, through ERK-mediated proteasomal degradation (355). Three splice variants of Bim exist, Bim<sub>EL</sub> (23 kDa), Bim<sub>L</sub> (15 kDa), and Bim<sub>S</sub> (12 kDa), with shorter isoforms having greater pro-apoptotic activity than Bim<sub>EL</sub> (428). We confirmed 154L/IL-4 co-culture to lead to a reduction in Bim<sub>EL</sub> expression with no change in Bim<sub>L</sub> or Bim<sub>S</sub> expression (Fig. 5.6A+B). Notably, although not reaching statistical

significance, a trend toward an increase in Bim<sub>EL</sub> expression in dasatinib-treated cells was preserved in 154/IL-4 co-culture (Fig. 5.6B).

As the level of CD154 expression achieved by stable expression in fibroblasts has been proposed to be supraphysiologic (355), the effect of dasatinib on changes in Bcl-2 family protein expression induced by culture of CLL cells in media supplemented with sCD154 and IL-4 was assessed. As synergy between CD154 and IL-4 signalling in the regulation of Bcl-2 protein expression has been described in CLL cells (293, 424), cells treated with or without dasatinib were cultured for 48 hr in four conditions: complete media alone; media supplemented with IL-4; media plus sCD154, or; both IL-4 and sCD154. At the end of experiments, cell viability was measured by Annexin V/VIaprobe FCM, and Bcl-2 family protein expression assessed by western blotting. A representative immunoblot is shown in Figure 5.7A. In untreated cells, up-regulation of both Mcl-1 and Bcl-x<sub>L</sub> was observed following incubation with both sCD154 and IL-4 (Fig. 5.7A). Dasatinib did not inhibit up-regulation of either Mcl-1 or Bcl-x<sub>L</sub> induced by combined sCD154/IL-4 stimulation (Fig. 5.7A), and had no effect on cell viability (Fig 5.7B). Of note, stimulation with either sCD154 or IL-4 alone slightly increased Mcl-1 and Bcl-x<sub>L</sub> expression. Dasatinib inhibited Mcl-1 expression induced by low-dose sCD154 alone (Fig. 5.7A), and retained the ability to induce apoptosis of these cells. Mcl-1 expression was unaffected by dasatinib in CLL cells co-cultured with IL-4 alone (Fig. 5.7A, and moreover this treatment completely abrogated the pro-apoptotic effect of dasatinib (Fig. 5.7B).

#### **5.3.4 CLL cell proliferation in 154L/IL-4 co-culture is not inhibited by dasatinib**

In addition to effects on cell viability and migration, dasatinib has been reported to exert antiproliferative effects on CML cells (429), and a number of non-haematopoietic malignant cell lines (430, 431). Although cells co-cultured in the 154L/IL-4 system were resistant to apoptosis on dasatinib treatment, we were interested to examine whether dasatinib may yet inhibit CLL cell proliferation in this model. In order to assess CLL cell division, cells were loaded with the fluorescent dye CFSE and co-cultured in the 154L/IL-4 proliferation assay, with or without dasatinib, as described in Section 2.2.9. Proliferation was assessed by FCM every three days. On the basis of CFSE dilution, CLL cell proliferation was evident from day 6 onwards (Fig. 5.8A), and dasatinib did not significantly inhibit proliferation in any sample assessed (n=6; Fig. 5.8A+B).

In order to assess whether long-term dasatinib treatment affected CLL cell viability in the 154L/IL-4 system, cells were counted by FCM at each time point. Both total cell counts (Fig. 5.9A) and percentage recovery of input cells (Fig. 5.9B) did not differ between untreated and dasatinib-treated cells throughout the experiment, confirming that 154L/IL-4 co-cultured CLL cells are resistant to dasatinib-induced apoptosis, even on prolonged drug exposure. Of interest, while dasatinib did not affect CLL cell viability or proliferation during these experiments, a striking difference in morphology of untreated and dasatinib-treated co-cultured was evident by the end of the culture period. Untreated CLL cells generally formed large cell aggregates, however dasatinib-treated cells remained more widely distributed across the stromal cell layer, suggesting effects of dasatinib on CLL cell migration and/or adhesion (Fig. 5.10).

### **5.3.5 Dasatinib retains the ability to sensitise CLL cells to fludarabine and chlorambucil in NT-L, but not 154L/IL-4 co-culture**

As synergy was observed between dasatinib and both chlorambucil and fludarabine (Section 3.3.7), experiments were performed to establish whether dasatinib retained the ability to chemosensitise CLL cells in stromal co-culture to these drugs. Rather than the concentrations of chemotherapeutic drugs used in combination with 100 nM dasatinib in synergy experiments (based on  $4 \times IC_{50}$  concentrations), 5  $\mu$ M fludarabine and 12.5  $\mu$ M chlorambucil were selected for use in these experiments, as they are nearer to the maximum clinically achievable concentrations (432, 433). Four drug treatment conditions were assessed: vehicle control; dasatinib; fludarabine (or chlorambucil), or; both dasatinib and fludarabine (or chlorambucil). CLL cells in each co-culture system were treated for 48 hr, following which apoptosis was assessed by FCM. Experiments were performed to assess drug treatments in each of five culture conditions as follows: media alone; NT-L co-culture; NT-L co-culture plus IL-4; 154L co-culture, or; 154L/IL-4 co-culture, in order to establish the individual contributions of IL-4 and CD154 to drug resistance. Although the level of apoptosis induced by drug treatments in NT-L co-cultured cells was markedly less than that in cells cultured in media alone, a trend for dasatinib to potentiate the effect of fludarabine was retained (Fig. 5.11A). 154L/IL-4 co-cultured cells were confirmed to be resistant to all drug treatments, predominantly due to CD154 stimulation, rather than the addition of IL-4 to stromal co-cultures (Fig. 5.11A). The ability of dasatinib to enhance the apoptotic effect of chlorambucil was also retained in NT-L co-culture, however CLL cells in 154L/IL-4

co-culture were also resistant to all treatments (Fig 5.11B). No differences in the appearance of stromal cell layers were visible following any of the drug treatments to suggest direct toxicity to stromal cells. The effect of dasatinib combinations was further assessed in NT-L co-cultured CLL cells only (Fig. 5.12A+B). Dasatinib significantly potentiated the pro-apoptotic effect of fludarabine in NT-L co-culture, with cells treated with the drug combination having a mean viability of  $58.8\% \pm 7\%$ , compared to  $76.5\% \pm 3.2\%$  in cells treated with fludarabine alone (Fig. 5.12A;  $p < 0.01$ ). Dasatinib also significantly increased apoptosis induced following chlorambucil treatment, with the mean viability of cells treated with the combination  $37\% \pm 9\%$ , compared with  $73.4\% \pm 8\%$  in cells treated with chlorambucil alone (Fig. 5.12B;  $p = 0.01$ ), confirming that dasatinib retains the ability to chemosensitise CLL cells in direct contact with stromal cells.

### **5.3.6 Synergy between dasatinib and Bcl-2 inhibitor I is lost on NT-L or 154L/IL-4 co-culture**

As our data demonstrated Bcl-2 protein up-regulation to be involved in the chemoresistant phenotype of 154L/IL-4 co-cultured CLL cells, and in view of the synergy observed between dasatinib and the BH3-mimetic Bcl-2 inhibitor I (Section 3.3.7), the possibility that the combination of dasatinib and Bcl-2 inhibitor I may overcome 154L/IL-4-induced chemoresistance was investigated. CLL cells cultured in each of the three culture conditions were treated with either: DMSO vehicle control; dasatinib; Bcl-2 inhibitor I, or; both dasatinib and Bcl-2 inhibitor I for 48 hr, then apoptosis assessed by FCM. While significant apoptosis was observed in treated cells cultured in media alone, NT-L or 154L/IL-4 co-cultured cells were completely resistant to apoptosis with all treatments (Fig. 5.13).

### **5.3.7 Dasatinib sensitises CLL cells to the HSP90 inhibitor 17-DMAG sensitises in both NT-L and 154L/IL-4 co-culture**

Dasatinib also exhibited synergy with the HSP90 inhibitor 17-DMAG (Section 3.3.7). As HSP90 is a chaperone protein involved in stabilising many kinases involved in cell signalling, including kinases key to both Akt and ERK MAPK signalling (330), the combination of dasatinib and 17-DMAG was assessed in co-cultured CLL cells, principally in order to assess whether the combination may overcome CLL cell chemoresistance in 154L/IL-4 co-culture. CLL cells are known to over-express HSP90 (331), however the influence of stromal co-culture on HSP90 expression has not been reported. In preliminary experiments we

observed NT-L co-culture, and moreover 154L/IL-4 co-culture to increase HSP90 expression in CLL cells (Fig. 5.14), which provided an additional rationale for investigation of dasatinib in combination with 17-DMAG in co-cultured CLL cells. Following 48 hr treatment 17-DMAG alone induced a degree of apoptosis of CLL cells in NT-L co-culture (Fig. 5.15), reducing mean cell viability from 95.5% to 65.4% ( $p>0.05$ ), however the pro-apoptotic effect became statistically significant on treatment with the combination of dasatinib and 17-DMAG, which reduced the mean cell viability to 42.4% ( $p=0.01$ ). Importantly, 17-DMAG also induced some apoptosis of 154L/IL-4 co-cultured CLL cells, reducing mean cell viability from 86.2% to 75% ( $p>0.05$ ; Fig 5.15). Again, the addition of dasatinib potentiated the effect of 17-DMAG alone, reducing mean cell viability to 67.7% ( $p=0.04$ ).

In view of these promising data, the effects of 48 hr treatment with 17-DMAG, dasatinib, or the inhibitor combination on irradiated NT-L and 154L cells cultured alone was assessed to determine whether these treatments caused direct toxicity to stromal cells (and therefore reduce the availability of survival signalling). Although dasatinib did not affect stromal cell viability, 17-DMAG or the drug combination did result in apoptosis of 30-40% of all cells (Fig. 5.16A). Despite this, visually the wells containing 17-DMAG still contained viable adherent stromal cells with the morphology of untreated cells (Fig. 5.16B). In view of the high expression of CD154 by transfected stromal cells, significant CD154 is likely to remain available to CLL cells. However, in view of this important potentially confounding factor, the effect of 17-DMAG on the protection provided by sCD154 and IL-4 in a cell-free system was assessed. CLL cells were treated as described above in media alone, or in media supplemented with sCD154 and IL-4 for 48 hr, following which apoptosis was assessed by FCM as before, and protein lysates also prepared. Whilst dasatinib-induced apoptosis was completely inhibited by sCD154 and IL-4, 17-DMAG induced apoptosis was unaffected, with the viability of CLL cells treated with 1  $\mu$ M 17-DMAG in media alone similar to that of cells treated in the presence of sCD154 and IL-4 (14.8 compared to 18.8% respectively; Fig. 5.17A). The immunoblot demonstrated that 17-DMAG, unlike dasatinib, completely inhibited up-regulation of Mcl-1 and Bcl-x<sub>L</sub> in the presence of sCD154 and IL-4 stimulation (Fig. 5.17B). Induction of apoptosis was confirmed by the cleavage of PARP. To investigate the mechanism responsible for these effects, the effect of 17-DMAG on Akt and MAPK signalling was assessed. CLL cells were treated as described above, however, protein lysates were prepared 2 hr after the

addition of sCD154 and IL-4 to culture media. In untreated cells, whilst little change in Akt phosphorylation was observed, sCD154/IL-4 stimulation increased the phosphorylation of p70 s6 kinase, JNK-, and p38-MAPK (Fig. 5.18). ERK phosphorylation was not seen at this time point using these experimental conditions. 17-DMAG inhibited p70 s6 kinase phosphorylation induced by sCD154/IL-4, with no effect on Akt, p38, or JNK phosphorylation, or total Akt protein expression. Although these data suggest that 17-DMAG inhibits PI-3K/Akt signalling on sCD154/IL-4 stimulation, further studies are required to establish this.

## 5.4 Discussion

The pro-apoptotic effect of dasatinib in CLL cells was significantly reduced by co-culture with NT-L stromal cells, in the presence or absence of CD154 and IL-4. Of note, dasatinib retained the ability to inhibit global tyrosine phosphorylation, including Lyn phosphorylation, in both co-culture systems, demonstrating that alternate signalling pathways are responsible for chemo-resistance in co-culture. Given the commonality of PI-3K and MAPKs in relaying anti-apoptotic and mitogenic signals downstream of a number of membrane-associated receptors, including CD40 and IL-4R, the effect of dasatinib on these kinases was compared between our culture conditions.

Basal ERK phosphorylation was detected in two of the five samples assessed in our study, consistent with previous reports demonstrating constitutive ERK phosphorylation in a subset of CLL samples only (191, 395). Although dasatinib inhibited basal ERK phosphorylation in both samples in our study, specific ERK inhibitors do not induce apoptosis of CLL cells *in vitro* (300, 434), suggesting that inhibition of ERK signalling is not the main pro-apoptotic mechanism of dasatinib. In contrast, we detected basal Akt Thr<sup>308</sup> phosphorylation in all five CLL samples assessed. Previous studies of Akt phosphorylation and kinase activity in unstimulated CLL cells have generated conflicting results. Ringshausen *et al.* demonstrated constitutive PI-3K activity in freshly isolated CLL cells, however no Akt phosphorylation on either Thr<sup>308</sup> or Ser<sup>473</sup>, and no Akt activity in kinase assays (434). In the present study, an attempt was made to assess Akt Ser<sup>473</sup> phosphorylation by immunoblotting, however no signal was detected; further optimisation of the antibody used is required. Barragan *et al.* also failed to detect Akt Ser<sup>473</sup> phosphorylation in a small number of CLL patient samples (300). However, other groups have both detected both Akt Thr<sup>308</sup> and Ser<sup>473</sup> phosphorylation in cultured CLL cells (435, 436), and demonstrated Akt kinase activity using a GSK-3 fusion protein substrate (435). Our experiments were performed using cryopreserved CLL cells. Previous studies have shown that cryopreservation does not significantly affect the ability to detect either ERK or Akt phosphorylation by immunoblotting (191, 436). The differences between studies of Akt activity in CLL cells may be explained by differences in either cell culture conditions or protein lysate preparation. The addition of albumin to cell culture media can activate PI-3K/Akt signalling in CLL cells (437); all studies described above used media containing FCS, however differences in albumin and cytokine

composition of FCS between laboratories may have led to variable levels of exogenous stimulation in culture. Alternatively, the failure of detection of Akt phosphorylation by some groups could be due to inadequate phosphatase inhibition during cell lysate preparation. Akt is rapidly inactivated *in vitro* by phosphatases including protein phosphatase 2A (PP2A) (438). In our experiments, microcystin, an inhibitor of PP1 and PP2A (439), was added to PBS used in washing steps prior to lysate preparation, which is likely to have facilitated phospho-Akt detection. The observation that PI-3K inhibitors (300, 434), and specific Akt inhibitors (436), induce apoptosis of CLL cells *in vitro* provides further evidence that PI-3K/Akt signalling is active and involved in the survival of cultured CLL cells.

Dasatinib inhibited basal Akt Thr<sup>308</sup> phosphorylation in only one of the five samples assessed. Inhibition of Akt phosphorylation by dasatinib would be expected, as a result of PI-3K inhibition, as Src kinases are upstream activators of PI-3K in BCR signal transduction (Section 1.5.2). Of note, variable inhibitory effects of PI-3K inhibitors on Akt phosphorylation in unstimulated CLL cells have been reported. Plate *et al.* reported LY294002 to induce caspase 8-dependent apoptosis of CLL cells, however suggested apoptosis was Akt-independent, as no inhibition of Akt phosphorylation or kinase activity was observed (435). However, two subsequent studies have shown that LY294002 inhibited Akt Thr<sup>308</sup> phosphorylation in CLL cells (436, 440), and one reported inhibition of Akt Ser<sup>473</sup> phosphorylation (436). In addition to regulation of activity by phosphorylation, Akt activity is also determined by intracellular localisation (164). The phosphorylation of p70 s6 kinase, a target kinase of the mTOR complex (Fig. 1.8), was therefore also assessed by immunoblotting as a further indicator of Akt activity. No p70 s6 kinase phosphorylation was seen in untreated CLL cells, suggesting little Akt activity.

In NT-L co-cultured CLL cells, the most striking observation was a significant increase in ERK phosphorylation, which was incompletely inhibited by dasatinib. Although a pro-survival role for ERK signalling in unstimulated CLL cells has not been confirmed, ERK activation has been proposed to account for the pro-survival effects of CXCR4 stimulation of CLL cells *in vitro* (242). One previous study found no inhibitory effect of 10  $\mu$ M PD98059 on the viability of CLL cells co-cultured with murine fibroblasts (360); however we found 40  $\mu$ M PD98059 to be the minimum concentration required to inhibit ERK phosphorylation in NT-L co-cultured CLL

cells. In the current work, PD98059 did slightly reduce CLL cell viability, suggesting ERK signalling does contribute to the anti-apoptotic effect of NT-L co-culture. Furthermore, PD98059 significantly potentiated the apoptotic effect of dasatinib in NT-L co-culture, confirming that ERK signalling contributes to dasatinib resistance under these conditions.

Stromal co-culture has been reported to sustain (360), or increase (254), Akt phosphorylation in CLL cells, and PI-3K inhibition abrogated the anti-apoptotic effect of co-culture with murine fibroblasts (360). Although we observed no significant change in Akt Thr<sup>308</sup> phosphorylation in NT-L co-cultured CLL cells, phosphorylation of p70 s6 kinase clearly increased. The reason for the disparity between Akt and p70 s6 kinase phosphorylation in our study is currently not clear. Of interest, there is evidence that mTOR activity may additionally be regulated by PI-3K/Akt independent mechanisms in certain haematological malignancies. In AML cells, in which Lyn is also over-expressed and constitutively active, a positive regulatory role of Lyn in the mTOR pathway downstream of Akt was demonstrated (205). In this study, inhibition of Lyn expression with siRNA significantly inhibited p70 s6 kinase phosphorylation, with no effect on Akt phosphorylation (205). In our experiments, dasatinib slightly reduced p70 s6 kinase phosphorylation in NT-L co-culture. Due to the upregulation of p70 s6 kinase phosphorylation in co-cultured cells, it is possible that the exposure times used in our study were too short to fully assess basal p70 s6 kinase phosphorylation in CLL cells cultured in media alone. Assessment of dasatinib or PP2 treatment on Akt and p70 s6 kinase phosphorylation in CLL cells cultured in media alone would be of interest to further assess whether similar regulation of mTOR by Src kinases occurs in CLL. Additionally, in follicular lymphoma cells, Syk has been established to contribute to mTOR activation, as measured by p70 s6 kinase phosphorylation, in an additional pathway independent of PI-3K/Akt signalling (441). Stromal co-culture has recently been demonstrated to increase Syk phosphorylation in CLL cells (442). Although p70 s6 kinase was not assessed in this study, it is possible that Syk activation may also contribute to p70 s6 kinase phosphorylation in NT-L co-cultured cells. The PI-3K inhibitor LY294002 reduced the viability of CLL cells in stromal co-culture, confirming previous reports (360, 412). Furthermore, LY294002 significantly increased CLL cell sensitivity to dasatinib, demonstrating PI-3K signalling to contribute to stromal cell-mediated resistance to dasatinib. In view of the increase in p70 s6 kinase phosphorylation in NT-L co-culture, it would

be interesting to establish whether mTOR inhibition also re-sensitises CLL cells to dasatinib, or whether other PI-3K/Akt dependent pathways are responsible. Whilst p38 MAPK has also been implicated in the anti-apoptotic effect of stromal co-culture in CLL cells (443), the p38 inhibitor SB203580 did not sensitise co-cultured cells to dasatinib in the present study. In conclusion, although dasatinib inhibits PI-3K/Akt and MAPK activation following BCR stimulation, activation of these kinases by stromal factors, CD154, and IL-4 is unaffected, and abrogates the pro-apoptotic effect of dasatinib.

Although this study has identified both PI-3K and ERK activation in CLL cells to be involved in the stromal cell adhesion-mediated resistance to dasatinib, the cell surface receptors activated by NT-L co-culture remain to be determined. The failure to detect SDF-1 mRNA by qRT-PCR in NT-L cells suggests that SDF-1/CXCR4 signalling is not responsible, although further assessment of SDF-1 expression at the protein level by immunoblotting, or enzyme-linked immunosorbent assay (ELISA) of NT-L cell culture media would be desirable to confirm this. The anti-apoptotic effect of NT-L cell co-culture on CLL cell viability has been demonstrated to be entirely dependent on direct cell contact, suggesting surface receptor-ligand interactions, rather than secreted factors, are responsible for increased survival (116). As outlined in Section 1.7.1.2, signalling through multiple integrin receptors, particularly VLA-4, has been demonstrated to inhibit both spontaneous and drug-induced apoptosis of CLL cells *in vitro*. In addition to up-regulation of integrin receptors such as CD49d on the surface of CLL cells driven by stromal co-culture (115), a number of inflammatory cytokines including IL-4 have been demonstrated to induce the expression of the VLA-4 ligand VCAM-1 on the surface of BM stromal cells (444), raising the possibility of a bi-directional positive reinforcement of cell adhesion between CLL cells and stromal cells. A recent study found CD38<sup>+</sup>/CD49d<sup>+</sup> CLL cells were able to attract monocytes via secretion of the chemokines CCL3 and CCL4, which in turn induced VCAM-1 expression on the surface of stromal cells, largely through secretion of TNF $\alpha$  (445). Whether IL-4 secreted by CLL-associated CD4<sup>+</sup> T lymphocytes, or by CLL cells themselves, can also upregulate VCAM-1 expression on BM stromal cells remains to be determined. It is also of great interest that DLBCL cell lines have been demonstrated to induce BAFF mRNA expression and increase BAFF secretion from co-cultured stromal cell lines, through a mechanism requiring direct cell-cell contact (446). In view of these data, it would be of great interest to assess

expression of both integrin receptor ligands such as fibronectin and VCAM-1, and also BAFF and APRIL, in NT-L cells, both following culture alone, and also following 48 hr co-culture with CLL cells, to assess whether CLL cells may directly regulate stromal cell protein expression. An alternative approach to further investigate the key interactions involved in cell adhesion-mediated apoptosis resistance would be to repeat NT-L co-culture experiments in the presence of blocking antibodies to integrin receptors on the CLL cell surface. Previous studies suggest that simultaneous blockade of several integrin receptors may be required to inhibit pro-survival signalling (221). Of note, a small peptide inhibitor of fibronectin/ $\beta$ 1 integrin interaction was recently demonstrated to re-sensitise AML cell lines cultured in fibronectin-coated plates to chemotherapeutic agents; furthermore the inhibitor prolonged survival in an *in vivo* AML mouse model (447).

Co-culture of CLL cells in the 154L/IL-4 system resulted in a further increase in p70 s6 kinase phosphorylation, accompanied by significant p38 and JNK MAPK phosphorylation, and none of the activated kinases were inhibited by dasatinib. That ERK or PI-3K inhibition failed to either overcome the protective effect of 154L/IL-4 co-culture, or sensitise CLL cells to dasatinib in this setting suggests a degree of functional overlap of pro-survival signals under these conditions. Indeed, this has previously been reported following CD40 stimulation of mature murine B lymphocytes (448). Dasatinib failed to overcome the up-regulation of Mcl-1 and Bcl-x<sub>L</sub> on CLL co-culture in the 154L/IL-4 system. Our results differ from a recent study reported by Hallaert *et al*, in which both imatinib and dasatinib reversed the upregulation of Mcl-1, Bcl-x<sub>L</sub>, and AI induced by co-culture of CLL cells with NIH3T3 fibroblasts stably transfected to express CD154 (355). A number of differences between the experimental approaches employed may account for the differing results obtained. Hallaert *et al*. co-cultured CLL cells for 48 hr in the presence or absence of 30  $\mu$ M dasatinib, a concentration far greater than the clinically achievable concentration of 100 nM used in our experiments. As described in Section 3.4, dasatinib used at such a concentration is likely to have a number of off-target effects. In the present study, CLL cells were placed in co-culture overnight prior to dasatinib treatment, in order to allow signalling networks to become established, as would be the case within the CLL microenvironment *in vivo*, whereas Hallaert *et al*. pre-treated CLL cells with 80  $\mu$ M dasatinib prior to adding cells to co-culture. It is also possible that the addition of IL-4 to the 154L cell co-culture media in our experiments may have contributed to

the differing results. Our observations that dasatinib inhibited Mcl-1 expression and induced apoptosis of CLL cells stimulated by low-dose sCD154 alone, while having no inhibitory effect on IL-4-induced Mcl-1 expression or survival are in support of this hypothesis. Furthermore, a clear synergistic effect on up-regulation of Bcl-x<sub>L</sub> and Mcl-1 was observed on CLL stimulation with the combination of sCD154 and IL-4. As CLL cells within LN and BM PCs adjacent to CD4<sup>+</sup> T lymphocytes expressing CD154 will likely also be exposed to IL-4 (219), we propose that our model may be more physiologically relevant than models studying CD154 stimulation alone.

Dasatinib did not inhibit the increase in survivin expression induced by 154L/IL-4 co-culture. Given these data, it was perhaps not unexpected that dasatinib failed to inhibit CLL cell proliferation in the 154L/IL-4 system. Nevertheless, as proliferation of normal B lymphocytes requires co-ordinated signalling through the BCR and co-stimulatory receptors such as CD40 (285), it remains possible that dasatinib may exert a net anti-proliferative effect on CLL cells stimulated through both receptors within PCs *in vivo*. In support of this, in T lymphocytes, proliferation induced by TCR engagement is inhibited by dasatinib, whereas proliferation stimulated by IL-2 signalling is unaffected (449). Also, in DLBCL cell lines, dasatinib induces a G<sub>1</sub>-S phase cell cycle arrest, due to inhibition of signalling pathways downstream of the BCR (385). It would be of interest to determine whether the addition of anti-IgM to the 154L/IL-4 co-culture system influences the kinetics of CLL cell proliferation, and if so, assess each condition in the presence or absence of dasatinib. CLL cell proliferation *in vitro* can also be induced by stimulation with CpG oligodeoxynucleotides (CpG ODN), which resemble unmethylated sequences of bacterial DNA (450, 451). CpG ODN stimulate Toll-like receptor 9 (TLR9), which activates a number of signalling pathways resulting in B cell proliferation and up-regulation of co-stimulatory receptors (451). It would also be interesting to investigate whether dasatinib affects CLL cell proliferation on CpG ODN stimulation.

We observed stromal co-culture to significantly reduce apoptosis induced by both fludarabine and chlorambucil, consistent with previous reports (223, 227). In addition to exhibiting synergy with chemotherapeutic agents in CLL cells cultured in media alone, dasatinib retained the ability to sensitise NT-L co-cultured CLL cells to apoptosis on treatment with fludarabine or chlorambucil. Although the mechanisms responsible for stromal cell adhesion-mediated resistance to

chemotherapeutic agents remain to be fully determined, it is interesting to note that direct contact between CLL cells and stromal cells has been demonstrated to increase expression of RAD51 and DNA ligase IV, involved in the repair of DNA damage (254). As inhibition of DNA repair has been proposed to account for the synergistic effects of dasatinib in combination with fludarabine and chlorambucil, this mechanism may also account for the chemosensitising effect of dasatinib in stromal co-culture. Further work to assess RAD51 phosphorylation in NT-L co-cultured CLL cells exposed to our experimental conditions would be informative. 154L/IL-4 co-cultured CLL cells were resistant to all drug combinations studied, demonstrating that whatever the chemosensitising mechanism active in NT-L co-culture, it is overcome by the pro-survival signalling pathways activated by CD154 and IL-4 stimulation. Our results again differ from the recent study by Hallaert *et al.*, which reported dasatinib (or imatinib) to sensitise CD154-expressing stromal co-cultured cells to fludarabine, and a number of novel therapeutic agents (355). In this study, in addition to using a significantly higher concentration of dasatinib than in our work (30  $\mu$ M), cells were co-cultured in the presence of dasatinib for 48 hr, then removed from the stromal layer, and treated with fludarabine while incubated in media alone. Furthermore, an exceedingly high concentration of fludarabine was employed in these experiments (100  $\mu$ M). Although further scheduling experiments may be performed, we show that CLL cells cultured with CD154-expressing cells alone are resistant to concurrent treatment with achievable concentrations of dasatinib and fludarabine. Although within CLL patients some recirculation of CLL cells between tissues and bloodstream could occur, a proportion of the CLL clone is likely to remain in contact with a supportive microenvironment during treatment courses, which was modelled in our experiments.

Our data suggest that CLL cells exposed to CD4<sup>+</sup> T lymphocytes within LN and BM are likely to be resistant to dasatinib as a single agent, or in combination with standard chemotherapy. Preliminary data from a phase II trial of dasatinib in chemo-refractory patients reported dasatinib to reduce patient LN size by over 50% in two-thirds of patients, often without significantly reducing the circulating lymphocyte count (374), suggesting that dasatinib may exert more complex *in vivo* effects on the leukaemic microenvironment than may be predicted from *in vitro* studies. Given the data presented in Chapter 4, this may be explained by effects of dasatinib on the SDF-1/CXCR4 axis, however there is also substantial evidence

to suggest that dasatinib may also modulate T cell support of CLL cells *in vivo*. It is important to consider that in our experimental system, the availability of IL-4 and CD154 is fixed, and immutable by dasatinib. Dasatinib has however been shown to inhibit many aspects of T lymphocyte function, without inducing apoptosis (449, 452). Dasatinib inhibited Akt and ERK phosphorylation following TCR stimulation (449), proposed to be due to inhibition of the Src kinase Lck (303), and prevented expression of the early activation markers CD38 and CD69 (449, 452). In addition, dasatinib can inhibit the secretion of IL-4 by stimulated CD4<sup>+</sup> T lymphocytes (453). Although not assessed by these groups, it is reasonable to suggest that such inhibition of early T cell activation may prevent up-regulation of CD154 expression. Furthermore, dasatinib inhibited the proliferation of murine CD4<sup>+</sup> T lymphocytes in a murine allogeneic transplantation model (449). Therefore, it is possible that by inhibiting proliferation, activation, and cytokine secretion of T lymphocytes *in vivo*, dasatinib may reduce the availability of T lymphocyte supportive factors including CD154 and IL-4, and indirectly overcome CD154/IL-4-mediated chemo-resistance. Of interest, inhibition of BCR signalling with the Syk inhibitor R406 reduced the secretion of the T cell chemokines CCL3 and CCL4 by CLL cells (195). It would be of great interest to confirm whether dasatinib also inhibits CCL3/CCL4 secretion following IgM stimulation, as this may represent another mechanism by which dasatinib inhibits supportive interactions between CLL cells and CD4<sup>+</sup> T lymphocytes.

To try to overcome CLL cell chemoresistance in 154L/IL-4 co-culture, dasatinib was assessed in combination with two novel agents, both of which exhibited synergy with dasatinib when assessed on culture in media alone. The pro-apoptotic effect of Bcl-2 inhibitor I was abrogated on stromal co-culture, and also failed to re-sensitise CLL cells to dasatinib. Given the lack of modulation of Bcl-2 family protein expression observed in NT-L co-cultured CLL cells, this result was surprising. A study of the potent BH3-mimetic ABT-737, which also binds both Bcl-2 and Bcl-x<sub>L</sub>, reported no significant reduction in activity in CLL cells co-cultured with stromal cells (329). ABT-737 has a reported nanomolar IC<sub>50</sub> for both Bcl-2 and Bcl-x<sub>L</sub> (328), compared to a low micromolar IC<sub>50</sub> reported for Bcl-2 inhibitor I (325). It is possible that the differing results may be explained by the effects of Bcl-2 inhibitor I being more sensitive to alterations in expression of Bcl-2 family proteins not assessed in the present body of work, although the findings do raise the possibility that the observed apoptosis induced by Bcl-2 inhibitor I in

media alone may be due to off-target effects on other signalling pathways. CLL cells co-cultured with stroma, CD154 and IL-4 were resistant to ABT-737, due to up-regulation of Bcl-2A1 and Bcl-x<sub>L</sub> (329). However, ABT-737 was able to sensitise CD154 co-cultured CLL cells to chemotherapy in some, but not all cases, suggested to be due to variations in Mcl-1 expression, which is not inhibited by ABT-737 (355). AT-101 is a BH3-mimetic inhibitor that binds to all Bcl-2 family anti-apoptotic proteins with high affinity, and has entered clinical trials in CLL (454). In pre-clinical assessment, the pro-apoptotic effect of AT-101 was not influenced by CLL co-culture with M2-10B4 stromal cells (454). Although the effect of AT-101 on CLL cells co-cultured in the presence of CD154 and IL-4 has not been reported, this agent would be an attractive candidate for investigation as an agent that may overcome resistance to dasatinib, and other drugs, in the 154L/IL-4 system.

In contrast, more promising results were obtained in experiments assessing the combination of dasatinib and 17-DMAG on co-cultured CLL cells. Our observation that NT-L, and more so 154L/IL-4 co-culture increased HSP90 expression in CLL cells is extremely interesting as it provides a possible mechanistic explanation for the promotion of Akt and MAPK signalling, linked to stromal cell adhesion-mediated chemoresistance. Of interest, IL-6 and ERK signalling in multiple myeloma cells cultured with BM stromal cells has recently been demonstrated to up-regulate HSP90 expression at the RNA and protein levels (455). Moreover, 17-DMAG induced apoptosis of myeloma cells in co-culture with stromal cells (455). In the present study, while a degree of protection from apoptosis was observed in NT-L, and more so in 154L/IL-4 co-culture, 17-DMAG alone induced a degree of apoptosis of co-cultured CLL cells. Notably, apoptosis was potentiated in both co-culture systems by the addition of dasatinib. The observation that dasatinib treatment slightly reduced HSP90 protein expression (Fig. 5.14) is of interest as it is possible that this could contribute to the synergy observed between the two drugs. Further assessment of the effect of dasatinib on both HSP90 RNA and protein expression in a larger sample cohort would provide valuable information on the potential utility of this drug combination.

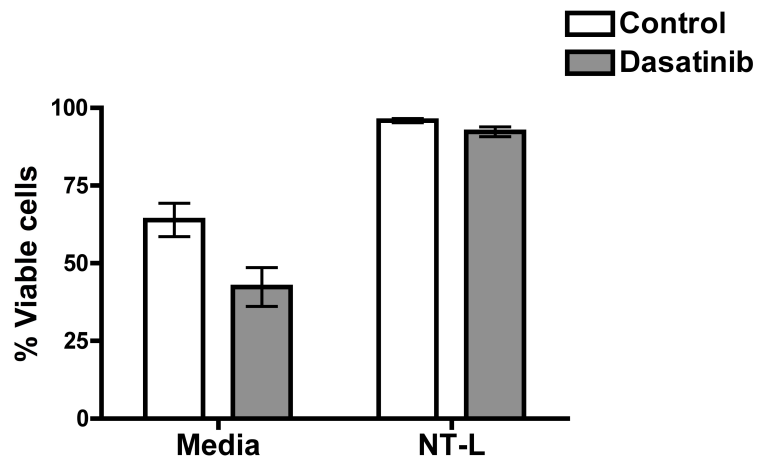
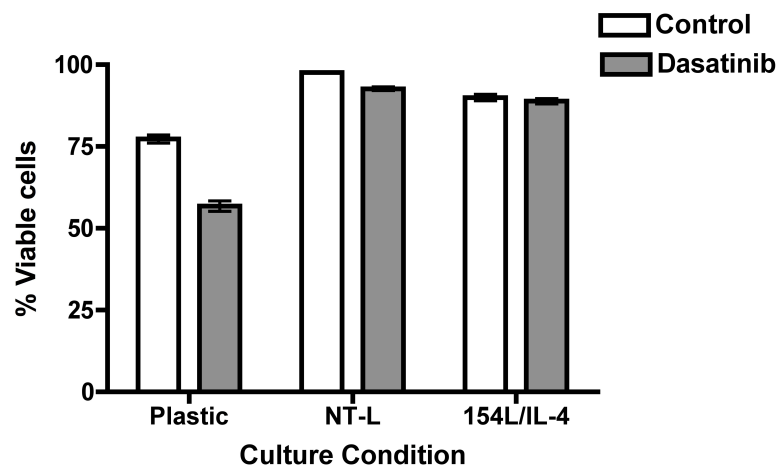
HSP90 inhibition using 17-AAG or 17-DMAG has been shown to result in inhibition of Akt phosphorylation in CLL cells (336), and degradation of a number of proteins including Akt, ZAP-70, the inhibitor of apoptosis protein XIAP, and the Bcl-2 protein Mcl-1 (332, 334, 335). In the present study, 17-DMAG-induced apoptosis

of CLL cells cultured in media alone was associated with inhibition of Mcl-1 and Bcl-x<sub>L</sub> protein levels, with little change in Bcl-2 expression. No change in Akt phosphorylation or total Akt protein level was seen in our experiments, however the 2 hr time point used in our experiments was shorter than that assessed in other studies. The effect of HSP90 inhibition on protein expression in CLL cells stimulated by CD154 and IL-4 has not been previously addressed. We demonstrated that 17-DMAG completely inhibited the up-regulation of Mcl-1 and Bcl-x<sub>L</sub> seen in untreated CLL cells following stimulation with sCD154 and IL-4, and induced a similar level of apoptosis as observed on treatment of unstimulated CLL cells. In sCD154/IL-4 stimulated cells, at 2 hr of treatment, 17-DMAG prevented the increase in p70 s6 kinase phosphorylation seen in control cells, however no effect was seen on Akt or MAPK phosphorylation or protein levels. As no significant activation of ERK was observed in untreated cells on sCD154/IL-4 stimulation, it is unlikely that ERK inhibition is responsible for the effects of 17-DMAG in this system. Although previous studies suggest that 17-DMAG may act primarily through inhibition of PI-3K/Akt signalling, further experiments assessing Akt and MAPK protein expression and phosphorylation over a longer time course are required to establish this.

As proteins involved in cell cycle regulation, including survivin and cdk4 are also HSP90 client proteins (330), it is tempting to speculate that CLL cell proliferation may also be inhibited by 17-DMAG. Notably, 17-DMAG treatment of mantle cell lymphoma cells results in down-regulation of cdk4 and c-myc, up-regulation of p21 and p27, and a G<sub>2</sub>/M cell cycle arrest (456). Furthermore, 17-DMAG inhibited proliferation of multiple myeloma cell lines in response to either endothelial cell contact or VEGF stimulation (457). Assessment of the effects of 17-DMAG, in the presence or absence of dasatinib, on CLL cells in the 154L/IL-4 proliferation assay would be of great interest, both to assess effects on proliferation and cell viability. If apoptosis were to be observed in these experiments, simultaneous assessment of CFSE fluorescence and markers of apoptosis such as Annexin V by FCM would allow determination of whether quiescent or proliferating cells were more sensitive to drug treatments.

In summary, the data presented in this chapter demonstrate that the pro-apoptotic effects of dasatinib as a single agent are abrogated by contact with stromal cells, in the presence or absence of IL-4. Although dasatinib sensitises CLL cells in stromal co-culture to conventional chemotherapeutic agents, cells additionally

stimulated by CD154 and IL-4 are highly resistant to established therapies. Dasatinib offers much as a novel therapeutic strategy for CLL, overcoming pro-survival signalling through the BCR, however given these data, dasatinib may be most effectively utilised in combination with agents that can overcome additional important antigen-independent signalling networks within the CLL microenvironment. The ability of targeted HSP90 inhibitors such as 17-DMAG to influence numerous signalling pathways that are conserved between several cell surface receptors, including antigen, cytokine, integrin, and chemokine receptors, make this class of agent an attractive candidate for further study on the effects on the CLL microenvironment. It is of interest that in multiple myeloma cell lines, in addition to anti-proliferative and pro-apoptotic effects, 17-DMAG also inhibited migration of cells toward both SDF-1 and VEGF (457). The synergy observed between dasatinib and 17-DMAG *in vitro*, which is retained in co-culture, demonstrates that this inhibitor combination has non-overlapping effects in CLL cells, and is worthy of further study.

**A****B**

**Figure 5.1 CLL cells co-cultured with stromal cells are significantly less sensitive to dasatinib**

CLL cells were incubated either in complete media alone, or co-cultured with irradiated NT-L cells overnight prior to treatment with dasatinib. Cells were then treated  $\pm$  100 nM dasatinib for 48 hr, following which apoptosis was assessed using Annexin V/Viaprobe staining by FCM. Each individual experiment was performed in triplicate. **A** Results are presented as the mean cell viability ( $\pm$  SEM) for cells treated in each condition (n=8). **B** CLL cells from one sample were cultured overnight in: media alone; NT-L co-culture, or; the 154L/IL-4 system. Cells were treated  $\pm$  100 nM dasatinib, in triplicate, for 48 hr. Apoptosis was assessed by Annexin V/Viaprobe staining by FCM, and the mean ( $\pm$  SEM) cell viabilities of cells treated as described shown.

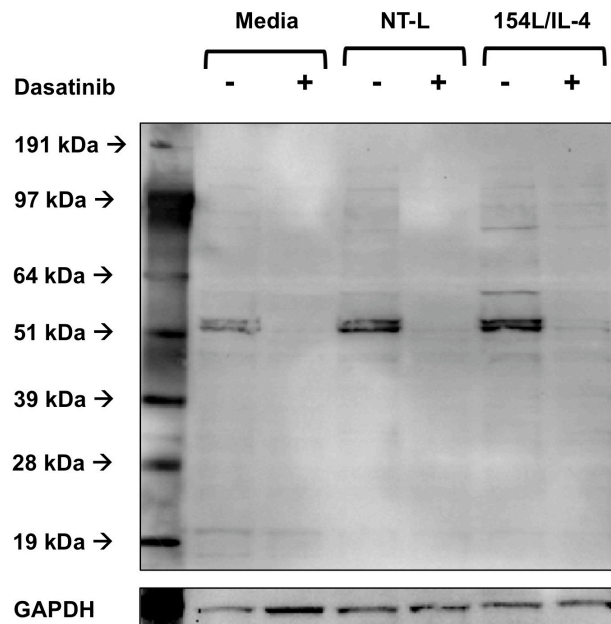


**Figure 5.2 Dasatinib retains the ability to inhibit tyrosine phosphorylation in CLL cells in NT-L or 154L/IL-4 co-culture**

CLL cells ( $2 \times 10^6$  per well) were cultured overnight in media alone, or in co-culture with NT-L cells, or in the 154L/IL-4 system prior to the experiment. Cells were then treated  $\pm$  100 nM dasatinib for 2 hr, then protein lysates prepared. Western blotting was performed with the 4G10 anti-phosphotyrosine antibody, and GAPDH assessed as a protein loading control. Molecular weights of the protein standards used are indicated.

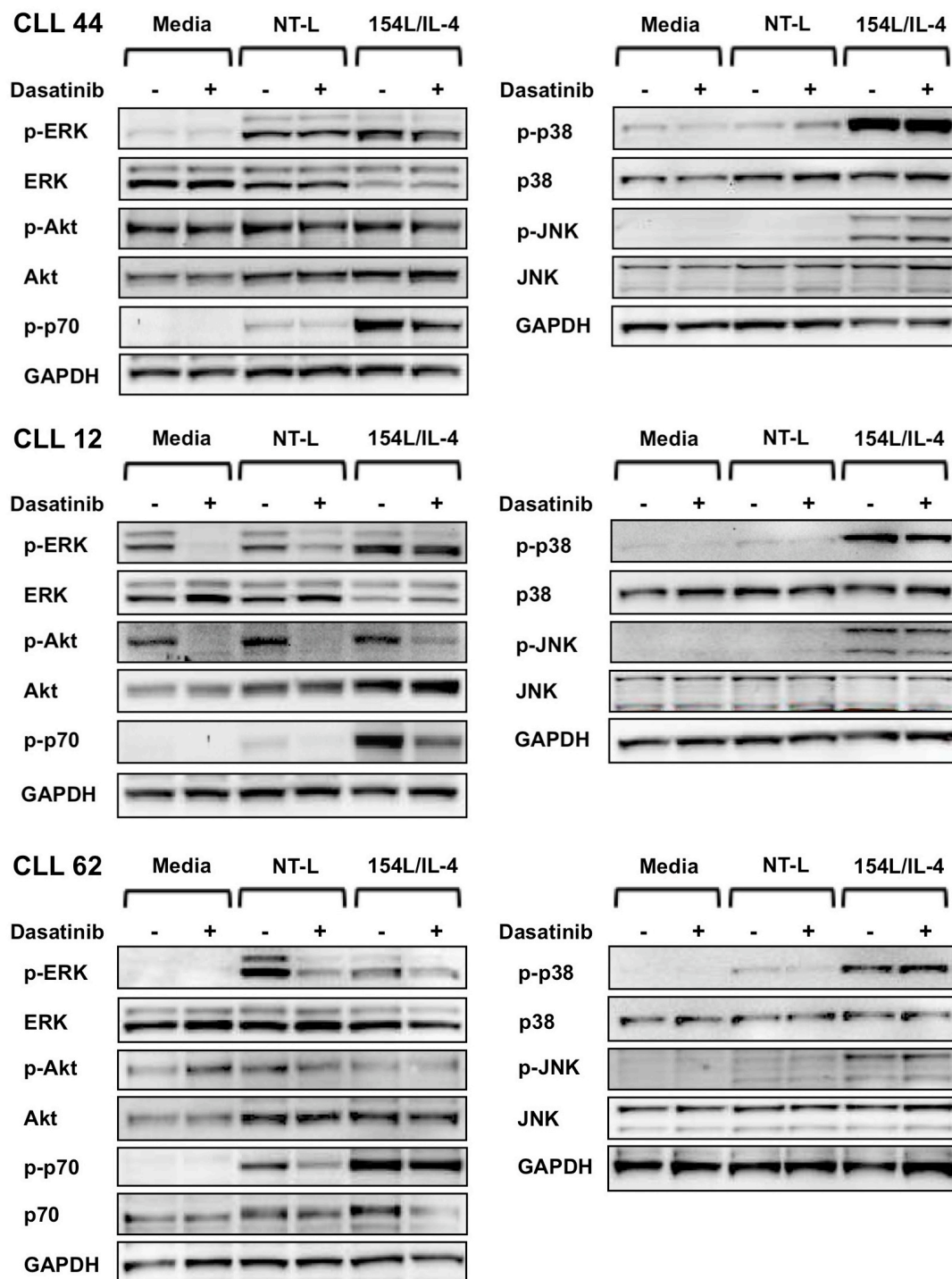


**Figure 5.3 NT-L and 154L/IL-4 co-culture induces activation of MAPK and Akt, which is not inhibited by dasatinib**

Cells ( $2 \times 10^6$ ) were cultured overnight in: complete media alone; NT-L co-culture, or; CD154/IL-4 co-culture. Cells were then treated with or without 100 nM dasatinib for 2 hr, and protein lysates prepared. Immunoblotting was performed with antibodies specific for phosphorylated and total Akt, p70 s6 kinase, ERK, p38, and JNK, with GAPDH included as a loading control. Five individual patient samples were assessed, and representative immunoblots from three patients are shown.

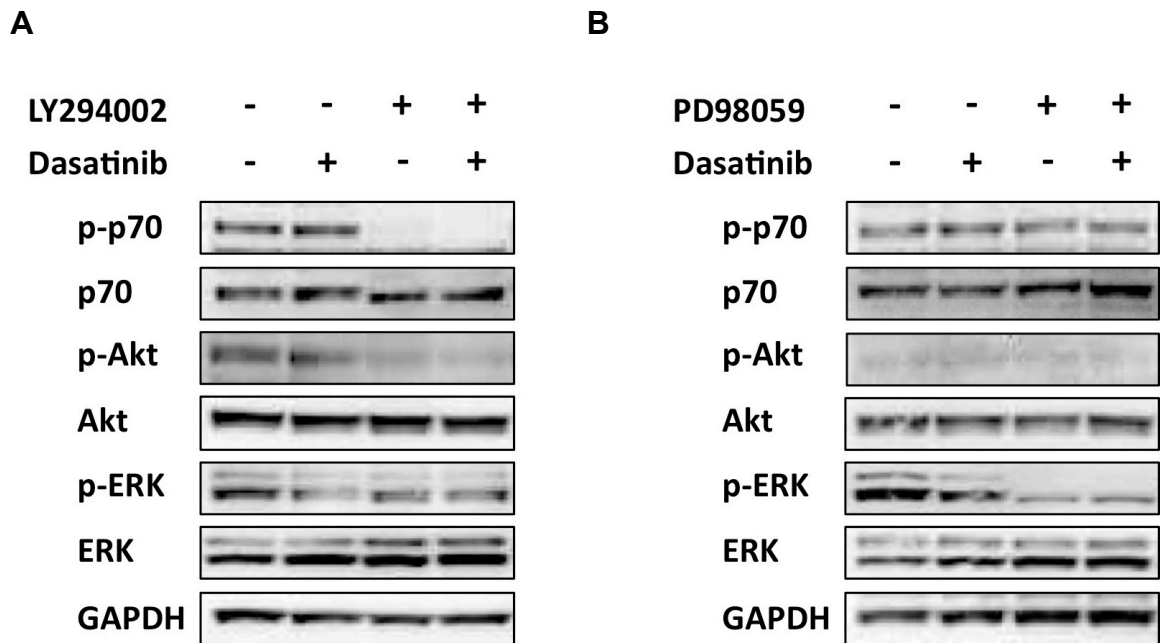
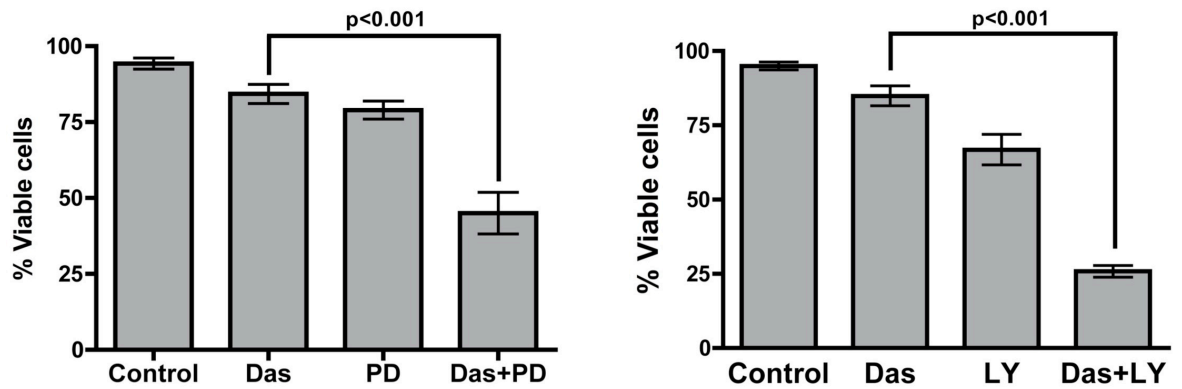


**Figure 5.4 PD98059 and LY294002 specifically inhibit ERK and Akt phosphorylation respectively in co-cultured CLL cells**

CLL cells ( $3 \times 10^6$ /ml) were co-cultured overnight in the CD154L/IL-4 system prior to treatment. **A** Cells were subsequently treated with either DMSO vehicle control, 10  $\mu$ M LY294002, 100 nM dasatinib, or both LY294002 and dasatinib for 2 hr ( $n=2$ ). **B** Cells were treated with either DMSO vehicle control, 40  $\mu$ M PD98059, 100 nM dasatinib, or both PD98059 and dasatinib for 2 hr ( $n=2$ ). At the end of experiments, protein lysates were prepared, and phosphorylation of Akt, p70 s6 kinase, and ERK assessed by western blotting. Immunoblots from one experiment are shown.

### A NT-L co-culture



### B 154L/IL-4 co-culture

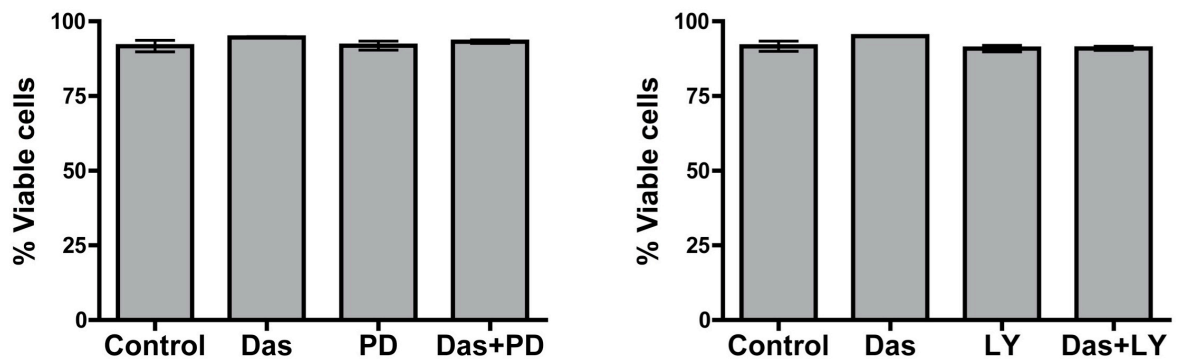


**Figure 5.5 PD98059 and LY294002 resensitise CLL cells to dasatinib in NT-L, but not 154L/IL-4 co-culture**

**A** CLL cells were co-cultured with NT-L cells overnight prior to treatments. Cells were then treated with 100 nM dasatinib (Das), 10  $\mu$ M LY294002 (LY) or 40  $\mu$ M PD98059 (PD), both Das and LY or PD, or DMSO vehicle control for 48 hr. Apoptosis was assessed by Annexin V/Viaprobe by FCM. The histogram plots show the mean ( $\pm$  SEM) viabilities of cells treated as described (n=5). **B** CLL cells were co-cultured in the CD154/IL-4 system overnight prior to treatment with inhibitors as described in A. The histograms show the mean ( $\pm$  SEM) viability of cells treated as indicated (n=3).

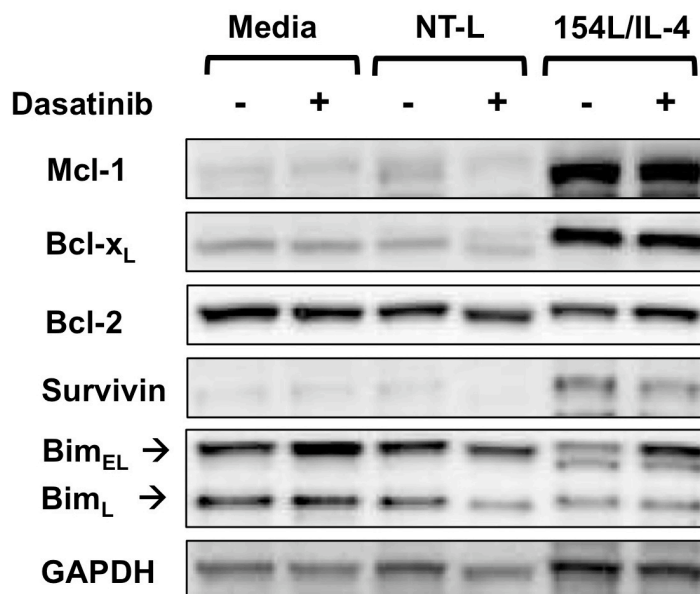


**Figure 5.6A Effects of dasatinib on Bcl-2 family protein and survivin expression in CLL cells cultured in media alone, or NT-L or 154L/IL-4 co-culture**

CLL cells ( $2 \times 10^6$ /well) were cultured overnight in media alone, in NT-L, or 154L/IL-4 co-culture prior to treatment. Cells were then treated with and without 100 nM dasatinib for 48 hr, and protein lysates prepared. Immunoblotting was performed to assess the expression of Bcl-2, Mcl-1, Bcl-x<sub>L</sub>, Bim, and survivin, using GAPDH as a protein loading control (n=5). A representative immunoblot from one experiment is shown.

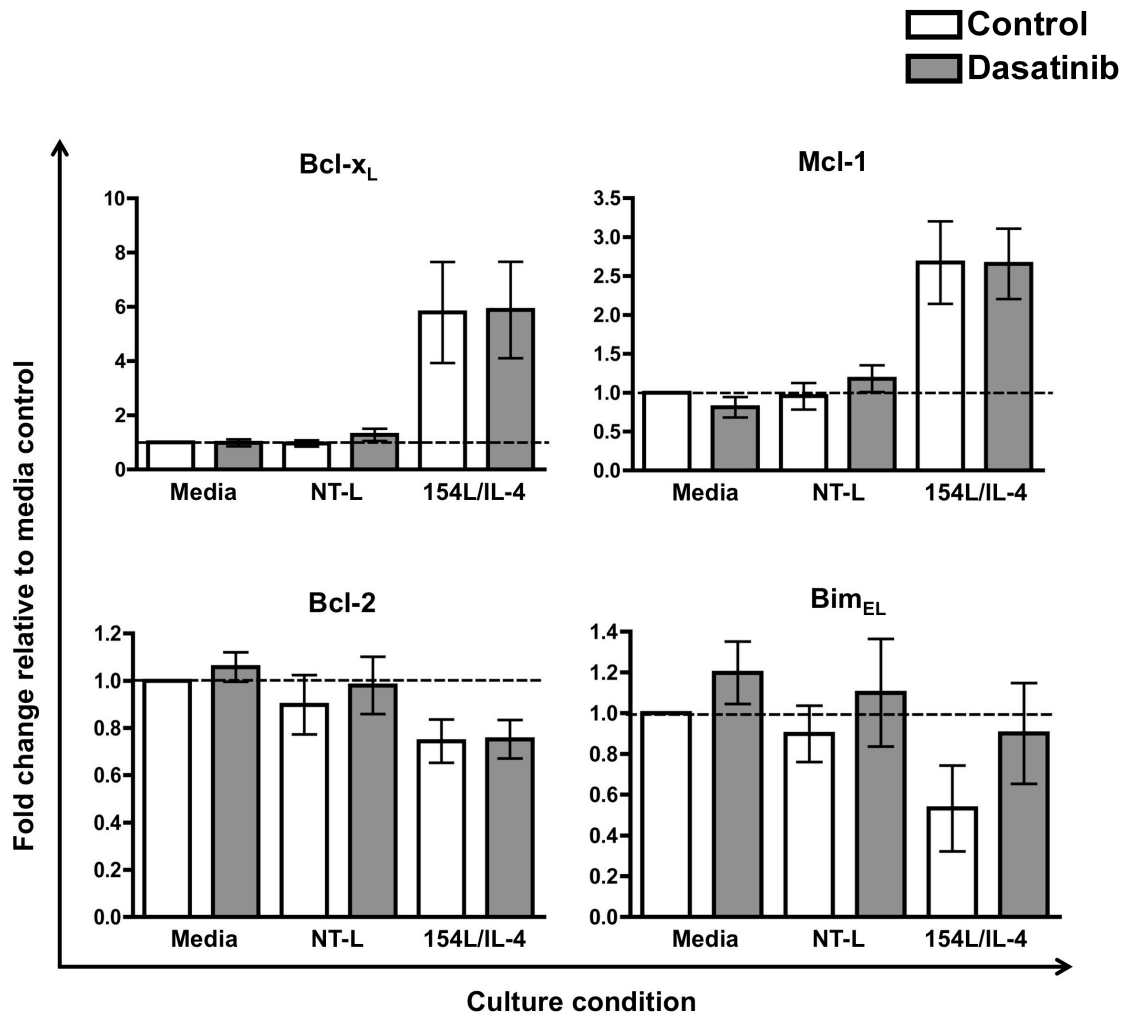
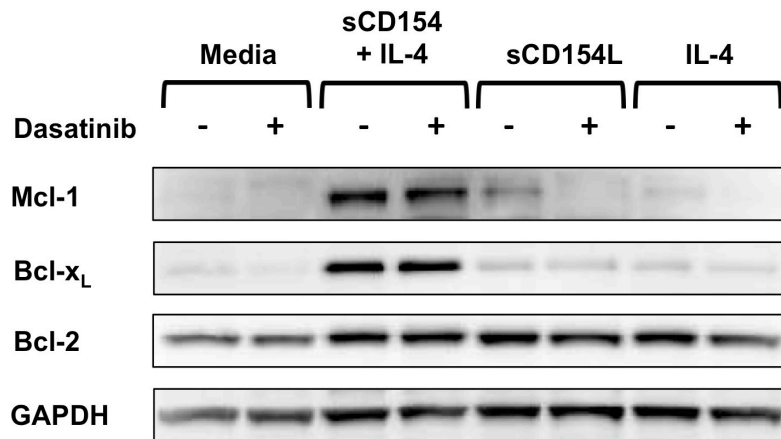


**Figure 5.6B Densitometric analysis of Bcl-2 family protein expression in CLL cells cultured in media alone, NT-L, and 154L/IL-4 co-culture in the presence or absence of dasatinib**

Densitometry was performed to quantitate the change in expression of Bcl-2 family proteins in each experimental condition, relative to expression in untreated control cells cultured in media alone. The histogram plots show the mean ( $\pm$  SEM) fold-change in protein expression (n=5).

**A**



**B**

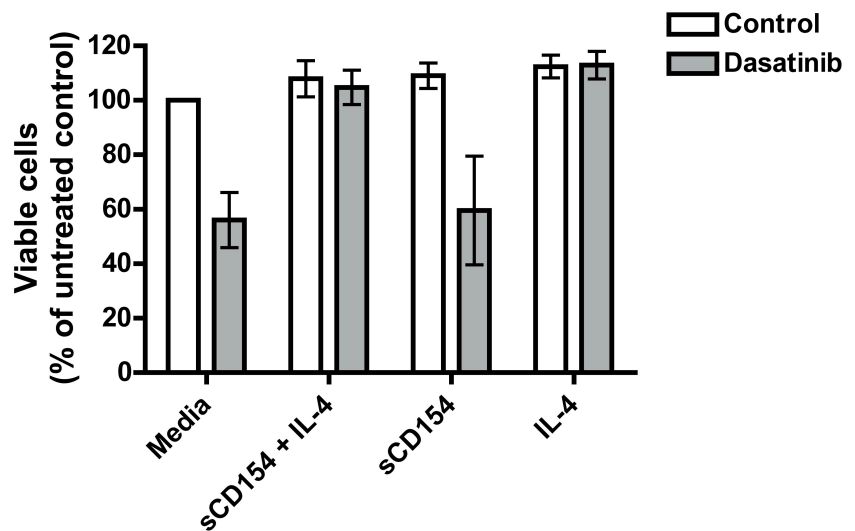


**Figure 5.7 Effect of dasatinib on Bcl-2 family protein expression induced by sCD154 and IL-4, alone and in combination**

CLL cells ( $2 \times 10^6$ /well) were treated  $\pm$  100 nM dasatinib for 30 min, followed by the addition of 100 ng/ml sCD154, 10 ng/ml IL-4, or both sCD154 and IL-4 for 48 hr ( $n=3$ ). At the end of experiments, apoptosis was assessed by Annexin V/Viaprobe staining by FCM, and protein lysates prepared. **A** Western blotting was performed to assess expression of Bcl-2, Mcl-1, Bcl-x<sub>L</sub>, and GAPDH, and a representative immunoblot shown. **B** The histogram plots show the mean ( $\pm$  SEM) viabilities of cells treated as indicated in all three experiments.

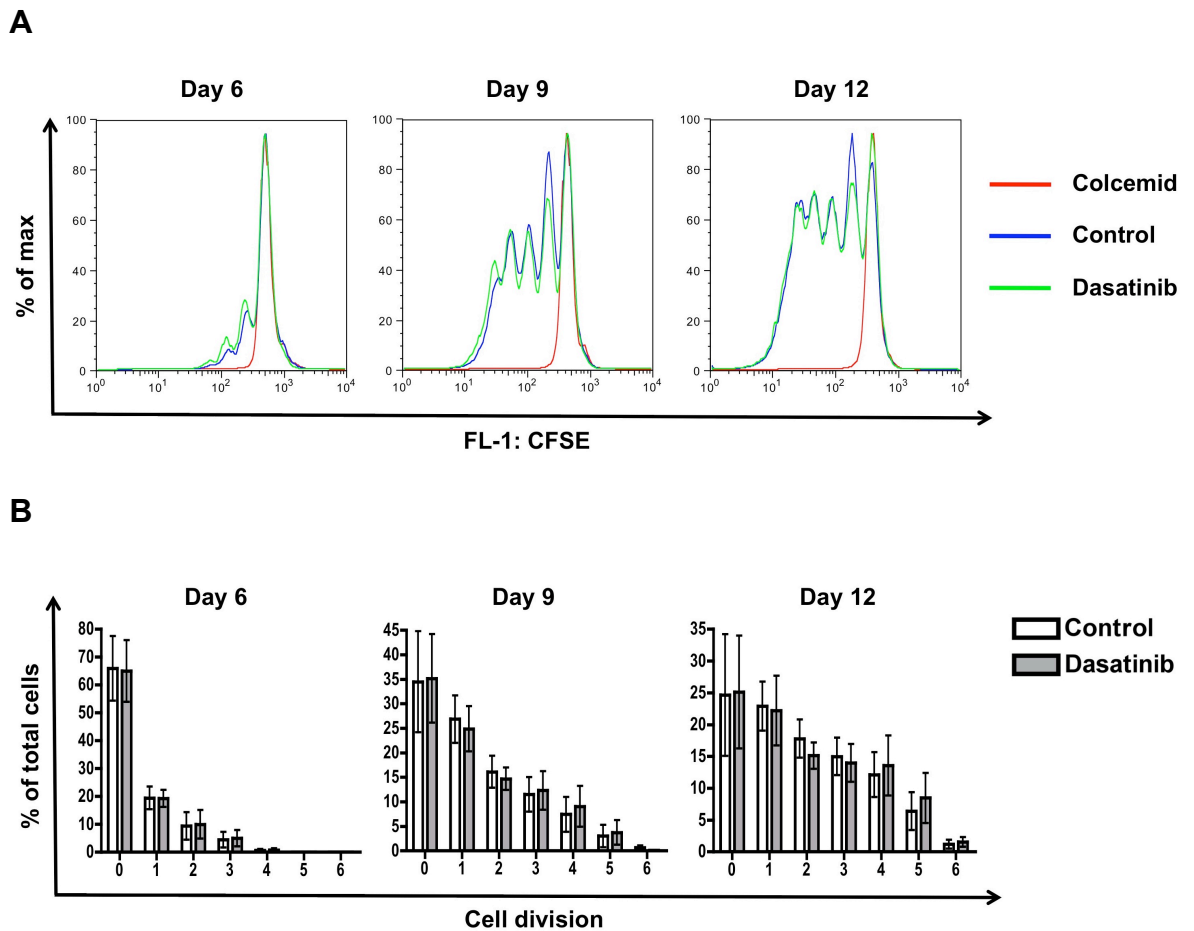
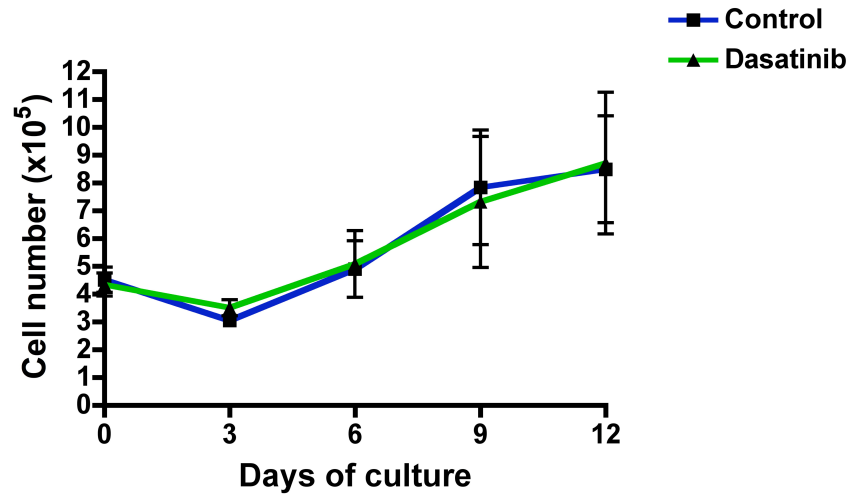


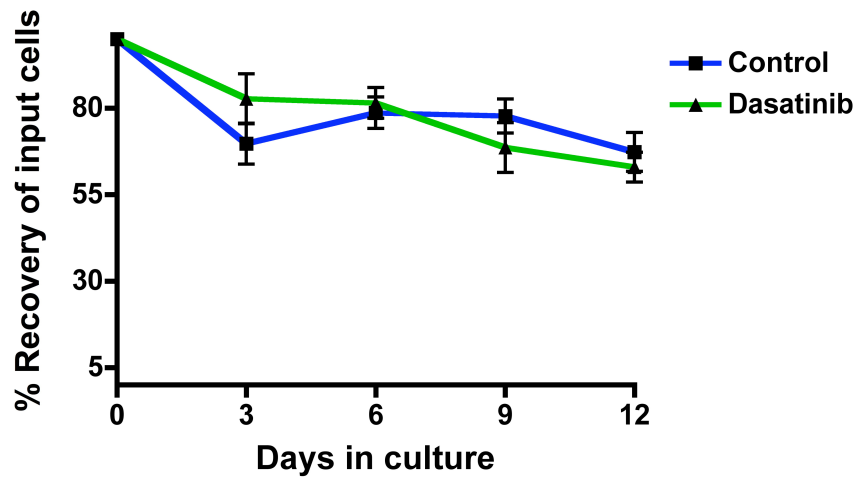
**Figure 5.8 Effect of dasatinib on CLL cell proliferation in the 154L/IL-4 system**

CLL cells were stained with CFSE and cultured with or without 100 nM dasatinib in the 12-day 154L/IL-4 co-culture system, as described in Section 2.2.9 ( $n=6$ ). FCM analysis was performed every 3 days as described in Section 2.3.9. **A** Day 6, 9, and 12 FACS histogram plots from one experiment are shown, gated on FSC/SSC and CD19 expression. The histogram of the colcemid control is shown in red, the untreated control sample in blue, and the dasatinib treated sample in green. **B** The histogram plots show the mean ( $\pm$  SEM) percentage of cells within each cell division at day 6, 9, and 12, calculated as described in Section 2.3.9.2, from analysis of all experiments ( $n=6$ ).

**A**

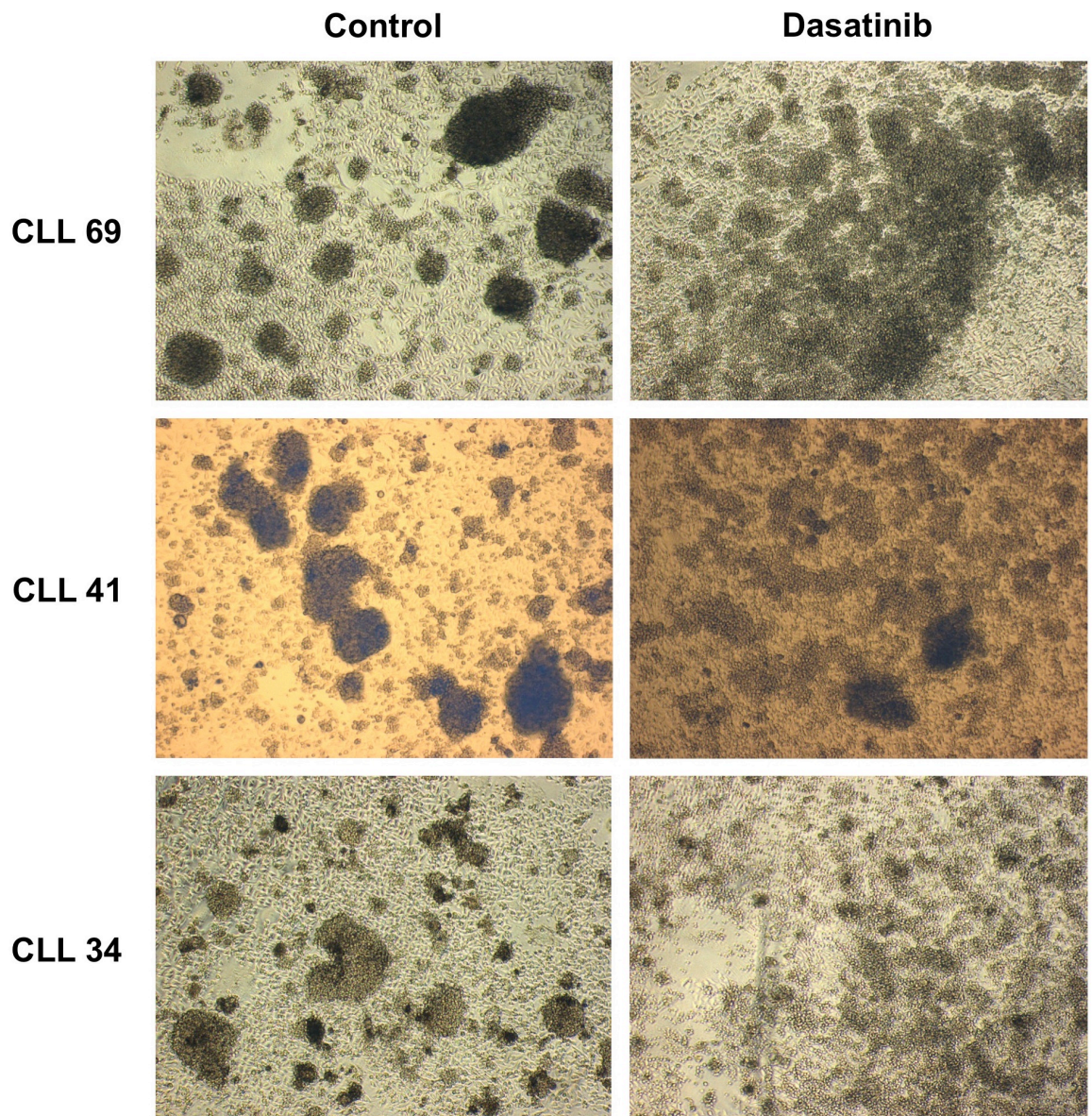


**B**



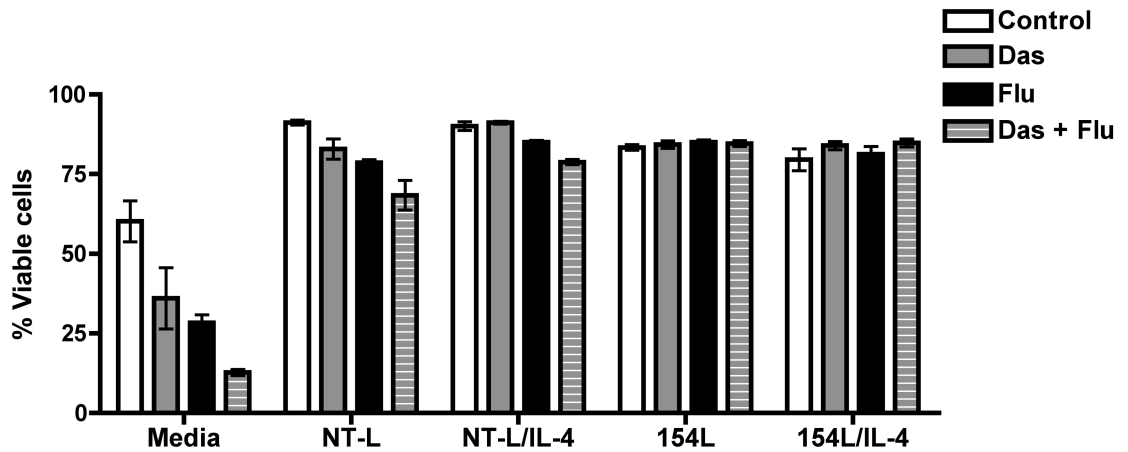
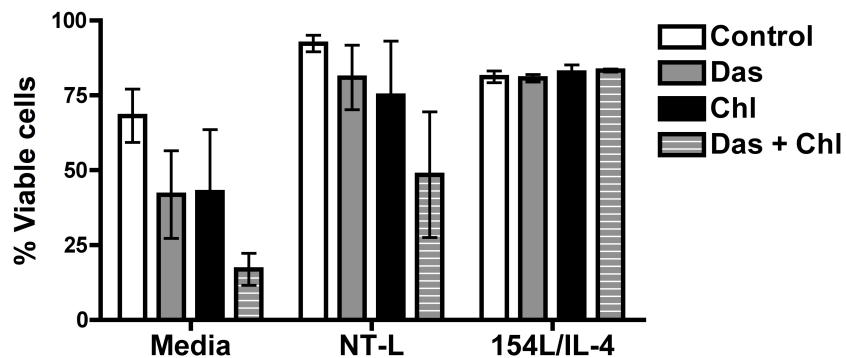
**Figure 5.9 Assessment of cell counts and percentage recovery of input cells in the 12 day 154L/IL-4 co-culture proliferation experiment.**

**A** At each time point, untreated and dasatinib-treated cells were counted by FCM, as described in Section 2.3.9.1. The graph depicts the mean ( $\pm$  SEM) cell counts determined in all experiments ( $n=6$ ). **B** The graph shows the mean ( $\pm$  SEM) percentage recovery of input cells, as described in Section 2.3.9.3, for all six experiments.



**Figure 5.10 Photographs of CLL cells following 12 days of co-culture in the 154L/IL-4 system with or without 100 nM dasatinib**

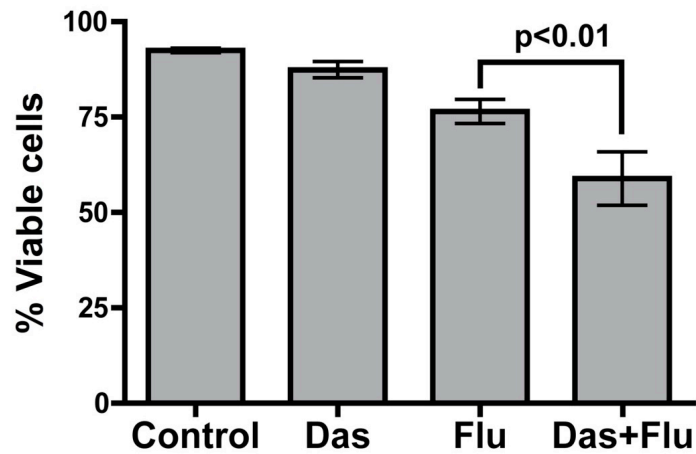
The photographs (4 x magnification) show representative images demonstrating the morphology of CLL cells at day 12 of 154L/IL-4 co-culture, in the presence or absence of dasatinib, in three representative patient samples.

**A****B**

**Figure 5.11 Comparison of the effect of dasatinib in combination with fludarabine or chlorambucil on CLL cells cultured in media or stromal co-culture systems**

**A** CLL cells were cultured overnight in the following conditions: media alone; NT-L co-culture; NTL co-culture with 10 ng/ml IL-4 added to culture media; 154L co-culture, or; 154L/IL-4 co-culture. Cells were subsequently treated with DMSO vehicle control, 100 nM dasatinib (Das), 5  $\mu$ M fludarabine (Flu), or both dasatinib and fludarabine for 48 hr, then apoptosis assessed by Annexin V/Viaprobe staining by FCM. The histogram plot shows the mean ( $\pm$  SEM) cell viabilities for cells treated as indicated (n=3). **B** CLL cells were cultured overnight in: media alone; NT-L co-culture, or; the CD154L/IL-4 system, prior to treatment with DMSO vehicle control, 100 nM dasatinib, 12.5  $\mu$ M chlorambucil (Chl), or both dasatinib and chlorambucil for 48 hr. Apoptosis was assessed using Annexin V/Viaprobe staining, and results are expressed as the mean ( $\pm$  SEM) cell viabilities in three independent experiments.

**A**



**B**

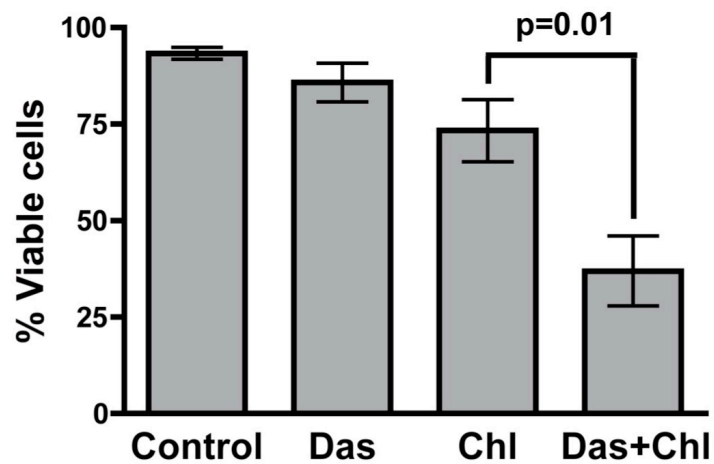


**Figure 5.12 Dasatinib retains the ability to sensitise CLL cells co-cultured with NT-L stromal cells to chlorambucil and fludarabine.**

CLL cells were co-cultured overnight with NT-L cells prior to treatment. **A** Cells were subsequently treated with DMSO vehicle control, 100 nM dasatinib (Das), 5  $\mu$ M fludarabine (Flu), or both Das and Flu for 48 hr, followed by assessment of apoptosis by Annexin V/Viaprobe staining. Data are presented as the mean ( $\pm$  SEM) viabilities of cells treated as indicated (n=7). **B** Cells were treated with DMSO vehicle control, 100 nM Das, 12.5  $\mu$ M chlorambucil (Chl), or both Das and Chl for 48 hr, followed by assessment of apoptosis by Annexin V/Viaprobe staining. Data are presented as the mean ( $\pm$  SEM) viabilities of cells treated as indicated (n=7).

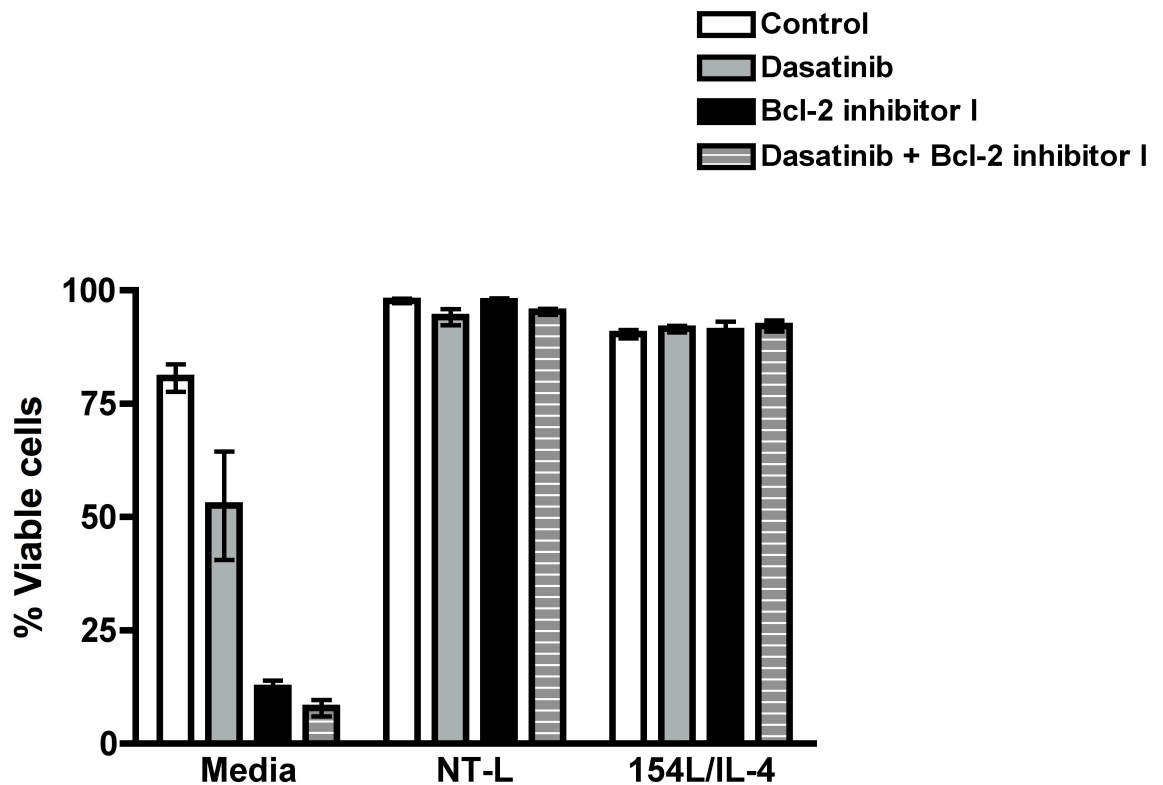
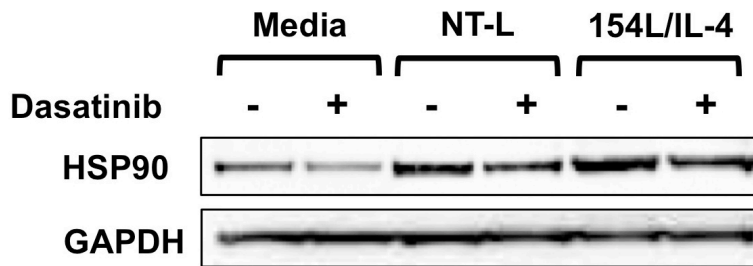


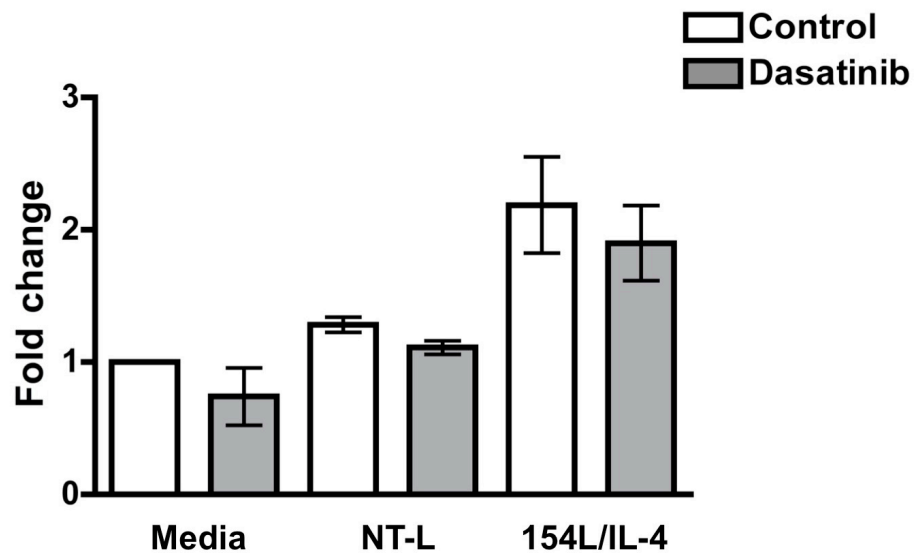
**Figure 5.13 Comparison of apoptosis induced by dasatinib in combination with Bcl-2 inhibitor I in CLL cells cultured in media alone or stromal co-culture.**

CLL cells were cultured overnight in media alone or in NT-L or 154L/IL-4 co-culture prior to treatment. Cells were subsequently treated with either: DMSO vehicle control; 100 nM dasatinib; 8  $\mu$ M Bcl-2 inhibitor I, or; both dasatinib and Bcl-2 inhibitor I for 48 hr, followed by assessment of apoptosis by Annexin V/Viaprobe staining by FCM. The histogram plots show the mean ( $\pm$  SEM) viabilities of cells treated as indicated (n=3).

**A**

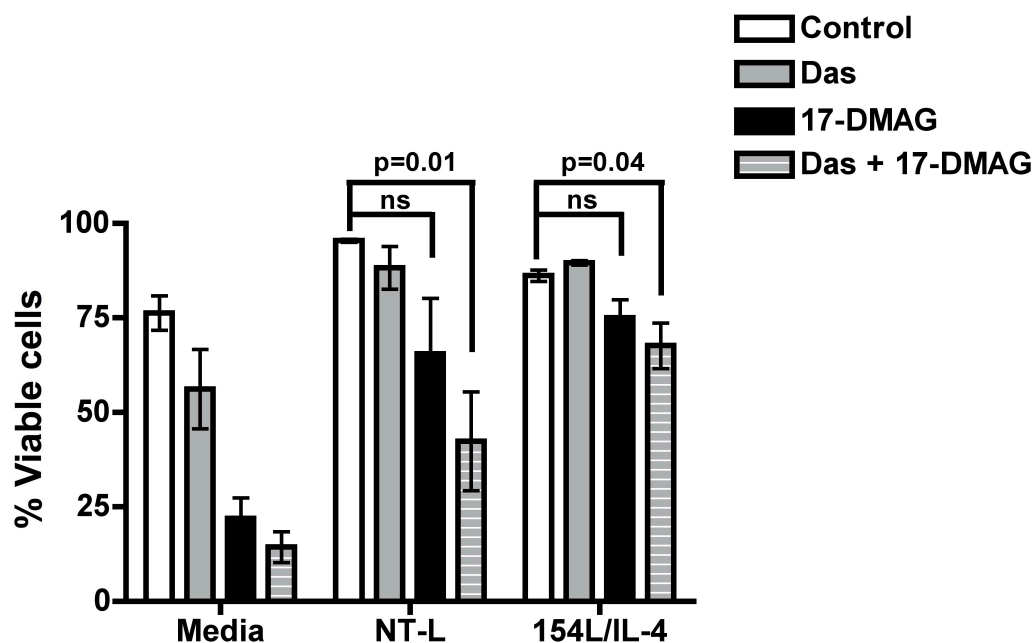


**B**



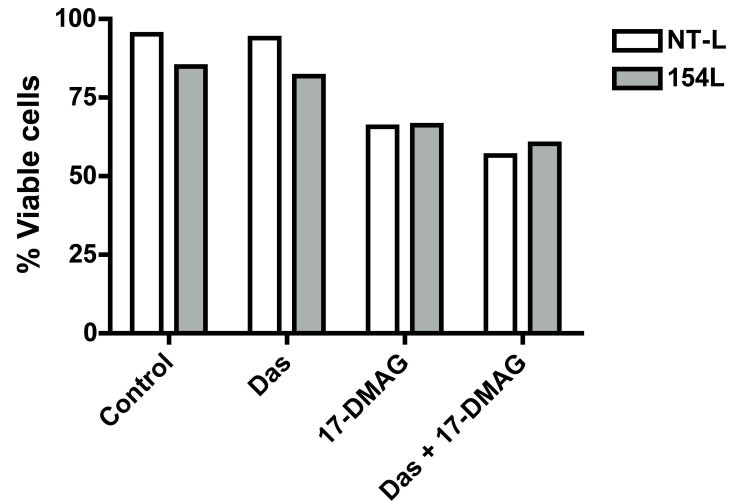
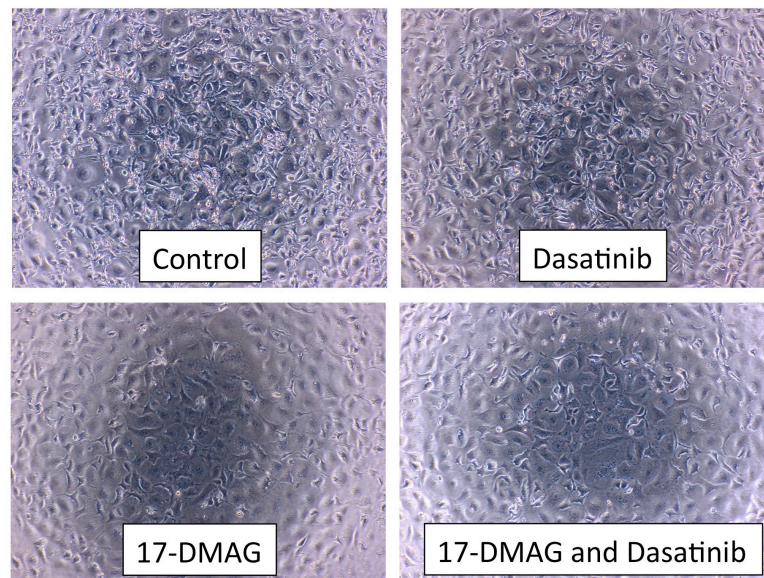
**Figure 5.14 HSP90 expression is increased in co-cultured CLL cells**

Immunoblots from experiments described in Figure 5.6, in which CLL cells in culture alone, or in NT-L, or 154L/IL-4 co-culture were treated in the presence or absence of 100 nM dasatinib for 48 hr were re-probed for expression of HSP90 (n=3). **A** One representative immunoblot is shown. **B** Densitometry was performed to quantitate HSP90 expression in each experimental condition in each experiment. Results are expressed as the mean ( $\pm$  SEM) fold-change in HSP90 expression in each condition relative to untreated cells cultured in media alone (n=3).



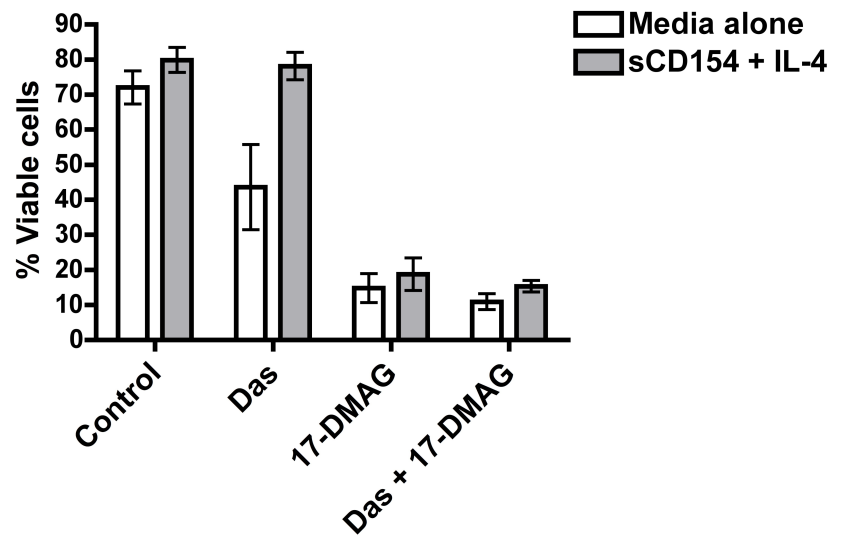
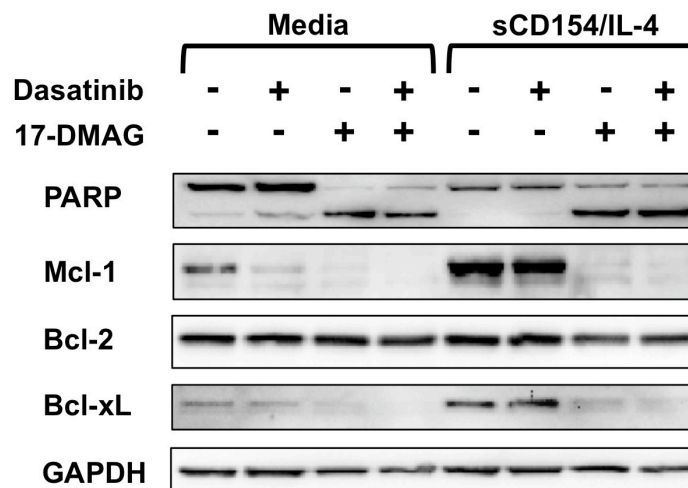
**Figure 5.15 Comparison of apoptosis induced by dasatinib and 17-DMAG in CLL cells cultured in media or stromal co-culture.**

CLL cells were cultured in media alone, or in NT-L or 154L/IL-4 co-culture overnight prior to treatment. Cells were then left untreated, or treated with 100 nM dasatinib (Das), 1  $\mu$ M 17-DMAG, or both dasatinib and 17-DMAG for 48 hr, then apoptosis assessed by Annexin V/Viaprobe staining by FCM. The histogram plots show the mean ( $\pm$  SEM) viabilities of cells treated as indicated (n=3).

**A****B**

**Figure 5.16 Effects of dasatinib and 17-DMAG on viability of NT-L and 154L cells**

Irradiated NT-L and CD154L stromal cells ( $1 \times 10^5$ ) were allowed to adhere to wells in a 24-well tissue culture plate overnight prior to treatment. Cells were then left untreated, or treated with 100 nM dasatinib, 1  $\mu$ M 17-DMAG, or both dasatinib and 17-DMAG for 48 hr. Cells were then photographed, removed from wells using trypsin, and apoptosis assessed by Annexin V/Viaprobe staining. **A** The histogram plots show the percentages of viable NT-L and CD154L stromal cells treated as indicated. **B** Photographs of CD154L cells treated as indicated (20 x magnification).

**A****B**

**Figure 5.17 Effect of dasatinib and 17-DMAG, alone and in combination, on CLL cells stimulated with sCD154 and IL-4**

CLL cells ( $3 \times 10^6/\text{ml}$ ) were either left untreated, or treated as follows: 100 nM dasatinib (Das); 1  $\mu\text{M}$  17-DMAG, or; both dasatinib and 17-DMAG. Following 30 min incubation, cells in each treatment arm were further treated with or without 100 ng/ml sCD154 and 10 ng/ml IL-4 for 48 hr. Apoptosis was assessed by Annexin V/Viaprobe staining, and protein lysates prepared. **A** The histogram plot shows the mean ( $\pm$  SEM) viabilities of cells treated as indicated ( $n=3$ ). **B** Immunoblotting was used to assess Bcl-2 family protein expression and PARP cleavage in treated cells ( $n=3$ ), and one representative immunoblot is shown.

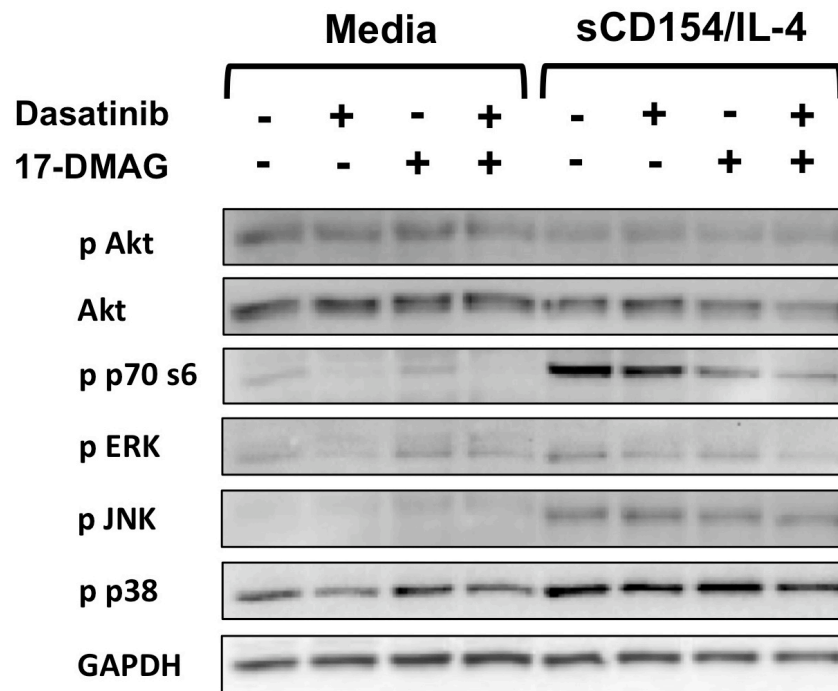


**Figure 5.18 17-DMAG selectively inhibits p70 s6 kinase phosphorylation in CLL cells following sCD154 and IL-4 stimulation**

CLL cells ( $3 \times 10^6$ /well) were either left untreated, or treated as follows: 100 nM dasatinib (Das); 1  $\mu$ M 17-DMAG, or; both Das and 17-DMAG. After 30 min incubation, cells in each treatment arm were further treated with or without 100 ng/ml sCD154 and 10 ng/ml IL-4 for 2 hr. Protein lysates were then prepared, western blotting performed used to assess phosphorylation of Akt, p70 s6 kinase, ERK, JNK, and p38, using GAPDH as a protein loading control. Total Akt was also assessed.

**Chapter 6:**  
**General Discussion**

## 6.1 Summary of results

The Src/c-Abl TKI dasatinib induced apoptosis of CLL cells *in vitro*, and exhibited synergy with established and novel therapeutic agents. The sensitivity of CLL cells to dasatinib correlated with the degree of inhibition of phosphorylation of Syk kinase, suggesting inhibition of tonic BCR signalling to account for its' anti-leukaemic effects. Dasatinib consistently inhibited BCR signalling following crosslinking of surface IgM, and inhibited the Mcl-1-dependent increase in survival on prolonged BCR stimulation. In addition, Src/c-Abl inhibition also inhibited Akt activation on CXCR4 stimulation, and impaired both chemotactic and pro-survival effects of SDF-1, demonstrating that the anti-leukaemic effects of dasatinib extend beyond direct effects on the BCR. Although dasatinib failed to inhibit additional survival signalling pathways induced by co-culture with stromal cells, the drug retained the ability to chemosensitise CLL cells to fludarabine and chlorambucil. Moreover, the combination of dasatinib and the HSP90 inhibitor 17-DMAG induced apoptosis of CLL cells co-cultured with stromal cells in the presence of CD154 and IL-4. In this chapter, the implications of these data for future pre-clinical investigation, and future clinical trials of Src/c-Abl TKI in CLL are discussed.

## 6.2 What could dasatinib add to current treatment algorithms in CLL?

The first clinical testing ground for novel therapies in any malignancy is in patients with advanced disease, who have exhausted established treatment modalities. In CLL, this is generally defined as patients refractory to purine analogue therapy (458). Therefore, the first question to address is whether dasatinib may benefit these patients, an issue which is currently being addressed in a number of phase I/II clinical trials (Table 6.1). Both studies of single-agent dasatinib, currently reported as abstracts (374, 459), have demonstrated a degree of clinical activity, in terms of reducing white cell counts and LN size. However only a minority of responding patients achieved the PR criteria as defined by the IWCLL (22). In view of the data suggesting that Syk and PLC $\gamma$  may serve as clinical biomarkers of response to dasatinib (Fig. 4.2 and (356)), incorporation of analysis of these proteins in patients treated with dasatinib in future clinical trials is warranted. As CLL cells with a high level of Syk expression, which we demonstrated to be less sensitive to dasatinib (Fig 4.4), have been shown to be more sensitive to Syk inhibitors *in vitro* (391), such patients may be best offered trials including clinical Syk inhibitors such as fostamatinib disodium (396). Our data suggest dasatinib may potentiate the clinical effects of both alkylating agents and purine analogues.

Whether dasatinib retains the ability to chemosensitise fludarabine-refractory CLL cells was not established in this study, however is an important clinical question for future study. Of note, a phase II trial assessing dasatinib in combination with fludarabine is ongoing (Table 6.1).

Looking to the future, it is important to consider whether dasatinib could add to initial therapy for CLL. The percentage of patients receiving chemo-immunotherapy as first-line treatment is set to increase. In practice, physically fit patients will receive FCR, whereas older patients with co-morbidities may be treated with combinations such as rituximab and chlorambucil, which demonstrated an increase in ORR and acceptable toxicity profile in a recent small phase II study (460). Whether dasatinib exhibits synergy with rituximab is currently unknown, however a phase I/II trial of dasatinib in combination with rituximab in the relapse setting is currently recruiting (Table 6.1). Although FCR has significantly improved the outcome of first-line treatment, CR is achieved by less than 50% of patients, with fewer MRD negative remissions (76). Given the survival benefit of achieving MRD-negativity, there is a rationale for considering more intensive combination strategies in selected patients. Combinations investigated to date include FCR in combination with either alemtuzumab (CFAR) or mitoxantrone (FCRM) (76). Both of these regimens increased MRD negative remission rates, but resulted in considerable toxicity. As significant neutropenia occurs in around a third of patients treated with single agent dasatinib (311), with FCR (76) the combination would likely result in significant BM suppression. As dasatinib induces a p53-independent mechanism of apoptosis, and preliminary investigations suggest CLL cells harbouring the 17p deletion are hypersensitive to dasatinib (365), the addition of dasatinib to FCR in patients with other high risk features (eg., unmutated CLL) could be a strategy to prevent selection of p53 mutated/deleted clones with therapy. Patients with 17p deletion or p53 mutation identified at diagnosis do not significantly benefit with FCR (76), and are currently treated with alemtuzumab, or high-dose methylprednisolone if the patient has bulky lymphadenopathy. As the ORR rate of alemtuzumab in this setting is only 40% (100), investigation of alemtuzumab combination therapies is also warranted. To date, two alemtuzumab combination trials in the relapse setting have been reported; the combination of alemtuzumab and fludarabine was effective (ORR 83%) and well tolerated, however a trial including alemtuzumab in combination with FC was terminated in view of excessive toxicity with this regimen (76). As

CD52 is also expressed on T lymphocytes, alemtuzumab causes significant T lymphocyte depletion, which has led to the inclusion of alemtuzumab in BM transplantation protocols as a strategy to reduce graft-versus host disease (461). The combination of agents such as dasatinib that inhibit BCR signalling, and alemtuzumab, which will reduce T cell support of CLL cells, may be considered a rational combination to assess in future clinical trials.

The improved PFS and OS observed in patients achieving an MRD negative remission has also led to interest in assessing consolidation therapy in patients who remain MRD positive at the end of standard chemotherapy (462).

Alemtuzumab consolidation following fludarabine-based chemotherapy has been reported to increase MRD negative CR rates and PFS (76), however significant infective toxicity was reported when alemtuzumab consolidation was commenced prior to three months from the end of chemotherapy (463). Failure to eradicate MRD in CLL is considered to be due to the failure to eradicate a proportion of the clone residing within supportive BM and LN stromal or PC microenvironments with chemotherapy (216), a hypothesis supported by our assessment of fludarabine and chlorambucil in 154L/IL-4 co-culture (Fig. 5.11). Novel therapeutic agents that disrupt microenvironmental pro-survival signalling pathways are rational drugs for investigation as consolidation therapy for patients remaining MRD positive following chemotherapy. Our co-culture data suggest that dasatinib monotherapy in this setting is unlikely to eradicate MRD, however the observation that dasatinib potentiated the pro-apoptotic effect of 17-DMAG in 154L/IL-4 co-culture (Fig. 5.14), demonstrates that further investigation of Src/c-Abl TKIs in combination approaches for this indication is justified.

### **6.3 Is there a potential role for dasatinib as maintenance therapy for CLL?**

Regardless of the quality of remission achieved with therapy, the majority of CLL patients still eventually relapse, and many become refractory to standard therapy (458). Prevention of relapse is therefore desirable, however a lack of suitable agents for maintenance therapy has limited this approach. IFN $\alpha$ , which was the first reported maintenance therapy trialled in CLL, during the 1990s, demonstrated no improvement in PFS or OS on long-term follow-up (464). During the last decade, studies demonstrating a significant increase in PFS with rituximab maintenance therapy in follicular lymphoma reignited interest in maintenance treatment of CLL (465). Although initial studies of rituximab maintenance administered at six-monthly intervals in CLL were disappointing (465), an increase

in PFS was reported with a more intense monthly rituximab maintenance strategy, specifically administered to patients remaining MRD positive following fludarabine (466). Similar results have been reported with monthly maintenance alemtuzumab in this setting (467).

As outlined in Section 1.4, a current model of CLL biology suggests that disease progression is governed by the ability of malignant cells to respond to antigenic stimulation through the BCR, although the culprit antigens remain to be fully characterised (145). According to this model, continuous inhibition of BCR signalling could reduce the rate of CLL cell proliferation, and hence the probability of clonal evolution and likelihood of relapse. As dasatinib consistently inhibited BCR signal transduction in CLL cells following crosslinking of the BCR, the most pertinent outstanding question is perhaps whether all, or indeed any, progressive CLL clones continue to depend on antigenic stimulation for proliferation. An alternative view of CLL progression suggests that, although BCR signalling is undoubtedly involved in the pathogenesis of CLL, once the malignant clone is established, proliferation may be primarily driven by BCR-independent stimuli including IL-4, CD154, VEGF, or BAFF (189). That *in vitro* CLL cell proliferation can be induced by IL-4 and CD154 in the absence of antigenic stimulation is in support of this hypothesis. As the contribution of ongoing BCR stimulation to CLL progression remains to be fully determined, it would seem reasonable to consider formally assessing dasatinib maintenance therapy in the context of a clinical trial in selected patients, for example, those with adverse prognostic features who remain MRD positive following chemotherapy.

#### **6.4 Novel therapeutic agents with the potential to target the leukaemic microenvironment in CLL**

The full array of the investigational agents targeting microenvironmental pro-survival signalling pathways in CLL that are in pre-clinical or early clinical testing is too broad to discuss in detail here (reviewed in (301)). Below, agents that are of particular interest for future study in combination with dasatinib are discussed.

In recent years, lenalidomide, an analogue of thalidomide, has been investigated as a novel therapeutic agent in CLL. Initially investigated in multiple myeloma as an anti-angiogenic agent, lenalidomide has now been ascribed numerous potential modes of action, including cytokine and immune modulation (468). Lenalidomide has been demonstrated to positively regulate both CD4<sup>+</sup> and CD8<sup>+</sup> T lymphocyte

activation, increase expression of CD154 on T cells, and promote T cell proliferation following TCR stimulation (468). Although these actions may seem detrimental for a CLL therapy in view of the established supportive role of CD4<sup>+</sup> T lymphocytes in CLL pathogenesis, lenalidomide also reversed the defect in immune synapse formation between CLL cells and autologous CD4<sup>+</sup> and CD8<sup>+</sup> T cells, both *in vitro*, and also *in vivo* in CLL patients (275). Lenalidomide itself does not induce apoptosis of CLL cells *in vitro*, rather the drug induces an activated B cell phenotype in CLL cells, increasing their expression of CD40 and CD86 (469). Moreover, lenalidomide up-regulated CLL cell expression of CD154, and increased the efficacy of CLL cells to co-stimulate normal B cells to produce antibodies, including CLL-directed antibodies, suggesting the drug may reverse the defective humoral immunity characteristic of CLL patients (470). Initial clinical trials of lenalidomide in CLL, using dosing schedules optimised in multiple myeloma (25 mg daily for 21 days of 28 day cycles), were complicated by frequent significant tumour lysis syndrome (TLS) and tumour flare reactions, the latter characterised by painful enlarged LN and bone pain (469, 471). The exact mechanism of tumour flare following lenalidomide remains under investigation, but has been proposed to occur as a result of B cell activation (469). Subsequent studies using lower dose continuous lenalidomide (starting dose 10 mg daily) demonstrated durable (over 12 month) clinical responses in heavily pre-treated mainly high-risk patients, with less severe tumour flare reactions (472). Furthermore, lenalidomide has recently been reported to achieve an ORR of 38% and CR rate of 19% in patients with relapsed CLL and either 11q or 17p deletion (473). A phase I/II trial of dasatinib in combination with lenalidomide has recently started recruiting (Table 6.1). Concurrent inhibition of dysregulated BCR signalling in CLL cells with dasatinib, and correction of the acquired immune defects characteristic of CLL with lenalidomide is an attractive therapeutic approach. However, a reasonable concern is that the inhibitory effects of dasatinib on BCR (as shown in CLL cells) and TCR signalling (372), may counteract the positive immunomodulatory effects of lenalidomide.

Another novel class of agent investigated over the last decade are cyclin-dependent kinase inhibitors (CDKI). The most extensively investigated agent is flavopiridol, an ATP-competitive inhibitor of CDK-1, -2, -4, -6, and -7 (474). Initial *in vitro* studies demonstrated flavopiridol to induce apoptosis of CLL cells through a p53-independent mechanism, and notably, apoptosis was not inhibited by IL-4

(475). The mechanism of toxicity to non-cycling CLL cells has been established to be due to transcriptional inhibition of anti-apoptotic proteins, particularly Mcl-1, which has a rapid turnover (474). This effect was mediated by inhibition of CDK7 and CDK9, which phosphorylate the C terminal domain of a subunit of RNA polymerase II (474). In a phase I study, flavopiridol achieved durable PR in 45% of refractory CLL patients. The notable side effects in this study were neutropenia (77%) and TLS (55%). Similar response rates have been reported in patients with 11q or 17p deletions and those without high-risk cytogenetic abnormalities (476). A number of additional CDKI are in development, including SNS-032, roscovitine, and the potent roscovitine analogue CR8 (477, 478). In addition to inhibition of anti-apoptotic proteins, this class of agent may inhibit CLL cell proliferation driven by microenvironmental interactions within the PC. Assessment of CDKI *in vitro* in the 154L/IL-4 system, in the presence or absence of dasatinib would be of great interest.

The HSP90 inhibitor 17-DMAG to induced apoptosis of CLL cells in the 154L/IL-4 system (Fig. 5.14), and exhibited synergy with dasatinib (Fig. 3.17). Very recently, three phase I clinical trials of 17-DMAG have been reported, notably one trial in AML (479-481). In two of these trials, including the AML study, 17-DMAG was administered twice weekly by intravenous infusion, and the maximum tolerated dose determined to be 21-24mg/m<sup>2</sup>. At this dosing schedule, the plasma C<sub>max</sub> was measured as 475-499 ng/ml between studies (0.8 μM), which is above the IC<sub>50</sub> in CLL cells determined in this study. In AML, of 17 patients mostly refractory to standard induction chemotherapy, four responded, three achieved CR with incomplete BM recovery (479). Using these schedules, toxicities included reversible renal dysfunction, peripheral neuropathy, fatigue, nausea, and musculoskeletal pain (479, 481). These side effects are largely non-overlapping with those of dasatinib, suggesting the combination may be clinically tolerated.

In addition to BCR signalling-related genes, genes related to NF-κB signalling are differentially expressed in unmutated as compared to mutated CLL (482).

Moreover, Rel A expression has been identified as an independent prognostic marker of survival in CLL (359). The novel NF-κB inhibitor LC-1 inhibited Rel A DNA-binding and induced apoptosis of CLL cells *in vitro* (483). In addition, LC-1 induced apoptosis was not inhibited by either CD154 or IL-4 stimulation (483). Given these data, and the importance of both BCR and NF-κB signalling to CLL

progression, LC-1 is another rational agent for future study in combination with dasatinib.

### **6.5 The potential for assessment of novel dasatinib combination therapies in mouse models of CLL .**

Although the *in vitro* co-culture model systems such as those used in this study likely reflect *in vivo* drug efficacy more closely than studies performed on CLL cells in media alone, they cannot completely substitute for preclinical assessment in animal models. In co-culture models, cell location is fixed, and the analysis of drug effects on purified CLL cells does not allow assessment of the effect of novel therapies on the complex signalling networks now known to involve the coordinated regulation of many cell types within the microenvironment, including T cells and monocytes. *In vivo* animal models are also required to assess drug pharmacokinetics, scheduling, and toxicity prior to clinical trial (484). In contrast to other leukaemias, murine xenograft models of CLL using primary cells have been very difficult to establish despite injection of high numbers of CLL cells into immuno-compromised mice, with the most promising reported model failing to sustain stable engraftment over a 12 week period (485).

A number of transgenic murine models have been developed, reviewed in (486), with the most extensively characterised of these being the Tcl-1 model, in which Tcl-1 is constitutively expressed in B cells under the control of an IgH E $\mu$  enhancer (487). These mice develop progressive accumulation of CD5<sup>+</sup> B lymphocytes in the peritoneum by 2 months, spleen by 3-5 months, and BM by 5-8 months (487). The BCRs used by Tcl-1 transgenic mice are predominantly unmutated, and of note, frequently have specificity for auto-antigens, suggesting this model is representative of aggressive CLL (488). Functional T cell abnormalities have also been described to associate with the lymphoproliferative disorder (489). The translational potential of this model was supported by the demonstration of a response to fludarabine treatment (490). Within our laboratory, a novel mouse model that bears many of the hallmarks of human CLL has been established (491). Following stable transfection of a dominant-negative PKC $\alpha$  (PKC $\alpha$ -KR) in haemopoietic progenitor cells enriched from foetal liver, and subsequent culture in B-cell co-culture systems, an outgrowth of cells with the surface phenotype of human CLL cells: CD19<sup>hi</sup>, CD5<sup>+</sup>, CD23<sup>+</sup>, IgM<sup>lo</sup>, was observed, associated with increased expression of Bcl-2 (491). Injection of these cells into RAG-1<sup>-/-</sup> mice resulted in progressive accumulation within lymphoreticular tissues. Moreover, on

*ex vivo* culture, the cells arrested in G<sub>0</sub>/G<sub>1</sub>, akin to human CLL cells (491). Although PKC $\alpha$  has not been implicated thus far in the pathogenesis of the human leukaemia, initial studies in our laboratory, in addition to a previous report, have noted low PKC $\alpha$  expression at the protein level in CLL cells (unpublished observations and (189)). Further studies are ongoing within our laboratory to further characterise this model, and develop its' translational potential. Future extension of this work would certainly involve assessment of novel drug combinations, determined on testing in our stromal co-culture systems, *in vivo* in the PKC $\alpha$ -KR model.

## **6.6 The future of targeted therapy in CLL**

The work presented here on the Src/Abl TKI dasatinib highlights many salient points relevant to the pursuit of any targeted therapy for CLL. First, the heterogeneity of CLL presents difficulties from the outset in establishing whether an identified dysregulated signalling protein has therapeutic potential. In this study, we have confirmed that tonic BCR signalling is a valid target for pharmacological intervention in CLL, however demonstrated that a varied therapeutic armoury is likely required to inhibit this pathway in individual patients, given the correlation observed between dasatinib sensitivity and Syk kinase expression and phosphorylation. Current evidence suggests that similar heterogeneity in regulatory protein expression exists in other key CLL signalling pathways, for example in RelA expression in the NF- $\kappa$ B pathway (359). Two broad strategies may be employed in future to determine which patients may benefit from novel targeted agents in CLL. Full molecular analysis of the signalling pathway to be targeted, using technology such as gene expression arrays, would provide detailed information, however is outwith the scope of a routine diagnostic laboratory. *In vitro* drug sensitivity screening assays may be performed against a range of novel agents, however studies to date have often shown a poor relationship between *in vitro* sensitivity and *in vivo* clinical response. It is therefore imperative that these issues are addressed within future clinical trial protocols, in order to validate potential clinical biomarkers.

Our studies also demonstrate the important point that a number of conserved signalling pathways, including the PI-3K/Akt and MAPK pathways, function to maintain CLL cell survival and direct proliferation. As these pathways are activated by many microenvironmental stimuli, targeted inhibition of individual proximal receptor signalling pathways may not impact significantly on the net

balance of pro-survival signalling induced in CLL cells by the microenvironment. Although we demonstrated dasatinib to exert direct effects on CXCR4 signalling in addition to BCR signal transduction, the drug was unable to inhibit PI-3K/Akt or MAPK signalling induced by other stromal factors, CD154 and IL-4. As the key microenvironmental interactions that support the survival and proliferation of CLL cells are more constant than the apparent heterogeneity in intrinsic signalling dysregulation that leads to CLL leukaemogenesis, inhibitors targeted toward the microenvironment may be effective across patient subgroups. In conclusion, the future success of targeted therapy in CLL will likely be in combination strategies, able to target both the CLL cells and microenvironmental signalling. Although our understanding of CLL biology has been transformed in the last decade, the challenge for the next remains to understand how to translate the biological information into improved outcomes for CLL patients.

## **6.7 Concluding remarks**

These data provide a comprehensive *in vitro* assessment of the anti-leukaemic effects of the Src/c-Abl TKI dasatinib on CLL cells *in vitro*. Further investigation of rational dasatinib drug combinations, in the co-culture model systems and our mouse model system will provide data which may form the basis for future clinical trials in CLL.

**Table 6.1 Current phase I/II clinical trials of dasatinib in relapsed/refractory CLL**

<b>Trial Number + Investigational Drugs</b>	<b>Phase</b>	<b>Dosing Schedule</b>	<b>Status</b>
NCT00829647 <b>Dasatinib + Lenalidomide</b>	I/II	Daily oral dasatinib (start at 70 mg) + Daily oral Lenalidomide (start at 2.5 mg)	Recruiting
NCT00949988 <b>Dasatinib + Rituximab</b>	I/II	Daily oral dasatinib (100-140 mg) + IV rituximab (375mg/m <sup>2</sup> cycle 1; 500 mg/m <sup>2</sup> cycle 2 onwards)  Up to six 28 day cycles	Recruiting
NCT01051115 <b>Dasatinib + Fludarabine</b>	II	Daily oral dasatinib (100 mg)  If less than partial response at day 28 oral fludarabine (40 mg/m <sup>2</sup> for 3 days every 28 days) will be added for up to six cycles	Recruiting
NCT00438854 <b>Dasatinib</b>	II	Daily oral dasatinib (dose not specified)	Closed
NCT00364286 <b>Dasatinib</b>	II	Daily oral dasatinib (50 mg twice daily)	Closed

\* Further details available at: <http://clinicaltrials.gov/>

## Bibliography

1. Janeway C, Murphy K, Travers P, Walport M. Janeway's Immunobiology (Seventh Edition). Seventh ed: Garland Science, Taylor and Francis Group; 2008.
2. Reth M. Antigen receptor tail clue. *Nature*. 1989;338(6214):383-4.
3. Niino H, Clark EA. Regulation of B-cell fate by antigen-receptor signals. *Nat Rev Immunol*. 2002;2(12):945-56.
4. Gauld SB, Merrell KT, Cambier JC. Silencing of autoreactive B cells by anergy: a fresh perspective. *Curr Opin Immunol*. 2006;18(3):292-7.
5. Allen CD, Okada T, Cyster JG. Germinal-center organization and cellular dynamics. *Immunity*. 2007;27(2):190-202.
6. Garside P, Ingulli E, Merica RR, Johnson JG, Noelle RJ, Jenkins MK. Visualization of specific B and T lymphocyte interactions in the lymph node. *Science*. 1998;281(5373):96-9.
7. Cyster JG, Ansel KM, Reif K, Ekland EH, Hyman PL, Tang HL, *et al*. Follicular stromal cells and lymphocyte homing to follicles. *Immunol Rev*. 2000;176:181-93.
8. Guzman-Rojas L, Sims-Mourtada JC, Rangel R, Martinez-Valdez H. Life and death within germinal centres: a double-edged sword. *Immunology*. 2002;107(2):167-75.
9. Allen CD, Ansel KM, Low C, Lesley R, Tamamura H, Fujii N, *et al*. Germinal center dark and light zone organization is mediated by CXCR4 and CXCR5. *Nat Immunol*. 2004;5(9):943-52.
10. Muramatsu M, Kinoshita K, Fagarasan S, Yamada S, Shinkai Y, Honjo T. Class switch recombination and hypermutation require activation-induced cytidine deaminase (AID), a potential RNA editing enzyme. *Cell*. 2000;102(5):553-63.
11. Di Noia JM, Neuberger MS. Molecular mechanisms of antibody somatic hypermutation. *Annu Rev Biochem*. 2007;76:1-22.
12. Wagner SD, Neuberger MS. Somatic hypermutation of immunoglobulin genes. *Annu Rev Immunol*. 1996;14:441-57.
13. Phan RT, Dalla-Favera R. The BCL6 proto-oncogene suppresses p53 expression in germinal-centre B cells. *Nature*. 2004;432(7017):635-9.
14. LeBien TW, Tedder TF. B lymphocytes: how they develop and function. *Blood*. 2008;112(5):1570-80.
15. Weiss LM, Warnke RA, Sklar J, Cleary ML. Molecular analysis of the t(14;18) chromosomal translocation in malignant lymphomas. *N Engl J Med*. 1987;317(19):1185-9.

16. Dyer MJ, Zani VJ, Lu WZ, O'Byrne A, Mould S, Chapman R, *et al.* BCL2 translocations in leukemias of mature B cells. *Blood*. 1994;83(12):3682-8.
17. Chiorazzi N, Rai KR, Ferrarini M. Chronic lymphocytic leukemia. *N Engl J Med*. 2005;352(8):804-15.
18. Rozman C, Montserrat E. Chronic lymphocytic leukemia. *N Engl J Med*. 1995;333(16):1052-7.
19. de Lima M, O'Brien S, Lerner S, Keating MJ. Chronic lymphocytic leukemia in the young patient. *Semin Oncol*. 1998;25(1):107-16.
20. Ghia P, Ferreri AM, Galigaris-Cappio F. Chronic lymphocytic leukemia. *Crit Rev Oncol Hematol*. 2007;64(3):234-46.
21. Houlston RS, Sellick G, Yuille M, Matutes E, Catovsky D. Causation of chronic lymphocytic leukemia--insights from familial disease. *Leuk Res*. 2003;27(10):871-6.
22. Hallek M, Cheson BD, Catovsky D, Caligaris-Cappio F, Dighiero G, Dohner H, *et al.* Guidelines for the diagnosis and treatment of chronic lymphocytic leukemia: a report from the International Workshop on Chronic Lymphocytic Leukemia (IWCLL) updating the National Cancer Institute-Working Group (NCI-WG) 1996 guidelines. *Blood*. 2008;111(12):5446-56.
23. Moreau EJ, Matutes E, A'Hern RP, Morilla AM, Morilla RM, Owusu-Ankomah KA, *et al.* Improvement of the chronic lymphocytic leukemia scoring system with the monoclonal antibody SN8 (CD79b). *Am J Clin Pathol*. 1997;108(4):378-82.
24. Rawstron AC, Green MJ, Kuzmicki A, Kennedy B, Fenton JA, Evans PA, *et al.* Monoclonal B lymphocytes with the characteristics of "indolent" chronic lymphocytic leukemia are present in 3.5% of adults with normal blood counts. *Blood*. 2002;100(2):635-9.
25. Marti GE, Rawstron AC, Ghia P, Hillmen P, Houlston RS, Kay N, *et al.* Diagnostic criteria for monoclonal B-cell lymphocytosis. *Br J Haematol*. 2005;130(3):325-32.
26. Shanafelt TD, Ghia P, Lanasa MC, Landgren O, Rawstron AC. Monoclonal B-cell lymphocytosis (MBL): biology, natural history and clinical management. *Leukemia*. 2010;24(3):512-20.
27. Fairley GH, Scott RB. Hypogammaglobulinaemia in chronic lymphatic leukaemia. *Br Med J*. 1961;2(5257):920-4.
28. Hamblin TJ, Oscier DG, Young BJ. Autoimmunity in chronic lymphocytic leukaemia. *J Clin Pathol*. 1986;39(7):713-6.
29. Dearden C. Disease-specific complications of chronic lymphocytic leukemia. *Hematology Am Soc Hematol Educ Program*. 2008:450-6.
30. Tsimberidou AM, Wen S, McLaughlin P, O'Brien S, Wierda WG, Lerner S, *et al.* Other malignancies in chronic lymphocytic leukemia/small lymphocytic lymphoma. *J Clin Oncol*. 2009;27(6):904-10.

31. Rai KR, Sawitsky A, Cronkite EP, Chanana AD, Levy RN, Pasternack BS. Clinical staging of chronic lymphocytic leukemia. *Blood*. 1975;46(2):219-34.
32. Binet JL, Auquier A, Dighiero G, Chastang C, Piguët H, Goasguen J, *et al.* A new prognostic classification of chronic lymphocytic leukemia derived from a multivariate survival analysis. *Cancer*. 1981;48(1):198-206.
33. Vinolas N, Reverter JC, Urbano-Ispizua A, Montserrat E, Rozman C. Lymphocyte doubling time in chronic lymphocytic leukemia: an update of its prognostic significance. *Blood Cells*. 1987;12(2):457-70.
34. Mauro FR, De Rossi G, Burgio VL, Caruso R, Giannarelli D, Monarca B, *et al.* Prognostic value of bone marrow histology in chronic lymphocytic leukemia. A study of 335 untreated cases from a single institution. *Haematologica*. 1994;79(4):334-41.
35. Fais F, Ghiotto F, Hashimoto S, Sellars B, Valetto A, Allen SL, *et al.* Chronic lymphocytic leukemia B cells express restricted sets of mutated and unmutated antigen receptors. *J Clin Invest*. 1998;102(8):1515-25.
36. Maloum K, Davi F, Merle-Beral H, Pritsch O, Magnac C, Vuillier F, *et al.* Expression of unmutated VH genes is a detrimental prognostic factor in chronic lymphocytic leukemia. *Blood*. 2000;96(1):377-9.
37. Damle RN, Wasil T, Fais F, Ghiotto F, Valetto A, Allen SL, *et al.* Ig V gene mutation status and CD38 expression as novel prognostic indicators in chronic lymphocytic leukemia. *Blood*. 1999;94(6):1840-7.
38. Hamblin TJ, Davis Z, Gardiner A, Oscier DG, Stevenson FK. Unmutated Ig V(H) genes are associated with a more aggressive form of chronic lymphocytic leukemia. *Blood*. 1999;94(6):1848-54.
39. Crespo M, Bosch F, Villamor N, Bellosillo B, Colomer D, Rozman M, *et al.* ZAP-70 expression as a surrogate for immunoglobulin-variable-region mutations in chronic lymphocytic leukemia. *N Engl J Med*. 2003;348(18):1764-75.
40. Wiestner A, Rosenwald A, Barry TS, Wright G, Davis RE, Henrikson SE, *et al.* ZAP-70 expression identifies a chronic lymphocytic leukemia subtype with unmutated immunoglobulin genes, inferior clinical outcome, and distinct gene expression profile. *Blood*. 2003;101(12):4944-51.
41. Au-Yeung BB, Deindl S, Hsu LY, Palacios EH, Levin SE, Kuriyan J, *et al.* The structure, regulation, and function of ZAP-70. *Immunol Rev*. 2009;228(1):41-57.
42. Schweighoffer E, Vanes L, Mathiot A, Nakamura T, Tybulewicz VL. Unexpected requirement for ZAP-70 in pre-B cell development and allelic exclusion. *Immunity*. 2003;18(4):523-33.
43. Nolz JC, Tschumper RC, Pittner BT, Darce JR, Kay NE, Jelinek DF. ZAP-70 is expressed by a subset of normal human B-lymphocytes displaying an activated phenotype. *Leukemia*. 2005;19(6):1018-24.

44. Shankey TV, Forman M, Scibelli P, Cobb J, Smith CM, Mills R, *et al.* An optimized whole blood method for flow cytometric measurement of ZAP-70 protein expression in chronic lymphocytic leukemia. *Cytometry B Clin Cytom.* 2006;70(4):259-69.
45. Chen YH, Peterson LC, Dittmann D, Evens A, Rosen S, Khoong A, *et al.* Comparative analysis of flow cytometric techniques in assessment of ZAP-70 expression in relation to IgVH mutational status in chronic lymphocytic leukemia. *Am J Clin Pathol.* 2007;127(2):182-91.
46. Rassenti LZ, Jain S, Keating MJ, Wierda WG, Grever MR, Byrd JC, *et al.* Relative value Of ZAP-70, CD38, and immunoglobulin mutation status in predicting aggressive disease in chronic lymphocytic leukemia. *Blood.* 2008 Jun;112(5):1923-30.
47. Hamblin TJ, Orchard JA, Gardiner A, Oscier DG, Davis Z, Stevenson FK. Immunoglobulin V genes and CD38 expression in CLL. *Blood.* 2000;95(7):2455-7.
48. Jelinek DF, Tschumper RC, Geyer SM, Bone ND, Dewald GW, Hanson CA, *et al.* Analysis of clonal B-cell CD38 and immunoglobulin variable region sequence status in relation to clinical outcome for B-chronic lymphocytic leukaemia. *Br J Haematol.* 2001;115(4):854-61.
49. Del Poeta G, Maurillo L, Venditti A, Buccisano F, Epiceno AM, Capelli G, *et al.* Clinical significance of CD38 expression in chronic lymphocytic leukemia. *Blood.* 2001;98(9):2633-9.
50. D'Arena G, Musto P, Cascavilla N, Dell'Olio M, Di Renzo N, Perla G, *et al.* CD38 expression correlates with adverse biological features and predicts poor clinical outcome in B-cell chronic lymphocytic leukemia. *Leuk Lymphoma.* 2001;42(1-2):109-14.
51. Morilla A, Gonzalez de Castro D, Del Giudice I, Osuji N, Else M, Morilla R, *et al.* Combinations of ZAP-70, CD38 and IGHV mutational status as predictors of time to first treatment in CLL. *Leuk Lymphoma.* 2008;49(11):2108-15.
52. Del Giudice I, Morilla A, Osuji N, Matutes E, Morilla R, Burford A, *et al.* Zeta-chain associated protein 70 and CD38 combined predict the time to first treatment in patients with chronic lymphocytic leukemia. *Cancer.* 2005;104(10):2124-32.
53. Juliusson G, Oscier DG, Fitchett M, Ross FM, Stockdill G, Mackie MJ, *et al.* Prognostic subgroups in B-cell chronic lymphocytic leukemia defined by specific chromosomal abnormalities. *N Engl J Med.* 1990;323(11):720-4.
54. Dohner H, Stilgenbauer S, Fischer K, Bentz M, Lichter P. Cytogenetic and molecular cytogenetic analysis of B cell chronic lymphocytic leukemia: specific chromosome aberrations identify prognostic subgroups of patients and point to loci of candidate genes. *Leukemia.* 1997;11 Suppl 2:S19-24.
55. Dohner H, Stilgenbauer S, Benner A, Leupolt E, Krober A, Bullinger L, *et al.* Genomic aberrations and survival in chronic lymphocytic leukemia. *N Engl J Med.* 2000;343(26):1910-6.

56. Calin GA, Dumitru CD, Shimizu M, Bichi R, Zupo S, Noch E, *et al.* Frequent deletions and down-regulation of micro- RNA genes miR15 and miR16 at 13q14 in chronic lymphocytic leukemia. *Proc Natl Acad Sci U S A.* 2002;99(24):15524-9.
57. Cimmino A, Calin GA, Fabbri M, Iorio MV, Ferracin M, Shimizu M, *et al.* miR-15 and miR-16 induce apoptosis by targeting BCL2. *Proc Natl Acad Sci U S A.* 2005;102(39):13944-9.
58. Klein U, Lia M, Crespo M, Siegel R, Shen Q, Mo T, *et al.* The DLEU2/miR-15a/16-1 Cluster Controls B Cell Proliferation and Its Deletion Leads to Chronic Lymphocytic Leukemia. *Cancer Cell.* 2010;17(1):28-40.
59. Rossi D, Cerri M, Deambrogi C, Sozzi E, Cresta S, Rasi S, *et al.* The prognostic value of TP53 mutations in chronic lymphocytic leukemia is independent of Del17p13: implications for overall survival and chemorefractoriness. *Clin Cancer Res.* 2009;15(3):995-1004.
60. Malcikova J, Smardova J, Rocnova L, Tichy B, Kuglik P, Vranova V, *et al.* Monoallelic and biallelic inactivation of TP53 gene in chronic lymphocytic leukemia: selection, impact on survival, and response to DNA damage. *Blood.* 2009;114(26):5307-14.
61. Dicker F, Herholz H, Schnittger S, Nakao A, Patten N, Wu L, *et al.* The detection of TP53 mutations in chronic lymphocytic leukemia independently predicts rapid disease progression and is highly correlated with a complex aberrant karyotype. *Leukemia.* 2009;23(1):117-24.
62. Eclache V, Caulet-Maugendre S, Poirel HA, Djemai M, Robert J, Lejeune F, *et al.* Cryptic deletion involving the ATM locus at 11q22.3 approximately q23.1 in B-cell chronic lymphocytic leukemia and related disorders. *Cancer Genet Cytogenet.* 2004;152(1):72-6.
63. Zenz T, Mohr J, Edelmann J, Sarno A, Hoth P, Heuberger M, *et al.* Treatment resistance in chronic lymphocytic leukemia: the role of the p53 pathway. *Leuk Lymphoma.* 2009;50(3):510-3.
64. Stankovic T, Weber P, Stewart G, Bedenham T, Murray J, Byrd PJ, *et al.* Inactivation of ataxia telangiectasia mutated gene in B-cell chronic lymphocytic leukaemia. *Lancet.* 1999;353(9146):26-9.
65. Dohner H, Stilgenbauer S, James MR, Benner A, Weilguni T, Bentz M, *et al.* 11q deletions identify a new subset of B-cell chronic lymphocytic leukemia characterized by extensive nodal involvement and inferior prognosis. *Blood.* 1997;89(7):2516-22.
66. Oscier DG, Matutes E, Copplestone A, Pickering RM, Chapman R, Gillingham R, *et al.* Atypical lymphocyte morphology: an adverse prognostic factor for disease progression in stage A CLL independent of trisomy 12. *Br J Haematol.* 1997;98(4):934-9.
67. Tefferi A, Bartholmai BJ, Witzig TE, Jenkins RB, Li CY, Hanson CA, *et al.* Clinical correlations of immunophenotypic variations and the presence of trisomy 12 in B-cell chronic lymphocytic leukemia. *Cancer Genet Cytogenet.* 1997;95(2):173-7.

68. Cuneo A, Rigolin GM, Bigoni R, De Angeli C, Veronese A, Cavazzini F, *et al.* Chronic lymphocytic leukemia with 6q- shows distinct hematological features and intermediate prognosis. *Leukemia*. 2004;18(3):476-83.
69. Mauro FR, Foa R, Giannarelli D, Cordone I, Crescenzi S, Pescarmona E, *et al.* Clinical characteristics and outcome of young chronic lymphocytic leukemia patients: a single institution study of 204 cases. *Blood*. 1999;94(2):448-54.
70. Dighiero G, Maloum K, Desablens B, Cazin B, Navarro M, Leblay R, *et al.* Chlorambucil in indolent chronic lymphocytic leukemia. French Cooperative Group on Chronic Lymphocytic Leukemia. *N Engl J Med*. 1998;338(21):1506-14.
71. Shustik C, Mick R, Silver R, Sawitsky A, Rai K, Shapiro L. Treatment of early chronic lymphocytic leukemia: intermittent chlorambucil versus observation. *Hematol Oncol*. 1988;6(1):7-12.
72. Chemotherapeutic options in chronic lymphocytic leukemia: a meta-analysis of the randomized trials. CLL Trialists' Collaborative Group. *J Natl Cancer Inst*. 1999;91(10):861-8.
73. Dameshek W. Chronic lymphocytic leukemia--an accumulative disease of immunologically incompetent lymphocytes. *Blood*. 1967;29(4):Suppl:566-84.
74. Keating MJ, O'Brien S, Lerner S, Koller C, Beran M, Robertson LE, *et al.* Long-term follow-up of patients with chronic lymphocytic leukemia (CLL) receiving fludarabine regimens as initial therapy. *Blood*. 1998;92(4):1165-71.
75. Rai KR, Peterson BL, Appelbaum FR, Kolitz J, Elias L, Shepherd L, *et al.* Fludarabine compared with chlorambucil as primary therapy for chronic lymphocytic leukemia. *N Engl J Med*. 2000;343(24):1750-7.
76. Hallek M. State-of-the-art treatment of chronic lymphocytic leukemia. *Hematology Am Soc Hematol Educ Program*. 2009:440-9.
77. Flinn IW, Byrd JC, Morrison C, Jamison J, Diehl LF, Murphy T, *et al.* Fludarabine and cyclophosphamide with filgrastim support in patients with previously untreated indolent lymphoid malignancies. *Blood*. 2000;96(1):71-5.
78. O'Brien SM, Kantarjian HM, Cortes J, Beran M, Koller CA, Giles FJ, *et al.* Results of the fludarabine and cyclophosphamide combination regimen in chronic lymphocytic leukemia. *J Clin Oncol*. 2001;19(5):1414-20.
79. Catovsky D, Richards S, Matutes E, Oscier D, Dyer MJ, Bezares RF, *et al.* Assessment of fludarabine plus cyclophosphamide for patients with chronic lymphocytic leukaemia (the LRF CLL4 Trial): a randomised controlled trial. *Lancet*. 2007;370(9583):230-9.
80. Bosch F, Ferrer A, Lopez-Guillermo A, Gine E, Bellosillo B, Villamor N, *et al.* Fludarabine, cyclophosphamide and mitoxantrone in the treatment of resistant or relapsed chronic lymphocytic leukaemia. *Br J Haematol*. 2002;119(4):976-84.

81. Keating M, O'Brien S. High-dose rituximab therapy in chronic lymphocytic leukemia. *Semin Oncol*. 2000;27(6 Suppl 12):86-90.
82. Huhn D, von Schilling C, Wilhelm M, Ho AD, Hallek M, Kuse R, *et al*. Rituximab therapy of patients with B-cell chronic lymphocytic leukemia. *Blood*. 2001;98(5):1326-31.
83. Byrd JC, Murphy T, Howard RS, Lucas MS, Goodrich A, Park K, *et al*. Rituximab using a thrice weekly dosing schedule in B-cell chronic lymphocytic leukemia and small lymphocytic lymphoma demonstrates clinical activity and acceptable toxicity. *J Clin Oncol*. 2001;19(8):2153-64.
84. O'Brien SM, Kantarjian H, Thomas DA, Giles FJ, Freireich EJ, Cortes J, *et al*. Rituximab dose-escalation trial in chronic lymphocytic leukemia. *J Clin Oncol*. 2001;19(8):2165-70.
85. Wierda W, O'Brien S, Wen S, Faderl S, Garcia-Manero G, Thomas D, *et al*. Chemoimmunotherapy with fludarabine, cyclophosphamide, and rituximab for relapsed and refractory chronic lymphocytic leukemia. *J Clin Oncol*. 2005;23(18):4070-8.
86. Keating MJ, O'Brien S, Albitar M, Lerner S, Plunkett W, Giles F, *et al*. Early results of a chemoimmunotherapy regimen of fludarabine, cyclophosphamide, and rituximab as initial therapy for chronic lymphocytic leukemia. *J Clin Oncol*. 2005;23(18):4079-88.
87. Goldman J. Monitoring minimal residual disease in BCR-ABL-positive chronic myeloid leukemia in the imatinib era. *Curr Opin Hematol*. 2005;12(1):33-9.
88. Raff T, Gokbuget N, Luschen S, Reutzel R, Ritgen M, Irmer S, *et al*. Molecular relapse in adult standard-risk ALL patients detected by prospective MRD monitoring during and after maintenance treatment: data from the GMALL 06/99 and 07/03 trials. *Blood*. 2007;109(3):910-5.
89. Buccisano F, Maurillo L, Gattei V, Del Poeta G, Del Principe MI, Cox MC, *et al*. The kinetics of reduction of minimal residual disease impacts on duration of response and survival of patients with acute myeloid leukemia. *Leukemia*. 2006;20(10):1783-9.
90. Sayala HA, Rawstron AC, Hillmen P. Minimal residual disease assessment in chronic lymphocytic leukaemia. *Best Pract Res Clin Haematol*. 2007;20(3):499-512.
91. Moreton P, Kennedy B, Lucas G, Leach M, Rassam SM, Haynes A, *et al*. Eradication of minimal residual disease in B-cell chronic lymphocytic leukemia after alemtuzumab therapy is associated with prolonged survival. *J Clin Oncol*. 2005;23(13):2971-9.
92. Dreger P, Corradini P, Kimby E, Michallet M, Milligan D, Schetelig J, *et al*. Indications for allogeneic stem cell transplantation in chronic lymphocytic leukemia: the EBMT transplant consensus. *Leukemia*. 2007;21(1):12-7.
93. Dreger P. Allogeneic transplantation for chronic lymphocytic leukemia. *Hematology Am Soc Hematol Educ Program*. 2009:602-9.

94. Gribben JG. Stem-cell transplantation in chronic lymphocytic leukaemia. *Best Pract Res Clin Haematol.* 2007;20(3):513-27.
95. Dohner H, Fischer K, Bentz M, Hansen K, Benner A, Cabot G, *et al.* p53 gene deletion predicts for poor survival and non-response to therapy with purine analogs in chronic B-cell leukemias. *Blood.* 1995;85(6):1580-9.
96. Montserrat E, Lopez-Lorenzo JL, Manso F, Martin A, Prieto E, Arias-Sampedro J, *et al.* Fludarabine in resistant or relapsing B-cell chronic lymphocytic leukemia: the Spanish Group experience. *Leuk Lymphoma.* 1996;21(5-6):467-72.
97. Perkins JG, Flynn JM, Howard RS, Byrd JC. Frequency and type of serious infections in fludarabine-refractory B-cell chronic lymphocytic leukemia and small lymphocytic lymphoma: implications for clinical trials in this patient population. *Cancer.* 2002;94(7):2033-9.
98. Rosenwald A, Chuang EY, Davis RE, Wiestner A, Alizadeh AA, Arthur DC, *et al.* Fludarabine treatment of patients with chronic lymphocytic leukemia induces a p53-dependent gene expression response. *Blood.* 2004;104(5):1428-34.
99. Thornton PD, Matutes E, Bosanquet AG, Lakhani AK, Grech H, Ropner JE, *et al.* High dose methylprednisolone can induce remissions in CLL patients with p53 abnormalities. *Ann Hematol.* 2003;82(12):759-65.
100. Lozanski G, Heerema NA, Flinn IW, Smith L, Harbison J, Webb J, *et al.* Alemtuzumab is an effective therapy for chronic lymphocytic leukemia with p53 mutations and deletions. *Blood.* 2004;103(9):3278-81.
101. Keating MJ, Flinn I, Jain V, Binet JL, Hillmen P, Byrd J, *et al.* Therapeutic role of alemtuzumab (Campath-1H) in patients who have failed fludarabine: results of a large international study. *Blood.* 2002;99(10):3554-61.
102. Montserrat E, Moreno C, Esteve J, Urbano-Ispizua A, Gine E, Bosch F. How I treat refractory CLL. *Blood.* 2006;107(4):1276-83.
103. Andreeff M, Darzynkiewicz Z, Sharpless TK, Clarkson BD, Melamed MR. Discrimination of human leukemia subtypes by flow cytometric analysis of cellular DNA and RNA. *Blood.* 1980;55(2):282-93.
104. Hanada M, Delia D, Aiello A, Stadtmauer E, Reed JC. bcl-2 gene hypomethylation and high-level expression in B-cell chronic lymphocytic leukemia. *Blood.* 1993;82(6):1820-8.
105. Oscier D, Fitchett M, Herbert T, Lambert R. Karyotypic evolution in B-cell chronic lymphocytic leukaemia. *Genes Chromosomes Cancer.* 1991;3(1):16-20.
106. Marti GE, Faguet GB, Stewart C, Branham P, Carter PH, Washington GC, *et al.* Evolution of leukemic heterogeneity of human B-CLL lymphocytes between and within patients. *Curr Top Microbiol Immunol.* 1992;182:303-11.

107. Hakim I, Rechavi G, Brok-Simoni F, Grossman Z, Amariglio N, Mandel M, *et al.* Analysis of rearranged immunoglobulin genes indicating a process of clonal evolution in chronic lymphocytic leukaemia. *Br J Haematol.* 1993;84(3):436-42.
108. Crossen PE, Tully SM, Benjes SM, Hollings PE, Beard ME, Nimmo JC, *et al.* Oligoclonal B-cell leukemia characterized by spontaneous cell division and telomere association. *Genes Chromosomes Cancer.* 1993;8(1):49-59.
109. Damle RN, Batliwalla FM, Ghiotto F, Valetto A, Albesiano E, Sison C, *et al.* Telomere length and telomerase activity delineate distinctive replicative features of the B-CLL subgroups defined by immunoglobulin V gene mutations. *Blood.* 2004;103(2):375-82.
110. Bechter OE, Eisterer W, Pall G, Hilbe W, Kuhr T, Thaler J. Telomere length and telomerase activity predict survival in patients with B cell chronic lymphocytic leukemia. *Cancer Res.* 1998;58(21):4918-22.
111. Trentin L, Ballon G, Ometto L, Perin A, Basso U, Chieco-Bianchi L, *et al.* Telomerase activity in chronic lymphoproliferative disorders of B-cell lineage. *Br J Haematol.* 1999;106(3):662-8.
112. Messmer BT, Messmer D, Allen SL, Kolitz JE, Kudalkar P, Cesar D, *et al.* In vivo measurements document the dynamic cellular kinetics of chronic lymphocytic leukemia B cells. *J Clin Invest.* 2005;115(3):755-64.
113. Schmid C, Isaacson PG. Proliferation centres in B-cell malignant lymphoma, lymphocytic (B-CLL): an immunophenotypic study. *Histopathology.* 1994;24(5):445-51.
114. Caligaris-Cappio F. Role of the microenvironment in chronic lymphocytic leukaemia. *Br J Haematol.* 2003;123(3):380-8.
115. Plander M, Seegers S, Ugocsai P, Diermeier-Daucher S, Ivanyi J, Schmitz G, *et al.* Different proliferative and survival capacity of CLL-cells in a newly established in vitro model for pseudofollicles. *Leukemia.* 2009;23(11):2118-28.
116. Willimott S, Baou M, Huf S, Wagner SD. Separate cell culture conditions to promote proliferation or quiescent cell survival in chronic lymphocytic leukemia. *Leuk Lymphoma.* 2007;48(8):1647-50.
117. Caligaris-Cappio F, Ghia P. The normal counterpart to the chronic lymphocytic leukemia B cell. *Best Pract Res Clin Haematol.* 2007;20(3):385-97.
118. Damle RN, Ghiotto F, Valetto A, Albesiano E, Fais F, Yan XJ, *et al.* B-cell chronic lymphocytic leukemia cells express a surface membrane phenotype of activated, antigen-experienced B lymphocytes. *Blood.* 2002;99(11):4087-93.
119. Rosenwald A, Alizadeh AA, Widhopf G, Simon R, Davis RE, Yu X, *et al.* Relation of gene expression phenotype to immunoglobulin mutation genotype in B cell chronic lymphocytic leukemia. *J Exp Med.* 2001;194(11):1639-47.

120. Klein U, Tu Y, Stolovitzky GA, Mattioli M, Cattoretti G, Husson H, *et al.* Gene expression profiling of B cell chronic lymphocytic leukemia reveals a homogeneous phenotype related to memory B cells. *J Exp Med.* 2001;194(11):1625-38.
121. Potter KN, Orchard J, Critchley E, Mockridge CI, Jose A, Stevenson FK. Features of the overexpressed V1-69 genes in the unmutated subset of chronic lymphocytic leukemia are distinct from those in the healthy elderly repertoire. *Blood.* 2003;101(8):3082-4.
122. Widhopf GF, 2nd, Kipps TJ. Normal B cells express 51p1-encoded Ig heavy chains that are distinct from those expressed by chronic lymphocytic leukemia B cells. *J Immunol.* 2001;166(1):95-102.
123. Tobin G, Thunberg U, Johnson A, Eriksson I, Soderberg O, Karlsson K, *et al.* Chronic lymphocytic leukemias utilizing the VH3-21 gene display highly restricted Vlambda2-14 gene use and homologous CDR3s: implicating recognition of a common antigen epitope. *Blood.* 2003;101(12):4952-7.
124. Widhopf GF, 2nd, Rassenti LZ, Toy TL, Gribben JG, Wierda WG, Kipps TJ. Chronic lymphocytic leukemia B cells of more than 1% of patients express virtually identical immunoglobulins. *Blood.* 2004;104(8):2499-504.
125. Messmer BT, Albesiano E, Efremov DG, Ghiotto F, Allen SL, Kolitz J, *et al.* Multiple distinct sets of stereotyped antigen receptors indicate a role for antigen in promoting chronic lymphocytic leukemia. *J Exp Med.* 2004;200(4):519-25.
126. Tobin G, Thunberg U, Karlsson K, Murray F, Laurell A, Willander K, *et al.* Subsets with restricted immunoglobulin gene rearrangement features indicate a role for antigen selection in the development of chronic lymphocytic leukemia. *Blood.* 2004;104(9):2879-85.
127. Stamatopoulos K, Belessi C, Moreno C, Boudjograh M, Guida G, Smilevska T, *et al.* Over 20% of patients with chronic lymphocytic leukemia carry stereotyped receptors: Pathogenetic implications and clinical correlations. *Blood.* 2007;109(1):259-70.
128. Murray F, Darzentas N, Hadzidimitriou A, Tobin G, Boudjogra M, Scielzo C, *et al.* Stereotyped patterns of somatic hypermutation in subsets of patients with chronic lymphocytic leukemia: implications for the role of antigen selection in leukemogenesis. *Blood.* 2008;111(3):1524-33.
129. Hadzidimitriou A, Darzentas N, Murray F, Smilevska T, Arvaniti E, Tresoldi C, *et al.* Evidence for the significant role of immunoglobulin light chains in antigen recognition and selection in chronic lymphocytic leukemia. *Blood.* 2009;113(2):403-11.
130. Ghia P, Stamatopoulos K, Belessi C, Moreno C, Stella S, Guida G, *et al.* Geographic patterns and pathogenetic implications of IGHV gene usage in chronic lymphocytic leukemia: the lesson of the IGHV3-21 gene. *Blood.* 2005;105(4):1678-85.
131. Rossi D, Spina V, Cerri M, Rasi S, Deambrogi C, De Paoli L, *et al.* Stereotyped B-cell receptor is an independent risk factor of chronic

- lymphocytic leukemia transformation to richter syndrome. *Clin Cancer Res.* 2009;15(13):4415-22.
132. Sthoeger ZM, Wakai M, Tse DB, Vinciguerra VP, Allen SL, Budman DR, *et al.* Production of autoantibodies by CD5-expressing B lymphocytes from patients with chronic lymphocytic leukemia. *J Exp Med.* 1989;169(1):255-68.
  133. Borche L, Lim A, Binet JL, Dighiero G. Evidence that chronic lymphocytic leukemia B lymphocytes are frequently committed to production of natural autoantibodies. *Blood.* 1990;76(3):562-9.
  134. Herve M, Xu K, Ng YS, Wardemann H, Albesiano E, Messmer BT, *et al.* Unmutated and mutated chronic lymphocytic leukemias derive from self-reactive B cell precursors despite expressing different antibody reactivity. *J Clin Invest.* 2005;115(6):1636-43.
  135. Seiler T, Woelfle M, Yancopoulos S, Catera R, Li W, Hatzi K, *et al.* Characterization of structurally defined epitopes recognized by monoclonal antibodies produced by chronic lymphocytic leukemia B cells. *Blood.* 2009;114(17):3615-24.
  136. Lanemo Myhrinder A, Hellqvist E, Sidorova E, Soderberg A, Baxendale H, Dahle C, *et al.* A new perspective: molecular motifs on oxidized-LDL, apoptotic cells, and bacteria are targets for chronic lymphocytic leukemia antibodies. *Blood.* 2008;111(7):3838-48.
  137. Catera R, Silverman GJ, Hatzi K, Seiler T, Didier S, Zhang L, *et al.* Chronic lymphocytic leukemia cells recognize conserved epitopes associated with apoptosis and oxidation. *Mol Med.* 2008;14(11-12):665-74.
  138. Chu CC, Catera R, Hatzi K, Yan XJ, Zhang L, Wang XB, *et al.* Chronic lymphocytic leukemia antibodies with a common stereotypic rearrangement recognize nonmuscle myosin heavy chain IIA. *Blood.* 2008;112(13):5122-9.
  139. Landgren O, Rapkin JS, Caporaso NE, Mellemkjaer L, Gridley G, Goldin LR, *et al.* Respiratory tract infections and subsequent risk of chronic lymphocytic leukemia. *Blood.* 2007;109(5):2198-201.
  140. Silverman GJ. B-cell superantigens. *Immunol Today.* 1997;18(8):379-86.
  141. Bomben R, Dal-Bo M, Benedetti D, Capello D, Forconi F, Marconi D, *et al.* Expression of mutated IGHV3-23 genes in chronic lymphocytic leukemia identifies a disease subset with peculiar clinical and biological features. *Clin Cancer Res.* 2010;16(2):620-8.
  142. Forconi F, Potter KN, Wheatley I, Darzentas N, Sozzi E, Stamatopoulos K, *et al.* The normal IGHV1-69-derived B-cell repertoire contains stereotypic patterns characteristic of unmutated CLL. *Blood.* 2010;115(1):71-7.
  143. Scheeren FA, Nagasawa M, Weijer K, Cupedo T, Kirberg J, Legrand N, *et al.* T cell-independent development and induction of somatic hypermutation in human IgM+ IgD+ CD27+ B cells. *J Exp Med.* 2008;205(9):2033-42.

144. Tsuiji M, Yurasov S, Velinzon K, Thomas S, Nussenzweig MC, Wardemann H. A checkpoint for autoreactivity in human IgM+ memory B cell development. *J Exp Med*. 2006;203(2):393-400.
145. Ghia P, Chiorazzi N, Stamatopoulos K. Microenvironmental influences in chronic lymphocytic leukaemia: the role of antigen stimulation. *J Intern Med*. 2008;264(6):549-62.
146. Sutton LA, Kostareli E, Hadzidimitriou A, Darzentas N, Tsaftaris A, Anagnostopoulos A, *et al*. Extensive intraclonal diversification in a subgroup of chronic lymphocytic leukemia patients with stereotyped IGHV4-34 receptors: implications for ongoing interactions with antigen. *Blood*. 2009;114(20):4460-8.
147. Carrasco YR, Batista FD. B cell recognition of membrane-bound antigen: an exquisite way of sensing ligands. *Curr Opin Immunol*. 2006;18(3):286-91.
148. Kurosaki T, Hikida M. Tyrosine kinases and their substrates in B lymphocytes. *Immunol Rev*. 2009;228(1):132-48.
149. Depoil D, Weber M, Treanor B, Fleire SJ, Carrasco YR, Harwood NE, *et al*. Early events of B cell activation by antigen. *Sci Signal*. 2009;2(63):pt1.
150. Batista FD, Iber D, Neuberger MS. B cells acquire antigen from target cells after synapse formation. *Nature*. 2001;411(6836):489-94.
151. Fleire SJ, Goldman JP, Carrasco YR, Weber M, Bray D, Batista FD. B cell ligand discrimination through a spreading and contraction response. *Science*. 2006;312(5774):738-41.
152. Treanor B, Harwood NE, Batista FD. Microsignalosomes: spatially resolved receptor signalling. *Biochem Soc Trans*. 2009;37(Pt 5):1014-8.
153. Gupta N, DeFranco AL. Lipid rafts and B cell signaling. *Semin Cell Dev Biol*. 2007;18(5):616-26.
154. Kurosaki T. Genetic analysis of B cell antigen receptor signaling. *Annu Rev Immunol*. 1999;17:555-92.
155. Dal Porto JM, Gauld SB, Merrell KT, Mills D, Pugh-Bernard AE, Cambier J. B cell antigen receptor signaling 101. *Mol Immunol*. 2004;41(6-7):599-613.
156. Fu C, Turck CW, Kurosaki T, Chan AC. BLNK: a central linker protein in B cell activation. *Immunity*. 1998;9(1):93-103.
157. Saito K, Scharenberg AM, Kinet JP. Interaction between the Btk PH domain and phosphatidylinositol-3,4,5-trisphosphate directly regulates Btk. *J Biol Chem*. 2001;276(19):16201-6.
158. Dolmetsch RE, Lewis RS, Goodnow CC, Healy JI. Differential activation of transcription factors induced by Ca<sup>2+</sup> response amplitude and duration. *Nature*. 1997;386(6627):855-8.

159. Saijo K, Mecklenbrauker I, Santana A, Leitger M, Schmedt C, Tarakhovsky A. Protein kinase C beta controls nuclear factor kappaB activation in B cells through selective regulation of the IkappaB kinase alpha. *J Exp Med.* 2002;195(12):1647-52.
160. Tan SL, Parker PJ. Emerging and diverse roles of protein kinase C in immune cell signalling. *Biochem J.* 2003;376(Pt 3):545-52.
161. Platanias LC. Map kinase signaling pathways and hematologic malignancies. *Blood.* 2003;101(12):4667-79.
162. Koyasu S. The role of PI3K in immune cells. *Nat Immunol.* 2003;4(4):313-9.
163. Astoul E, Watton S, Cantrell D. The dynamics of protein kinase B regulation during B cell antigen receptor engagement. *J Cell Biol.* 1999;145(7):1511-20.
164. Meier R, Alessi DR, Cron P, Andjelkovic M, Hemmings BA. Mitogenic activation, phosphorylation, and nuclear translocation of protein kinase Bbeta. *J Biol Chem.* 1997;272(48):30491-7.
165. Datta SR, Dudek H, Tao X, Masters S, Fu H, Gotoh Y, *et al.* Akt phosphorylation of BAD couples survival signals to the cell-intrinsic death machinery. *Cell.* 1997;91(2):231-41.
166. Cardone MH, Roy N, Stennicke HR, Salvesen GS, Franke TF, Stanbridge E, *et al.* Regulation of cell death protease caspase-9 by phosphorylation. *Science.* 1998;282(5392):1318-21.
167. Datta SR, Brunet A, Greenberg ME. Cellular survival: a play in three Akts. *Genes Dev.* 1999;13(22):2905-27.
168. Bjornsti MA, Houghton PJ. The TOR pathway: a target for cancer therapy. *Nat Rev Cancer.* 2004;4(5):335-48.
169. Li HL, Davis W, Pure E. Suboptimal cross-linking of antigen receptor induces Syk-dependent activation of p70S6 kinase through protein kinase C and phosphoinositol 3-kinase. *J Biol Chem.* 1999;274(14):9812-20.
170. Gilmore TD. Introduction to NF-kappaB: players, pathways, perspectives. *Oncogene.* 2006;25(51):6680-4.
171. Pasparakis M, Schmidt-Supprian M, Rajewsky K. IkappaB kinase signaling is essential for maintenance of mature B cells. *J Exp Med.* 2002;196(6):743-52.
172. Lam KP, Kuhn R, Rajewsky K. In vivo ablation of surface immunoglobulin on mature B cells by inducible gene targeting results in rapid cell death. *Cell.* 1997;90(6):1073-83.
173. Fuentes-Panana EM, Bannish G, Monroe JG. Basal B-cell receptor signaling in B lymphocytes: mechanisms of regulation and role in positive selection, differentiation, and peripheral survival. *Immunol Rev.* 2004;197:26-40.

174. Monroe JG. Ligand-independent tonic signaling in B-cell receptor function. *Curr Opin Immunol.* 2004;16(3):288-95.
175. Saijo K, Schmedt C, Su IH, Karasuyama H, Lowell CA, Reth M, *et al.* Essential role of Src-family protein tyrosine kinases in NF-kappaB activation during B cell development. *Nat Immunol.* 2003;4(3):274-9.
176. Muljo SA, Schlissel MS. A small molecule Abl kinase inhibitor induces differentiation of Abelson virus-transformed pre-B cell lines. *Nat Immunol.* 2003;4(1):31-7.
177. Roose JP, Diehn M, Tomlinson MG, Lin J, Alizadeh AA, Botstein D, *et al.* T cell receptor-independent basal signaling via Erk and Abl kinases suppresses RAG gene expression. *PLoS Biol.* 2003;1(2):E53.
178. Chiorazzi N, Hatzi K, Albesiano E. B-cell chronic lymphocytic leukemia, a clonal disease of B lymphocytes with receptors that vary in specificity for (auto)antigens. *Ann N Y Acad Sci.* 2005;1062:1-12.
179. Hivroz C, Geny B, Brouet JC, Grillot-Courvalin C. Altered signal transduction secondary to surface IgM cross-linking on B-chronic lymphocytic leukemia cells. Differential activation of the phosphatidylinositol-specific phospholipase C. *J Immunol.* 1990;144(6):2351-8.
180. Lankester AC, van Schijndel GM, van der Schoot CE, van Oers MH, van Noesel CJ, van Lier RA. Antigen receptor nonresponsiveness in chronic lymphocytic leukemia B cells. *Blood.* 1995;86(3):1090-7.
181. Lanham S, Hamblin T, Oscier D, Ibbotson R, Stevenson F, Packham G. Differential signaling via surface IgM is associated with VH gene mutational status and CD38 expression in chronic lymphocytic leukemia. *Blood.* 2003;101(3):1087-93.
182. Allsup DJ, Kamiguti AS, Lin K, Sherrington PD, Matrai Z, Slupsky JR, *et al.* B-cell receptor translocation to lipid rafts and associated signaling differ between prognostically important subgroups of chronic lymphocytic leukemia. *Cancer Res.* 2005;65(16):7328-37.
183. Chen L, Widhopf G, Huynh L, Rassenti L, Rai KR, Weiss A, *et al.* Expression of ZAP-70 is associated with increased B-cell receptor signaling in chronic lymphocytic leukemia. *Blood.* 2002;100(13):4609-14.
184. Chen L, Huynh L, Apgar J, Tang L, Rassenti L, Weiss A, *et al.* ZAP-70 enhances IgM signaling independent of its kinase activity in chronic lymphocytic leukemia. *Blood.* 2008;111(5):2685-92.
185. Deglesne PA, Chevallier N, Letestu R, Baran-Marszak F, Beitar T, Salanoubat C, *et al.* Survival response to B-cell receptor ligation is restricted to progressive chronic lymphocytic leukemia cells irrespective of Zap70 expression. *Cancer Res.* 2006;66(14):7158-66.
186. Zupo S, Isnardi L, Megna M, Massara R, Malavasi F, Dono M, *et al.* CD38 expression distinguishes two groups of B-cell chronic lymphocytic

- leukemias with different responses to anti-IgM antibodies and propensity to apoptosis. *Blood*. 1996;88(4):1365-74.
187. Mockridge CI, Potter KN, Wheatley I, Neville LA, Packham G, Stevenson FK. Reversible anergy of sIgM-mediated signaling in the two subsets of CLL defined by VH-gene mutational status. *Blood*. 2007;109(10):4424-31.
  188. Herling M, Patel KA, Weit N, Lilienthal N, Hallek M, Keating MJ, *et al.* High TCL1 levels are a marker of B-cell receptor pathway responsiveness and adverse outcome in chronic lymphocytic leukemia. *Blood*. 2009;114(21):4675-86.
  189. Abrams ST, Lakum T, Lin K, Jones GM, Treweeke AT, Farahani M, *et al.* B-cell receptor signaling in chronic lymphocytic leukemia cells is regulated by overexpressed active protein kinase Cbeta1. *Blood*. 2007;109(3):1193-201.
  190. Semichon M, Merle-Beral H, Lang V, Bismuth G. Normal Syk protein level but abnormal tyrosine phosphorylation in B-CLL cells. *Leukemia*. 1997;11(11):1921-8.
  191. Muzio M, Apollonio B, Scielzo C, Frenquelli M, Vandoni I, Boussiotis V, *et al.* Constitutive activation of distinct BCR-signaling pathways in a subset of CLL patients: a molecular signature of anergy. *Blood*. 2008;112(1):188-95.
  192. Petlickovski A, Laurenti L, Li X, Marietti S, Chiusolo P, Sica S, *et al.* Sustained signaling through the B-cell receptor induces Mcl-1 and promotes survival of chronic lymphocytic leukemia B cells. *Blood*. 2005;105(12):4820-7.
  193. Gauld SB, Benschop RJ, Merrell KT, Cambier JC. Maintenance of B cell anergy requires constant antigen receptor occupancy and signaling. *Nat Immunol*. 2005;6(11):1160-7.
  194. Bernal A, Pastore RD, Asgary Z, Keller SA, Cesarman E, Liou HC, *et al.* Survival of leukemic B cells promoted by engagement of the antigen receptor. *Blood*. 2001;98(10):3050-7.
  195. Quiroga MP, Balakrishnan K, Kurtova AV, Sivina M, Keating MJ, Wierda WG, *et al.* B cell antigen receptor signaling enhances chronic lymphocytic leukemia cell migration and survival: specific targeting with a novel Syk inhibitor, R406. *Blood*. 2009;114(5):1029-37.
  196. Longo PG, Laurenti L, Gobessi S, Sica S, Leone G, Efremov DG. The Akt/Mcl-1 pathway plays a prominent role in mediating antiapoptotic signals downstream of the B-cell receptor in chronic lymphocytic leukemia B cells. *Blood*. 2008;111(2):846-55.
  197. Kitada S, Andersen J, Akar S, Zapata JM, Takayama S, Krajewski S, *et al.* Expression of apoptosis-regulating proteins in chronic lymphocytic leukemia: correlations with In vitro and In vivo chemoresponses. *Blood*. 1998;91(9):3379-89.
  198. Stilgenbauer S, Sander S, Bullinger L, Benner A, Leupolt E, Winkler D, *et al.* Clonal evolution in chronic lymphocytic leukemia: acquisition of high-risk

- genomic aberrations associated with unmutated VH, resistance to therapy, and short survival. *Haematologica*. 2007;92(9):1242-5.
199. Guarini A, Chiaretti S, Tavolaro S, Maggio R, Peragine N, Citarella F, *et al*. BCR-ligation induced by IgM stimulation results in gene expression and functional changes only in IgVH unmutated chronic lymphocytic leukemia (CLL) cells. *Blood*. 2008;112(3):1923-30.
  200. Ingley E. Src family kinases: regulation of their activities, levels and identification of new pathways. *Biochim Biophys Acta*. 2008;1784(1):56-65.
  201. Xu Y, Harder KW, Huntington ND, Hibbs ML, Tarlinton DM. Lyn tyrosine kinase: accentuating the positive and the negative. *Immunity*. 2005;22(1):9-18.
  202. Hibbs ML, Tarlinton DM, Armes J, Grail D, Hodgson G, Maglitta R, *et al*. Multiple defects in the immune system of Lyn-deficient mice, culminating in autoimmune disease. *Cell*. 1995;83(2):301-11.
  203. Contri A, Brunati AM, Trentin L, Cabrelle A, Miorin M, Cesaro L, *et al*. Chronic lymphocytic leukemia B cells contain anomalous Lyn tyrosine kinase, a putative contribution to defective apoptosis. *J Clin Invest*. 2005;115(2):369-78.
  204. Hussein K, von Neuhoff N, Busche G, Buhr T, Kreipe H, Bock O. Opposite expression pattern of Src kinase Lyn in acute and chronic haematological malignancies. *Ann Hematol*. 2009;88(11):1059-67.
  205. Dos Santos C, Demur C, Bardet V, Prade-Houdellier N, Payrastre B, Recher C. A critical role for Lyn in acute myeloid leukemia. *Blood*. 2008;111(4):2269-79.
  206. Donato NJ, Wu JY, Stapley J, Gallick G, Lin H, Arlinghaus R, *et al*. BCR-ABL independence and LYN kinase overexpression in chronic myelogenous leukemia cells selected for resistance to STI571. *Blood*. 2003;101(2):690-8.
  207. Hu Y, Liu Y, Pelletier S, Buchdunger E, Warmuth M, Fabbro D, *et al*. Requirement of Src kinases Lyn, Hck and Fgr for BCR-ABL1-induced B-lymphoblastic leukemia but not chronic myeloid leukemia. *Nat Genet*. 2004;36(5):453-61.
  208. Tanaka H, Takeuchi M, Takeda Y, Sakai S, Abe D, Ohwada C, *et al*. Identification of a novel TEL-Lyn fusion gene in primary myelofibrosis. *Leukemia*. 2010;24(1):197-200.
  209. Tauzin S, Ding H, Khatib K, Ahmad I, Burdevet D, van Echten-Deckert G, *et al*. Oncogenic association of the Cbp/PAG adaptor protein with the Lyn tyrosine kinase in human B-NHL rafts. *Blood*. 2008;111(4):2310-20.
  210. Tybulewicz VL, Crawford CE, Jackson PK, Bronson RT, Mulligan RC. Neonatal lethality and lymphopenia in mice with a homozygous disruption of the c-abl proto-oncogene. *Cell*. 1991;65(7):1153-63.

211. Zipfel PA, Grove M, Blackburn K, Fujimoto M, Tedder TF, Pendergast AM. The c-Abl tyrosine kinase is regulated downstream of the B cell antigen receptor and interacts with CD19. *J Immunol.* 2000;165(12):6872-9.
212. Lin K, Glenn MA, Harris RJ, Duckworth AD, Dennett S, Cawley JC, *et al.* c-Abl expression in chronic lymphocytic leukemia cells: clinical and therapeutic implications. *Cancer Res.* 2006;66(15):7801-9.
213. Aloyz R, Grzywacz K, Xu ZY, Loignon M, Alaoui-Jamali MA, Panasci L. Imatinib sensitizes CLL lymphocytes to chlorambucil. *Leukemia.* 2004;18(3):409-14.
214. Albini A, Sporn MB. The tumour microenvironment as a target for chemoprevention. *Nat Rev Cancer.* 2007;7(2):139-47.
215. Lane SW, Scadden DT, Gilliland DG. The leukemic stem cell niche: current concepts and therapeutic opportunities. *Blood.* 2009;114(6):1150-7.
216. Burger JA, Ghia P, Rosenwald A, Caligaris-Cappio F. The microenvironment in mature B-cell malignancies: a target for new treatment strategies. *Blood.* 2009;114(16):3367-75.
217. Collins RJ, Verschuer LA, Harmon BV, Prentice RL, Pope JH, Kerr JF. Spontaneous programmed death (apoptosis) of B-chronic lymphocytic leukaemia cells following their culture in vitro. *Br J Haematol.* 1989;71(3):343-50.
218. Rozman C, Hernandez-Nieto L, Montserrat E, Bruges R. Prognostic significance of bone-marrow patterns in chronic lymphocytic leukaemia. *Br J Haematol.* 1981;47(4):529-37.
219. Stevenson FK, Caligaris-Cappio F. Chronic lymphocytic leukemia: revelations from the B-cell receptor. *Blood.* 2004;103(12):4389-95.
220. Panayiotidis P, Jones D, Ganeshaguru K, Foroni L, Hoffbrand AV. Human bone marrow stromal cells prevent apoptosis and support the survival of chronic lymphocytic leukaemia cells in vitro. *Br J Haematol.* 1996;92(1):97-103.
221. Lagneaux L, Delforge A, Bron D, De Bruyn C, Stryckmans P. Chronic lymphocytic leukemic B cells but not normal B cells are rescued from apoptosis by contact with normal bone marrow stromal cells. *Blood.* 1998;91(7):2387-96.
222. Pedersen IM, Kitada S, Leoni LM, Zapata JM, Karras JG, Tsukada N, *et al.* Protection of CLL B cells by a follicular dendritic cell line is dependent on induction of Mcl-1. *Blood.* 2002;100(5):1795-801.
223. Kay NE, Shanafelt TD, Strege AK, Lee YK, Bone ND, Raza A. Bone biopsy derived marrow stromal elements rescue chronic lymphocytic leukemia B-cells from spontaneous and drug induced cell death and facilitates an "angiogenic switch". *Leuk Res.* 2007;31(7):899-906.

224. Mudry RE, Fortney JE, York T, Hall BM, Gibson LF. Stromal cells regulate survival of B-lineage leukemic cells during chemotherapy. *Blood*. 2000;96(5):1926-32.
225. Damiano JS, Hazlehurst LA, Dalton WS. Cell adhesion-mediated drug resistance (CAM-DR) protects the K562 chronic myelogenous leukemia cell line from apoptosis induced by BCR/ABL inhibition, cytotoxic drugs, and gamma-irradiation. *Leukemia*. 2001;15(8):1232-9.
226. Nefedova Y, Landowski TH, Dalton WS. Bone marrow stromal-derived soluble factors and direct cell contact contribute to de novo drug resistance of myeloma cells by distinct mechanisms. *Leukemia*. 2003;17(6):1175-82.
227. Kurtova AV, Balakrishnan K, Chen R, Ding W, Schnabl S, Quiroga MP, *et al*. Diverse marrow stromal cells protect CLL cells from spontaneous and drug-induced apoptosis: development of a reliable and reproducible system to assess stromal cell adhesion-mediated drug resistance. *Blood*. 2009;114(20):4441-50.
228. Rawstron AC, Kennedy B, Evans PA, Davies FE, Richards SJ, Haynes AP, *et al*. Quantitation of minimal disease levels in chronic lymphocytic leukemia using a sensitive flow cytometric assay improves the prediction of outcome and can be used to optimize therapy. *Blood*. 2001;98(1):29-35.
229. Kucia M, Jankowski K, Reza R, Wysoczynski M, Bandura L, Allendorf DJ, *et al*. CXCR4-SDF-1 signalling, locomotion, chemotaxis and adhesion. *J Mol Histol*. 2004;35(3):233-45.
230. Burger JA, Burger M, Kipps TJ. Chronic lymphocytic leukemia B cells express functional CXCR4 chemokine receptors that mediate spontaneous migration beneath bone marrow stromal cells. *Blood*. 1999;94(11):3658-67.
231. Busillo JM, Benovic JL. Regulation of CXCR4 signaling. *Biochim Biophys Acta*. 2007;1768(4):952-63.
232. Amara A, Lorthioir O, Valenzuela A, Magerus A, Thelen M, Montes M, *et al*. Stromal cell-derived factor-1alpha associates with heparan sulfates through the first beta-strand of the chemokine. *J Biol Chem*. 1999;274(34):23916-25.
233. Ganju RK, Brubaker SA, Meyer J, Dutt P, Yang Y, Qin S, *et al*. The alpha-chemokine, stromal cell-derived factor-1alpha, binds to the transmembrane G-protein-coupled CXCR-4 receptor and activates multiple signal transduction pathways. *J Biol Chem*. 1998;273(36):23169-75.
234. Zhang XF, Wang JF, Matczak E, Proper JA, Gropman JE. Janus kinase 2 is involved in stromal cell-derived factor-1alpha-induced tyrosine phosphorylation of focal adhesion proteins and migration of hematopoietic progenitor cells. *Blood*. 2001;97(11):3342-8.
235. Chernock RD, Cherla RP, Ganju RK. SHP2 and cbl participate in alpha-chemokine receptor CXCR4-mediated signaling pathways. *Blood*. 2001;97(3):608-15.

236. Cox BD, Natarajan M, Stettner MR, Gladson CL. New concepts regarding focal adhesion kinase promotion of cell migration and proliferation. *J Cell Biochem.* 2006;99(1):35-52.
237. Ma Q, Jones D, Springer TA. The chemokine receptor CXCR4 is required for the retention of B lineage and granulocytic precursors within the bone marrow microenvironment. *Immunity.* 1999;10(4):463-71.
238. Ma Q, Jones D, Borghesani PR, Segal RA, Nagasawa T, Kishimoto T, *et al.* Impaired B-lymphopoiesis, myelopoiesis, and derailed cerebellar neuron migration in CXCR4- and SDF-1-deficient mice. *Proc Natl Acad Sci U S A.* 1998;95(16):9448-53.
239. Shen W, Bendall LJ, Gottlieb DJ, Bradstock KF. The chemokine receptor CXCR4 enhances integrin-mediated in vitro adhesion and facilitates engraftment of leukemic precursor-B cells in the bone marrow. *Exp Hematol.* 2001;29(12):1439-47.
240. Bleul CC, Schultze JL, Springer TA. B lymphocyte chemotaxis regulated in association with microanatomic localization, differentiation state, and B cell receptor engagement. *J Exp Med.* 1998;187(5):753-62.
241. Mohle R, Failenschmid C, Bautz F, Kanz L. Overexpression of the chemokine receptor CXCR4 in B cell chronic lymphocytic leukemia is associated with increased functional response to stromal cell-derived factor-1 (SDF-1). *Leukemia.* 1999;13(12):1954-9.
242. Burger JA, Tsukada N, Burger M, Zvaifler NJ, Dell'Aquila M, Kipps TJ. Blood-derived nurse-like cells protect chronic lymphocytic leukemia B cells from spontaneous apoptosis through stromal cell-derived factor-1. *Blood.* 2000;96(8):2655-63.
243. Abram CL, Lowell CA. The ins and outs of leukocyte integrin signaling. *Annu Rev Immunol.* 2009;27:339-62.
244. Vincent AM, Cawley JC, Burthem J. Integrin function in chronic lymphocytic leukemia. *Blood.* 1996;87(11):4780-8.
245. Molica S, Dattilo A, Mannella A, Levato D. Intercellular adhesion molecules (ICAMs) 2 and 3 are frequently expressed in B cell chronic lymphocytic leukemia. *Leukemia.* 1996;10(5):907-8.
246. De Rossi G, Zarcone D, Mauro F, Cerruti G, Tenca C, Puccetti A, *et al.* Adhesion molecule expression on B-cell chronic lymphocytic leukemia cells: malignant cell phenotypes define distinct disease subsets. *Blood.* 1993;81(10):2679-87.
247. Behr SI, Korinth D, Schriever F. Differential adhesion pattern of B cell chronic lymphocytic leukemia cells. *Leukemia.* 1998;12(1):71-7.
248. de la Fuente MT, Casanova B, Garcia-Gila M, Silva A, Garcia-Pardo A. Fibronectin interaction with alpha4beta1 integrin prevents apoptosis in B cell chronic lymphocytic leukemia: correlation with Bcl-2 and Bax. *Leukemia.* 1999;13(2):266-74.

249. de la Fuente MT, Casanova B, Moyano JV, Garcia-Gila M, Sanz L, Garcia-Marco J, *et al.* Engagement of alpha4beta1 integrin by fibronectin induces in vitro resistance of B chronic lymphocytic leukemia cells to fludarabine. *J Leukoc Biol.* 2002;71(3):495-502.
250. Gattei V, Bulian P, Del Principe MI, Zucchetto A, Maurillo L, Buccisano F, *et al.* Relevance of CD49d protein expression as overall survival and progressive disease prognosticator in chronic lymphocytic leukemia. *Blood.* 2008;111(2):865-73.
251. Shanafelt TD, Geyer SM, Bone ND, Tschumper RC, Witzig TE, Nowakowski GS, *et al.* CD49d expression is an independent predictor of overall survival in patients with chronic lymphocytic leukaemia: a prognostic parameter with therapeutic potential. *Br J Haematol.* 2008;140(5):537-46.
252. Nuckel H, Switala M, Collins CH, Sellmann L, Grosse-Wilde H, Duhrsen U, *et al.* High CD49d protein and mRNA expression predicts poor outcome in chronic lymphocytic leukemia. *Clin Immunol.* 2009;131(3):472-80.
253. Kay NE, Bone ND, Tschumper RC, Howell KH, Geyer SM, Dewald GW, *et al.* B-CLL cells are capable of synthesis and secretion of both pro- and anti-angiogenic molecules. *Leukemia.* 2002;16(5):911-9.
254. Edelmann J, Klein-Hitpass L, Carpinteiro A, Fuhrer A, Sellmann L, Stilgenbauer S, *et al.* Bone marrow fibroblasts induce expression of PI3K/NF-kappaB pathway genes and a pro-angiogenic phenotype in CLL cells. *Leuk Res.* 2008;32(10):1565-72.
255. Lee YK, Bone ND, Strege AK, Shanafelt TD, Jelinek DF, Kay NE. VEGF receptor phosphorylation status and apoptosis is modulated by a green tea component, epigallocatechin-3-gallate (EGCG), in B-cell chronic lymphocytic leukemia. *Blood.* 2004;104(3):788-94.
256. Veronese L, Tournilhac O, Verrelle P, Davi F, Dighiero G, Chautard E, *et al.* Strong correlation between VEGF and MCL-1 mRNA expression levels in B-cell chronic lymphocytic leukemia. *Leuk Res.* 2009;33(12):1623-6.
257. Molica S, Vitelli G, Levato D, Ricciotti A, Digiesi G. Clinicoprognostic implications of increased serum levels of vascular endothelial growth factor and basic fibroblastic growth factor in early B-cell chronic lymphocytic leukaemia. *Br J Cancer.* 2002;86(1):31-5.
258. Tsukada N, Burger JA, Zvaifler NJ, Kipps TJ. Distinctive features of "nurselike" cells that differentiate in the context of chronic lymphocytic leukemia. *Blood.* 2002;99(3):1030-7.
259. Nishio M, Endo T, Tsukada N, Ohata J, Kitada S, Reed JC, *et al.* Nurselike cells express BAFF and APRIL, which can promote survival of chronic lymphocytic leukemia cells via a paracrine pathway distinct from that of SDF-1alpha. *Blood.* 2005;106(3):1012-20.
260. Mackay F, Schneider P, Rennert P, Browning J. BAFF AND APRIL: a tutorial on B cell survival. *Annu Rev Immunol.* 2003;21:231-64.

261. Planelles L, Carvalho-Pinto CE, Hardenberg G, Smaniotto S, Savino W, Gomez-Caro R, *et al.* APRIL promotes B-1 cell-associated neoplasm. *Cancer Cell.* 2004;6(4):399-408.
262. Novak AJ, Bram RJ, Kay NE, Jelinek DF. Aberrant expression of B-lymphocyte stimulator by B chronic lymphocytic leukemia cells: a mechanism for survival. *Blood.* 2002;100(8):2973-9.
263. Kern C, Cornuel JF, Billard C, Tang R, Rouillard D, Stenou V, *et al.* Involvement of BAFF and APRIL in the resistance to apoptosis of B-CLL through an autocrine pathway. *Blood.* 2004;103(2):679-88.
264. Endo T, Nishio M,ENZLER T, Cottam HB, Fukuda T, James DF, *et al.* BAFF and APRIL support chronic lymphocytic leukemia B-cell survival through activation of the canonical NF-kappaB pathway. *Blood.* 2007;109(2):703-10.
265. Planelles L, Castillo-Gutierrez S, Medema JP, Morales-Luque A, Merle-Beral H, Hahne M. APRIL but not BLyS serum levels are increased in chronic lymphocytic leukemia: prognostic relevance of APRIL for survival. *Haematologica.* 2007;92(9):1284-5.
266. Bojarska-Junak A, Hus I, Chocholska S, Wasik-Szczepanek E, Sieklucka M, Dmoszynska A, *et al.* BAFF and APRIL expression in B-cell chronic lymphocytic leukemia: Correlation with biological and clinical features. *Leuk Res.* 2009;33(10):1319-27.
267. Molica S, Digiesi G, Mauro F, Mirabelli R, Cutrona G, Vitelli G, *et al.* Increased serum BAFF (B-cell activating factor of the TNF family) level is a peculiar feature associated with familial chronic lymphocytic leukemia. *Leuk Res.* 2009;33(1):162-5.
268. Deaglio S, Vaisitti T, Bergui L, Bonello L, Horenstein AL, Tamagnone L, *et al.* CD38 and CD100 lead a network of surface receptors relaying positive signals for B-CLL growth and survival. *Blood.* 2005;105(8):3042-50.
269. Deaglio S, Vaisitti T, Aydin S, Ferrero E, Malavasi F. In-tandem insight from basic science combined with clinical research: CD38 as both marker and key component of the pathogenetic network underlying chronic lymphocytic leukemia. *Blood.* 2006;108(4):1135-44.
270. Mellstedt H, Choudhury A. T and B cells in B-chronic lymphocytic leukaemia: Faust, Mephistopheles and the pact with the Devil. *Cancer Immunol Immunother.* 2006;55(2):210-20.
271. Serrano D, Monteiro J, Allen SL, Kolitz J, Schulman P, Lichtman SM, *et al.* Clonal expansion within the CD4+CD57+ and CD8+CD57+ T cell subsets in chronic lymphocytic leukemia. *J Immunol.* 1997;158(3):1482-9.
272. Porakishvili N, Roschupkina T, Kalber T, Jewell AP, Patterson K, Yong K, *et al.* Expansion of CD4+ T cells with a cytotoxic phenotype in patients with B-chronic lymphocytic leukaemia (B-CLL). *Clin Exp Immunol.* 2001;126(1):29-36.
273. Rossmann ED, Jeddi-Tehrani M, Osterborg A, Mellstedt H. T-cell signaling and costimulatory molecules in B-chronic lymphocytic leukemia (B-CLL): an

- increased abnormal expression by advancing stage. *Leukemia*. 2003;17(11):2252-4.
274. Van den Hove LE, Van Gool SW, Vandenberghe P, Bakkus M, Thielemans K, Boogaerts MA, *et al.* CD40 triggering of chronic lymphocytic leukemia B cells results in efficient alloantigen presentation and cytotoxic T lymphocyte induction by up-regulation of CD80 and CD86 costimulatory molecules. *Leukemia*. 1997;11(4):572-80.
275. Ramsay AG, Johnson AJ, Lee AM, Gorgun G, Le Dieu R, Blum W, *et al.* Chronic lymphocytic leukemia T cells show impaired immunological synapse formation that can be reversed with an immunomodulating drug. *J Clin Invest*. 2008;118(7):2427-37.
276. Krackhardt AM, Harig S, Witzens M, Broderick R, Barrett P, Gribben JG. T-cell responses against chronic lymphocytic leukemia cells: implications for immunotherapy. *Blood*. 2002;100(1):167-73.
277. Tinhofer I, Weiss L, Gassner F, Rubenzer G, Holler C, Greil R. Difference in the relative distribution of CD4+ T-cell subsets in B-CLL with mutated and unmutated immunoglobulin (Ig) VH genes: implication for the course of disease. *J Immunother*. 2009;32(3):302-9.
278. Roth A, de Beer D, Nuckel H, Sellmann L, Duhrsen U, Durig J, *et al.* Significantly shorter telomeres in T-cells of patients with ZAP-70(+)/CD38(+) chronic lymphocytic leukaemia. *Br J Haematol*. 2008;143(3):383-6.
279. Ghia P, Strola G, Granziero L, Geuna M, Guida G, Sallusto F, *et al.* Chronic lymphocytic leukemia B cells are endowed with the capacity to attract CD4+, CD40L+ T cells by producing CCL22. *Eur J Immunol*. 2002;32(5):1403-13.
280. Pizzolo G, Chilosi M, Ambrosetti A, Semenzato G, Fiore-Donati L, Perona G. Immunohistologic study of bone marrow involvement in B-chronic lymphocytic leukemia. *Blood*. 1983;62(6):1289-96.
281. Patten PE, Buggins AG, Richards J, Wotherspoon A, Salisbury J, Mufti GJ, *et al.* CD38 expression in chronic lymphocytic leukemia is regulated by the tumor microenvironment. *Blood*. 2008;111(10):5173-81.
282. Rossmann ED, Lewin N, Jeddi-Tehrani M, Osterborg A, Mellstedt H. Intracellular T cell cytokines in patients with B cell chronic lymphocytic leukaemia (B-CLL). *Eur J Haematol*. 2002;68(5):299-306.
283. Podhorecka M, Dmoszynska A, Rolinski J, Wasik E. T type 1/type 2 subsets balance in B-cell chronic lymphocytic leukemia--the three-color flow cytometry analysis. *Leuk Res*. 2002;26(7):657-60.
284. Gorgun G, Holderried TA, Zahrieh D, Neuberg D, Gribben JG. Chronic lymphocytic leukemia cells induce changes in gene expression of CD4 and CD8 T cells. *J Clin Invest*. 2005;115(7):1797-805.
285. Bishop GA, Hostager BS. The CD40-CD154 interaction in B cell-T cell liaisons. *Cytokine Growth Factor Rev*. 2003;14(3-4):297-309.

286. Harnett MM. CD40: a growing cytoplasmic tale. *Sci STKE*. 2004;(237):pe25.
287. Schattner EJ. CD40 ligand in CLL pathogenesis and therapy. *Leuk Lymphoma*. 2000;37(5-6):461-72.
288. Furman RR, Asgary Z, Mascarenhas JO, Liou HC, Schattner EJ. Modulation of NF-kappa B activity and apoptosis in chronic lymphocytic leukemia B cells. *J Immunol*. 2000;164(4):2200-6.
289. Kitada S, Zapata JM, Andreeff M, Reed JC. Bryostatins and CD40-ligand enhance apoptosis resistance and induce expression of cell survival genes in B-cell chronic lymphocytic leukaemia. *Br J Haematol*. 1999;106(4):995-1004.
290. Kater AP, Evers LM, Remmerswaal EB, Jaspers A, Oosterwijk MF, van Lier RA, *et al*. CD40 stimulation of B-cell chronic lymphocytic leukaemia cells enhances the anti-apoptotic profile, but also Bid expression and cells remain susceptible to autologous cytotoxic T-lymphocyte attack. *Br J Haematol*. 2004;127(4):404-15.
291. Dicker F, Kater AP, Prada CE, Fukuda T, Castro JE, Sun G, *et al*. CD154 induces p73 to overcome the resistance to apoptosis of chronic lymphocytic leukemia cells lacking functional p53. *Blood*. 2006;108(10):3450-7.
292. Smit LA, Hallaert DY, Spijker R, de Goeij B, Jaspers A, Kater AP, *et al*. Differential Noxa/Mcl-1 balance in peripheral versus lymph node chronic lymphocytic leukemia cells correlates with survival capacity. *Blood*. 2007;109(4):1660-8.
293. Fluckiger AC, Rossi JF, Bussel A, Bryon P, Banchereau J, Defrance T. Responsiveness of chronic lymphocytic leukemia B cells activated via surface Igs or CD40 to B-cell tropic factors. *Blood*. 1992;80(12):3173-81.
294. Crawford DH, Catovsky D. In vitro activation of leukaemic B cells by interleukin-4 and antibodies to CD40. *Immunology*. 1993;80(1):40-4.
295. Kay NE, Pittner BT. IL-4 biology: impact on normal and leukemic CLL B cells. *Leuk Lymphoma*. 2003;44(6):897-903.
296. Douglas RS, Capocasale RJ, Lamb RJ, Nowell PC, Moore JS. Chronic lymphocytic leukemia B cells are resistant to the apoptotic effects of transforming growth factor-beta. *Blood*. 1997;89(3):941-7.
297. Mainou-Fowler T, Miller S, Proctor SJ, Dickinson AM. The levels of TNF alpha, IL4 and IL10 production by T-cells in B-cell chronic lymphocytic leukaemia (B-CLL). *Leuk Res*. 2001;25(2):157-63.
298. Williams JF, Petrus MJ, Wright JA, Husebekk A, Fellowes V, Read EJ, *et al*. fas-mediated lysis of chronic lymphocytic leukaemia cells: role of type I versus type II cytokines and autologous fasL-expressing T cells. *Br J Haematol*. 1999;107(1):99-105.
299. Kay NE, Han L, Bone N, Williams G. Interleukin 4 content in chronic lymphocytic leukaemia (CLL) B cells and blood CD8+ T cells from B-CLL

- patients: impact on clonal B-cell apoptosis. *Br J Haematol.* 2001;112(3):760-7.
300. Barragan M, Bellosillo B, Campas C, Colomer D, Pons G, Gil J. Involvement of protein kinase C and phosphatidylinositol 3-kinase pathways in the survival of B-cell chronic lymphocytic leukemia cells. *Blood.* 2002;99(8):2969-76.
  301. Pleyer L, Egle A, Hartmann TN, Greil R. Molecular and cellular mechanisms of CLL: novel therapeutic approaches. *Nat Rev Clin Oncol.* 2009;6(7):405-18.
  302. Sawyers CL. Chronic myeloid leukemia. *N Engl J Med.* 1999;340(17):1330-40.
  303. Lombardo LJ, Lee FY, Chen P, Norris D, Barrish JC, Behnia K, *et al.* Discovery of N-(2-chloro-6-methyl-phenyl)-2-(6-(4-(2-hydroxyethyl)-piperazin-1-yl)-2-methylpyrimidin-4-ylamino)thiazole-5-carboxamide (BMS-354825), a dual Src/Abl kinase inhibitor with potent antitumor activity in preclinical assays. *J Med Chem.* 2004;47(27):6658-61.
  304. Tokarski JS, Newitt JA, Chang CY, Cheng JD, Wittekind M, Kiefer SE, *et al.* The structure of Dasatinib (BMS-354825) bound to activated ABL kinase domain elucidates its inhibitory activity against imatinib-resistant ABL mutants. *Cancer Res.* 2006;66(11):5790-7.
  305. Hantschel O, Rix U, Schmidt U, Burckstummer T, Kneidinger M, Schutze G, *et al.* The Btk tyrosine kinase is a major target of the Bcr-Abl inhibitor dasatinib. *Proc Natl Acad Sci U S A.* 2007;104(33):13283-8.
  306. Hantschel O, Rix U, Superti-Furga G. Target spectrum of the BCR-ABL inhibitors imatinib, nilotinib and dasatinib. *Leuk Lymphoma.* 2008;49(4):615-9.
  307. Rix U, Hantschel O, Durnberger G, Remsing Rix LL, Planyavsky M, Fernbach NV, *et al.* Chemical proteomic profiles of the BCR-ABL inhibitors imatinib, nilotinib, and dasatinib reveal novel kinase and nonkinase targets. *Blood.* 2007;110(12):4055-63.
  308. Luo FR, Yang Z, Camuso A, Smykla R, McGlinchey K, Fager K, *et al.* Dasatinib (BMS-354825) pharmacokinetics and pharmacodynamic biomarkers in animal models predict optimal clinical exposure. *Clin Cancer Res.* 2006;12(23):7180-6.
  309. Talpaz M, Shah NP, Kantarjian H, Donato N, Nicoll J, Paquette R, *et al.* Dasatinib in imatinib-resistant Philadelphia chromosome-positive leukemias. *N Engl J Med.* 2006;354(24):2531-41.
  310. Hochhaus A, Kantarjian HM, Baccarani M, Lipton JH, Apperley JF, Druker BJ, *et al.* Dasatinib induces notable hematologic and cytogenetic responses in chronic-phase chronic myeloid leukemia after failure of imatinib therapy. *Blood.* 2007;109(6):2303-9.
  311. Shah NP, Kantarjian HM, Kim DW, Rea D, Dorlhiac-Llacer PE, Milone JH, *et al.* Intermittent target inhibition with dasatinib 100 mg once daily

preserves efficacy and improves tolerability in imatinib-resistant and -intolerant chronic-phase chronic myeloid leukemia. *J Clin Oncol*. 2008;26(19):3204-12.

312. Johnson FM, Saigal B, Talpaz M, Donato NJ. Dasatinib (BMS-354825) tyrosine kinase inhibitor suppresses invasion and induces cell cycle arrest and apoptosis of head and neck squamous cell carcinoma and non-small cell lung cancer cells. *Clin Cancer Res*. 2005;11(19 Pt 1):6924-32.
313. Nam S, Kim D, Cheng JQ, Zhang S, Lee JH, Buettner R, *et al*. Action of the Src family kinase inhibitor, dasatinib (BMS-354825), on human prostate cancer cells. *Cancer Res*. 2005;65(20):9185-9.
314. Adams JM, Cory S. The Bcl-2 apoptotic switch in cancer development and therapy. *Oncogene*. 2007;26(9):1324-37.
315. Adams JM. Ways of dying: multiple pathways to apoptosis. *Genes Dev*. 2003;17(20):2481-95.
316. Taylor RC, Cullen SP, Martin SJ. Apoptosis: controlled demolition at the cellular level. *Nat Rev Mol Cell Biol*. 2008;9(3):231-41.
317. Castedo M, Ferri K, Roumier T, Metivier D, Zamzami N, Kroemer G. Quantitation of mitochondrial alterations associated with apoptosis. *J Immunol Methods*. 2002;265(1-2):39-47.
318. Adams JM, Cory S. Bcl-2-regulated apoptosis: mechanism and therapeutic potential. *Curr Opin Immunol*. 2007;19(5):488-96.
319. Kang MH, Reynolds CP. Bcl-2 inhibitors: targeting mitochondrial apoptotic pathways in cancer therapy. *Clin Cancer Res*. 2009;15(4):1126-32.
320. Pepper C, Hoy T, Bentley P. Elevated Bcl-2/Bax are a consistent feature of apoptosis resistance in B-cell chronic lymphocytic leukaemia and are correlated with in vivo chemoresistance. *Leuk Lymphoma*. 1998;28(3-4):355-61.
321. Pepper C, Thomas A, Hoy T, Cotter F, Bentley P. Antisense-mediated suppression of Bcl-2 highlights its pivotal role in failed apoptosis in B-cell chronic lymphocytic leukaemia. *Br J Haematol*. 1999;107(3):611-5.
322. Pepper C, Hooper K, Thomas A, Hoy T, Bentley P. Bcl-2 antisense oligonucleotides enhance the cytotoxicity of chlorambucil in B-cell chronic lymphocytic leukaemia cells. *Leuk Lymphoma*. 2001;42(3):491-8.
323. O'Brien SM, Cunningham CC, Golenkov AK, Turkina AG, Novick SC, Rai KR. Phase I to II multicenter study of oblimersen sodium, a Bcl-2 antisense oligonucleotide, in patients with advanced chronic lymphocytic leukemia. *J Clin Oncol*. 2005;23(30):7697-702.
324. O'Brien S, Moore JO, Boyd TE, Larratt LM, Skotnicki A, Koziner B, *et al*. Randomized phase III trial of fludarabine plus cyclophosphamide with or without oblimersen sodium (Bcl-2 antisense) in patients with relapsed or refractory chronic lymphocytic leukemia. *J Clin Oncol*. 2007;25(9):1114-20.

325. Enyedy IJ, Ling Y, Nacro K, Tomita Y, Wu X, Cao Y, *et al.* Discovery of small-molecule inhibitors of Bcl-2 through structure-based computer screening. *J Med Chem.* 2001;44(25):4313-24.
326. Campas C, Cosialls AM, Barragan M, Iglesias-Serret D, Santidrian AF, Coll-Mulet L, *et al.* Bcl-2 inhibitors induce apoptosis in chronic lymphocytic leukemia cells. *Exp Hematol.* 2006;34(12):1663-9.
327. Vogler M, Dinsdale D, Sun XM, Young KW, Butterworth M, Nicotera P, *et al.* A novel paradigm for rapid ABT-737-induced apoptosis involving outer mitochondrial membrane rupture in primary leukemia and lymphoma cells. *Cell Death Differ.* 2008;15(5):820-30.
328. Del Gaizo Moore V, Brown JR, Certo M, Love TM, Novina CD, Letai A. Chronic lymphocytic leukemia requires BCL2 to sequester prodeath BIM, explaining sensitivity to BCL2 antagonist ABT-737. *J Clin Invest.* 2007;117(1):112-21.
329. Vogler M, Butterworth M, Majid A, Walewska RJ, Sun XM, Dyer MJ, *et al.* Concurrent up-regulation of BCL-XL and BCL2A1 induces approximately 1000-fold resistance to ABT-737 in chronic lymphocytic leukemia. *Blood.* 2009;113(18):4403-13.
330. Banerji U. Heat shock protein 90 as a drug target: some like it hot. *Clin Cancer Res.* 2009;15(1):9-14.
331. Dempsey NC, Leoni F, Ireland HE, Hoyle C, Williams JH. Differential heat shock protein localization in chronic lymphocytic leukemia. *J Leukoc Biol.* 2010;87(3):467-76.
332. Castro JE, Prada CE, Loria O, Kamal A, Chen L, Burrows FJ, *et al.* ZAP-70 is a novel conditional heat shock protein 90 (Hsp90) client: inhibition of Hsp90 leads to ZAP-70 degradation, apoptosis, and impaired signaling in chronic lymphocytic leukemia. *Blood.* 2005;106(7):2506-12.
333. Neckers L. Hsp90 inhibitors as novel cancer chemotherapeutic agents. *Trends Mol Med.* 2002;8(4 Suppl):S55-61.
334. Jones DT, Addison E, North JM, Lowdell MW, Hoffbrand AV, Mehta AB, *et al.* Geldanamycin and herbimycin A induce apoptotic killing of B chronic lymphocytic leukemia cells and augment the cells' sensitivity to cytotoxic drugs. *Blood.* 2004;103(5):1855-61.
335. Johnson AJ, Wagner AJ, Cheney CM, Smith LL, Lucas DM, Guster SK, *et al.* Rituximab and 17-allylamino-17-demethoxygeldanamycin induce synergistic apoptosis in B-cell chronic lymphocytic leukaemia. *Br J Haematol.* 2007;139(5):837-44.
336. Lin K, Rockliffe N, Johnson GG, Sherrington PD, Pettitt AR. Hsp90 inhibition has opposing effects on wild-type and mutant p53 and induces p21 expression and cytotoxicity irrespective of p53/ATM status in chronic lymphocytic leukaemia cells. *Oncogene.* 2008;27(17):2445-55.
337. Milanesi E, Costantini P, Gambalunga A, Colonna R, Petronilli V, Cabrelle A, *et al.* The mitochondrial effects of small organic ligands of BCL-2:

- sensitization of BCL-2-overexpressing cells to apoptosis by a pyrimidine-2,4,6-trione derivative. *J Biol Chem*. 2006;281(15):10066-72.
338. Quah BJ, Warren HS, Parish CR. Monitoring lymphocyte proliferation in vitro and in vivo with the intracellular fluorescent dye carboxyfluorescein diacetate succinimidyl ester. *Nat Protoc*. 2007;2(9):2049-56.
339. Grynkiewicz G, Poenie M, Tsien RY. A new generation of Ca<sup>2+</sup> indicators with greatly improved fluorescence properties. *J Biol Chem*. 1985;260(6):3440-50.
340. Chou TC. Theoretical basis, experimental design, and computerized simulation of synergism and antagonism in drug combination studies. *Pharmacol Rev*. 2006;58(3):621-81.
341. Peng B, Hayes M, Resta D, Racine-Poon A, Druker BJ, Talpaz M, *et al*. Pharmacokinetics and pharmacodynamics of imatinib in a phase I trial with chronic myeloid leukemia patients. *J Clin Oncol*. 2004;22(5):935-42.
342. Dasatinib (BMS-354825) Oncologic Drug Advisory Committee (ODAC) Briefing Document, NDA 21-986: Bristol-Myers-Squibb Company 2006.
343. Koopman G, Reutelingsperger CP, Kuijten GA, Keehnen RM, Pals ST, van Oers MH. Annexin V for flow cytometric detection of phosphatidylserine expression on B cells undergoing apoptosis. *Blood*. 1994;84(5):1415-20.
344. Hammill AK, Uhr JW, Scheuermann RH. Annexin V staining due to loss of membrane asymmetry can be reversible and precede commitment to apoptotic death. *Exp Cell Res*. 1999;251(1):16-21.
345. Tait SW, Green DR. Caspase-independent cell death: leaving the set without the final cut. *Oncogene*. 2008;27(50):6452-61.
346. Conus S, Simon HU. Cathepsins: key modulators of cell death and inflammatory responses. *Biochem Pharmacol*. 2008;76(11):1374-82.
347. Snead JL, O'Hare T, Adrian LT, Eide CA, Lange T, Druker BJ, *et al*. Acute dasatinib exposure commits Bcr-Abl-dependent cells to apoptosis. *Blood*. 2009;114(16):3459-63.
348. Trentin L, Frasson M, Donella-Deana A, Frezzato F, Pagano MA, Tibaldi E, *et al*. Geldanamycin-induced Lyn dissociation from aberrant HSP90-stabilized cytosolic complex is an early event in apoptotic mechanisms in B-chronic lymphocytic leukemia. *Blood*. 2008;112(12):4665-74.
349. Scielzo C, Ghia P, Conti A, Bachi A, Guida G, Geuna M, *et al*. HS1 protein is differentially expressed in chronic lymphocytic leukemia patient subsets with good or poor prognoses. *J Clin Invest*. 2005;115(6):1644-50.
350. Amrein L, Hernandez TA, Ferrario C, Johnston J, Gibson SB, Panasci L, *et al*. Dasatinib sensitizes primary chronic lymphocytic leukaemia lymphocytes to chlorambucil and fludarabine in vitro. *Br J Haematol*. 2008;143(5):698-706.

351. Abts H, Jucker M, Diehl V, Tesch H. Human chronic lymphocytic leukemia cells regularly express mRNAs of the protooncogenes *lck* and *c-fgr*. *Leuk Res.* 1991;15(11):987-97.
352. Majolini MB, D'Elis MM, Galieni P, Boncristiano M, Lauria F, Del Prete G, *et al.* Expression of the T-cell-specific tyrosine kinase *Lck* in normal B-1 cells and in chronic lymphocytic leukemia B cells. *Blood.* 1998;91(9):3390-6.
353. Veldurthy A, Patz M, Hagist S, Pallasch CP, Wendtner CM, Hallek M, *et al.* The kinase inhibitor dasatinib induces apoptosis in chronic lymphocytic leukemia cells in vitro with preference for a subgroup of patients with unmutated IgVH genes. *Blood.* 2008;112:1443-52.
354. Ke J, Chelvarajan RL, Sindhava V, Robertson DA, Lekakis L, Jennings CD, *et al.* Anomalous constitutive Src kinase activity promotes B lymphoma survival and growth. *Mol Cancer.* 2009;8:132.
355. Hallaert DY, Jaspers A, van Noesel CJ, van Oers MH, Kater AP, Eldering E. *c-Abl* kinase inhibitors overcome CD40-mediated drug resistance in CLL; Implications for therapeutic targeting of chemoresistant niches. *Blood.* 2008;112(13):5141-9.
356. Song Z, Lu P, Furman RR, Leonard JP, Martin P, Tyrell L, *et al.* Activities of SYK and PLCgamma2 predict apoptotic response of CLL cells to SRC tyrosine kinase inhibitor dasatinib. *Clin Cancer Res.* 2010;16(2):587-99.
357. Tavolaro S, Chiaretti S, Messina M, Peragine N, Del Giudice I, Marinelli M, *et al.* Gene expression profile of protein kinases reveals a distinctive signature in chronic lymphocytic leukemia and in vitro experiments support a role of second generation protein kinase inhibitors. *Leuk Res.* 2010 (in press).
358. Tecchio C, Nichele I, Todeschini G, Pizzolo G, Ambrosetti A. Dasatinib-induced response in a rare case of chronic lymphocytic leukaemia associated with chronic myeloid leukaemia. *Br J Haematol.* 2009;146(2):222-3.
359. Hewamana S, Lin TT, Rowntree C, Karunanithi K, Pratt G, Hills R, *et al.* Rel A Is an Independent Biomarker of Clinical Outcome in Chronic Lymphocytic Leukemia. *J Clin Oncol.* 2009;27(5):763-9.
360. Cuni S, Perez-Aciego P, Perez-Chacon G, Vargas JA, Sanchez A, Martin-Saavedra FM, *et al.* A sustained activation of PI3K/NF-kappaB pathway is critical for the survival of chronic lymphocytic leukemia B cells. *Leukemia.* 2004;18(8):1391-400.
361. Chow KU, Nowak D, Hofmann W, Schneider B, Hofmann WK. Imatinib induces apoptosis in CLL lymphocytes with high expression of Par-4. *Leukemia.* 2005;19(6):1103-5.
362. Ranganathan P, Rangnekar VM. Regulation of cancer cell survival by Par-4. *Ann N Y Acad Sci.* 2005;1059:76-85.

363. Boehrer S, Kukoc-Zivojnov N, Nowak D, Bergmann M, Baum C, Puccetti E, *et al.* Upon drug-induced apoptosis expression of prostate-apoptosis-response-gene-4 promotes cleavage of caspase-8, bid and mitochondrial release of cytochrome c. *Hematology*. 2004;9(5-6):425-31.
364. Brieger A, Boehrer S, Schaaf S, Nowak D, Ruthardt M, Kim SZ, *et al.* In bcr-abl-positive myeloid cells resistant to conventional chemotherapeutic agents, expression of Par-4 increases sensitivity to imatinib (STI571) and histone deacetylase-inhibitors. *Biochem Pharmacol*. 2004;68(1):85-93.
365. Amrein L, Panasci L, Gibson SB, Johnston JB, Soulieres D, Aloyz R. Primary del 17 chronic lymphocytic leukaemia lymphocytes are hypersensitive to dasatinib in vitro. *Br J Haematol*. 2009;147(3):396-8.
366. Bitomsky N, Hofmann TG. Apoptosis and autophagy: Regulation of apoptosis by DNA damage signalling - roles of p53, p73 and HIPK2. *FEBS J*. 2009;276(21):6074-83.
367. Steele AJ, Prentice AG, Hoffbrand AV, Yogashangary BC, Hart SM, Nacheva EP, *et al.* p53-mediated apoptosis of CLL cells: evidence for a transcription-independent mechanism. *Blood*. 2008;112(9):3827-34.
368. Pitini V, Arrigo C, Altavilla G. Dasatinib induces a response in chronic lymphocytic leukemia. *Blood*. 2009;113(2):498.
369. Nowak D, Boehrer S, Hochmuth S, Trepohl B, Hofmann W, Hoelzer D, *et al.* Src kinase inhibitors induce apoptosis and mediate cell cycle arrest in lymphoma cells. *Anticancer Drugs*. 2007;18(9):981-95.
370. Jia SH, Parodo J, Kapus A, Rotstein OD, Marshall JC. Dynamic regulation of neutrophil survival through tyrosine phosphorylation or dephosphorylation of caspase-8. *J Biol Chem*. 2008;283(9):5402-13.
371. Chowdhury I, Tharakan B, Bhat GK. Caspases - an update. *Comp Biochem Physiol B Biochem Mol Biol*. 2008;151(1):10-27.
372. Blake S, Hughes TP, Mayrhofer G, Lyons AB. The Src/ABL kinase inhibitor dasatinib (BMS-354825) inhibits function of normal human T-lymphocytes in vitro. *Clin Immunol*. 2008;127(3):330-9.
373. Monroe JG. ITAM-mediated tonic signalling through pre-BCR and BCR complexes. *Nat Rev Immunol*. 2006;6(4):283-94.
374. Amrein PC, Attar E, Takvorian T, Hochberg E, Ballen K, Leahy KM, *et al.* Dasatinib Has Activity in Relapsed/Refractory Chronic Lymphocytic Leukaemia (CLL/SLL), a Phase II Trial *Blood*. 2008;112(11): abstract 3162.
375. Begleiter A, Mowat M, Israels LG, Johnston JB. Chlorambucil in chronic lymphocytic leukemia: mechanism of action. *Leuk Lymphoma*. 1996;23(3-4):187-201.
376. Torres-Garcia SJ, Cousineau L, Caplan S, Panasci L. Correlation of resistance to nitrogen mustards in chronic lymphocytic leukemia with enhanced removal of melphalan-induced DNA cross-links. *Biochem Pharmacol*. 1989;38(18):3122-3.

377. Yoshida K, Yamaguchi T, Natsume T, Kufe D, Miki Y. JNK phosphorylation of 14-3-3 proteins regulates nuclear targeting of c-Abl in the apoptotic response to DNA damage. *Nat Cell Biol.* 2005;7(3):278-85.
378. Yuan ZM, Huang Y, Ishiko T, Nakada S, Utsugisawa T, Kharbanda S, *et al.* Regulation of Rad51 function by c-Abl in response to DNA damage. *J Biol Chem.* 1998;273(7):3799-802.
379. Chen G, Yuan SS, Liu W, Xu Y, Trujillo K, Song B, *et al.* Radiation-induced assembly of Rad51 and Rad52 recombination complex requires ATM and c-Abl. *J Biol Chem.* 1999;274(18):12748-52.
380. Pettitt AR. Mechanism of action of purine analogues in chronic lymphocytic leukaemia. *Br J Haematol.* 2003;121(5):692-702.
381. Kraus M, Alimzhanov MB, Rajewsky N, Rajewsky K. Survival of resting mature B lymphocytes depends on BCR signaling via the Igalpha/beta heterodimer. *Cell.* 2004;117(6):787-800.
382. Gururajan M, Jennings CD, Bondada S. Cutting edge: constitutive B cell receptor signaling is critical for basal growth of B lymphoma. *J Immunol.* 2006;176(10):5715-9.
383. Chen L, Monti S, Juszczynski P, Daley J, Chen W, Witzig TE, *et al.* SYK-dependent tonic B-cell receptor signaling is a rational treatment target in diffuse large B-cell lymphoma. *Blood.* 2008;111(4):2230-7.
384. Young RM, Hardy IR, Clarke RL, Lundy N, Pine P, Turner BC, *et al.* Mouse models of non-Hodgkin lymphoma reveal Syk as an important therapeutic target. *Blood.* 2009;113(11):2508-16.
385. Yang C, Lu P, Lee FY, Chadburn A, Barrientos JC, Leonard JP, *et al.* Tyrosine kinase inhibition in diffuse large B-cell lymphoma: molecular basis for antitumor activity and drug resistance of dasatinib. *Leukemia.* 2008;22(9):1755-66.
386. Guinamard R, Signoret N, Ishiai M, Marsh M, Kurosaki T, Ravetch JV. B cell antigen receptor engagement inhibits stromal cell-derived factor (SDF)-1alpha chemotaxis and promotes protein kinase C (PKC)-induced internalization of CXCR4. *J Exp Med.* 1999;189(9):1461-6.
387. Casamayor-Palleja M, Mondiere P, Verschelde C, Bella C, Defrance T. BCR ligation reprograms B cells for migration to the T zone and B-cell follicle sequentially. *Blood.* 2002;99(6):1913-21.
388. Vlad A, Deglesne PA, Letestu R, Saint-Georges S, Chevallier N, Baran-Marszak F, *et al.* Down-regulation of CXCR4 and CD62L in chronic lymphocytic leukemia cells is triggered by B-cell receptor ligation and associated with progressive disease. *Cancer Res.* 2009;69(16):6387-95.
389. Geahlen RL. Syk and pTyr'd: Signaling through the B cell antigen receptor. *Biochim Biophys Acta.* 2009;1793(7):1115-27.

390. Michie AM, Trop S, Wiest DL, Zuniga-Pflucker JC. Extracellular signal-regulated kinase (ERK) activation by the pre-T cell receptor in developing thymocytes in vivo. *J Exp Med*. 1999;190(11):1647-56.
391. Buchner M, Fuchs S, Prinz G, Pfeifer D, Bartholome K, Burger M, *et al*. Spleen tyrosine kinase is overexpressed and represents a potential therapeutic target in chronic lymphocytic leukemia. *Cancer Res*. 2009;69(13):5424-32.
392. Serrels A, Macpherson IR, Evans TR, Lee FY, Clark EA, Sansom OJ, *et al*. Identification of potential biomarkers for measuring inhibition of Src kinase activity in colon cancer cells following treatment with dasatinib. *Mol Cancer Ther*. 2006;5(12):3014-22.
393. Burger M, Hartmann T, Krome M, Rawluk J, Tamamura H, Fujii N, *et al*. Small peptide inhibitors of the CXCR4 chemokine receptor (CD184) antagonize the activation, migration, and antiapoptotic responses of CXCL12 in chronic lymphocytic leukemia B cells. *Blood*. 2005;106(5):1824-30.
394. Baudot AD, Jeandel PY, Mouska X, Maurer U, Tartare-Deckert S, Raynaud SD, *et al*. The tyrosine kinase Syk regulates the survival of chronic lymphocytic leukemia B cells through PKCdelta and proteasome-dependent regulation of Mcl-1 expression. *Oncogene*. 2009;28(37):3261-73.
395. Gobessi S, Laurenti L, Longo PG, Carsetti L, Berno V, Sica S, *et al*. Inhibition of constitutive and BCR-induced Syk activation downregulates Mcl-1 and induces apoptosis in chronic lymphocytic leukemia B cells. *Leukemia*. 2009;23(4):686-97.
396. Friedberg JW, Sharman J, Sweetenham J, Johnston PB, Vose JM, Lacasce A, *et al*. Inhibition of Syk with fostamatinib disodium has significant clinical activity in non Hodgkin's lymphoma and chronic lymphocytic leukemia. *Blood*. 2010;115(13):2578-85.
397. Rolli V, Gallwitz M, Wossning T, Flemming A, Schamel WW, Zurn C, *et al*. Amplification of B cell antigen receptor signaling by a Syk/ITAM positive feedback loop. *Mol Cell*. 2002;10(5):1057-69.
398. Chen L, Juszczynski P, Takeyama K, Aguiar RC, Shipp MA. Protein tyrosine phosphatase receptor-type O truncated (PTPROt) regulates SYK phosphorylation, proximal B-cell-receptor signaling, and cellular proliferation. *Blood*. 2006;108(10):3428-33.
399. Motiwala T, Majumder S, Kutay H, Smith DS, Neuberg DS, Lucas DM, *et al*. Methylation and silencing of protein tyrosine phosphatase receptor type O in chronic lymphocytic leukemia. *Clin Cancer Res*. 2007;13(11):3174-81.
400. Juszczynski P, Chen L, O'Donnell E, Polo JM, Ranuncolo SM, Dalla-Favera R, *et al*. BCL6 modulates tonic BCR signaling in diffuse large B-cell lymphomas by repressing the SYK phosphatase, PTPROt. *Blood*. 2009;114(26):5315-21.
401. Shor AC, Keschman EA, Lee FY, Muro-Cacho C, Letson GD, Trent JC, *et al*. Dasatinib inhibits migration and invasion in diverse human sarcoma cell

- lines and induces apoptosis in bone sarcoma cells dependent on SRC kinase for survival. *Cancer Res.* 2007;67(6):2800-8.
402. Tsao AS, He D, Saigal B, Liu S, Lee JJ, Bakkannagari S, *et al.* Inhibition of c-Src expression and activation in malignant pleural mesothelioma tissues leads to apoptosis, cell cycle arrest, and decreased migration and invasion. *Mol Cancer Ther.* 2007;6(7):1962-72.
403. Buettner R, Mesa T, Vultur A, Lee F, Jove R. Inhibition of Src family kinases with dasatinib blocks migration and invasion of human melanoma cells. *Mol Cancer Res.* 2008;6(11):1766-74.
404. Ozkal S, Paterson JC, Tedoldi S, Hansmann ML, Kargi A, Manek S, *et al.* Focal adhesion kinase (FAK) expression in normal and neoplastic lymphoid tissues. *Pathol Res Pract.* 2009;205(11):781-8.
405. Le Y, Honczarenko M, Glodek AM, Ho DK, Silberstein LE. CXC chemokine ligand 12-induced focal adhesion kinase activation and segregation into membrane domains is modulated by regulator of G protein signaling 1 in pro-B cells. *J Immunol.* 2005;174(5):2582-90.
406. Le Y, Zhu BM, Harley B, Park SY, Kobayashi T, Manis JP, *et al.* SOCS3 protein developmentally regulates the chemokine receptor CXCR4-FAK signaling pathway during B lymphopoiesis. *Immunity.* 2007;27(5):811-23.
407. Ptasznik A, Urbanowska E, Chinta S, Costa MA, Katz BA, Stanislaus MA, *et al.* Crosstalk between BCR/ABL oncoprotein and CXCR4 signaling through a Src family kinase in human leukemia cells. *J Exp Med.* 2002;196(5):667-78.
408. Nakata Y, Tomkowicz B, Gewirtz AM, Ptasznik A. Integrin inhibition through Lyn-dependent cross talk from CXCR4 chemokine receptors in normal human CD34+ marrow cells. *Blood.* 2006;107(11):4234-9.
409. Pleiman CM, Hertz WM, Cambier JC. Activation of phosphatidylinositol-3' kinase by Src-family kinase SH3 binding to the p85 subunit. *Science.* 1994;263(5153):1609-12.
410. Ptasznik A, Traynor-Kaplan A, Bokoch GM. G protein-coupled chemoattractant receptors regulate Lyn tyrosine kinase. Shc adapter protein signaling complexes. *J Biol Chem.* 1995;270(34):19969-73.
411. Fox JA, Ung K, Tanlimco SG, Jirik FR. Disruption of a single Pten allele augments the chemotactic response of B lymphocytes to stromal cell-derived factor-1. *J Immunol.* 2002;169(1):49-54.
412. Niedermeier M, Hennessy BT, Knight ZA, Henneberg M, Hu J, Kurtova AV, *et al.* Isoform-selective phosphoinositide 3'-kinase inhibitors inhibit CXCR4 signaling and overcome stromal cell-mediated drug resistance in chronic lymphocytic leukemia: a novel therapeutic approach. *Blood.* 2009;113(22):5549-57.
413. Matsusaka S, Tohyama Y, He J, Shi Y, Hazama R, Kadono T, *et al.* Protein-tyrosine kinase, Syk, is required for CXCL12-induced polarization of B cells. *Biochem Biophys Res Commun.* 2005;328(4):1163-9.

414. Juarez JG, Thien M, Dela Pena A, Baraz R, Bradstock KF, Bendall LJ. CXCR4 mediates the homing of B cell progenitor acute lymphoblastic leukaemia cells to the bone marrow via activation of p38MAPK. *Br J Haematol.* 2009;145(4):491-9.
415. Kurtova A, Sivina M, Quiroga MP, Wierda WG, Keating MJ, Burger JA. The Immunophenotype Signature CD49d+CD38+ Identifies Chronic Lymphocytic Leukemia Cases with a Higher Potential for Migration Beneath Marrow Stromal Cells. *ASH Annual Meeting Abstracts.* 2009;114(22): abstract 356.
416. Zucchetto A, Vaisitti T, Benedetti D, Bomben R, Dal-Bo M, Degan M, *et al.* CD38 CD49d Are Physically and Functionally Associated in B-Cell Chronic Lymphocytic Leukemia Cells. *ASH Annual Meeting Abstracts.* 2009;114(22): abstract 357.
417. Buggins AGS, Levi A, Gohil S, Fishlock K, Patten PE, Yallop D, *et al.* Evidence for A Macromolecular Complex in Poor Prognostic CLL That Contains CD38, CD49d, CD44, MMP-9 and ZAP-70. *ASH Annual Meeting Abstracts.* 2009;114(22): abstract 2334.
418. Constantin G, Majeed M, Giagulli C, Piccio L, Kim JY, Butcher EC, *et al.* Chemokines trigger immediate beta2 integrin affinity and mobility changes: differential regulation and roles in lymphocyte arrest under flow. *Immunity.* 2000;13(6):759-69.
419. Lopez-Giral S, Quintana NE, Cabrerizo M, Alfonso-Perez M, Sala-Valdes M, De Soria VG, *et al.* Chemokine receptors that mediate B cell homing to secondary lymphoid tissues are highly expressed in B cell chronic lymphocytic leukemia and non-Hodgkin lymphomas with widespread nodular dissemination. *J Leukoc Biol.* 2004;76(2):462-71.
420. Redondo-Munoz J, Jose Terol M, Garcia-Marco JA, Garcia-Pardo A. Matrix metalloproteinase-9 is up-regulated by CCL21/CCR7 interaction via extracellular signal-regulated kinase-1/2 signaling and is involved in CCL21-driven B-cell chronic lymphocytic leukemia cell invasion and migration. *Blood.* 2008;111(1):383-6.
421. Redondo-Munoz J, Escobar-Diaz E, Samaniego R, Terol MJ, Garcia-Marco JA, Garcia-Pardo A. MMP-9 in B-cell chronic lymphocytic leukemia is up-regulated by alpha4beta1 integrin or CXCR4 engagement via distinct signaling pathways, localizes to podosomes, and is involved in cell invasion and migration. *Blood.* 2006;108(9):3143-51.
422. Tretter T, Schuler M, Schneller F, Brass U, Esswein M, Aman MJ, *et al.* Direct cellular interaction with activated CD4(+) T cells overcomes hyporesponsiveness of B-cell chronic lymphocytic leukemia in vitro. *Cell Immunol.* 1998;189(1):41-50.
423. Jacob A, Pound JD, Challa A, Gordon J. Release of clonal block in B cell chronic lymphocytic leukaemia by engagement of co-operative epitopes on CD40. *Leuk Res.* 1998;22(4):379-82.

424. Grdisa M. Influence of CD40 ligation on survival and apoptosis of B-CLL cells in vitro. *Leuk Res.* 2003;27(10):951-6.
425. Granziero L, Ghia P, Circosta P, Gottardi D, Strola G, Geuna M, *et al.* Survivin is expressed on CD40 stimulation and interfaces proliferation and apoptosis in B-cell chronic lymphocytic leukemia. *Blood.* 2001;97(9):2777-83.
426. Willimott S, Baou M, Naresh K, Wagner SD. CD154 induces a switch in pro-survival Bcl-2 family members in chronic lymphocytic leukaemia. *Br J Haematol.* 2007;138(6):721-32.
427. Steelman LS, Abrams SL, Whelan J, Bertrand FE, Ludwig DE, Basecke J, *et al.* Contributions of the Raf/MEK/ERK, PI3K/PTEN/Akt/mTOR and Jak/STAT pathways to leukemia. *Leukemia.* 2008;22(4):686-707.
428. O'Connor L, Strasser A, O'Reilly LA, Hausmann G, Adams JM, Cory S, *et al.* Bim: a novel member of the Bcl-2 family that promotes apoptosis. *EMBO J.* 1998;17(2):384-95.
429. Copland M, Hamilton A, Elrick LJ, Baird JW, Allan EK, Jordanides N, *et al.* Dasatinib (BMS-354825) targets an earlier progenitor population than imatinib in primary CML but does not eliminate the quiescent fraction. *Blood.* 2006;107(11):4532-9.
430. Finn RS, Dering J, Ginther C, Wilson CA, Glaspy P, Tchekmedyian N, *et al.* Dasatinib, an orally active small molecule inhibitor of both the src and abl kinases, selectively inhibits growth of basal-type/"triple-negative" breast cancer cell lines growing in vitro. *Breast Cancer Res Treat.* 2007;105(3):319-26.
431. Timeus F, Crescenzo N, Fandi A, Doria A, Foglia L, Cordero di Montezemolo L. In vitro antiproliferative and antimigratory activity of dasatinib in neuroblastoma and Ewing sarcoma cell lines. *Oncol Rep.* 2008;19(2):353-9.
432. Silvennoinen R, Malminiemi K, Malminiemi O, Seppala E, Vilpo J. Pharmacokinetics of chlorambucil in patients with chronic lymphocytic leukaemia: comparison of different days, cycles and doses. *Pharmacol Toxicol.* 2000;87(5):223-8.
433. Foran JM, Oscier D, Orchard J, Johnson SA, Tighe M, Cullen MH, *et al.* Pharmacokinetic study of single doses of oral fludarabine phosphate in patients with "low-grade" non-Hodgkin's lymphoma and B-cell chronic lymphocytic leukemia. *J Clin Oncol.* 1999;17(5):1574-9.
434. Ringshausen I, Schneller F, Bogner C, Hipp S, Duyster J, Peschel C, *et al.* Constitutively activated phosphatidylinositol-3 kinase (PI-3K) is involved in the defect of apoptosis in B-CLL: association with protein kinase Cdelta. *Blood.* 2002;100(10):3741-8.
435. Plate JM. PI3-kinase regulates survival of chronic lymphocytic leukemia B-cells by preventing caspase 8 activation. *Leuk Lymphoma.* 2004;45(8):1519-29.

436. Zhuang J, Hawkins SF, Glenn MA, Lin K, Johnson GG, Carter A, *et al.* Akt is activated in chronic lymphocytic leukemia cells and delivers a pro-survival signal: the therapeutic potential of Akt inhibition. *Haematologica*. 2010;95(1):110-8.
437. Jones DT, Ganeshaguru K, Anderson RJ, Jackson TR, Bruckdorfer KR, Low SY, *et al.* Albumin activates the AKT signaling pathway and protects B-chronic lymphocytic leukemia cells from chlorambucil- and radiation-induced apoptosis. *Blood*. 2003;101(8):3174-80.
438. Millward TA, Zolnierowicz S, Hemmings BA. Regulation of protein kinase cascades by protein phosphatase 2A. *Trends Biochem Sci*. 1999;24(5):186-91.
439. Honkanen RE, Zwiller J, Moore RE, Daily SL, Khatra BS, Dukelow M, *et al.* Characterization of microcystin-LR, a potent inhibitor of type 1 and type 2A protein phosphatases. *J Biol Chem*. 1990;265(32):19401-4.
440. Barragan M, de Frias M, Iglesias-Serret D, Campas C, Castano E, Santidrian AF, *et al.* Regulation of Akt/PKB by phosphatidylinositol 3-kinase-dependent and -independent pathways in B-cell chronic lymphocytic leukemia cells: role of protein kinase C $\beta$ . *J Leukoc Biol*. 2006;80(6):1473-9.
441. Leseux L, Hamdi SM, Al Saati T, Capilla F, Recher C, Laurent G, *et al.* Syk-dependent mTOR activation in follicular lymphoma cells. *Blood*. 2006;108(13):4156-62.
442. Buchner M, Baer C, Prinz G, Dierks C, Burger M, Zenz T, *et al.* Spleen tyrosine kinase inhibition prevents chemokine- and integrin-mediated stromal protective effects in chronic lymphocytic leukemia. *Blood*. 2010 (in press).
443. Ringshausen I, Dechow T, Schneller F, Weick K, Oelsner M, Peschel C, *et al.* Constitutive activation of the MAPkinase p38 is critical for MMP-9 production and survival of B-CLL cells on bone marrow stromal cells. *Leukemia*. 2004;18(12):1964-70.
444. Dittel BN, McCarthy JB, Wayner EA, LeBien TW. Regulation of human B-cell precursor adhesion to bone marrow stromal cells by cytokines that exert opposing effects on the expression of vascular cell adhesion molecule-1 (VCAM-1). *Blood*. 1993;81(9):2272-82.
445. Zucchetto A, Benedetti D, Tripodo C, Bomben R, Dal Bo M, Marconi D, *et al.* CD38/CD31, the CCL3 and CCL4 chemokines, and CD49d/vascular cell adhesion molecule-1 are interchained by sequential events sustaining chronic lymphocytic leukemia cell survival. *Cancer Res*. 2009;69(9):4001-9.
446. Lwin T, Crespo LA, Wu A, Dessureault S, Shu HB, Moscinski LC, *et al.* Lymphoma cell adhesion-induced expression of B cell-activating factor of the TNF family in bone marrow stromal cells protects non-Hodgkin's B lymphoma cells from apoptosis. *Leukemia*. 2009;23(1):170-7.
447. Matsunaga T, Fukai F, Miura S, Nakane Y, Owaki T, Kodama H, *et al.* Combination therapy of an anticancer drug with the FNIII14 peptide of

- fibronectin effectively overcomes cell adhesion-mediated drug resistance of acute myelogenous leukemia. *Leukemia*. 2008;22(2):353-60.
448. Dadgostar H, Zarnegar B, Hoffmann A, Qin XF, Truong U, Rao G, *et al*. Cooperation of multiple signaling pathways in CD40-regulated gene expression in B lymphocytes. *Proc Natl Acad Sci U S A*. 2002;99(3):1497-502.
  449. Schade AE, Schieven GL, Townsend R, Jankowska AM, Susulic V, Zhang R, *et al*. Dasatinib, a small-molecule protein tyrosine kinase inhibitor, inhibits T-cell activation and proliferation. *Blood*. 2008;111(3):1366-77.
  450. Decker T, Schneller F, Sparwasser T, Tretter T, Lipford GB, Wagner H, *et al*. Immunostimulatory CpG-oligonucleotides cause proliferation, cytokine production, and an immunogenic phenotype in chronic lymphocytic leukemia B cells. *Blood*. 2000;95(3):999-1006.
  451. Longo PG, Laurenti L, Gobessi S, Petlickovski A, Pelosi M, Chiusolo P, *et al*. The Akt signaling pathway determines the different proliferative capacity of chronic lymphocytic leukemia B-cells from patients with progressive and stable disease. *Leukemia*. 2007;21(1):110-20.
  452. Weichsel R, Dix C, Wooldridge L, Clement M, Fenton-May A, Sewell AK, *et al*. Profound inhibition of antigen-specific T-cell effector functions by dasatinib. *Clin Cancer Res*. 2008;14(8):2484-91.
  453. Fei F, Yu Y, Schmitt A, Rojewski MT, Chen B, Gotz M, *et al*. Dasatinib inhibits the proliferation and function of CD4+CD25+ regulatory T cells. *Br J Haematol*. 2009;144(2):195-205.
  454. Balakrishnan K, Burger JA, Wierda WG, Gandhi V. AT-101 induces apoptosis in CLL B-cells and overcomes stromal cell-mediated Mcl-1 induction and drug resistance. *Blood*. 2009;113(1):149-53.
  455. Chatterjee M, Jain S, Stuhmer T, Andrulis M, Ungethum U, Kuban RJ, *et al*. STAT3 and MAPK signaling maintain overexpression of heat shock proteins 90alpha and beta in multiple myeloma cells, which critically contribute to tumor-cell survival. *Blood*. 2007;109(2):720-8.
  456. Rao R, Lee P, Fiskus W, Yang Y, Joshi R, Wang Y, *et al*. Co-treatment with heat shock protein 90 inhibitor 17-dimethylaminoethylamino-17-demethoxygeldanamycin (DMAG) and vorinostat: a highly active combination against human mantle cell lymphoma (MCL) cells. *Cancer Biol Ther*. 2009;8(13):1273-80.
  457. Huston A, Leleu X, Jia X, Moreau AS, Ngo HT, Runnels J, *et al*. Targeting Akt and heat shock protein 90 produces synergistic multiple myeloma cell cytotoxicity in the bone marrow microenvironment. *Clin Cancer Res*. 2008;14(3):865-74.
  458. O'Brien S. New Agents in the Treatment of CLL. *Hematology Am Soc Hematol Educ Program*. 2008:457-64.

459. Garg RJ, Wierda W, Fayad L, Estrov Z, Bickel SM, O'Brien S. Phase II Study of Dasatinib in Patients with Relapsed CLL. ASH Annual Meeting Abstracts. 2008;112(11): abstract 4197.
460. Hillmen P, Gribben JG, Follows GA, Milligan DW, Sayala HA, Moreton P, *et al.* An Open-Label Phase II Study to Investigate the Safety and Efficacy of Rituximab Plus Chlorambucil in Previously Untreated Patients with CD20-Positive B-Cell Chronic Lymphocytic Leukaemia (CLL). ASH Annual Meeting Abstracts. 2009;114(22): abstract 3428.
461. Delgado J, Pillai S, Benjamin R, Caballero D, Martino R, Nathwani A, *et al.* The effect of in vivo T cell depletion with alemtuzumab on reduced-intensity allogeneic hematopoietic cell transplantation for chronic lymphocytic leukemia. Biol Blood Marrow Transplant. 2008;14(11):1288-97.
462. Nabhan C, Coutre S, Hillmen P. Minimal residual disease in chronic lymphocytic leukaemia: is it ready for primetime? Br J Haematol. 2007;136(3):379-92.
463. Schweighofer CD, Ritgen M, Eichhorst BF, Busch R, Abenhardt W, Kneba M, *et al.* Consolidation with alemtuzumab improves progression-free survival in patients with chronic lymphocytic leukaemia (CLL) in first remission: long-term follow-up of a randomized phase III trial of the German CLL Study Group (GCLLSG). Br J Haematol. 2009;144(1):95-8.
464. Mauro FR, Zinzani P, Zaja F, Gentile M, Vegna ML, Stefoni V, *et al.* Fludarabine + prednisone +/- alpha-interferon followed or not by alpha-interferon maintenance therapy for previously untreated patients with chronic lymphocytic leukemia: long term results of a randomized study. Haematologica. 2003;88(12):1348-57.
465. Hainsworth JD, Litchy S, Barton JH, Houston GA, Hermann RC, Bradof JE, *et al.* Single-agent rituximab as first-line and maintenance treatment for patients with chronic lymphocytic leukemia or small lymphocytic lymphoma: a phase II trial of the Minnie Pearl Cancer Research Network. J Clin Oncol. 2003;21(9):1746-51.
466. Del Poeta G, Del Principe MI, Buccisano F, Maurillo L, Capelli G, Luciano F, *et al.* Consolidation and maintenance immunotherapy with rituximab improve clinical outcome in patients with B-cell chronic lymphocytic leukemia. Cancer. 2008;112(1):119-28.
467. Thieblemont C, Bouafia F, Hornez E, Dumontet C, Tartas S, Antal D, *et al.* Maintenance therapy with a monthly injection of alemtuzumab prolongs response duration in patients with refractory B-cell chronic lymphocytic leukemia/small lymphocytic lymphoma (B-CLL/SLL). Leuk Lymphoma. 2004;45(4):711-4.
468. Awan FT, Johnson AJ, Lapalombella R, Hu W, Lucas M, Fischer B, *et al.* Thalidomide and lenalidomide as new therapeutics for the treatment of chronic lymphocytic leukemia. Leuk Lymphoma. 2010;51(1):27-38.
469. Andritsos L, Johnson AJ, Lozanski G, Blum W, Kefauver C, Awan F, *et al.* Higher Doses of Lenalidomide Are Associated With Unacceptable Toxicity

Including Life Threatening Tumor Flare in Patients With Chronic Lymphocytic Leukemia. *J Clin Oncol*. 2008;26(15):2519-25.

470. Lapalombella R, Andritsos L, Liu Q, May SE, Browning R, Pham LV, *et al*. Lenalidomide treatment promotes CD154 expression on CLL cells and enhances production of antibodies by normal B Cells through a PI3-kinase dependent pathway. *Blood*. 2010;115(13):2619-29.
471. Chanan-Khan A, Miller KC, Musial L, Lawrence D, Padmanabhan S, Takeshita K, *et al*. Clinical efficacy of lenalidomide in patients with relapsed or refractory chronic lymphocytic leukemia: results of a phase II study. *J Clin Oncol*. 2006;24(34):5343-9.
472. Ferrajoli A, Lee BN, Schlette EJ, O'Brien SM, Gao H, Wen S, *et al*. Lenalidomide induces complete and partial remissions in patients with relapsed and refractory chronic lymphocytic leukemia. *Blood*. 2008;111(11):5291-7.
473. Sher T, Miller KC, Lawrence D, Whitworth A, Hernandez-Ilizaliturri F, Czuczman MS, *et al*. Efficacy of lenalidomide in patients with chronic lymphocytic leukemia with high-risk cytogenetics. *Leuk Lymphoma*. 2010;51(1):85-8.
474. Chen R, Keating MJ, Gandhi V, Plunkett W. Transcription inhibition by flavopiridol: mechanism of chronic lymphocytic leukemia cell death. *Blood*. 2005;106(7):2513-9.
475. Byrd JC, Shinn C, Waselenko JK, Fuchs EJ, Lehman TA, Nguyen PL, *et al*. Flavopiridol induces apoptosis in chronic lymphocytic leukemia cells via activation of caspase-3 without evidence of bcl-2 modulation or dependence on functional p53. *Blood*. 1998;92(10):3804-16.
476. Lin TS, Ruppert AS, Johnson AJ, Fischer B, Heerema NA, Andritsos LA, *et al*. Phase II study of flavopiridol in relapsed chronic lymphocytic leukemia demonstrating high response rates in genetically high-risk disease. *J Clin Oncol*. 2009;27(35):6012-8.
477. Chen R, Wierda WG, Chubb S, Hawtin RE, Fox JA, Keating MJ, *et al*. Mechanism of action of SNS-032, a novel cyclin-dependent kinase inhibitor, in chronic lymphocytic leukemia. *Blood*. 2009;113(19):4637-45.
478. Bettayeb K, Oumata N, Echaliier A, Ferandin Y, Endicott JA, Galons H, *et al*. CR8, a potent and selective, roscovitine-derived inhibitor of cyclin-dependent kinases. *Oncogene*. 2008;27(44):5797-807.
479. Lancet JE, Gojo I, Burton M, Quinn M, Tighe SM, Kersey K, *et al*. Phase I study of the heat shock protein 90 inhibitor alvespimycin (KOS-1022, 17-DMAG) administered intravenously twice weekly to patients with acute myeloid leukemia. *Leukemia*. 2010;24(4):699-705.
480. Ramanathan RK, Egorin MJ, Erlichman C, Remick SC, Ramalingam SS, Naret C, *et al*. Phase I Pharmacokinetic and Pharmacodynamic Study of 17-dimethylaminoethylamino-17-demethoxygeldanamycin, an Inhibitor of Heat-Shock Protein 90, in Patients With Advanced Solid Tumors. *J Clin Oncol*. 2010;28(9):1520-6.

481. Kummar S, Gutierrez ME, Gardner ER, Chen X, Figg WD, Zajac-Kaye M, *et al.* Phase I trial of 17-dimethylaminoethylamino-17-demethoxygeldanamycin (17-DMAG), a heat shock protein inhibitor, administered twice weekly in patients with advanced malignancies. *Eur J Cancer.* 2010;46(2):340-7.
482. Rodriguez A, Villuendas R, Yanez L, Gomez ME, Diaz R, Pollan M, *et al.* Molecular heterogeneity in chronic lymphocytic leukemia is dependent on BCR signaling: clinical correlation. *Leukemia.* 2007;21(9):1984-91.
483. Hewamana S, Lin TT, Jenkins C, Burnett AK, Jordan CT, Fegan C, *et al.* The novel nuclear factor-kappaB inhibitor LC-1 is equipotent in poor prognostic subsets of chronic lymphocytic leukemia and shows strong synergy with fludarabine. *Clin Cancer Res.* 2008;14(24):8102-11.
484. Olive KP, Tuveson DA. The use of targeted mouse models for preclinical testing of novel cancer therapeutics. *Clin Cancer Res.* 2006;12(18):5277-87.
485. Durig J, Ebeling P, Grabellus F, Sorg UR, Mollmann M, Schutt P, *et al.* A novel nonobese diabetic/severe combined immunodeficient xenograft model for chronic lymphocytic leukemia reflects important clinical characteristics of the disease. *Cancer Res.* 2007;67(18):8653-61.
486. Michie AM, Nakagawa R, McCaig AM. Murine models for chronic lymphocytic leukaemia. *Biochem Soc Trans.* 2007;35(Pt 5):1009-12.
487. Bichi R, Shinton SA, Martin ES, Koval A, Calin GA, Cesari R, *et al.* Human chronic lymphocytic leukemia modeled in mouse by targeted TCL1 expression. *Proc Natl Acad Sci U S A.* 2002;99(10):6955-60.
488. Yan XJ, Albesiano E, Zanesi N, Yancopoulos S, Sawyer A, Romano E, *et al.* B cell receptors in TCL1 transgenic mice resemble those of aggressive, treatment-resistant human chronic lymphocytic leukemia. *Proc Natl Acad Sci U S A.* 2006;103(31):11713-8.
489. Gorgun G, Ramsay AG, Holderried TA, Zahrieh D, Le Dieu R, Liu F, *et al.* E(mu)-TCL1 mice represent a model for immunotherapeutic reversal of chronic lymphocytic leukemia-induced T-cell dysfunction. *Proc Natl Acad Sci U S A.* 2009;106(15):6250-5.
490. Johnson AJ, Lucas DM, Muthusamy N, Smith LL, Edwards RB, De Lay MD, *et al.* Characterization of the TCL-1 transgenic mouse as a preclinical drug development tool for human chronic lymphocytic leukemia. *Blood.* 2006;108(4):1334-8.
491. Nakagawa R, Soh JW, Michie AM. Subversion of protein kinase C alpha signaling in hematopoietic progenitor cells results in the generation of a B-cell chronic lymphocytic leukemia-like population in vivo. *Cancer Res.* 2006;66(1):527-34.